SMALL MOLECULE GROWTH INHIBITORS FROM *Albatrellus flettii* AND *Sarcodon scabripes* NATIVE TO BRITISH COLUMBIA

by

Almas Yaqoob

Doctor of Pharmacy (Pharm-D), Hamdard University, Pakistan, 2012

THESIS SUBMITTED IN PARTIAL FULFILLMENT OF
THE REQUIREMENTS FOR THE DEGREE OF
MASTER OF SCIENCE
IN
BIOCHEMISTRY

UNIVERSITY OF NORTHERN BRITISH COLUMBIA

April 2019

Abstract

The first part of this thesis investigated the growth-inhibitory and immunomodulatory potential of six wild Canadian mushrooms. Out of 24 crude extracts, six showed strong growth-inhibitory activity, two exhibited strong immuno-stimulatory activity and nine demonstrated potent anti-inflammatory activity.

The second part of this thesis involved purification and characterization of growth-inhibitory compounds from *Albatrellus flettii*. Liquid-liquid extraction, Sephadex LH-20 and HPLC-Mass Spectrometry (HPLC-MS) were used to purify the three compounds of interest. NMR analyses confirmed their identity as grifolin, neogrifolin and confluentin. Grifolin and neogrifolin inhibited IMP1-KRas RNA interaction as demonstrated using an *in-vitro* fluorescent polarization assay. The three compounds suppressed KRas expression in SW480 and HT-29 human colon cancer cells. Confluentin, shown for the first time, to induce apoptosis and arrest cell cycle in SW480 cells.

The third part of this thesis involved the development of methods to purify growth-inhibitory compounds from *Sarcodon scabripes*. HPLC-MS detected some potential novel compounds.

Table of contents

List of Tables

List of Figures

List of Latin Binomials (fungi)

A. flettii	*Albatrellus flettii* Morse ex Pouzar.
C. unicolor	*Cerrena unicolor* Murril.
F. officinalis	*Fomitopsis officinalis* (Batsch) Bondartsev & Singer.
T. vaccinum	*Tricholoma vaccinum* (Schaeff.) P. Kumm.
T. versicolor	*Trametes versicolor* (L.) Lloyd.
S. scabripes	*Sarcodon scabripes* (Peck) Banker.

List of Abbreviations

$CDCl_3$	Chloroform-d
COSY-NMR	Correlation spectroscopy
DMEM	DMEM Dulbecco's Essential Eagle Media
DBPS	Dulbecco's Phosphate-Buffered Saline
ELISA	Enzyme-linked immunosorbent assay
EMEM	Eagle's Minimum Essential Medium (EMEM)
ESIMS	Electrospray Ionization Mass spectrophotometer
FBS	Fetal bovine serum
gDNA	Genomic DNA
HeLa	Henrietta Lacks cells
HPLC	High Pressure /Performance Liquid Chromatography
HSQC-NMR	Heteronuclear single quantum correlation
HT-29	Human colon adenocarcinoma cells
IMP-1	IGF2 mRNA-binding protein 1
MTT	3-(4,5-Dimethylthiazol-2-Yl)-2,5-Diphenyltetrazolium Bromide
KRAS	Kirsten rat sarcoma viral oncogene homolog.
NMR	Nuclear Magnetic Resonance
PCR	Polymerase Chain Reaction
RAW 264.7	Mouse macrophages
SW-480	Human colon adenocarcinoma cells
TMS	Tetramethyl silane
TNF-α	Tumor necrosis factor-α
^{1}H-NMR	Proton Nuclear Magnetic Resonance
^{13}C-NMR	Carbon (C-13) Nuclear Magnetic Resonance

Acknowledgements

First, I would like to say thank you “Dr. Chow Lee” for providing me with the opportunity to work in your lab on the mushroom project. Your office doors were always open whenever I needed your direction and you have been a great mentor throughout. Your constant motivation always kept me on the track and helped me grow academically and personally. I would also like to thank Drs Maggie Li, Hugues Massicotte, Keith Egger and Kerry Reimer for the much-needed technical guidance and perspicacious conversations that helped me understand the research results better. I would like to thank the Lee lab members for their unconditional help, especially Kashif Mehmood, Sebastian Mackedenski, Vicky Myhre, Belal Tafech, Hooi Xian, Mehreen Zeb, Sumreen Javed, Jake Da and Victor Liu for their support. Also, thanks to NALS members (Charles Bradshaw and Erwin Rehl) for providing the state-of-the-art facility for my experiments.

I am deeply indebted to my parents (Ms. Kausar Parveen and Mr. Muhammad Yaqoob) for their continuous emotional and financial support. My siblings (Lubna Yaqoob, Waqas Yaqoob, Awais Yaqoob and Hasnain Yaqoob) for their endless motivation. It is a delight to acknowledge those who have supported me over the last two years; I thank all my friends Muhammad Darwish, Hashim Nawaz, Gurbind Deo, Sukhpreet Buttar, Jatindar Khatra, Brendan Rieter, Jack Lofroth, Holly Cherniwchan, Muhammad Shubair and Fasahat Saeed for their unwavering support. Lastly, I would like to thank Kashif Mehmood for never letting me feel home sick and providing me with healthy meals every weekend.

Finally, I am tremendously appreciative of the efforts of Drs. Kaila Fadok and Elizabeth Dunn for their countless efforts teaching me the interpretation of NMR spectra.

Chapter 1: Introduction and literature review

1.1 Mushrooms are not just food

Fungi comprise the second largest kingdom of eukaryotic life on this planet (Schoch et al., 2012). Mushrooms are macro-fungi with a distinctive fruiting body, which can be either epigeous or hypogeous; they are large enough to be visible with the naked eye (Chang & Miles, 1992). Hypogeous mushrooms have their fruiting bodies below ground, while epigeous mushrooms have their fruiting bodies above ground. There is estimated to be about 1.5 million mushroom species but only about 10% are currently described (Hawksworth, 2012). Canada, specifically British Columbia (BC), has not been explored greatly for these valuable and interesting fungi. These facts and figures indicate the need to explore wild mushrooms from the vast and untapped regions of the world such as BC where novel mushrooms can be discovered, and their medicinal value can be determined.

Mushrooms are nutritionally important because they are low in calories, carbohydrates, fat, sodium, and cholesterol; they provide important nutrients including selenium, potassium, riboflavin, niacin, vitamin D, proteins, and fibers (Valverde et al., 2015). Both wild and commercial mushrooms are used as sources of nutrients and nutraceuticals. Most of the edible mushrooms have an added benefit of being anti-microbial and provide resistance to various diseases (Barros et al., 2015).

Aside from the oriental folk medicines, mushrooms have become more important in the last decade because of their promising medicinal properties (Lindequist et al., 2005). Medicinal Mushrooms are now proven to have anti-oxidant, anti-fungal, anti-bacterial, anti-viral, anti-allergic, antidiabetic, anti-parasitic, anti-atherogenic, hepato-protective, anti-cancer and immuno-modulatory activities among others (Lindequist et al., 2015). Mushrooms can also be used as

prophylactic agents against inflammation and tumorigenesis (Finimundy et al., 2013). For instance, anti-cancer agents from *Albatrellus confluens* have been reported to have effects against gastric cancer cells, nasopharyngeal carcinoma and osteosarcoma (Wu & Li, 2017). Thus, these mushrooms are not just part of our diet but rather encapsulate medicinal properties that can potentially be exploited by humans.

1.2 Mushrooms as ancient remedy

Mushrooms have been used as medicine for thousands of years by our ancestors. In the 5th century, the alchemist Tao Hongjing first described *Ganoderma lucidum* and *Dendropolyporus umbellatus* (Stamets & Zwickey, 2014). The use of *Ganoderma* and related species as a medicinal constituent in traditional medicines dates back thousands of years (Stamets & Zwickey, 2014). *Ganoderma lucidum* (Ling zhi) is commonly referred to as the mushroom of immortality in China, Japan and Korea (Pegler, 2002). In China and Japan particularly, hot water extracts of mushrooms are used for the treatment of several diseases (Dias et al., 2004). The medicinal use of mushrooms has a very long tradition in Asian countries, whereas their use in the Western culture is only slowly gaining attention. Moreover, the dried powder of *G. lucidum* is also used in eastern countries as a preventive household medicine or cure against various cancers like prostate and human breast cancer (Daniel et al., 2003).

Today, *Ganoderma lucidum* has been shown to contain 16,000 genes that code for many active compounds (Stamets & Zwickey, 2014). Although mushrooms have long been used by various ancient cultures, only from research done in the last decade has modern science been able to rediscover what the ancients knew long ago, that mushrooms can be a tremendous resource of powerful medicines (Stamets & Zwickey, 2014). Pharmacological activity includes hepatic and renal protection from oxidation through its prominent superoxide scavenging effects

(Shieh et al., 2011), enhancing innate immunity by activating NF-kappa-B (Kuo et al., 2006), and proven anti-cancer benefit by inducing apoptosis and causing mitochondrial damage (Kim et al., 2007). Among these therapeutic potentials, the immuno-modulating effects of *Ganoderma lucidum* gained special interest; the immuno-modulatory mechanism of action includes promoting the function of antigen-presenting cells, as well as encouraging the mononuclear phagocyte system, humoral immunity, and cellular immunity (Lin, 2005). Therefore, this strong history of traditional use of medicinal mushrooms supported by scientific research can be a hope for the eradication of chronic diseases including cancer.

1.3 Medicinal mushrooms and their compounds as a source of anti-proliferative activity

1.3.1 Anti-proliferative mushrooms

The feasibility of using mushroom-derived compounds exhibiting anti-cancer effects is becoming increasingly evident. The anti-cancer properties of compounds extracted and purified from mushrooms impart anti-tumor effects using one or a combination of the following mechanism(s): reactive oxygen species inducer, mitotic kinase inhibitor, signal transduction cascade modifier, angiogenesis inhibitor, and topoisomerase inhibitor. These mechanisms ultimately lead to apoptosis and an anti-proliferative response (Patel & Goyal, 2012**)**. One of the prominent anti-cancer compounds from the mushroom *Trametes versicolor* is Polysaccharide K (PSK), imparting anti-cancer effects by selectively activating the Toll like receptor 2 (TLR-2) in tumor-bearing neu transgenic mice after oral administration (Lu et al., 2011). *Inocybe umbrinella*, a toxic mushroom, is also reported to have a novel lectin that has shown anti-proliferative activity against hepatoma HepG2 cells and breast cancer MCF7 cells (Zhao et al., 2009). Similarly, studies on the anti-proliferative activity of mushroom extracts from *Auricularia auricula-judae, Pleurotus abalonus* and *Pleurotus sajor-caju* against U937 leukemia cells

showed that fungi do exhibit promising results (Friedman, 2016). Friedman (2016) also studied several mushroom extracts that have demonstrated the anti-tumor effect via anti-angiogenic pathways. The findings suggested that *Phellinus linteus* significantly inhibit proliferation, migration, tube formation and vascular endothelial growth factor receptor phosphorylation of human vein endothelial cells (Lee et al., 2010). The polysaccharide isolated from *Antrodia cinnamomea* also exhibit anti-angiogenic activity by down-regulating cyclin D1 expression via antagonizing vascular endothelial growth factor receptor signaling (Cheng et al., 2005).

Anti-proliferative activity can be due to changes in cell morphology, activation of caspase-like activities, release of cytochrome C into cytosol, or DNA fragmentation. Clitocine, a bioactive compound from *Leucopaxillus giganteus,* has shown apoptotic activity in human cervical cancer cells (HeLa), demonstrating the anti-proliferative potential of this purified moiety (Ren et al., 2008). Similarly, various terpenes also exhibit tumor growth-inhibitory properties. For example, terpenes isolated from the ethyl acetate-extract of *Hypsizigus marmoreus* exhibited strong tumor growth-inhibitory activity against murine sarcoma cells and against human tumor cell lines including U937 and HL-60 (Mizutani et al., 2006).

1.3.2 Cytotoxic Extracts

Mushroom extracts are also reputed to possess cytotoxic activity. Mushrooms extracts are not only used alone but also in combinational therapy to impart synergistic effects on tumor growth inhibition. Some of the prominent cytotoxic compounds and extracts will be described briefly here to highlight the potency of these mushrooms against cancer cell lines. A cytotoxic component, called suillin, isolated from the extract of the mushroom *Suillus placidus,* demonstrated a significant cytotoxic activity against human liver cancer cells (HepG2 cells, Hep3B cells, and SK-Hep-1) (Liu et al., 2009). The fungal extract of *Agaricus blazei* is also in

use by gynecological cancer patients undergoing cancer chemotherapy (Ahn et al., 2004). Similarly, hot water extracts of some common dietary mushrooms, including maitake, crimini, portabella, king oyster, and white button, have shown ability to reduce mitogenesis and induce apoptosis and cytotoxic activity in MCF7 human breast cancer cells (Martin et al., 2009). Among these mushrooms, maitake is well-known to have both immunomodulatory and antitumor properties; its 5% NaOH extract has previously been reported with potent cytotoxic effects and has shown promising results in reducing tumor cell viability due to apoptosis (Soares et al., 2011).

1.4 Overall Medicinal Prospects of Mushrooms

The spectrum of medicinal properties of mushrooms is not confined to anti-cancer activity, but rather they have also been documented to have other promising healing properties. These include antimicrobial (antiviral, antibacterial and anti-fungal), antiallergic, immunomodulating (both immuno-stimulating and anti-inflammatory), antiatherogenic, anti-diabetic (hypoglycemic), anti-oxidative (hepatoprotective) (Lindequist et al., 2015).

1.4.1 Anti-Bacterial Mushrooms

Many parts of the world are facing problems related to prevalence of infectious diseases and complications related to resistance to antibiotics. Prophylactically and therapeutically, antimicrobial drugs have been over-used, which has caused the bacterial strains to become resistant towards antibiotics (Klein et al., 2007). Compounds from mushroom extracts have shown both bactericidal and bacteriostatic potential. The type of activity exhibited by extracts can be related to the nature of bioactive compounds (Alves et al., 2012). For example, *Lentinus edodes* extracts have shown strong bactericidal activity against *Streptococcus pyogenes* (Hatvani, 2001). These extracts are helpful in killing bacteria responsible for oral infections and tooth

decay (Signoretto et al., 2011). Mushroom extracts have also proven their anti-microbial activity against very resistant strains of bacteria. For example, extracts from *Phellinus linteus* have shown antibacterial activity against methicillin resistant *Staphylococcus aureus* (Hur et al., 2004).

1.4.2 Cardiovascular diseases

The western world is suffering from a high level of mortality and morbidity related to cardiovascular diseases. Cardiovascular diseases can be linked with different metabolic markers including high density lipoproteins, low density lipoproteins, cholesterol and triglycerides. Metabolic markers for cardiovascular diseases are impacted positively (a decrease is noted), by several compounds present in mushrooms, such as low trans-isomers of unsaturated fatty acids, a low concentration of sodium, eritadenine, phenolic compounds, sterols (such as ergosterol), chitosan and triterpenes (Guillamón et al., 2010).

1.4.3 Anti-inflammatory

Overproduction of inflammatory mediators is a biological response of the immune system in response to pathogens. Inflammatory biomarkers include interleukins, tumor necrosis factor, nuclear factor-κB, intercellular adhesion molecule, cyclooxygenases, and prostaglandins (Elsayed et al., 2014). Mushrooms contain polysaccharides, terpenoids, phenolic compounds, and low molecular weight molecules, which have all shown strong anti-inflammatory properties (Elsayed et al., 2014). *Inonotus obliquus,* known as Chaga, is a well-known anti-inflammatory mushroom (Park et al., 2005). Various triterpenoids and steroids from *I. obliquus* were purified and found responsible for this anti-inflammatory potential in various *in-vitro* and *in-vivo* models (Park et al., 2005). Similarly, proteoglycan derived from the medicinal mushroom *Phellinus linteus* can prevent and treat collagen-induced arthritis (CIA) in mice (Kim et al., 2003).

1.4.4 Anti-oxidative

An antioxidant is a molecule capable of inhibiting the oxidation of other molecules (Kozarski et al., 2015). Imbalanced metabolism or an excess of reactive oxygen species can lead to oxidative stress in human systems. Dietary intake of antioxidant supplements can regulate oxidative homeostasis. Mushrooms have shown significant antioxidant properties due to their bioactive compounds, such as polyphenols, polysaccharides, vitamins, carotenoids and minerals. Their anti-oxidant mechanism can be primary (chain breaking, free radical scavengers) or secondary or preventive (Kozarski et al., 2015).

Kozarki et al. (2012) studied the anti-oxidative potential of four reputed mushrooms (*Ganoderma applanatum, G. lucidum*, *L. edodes* and *T. versicolor*) and, among these, four different extracts of *G. applanatum* and *L. edodes,* were the most potent. All four extracts demonstrated strong correlation between phenol and α-glucan levels and bioactivity, suggesting the possibility of the active molecule(s) to be phenolic and α-glucan derivatives (Kozarki et al. 2012).

1.5 Wild mushrooms in Canada: a source to discover new anti-cancer compounds

Canadian ecosystems, especially the habitats of British Columbia, provide favorable conditions for growth of many species of mushrooms. Classification of these mushrooms is complex, and it used to be based on their reproductive structures; these may be bracket, crust, truffle, morel, gilled, coral, jelly, toothed, bird's nest, pore, club, puffball, earthstar, stinkhorn cup, earth tongue mushrooms, along with many others (Arora 1986).

Wild mushrooms, especially from North America, are still mostly un-explored for their medicinal properties. Commercially available and wild edible mushrooms have long been consumed in Canada for their nutritional value, but prior to research at UNBC, there had been

only two studies on the bioactivity of wild mushrooms native to Canada. A new compound in *Ganoderma applanatum* collected from BC forests was reported (Ming et al., 2002), but there was no insight into its biological activity. A second study shows anti-inflammatory effects of *Inonotus obliquus* collected from northern Manitoba, but no compound characterization was provided (Van et al., 2009).

Three recent studies in Dr. Lee's lab have provided insights to the medicinal properties of several Canadian wild mushrooms; these were found to have immunomodulatory and growth-inhibitory activities. The first report on growth-inhibitory and immunomodulatory potential of BC wild mushrooms has provided a direction for further exploration (Smith et al., 2017). The second report was on a growth-inhibitory heteroglycan (GIPinv) polysaccharide isolated from *Paxillus involutus*. GIPinv (229KDa) has ability to induce apoptosis in HeLa cancer cells (Barad et al., 2018). The third study focused on a small molecular weight carbohydrate (5-25KDa) purified from *E. tinctorium* (Javed et al., 2017). The anti-inflammatory polysaccharide can inhibit the TNF-α production in LPS activated RAW 264.7 cells as well as ameliorate histamine-induced vasodilation in the 2A arterioles (*gluteus maximus* muscle) in mice (Javed et al., 2017). Based on these studies, it is clear that Canadian wild mushrooms are beneficial and a possible economical source of small and large molecules with potential for the treatment or prevention of many acute and chronic diseases.

1.6 Compounds with anti-proliferative activity

There are great variety of growth-inhibitory compounds when it comes to the size of molecules. The growth-inhibitory compounds are classified based on their size and chemical nature. Figure 1.1 provides a general classification of high molecular weight and small molecular compounds that have been isolated from mushrooms. A brief description of some of these compounds is provided below.

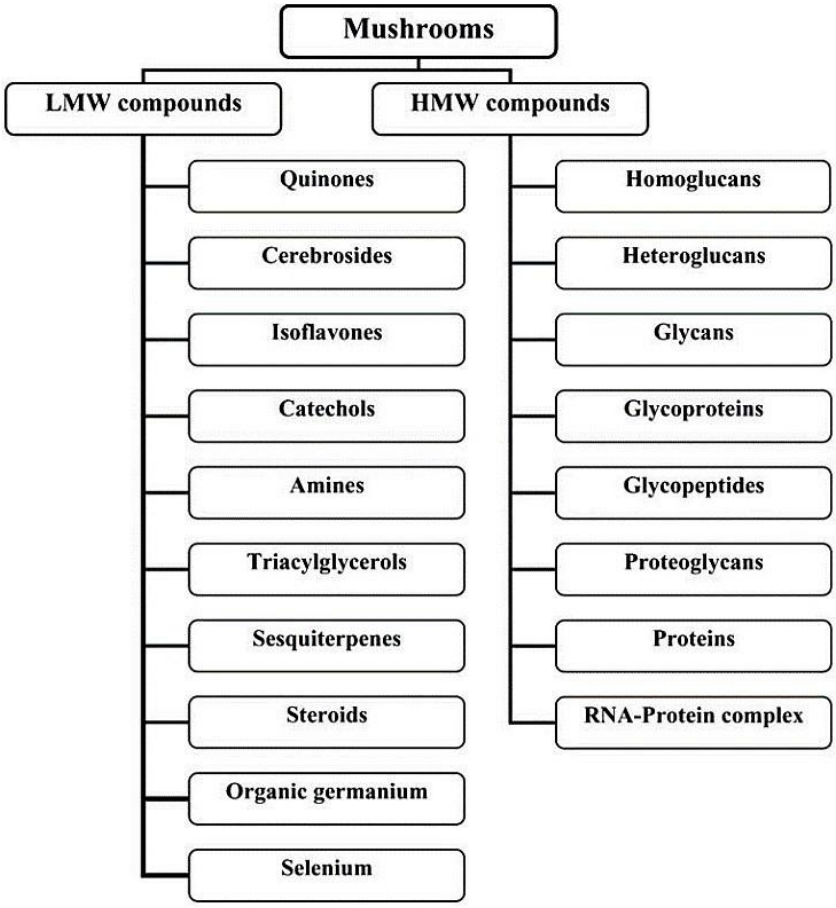

Figure 1.1 Classification of compounds with anti-tumor potential based on their molecular weight (Ferreira et al., 2010).

1.6.1 Large molecules (High Molecular weight compounds)

High-molecular-weight bioactive compounds isolated from mushrooms include homoglucan, heteroglucans, glycan, glycoproteins, glycopeptides, proteoglycans, proteins and RNA-protein complexes (Figure 1.1). Mushrooms contain high amounts of proteins, ranging from 10-40% of dry weight. These proteins should be cytotoxic in their nature for instance a cytotoxic high molecular weight protease purified from the dried fruiting bodies of *Cordyceps militaris* showed remarkable effects against different human cancer cell lines (Park et al., 2009). Alkaline protease, having the molecular weight of 15 kDa, isolated from fruiting bodies of *Amanita farinosa* was shown to dose-dependently inhibit proliferation of HepG2 cells (Sun et al., 2011). Similarly, a sulfated polysaccharide isolated from *Grifola frondosa* showed a concentration-dependent inhibition of proliferation in HepG2 cells by inducing apoptosis and causing cell cycle arrest at S phase (Wang et al., 2013). Likewise, the polysaccharide from *G. frondosa* and vitamin C, when tested in combination, showed the synergistic effects on hepatocellular carcinoma cells (SMMC-7721) by reducing the viability by 70%. This effect was observed because of cell cycle arrest at the G2/M phase (Zhao et al., 2016). Table 1.1 provides insights from the literature to some of the purified large molecules from fruiting bodies of the mushrooms.

Table 1. 1 Large compounds from mushroom and their biological properties

Mushroom species	Compounds	Biological activity	Reference
Polysaccharides:			
Paxillus involutus	GIP-inv polysaccharide	Anti-proliferative (apoptosis induction)	Barad et al., 2018.
Agaricus bisporus	RK2-Ab manno-galacto-glucan	Anti-proliferative (apoptosis induction)	Pires et al., 2017.
Flammulina velutipes	FVP2A, FVP2B and FVP2C	↑cellular NO formation, iL-1 production and TNF-α secretion in macrophages	Yin et al., 2010.
Sarcodon aspratus	Water-soluble polysaccharide (HCP)	Stimulate the proliferation of the cultured mice spleen lymphocyte	Han et al., 2011.
Lentinus edodes	Branched β-(1, 3)-glucan (LNT)	Induction of apoptosis, inhibition of proliferation	Xu et al., 2016.
Proteins/Enzymes:			
Ganoderma lucidum	Laccase	Inhibition of the activity of HIV-1 reverse transcriptase	Wang et al., 2006
	(FIP) fungal immunomodulatory protein	Enhanced the transcription of (IL)-2, IL-3, IL-4, interferon (IFN)-γ, (TNF)-α	Li et al., 2010.
Hypsizigus marmoreus	(RIP) Ribosome inactivating protein	↓ Proliferation of Hep G2 cells MCF-7 cells	Wong et al., 2008
Stachybotrys chlorohalonata	(FIP) Fungal immunomodulatory protein	Induced apoptosis and interrupt migration in A549 cells	Jiang et al., 2017
Ganoderma microsporum	(GIP) Ganoderma immunomodulatory protein	Down-regulation of TNF-a Induced Expression of Matrix Metalloproteinase 9	Lin et al., 2010.
Trametes versicolor	FIP-TVC	Enhanced the proliferation of splenocytes and human peripheral blood lymphocytes.	Li et al., 2011.

1.6.2 Small molecules (Low Molecular weight compounds)

Smaller compounds with anti-proliferative potential identified so far in mushrooms, include quinones, cerebrosides, isoflavones, catechol, amines, triacylglycerols, sesquiterpenes, steroids, organic germanium and selenium (Figure 1.1). Terpenoids can be phenolic in nature, such as Isopropyl 2,6-bis(1-phenylethyl)phenol isolated from the butanol extract of *Cordyceps bassiana.* This terpenoid has shown anti-proliferative and apoptotic activity on several cancer cell lines such as C6 glioma, MDA-MB-231, and A549 cells (Kim et al., 2015).

Terpenes also play a major role in inhibiting cancer cells growth. Ergosterol peroxide from Chaga exhibited anti-proliferative activity by down-regulating the β-catenin pathway in different colorectal cancer cell lines (Kang et al., 2015). Methanolic extracts contain the cytotoxic sterols, sterols with peroxide ring or an epoxide ring . Sterols extracted from the dried powder of cultured mycelium of *C. sinensis* showed significant cytotoxic activity on human cancer cell line HL60 (Matsuda et al., 2009).

Low molecular weight (LMW) polyphenolic compounds having polyhydroxylated benzyl, moiety in their structure are abundant in *Inonotus obliquus.* These low molecular weight polyphenolic compounds include caffeic acid, 3,4-dihydroxybenzalacetone, gallic acid, syringic acid, protocatechuic acid, 3,4-dihydroxybenzaldehyde and 2,5-dihydroxyterephthalic acid. These low molecular weight polyphenolic compounds were able to inhibit human topoisomerase II (Kuriyama et al., 2013). Some potent anti-cancer small molecules purified from the fruiting bodies of the mushrooms are shown in Table 1.2.

Table 1. 2 Small compounds from fruiting bodies of mushrooms and their biological properties

Mushroom species	Compounds	Biological activity	Reference
Terpenoids:			
Albatrellus confluens	Grifolin	Inducing apoptosis	Ye et al., 2005.
	Confluentin	Weak antagonist for human vanilloid receptor VR1	Hellwig et al., 2003.
Albatrellus flettii	Grifolin, Neogrifolin and Confluentin.	Anti-bacterial activity	Liu et al., 2010.
Albatrellus ovinus	3-hydroxyneogrifolin, 1-formylneogrifolin and 1-formyl-3-hydroxyneogrifolin	Antioxidative activity	Nukata et al., 2002.
	Grifolin, Neogrifolin		
Sarcodon scabrosus	Sarcodonin G	↓ Proliferation by inducing HeLa cell apoptosis	Mei et al., 2010.
	Scabronine A	Potent inductive activity of the nerve growth factor synthesis	Ohta et al., 1998.
	Scabronine G and H	Antibacterial and antifungal activity	Ma et al., 2010.
Pleurotus eryngii	Eryngiolide A	Moderate cytotoxicity against two human cancer lines in vitro	Wang et al., 2012.
Cyathus africanus	Cyathane diterpenes	Inhibition of nitric oxide production in LPS-activated macrophages	Han t al., 2013.
Ganoderma lucidum	Ganoderic acid A	Suppress growth and invasion of breast cancer cells by modulating AP-1 and NF-κB signaling	Jiang et al., 2008.
	Ganoderic acid T	Mitochondria mediated apoptosis in lung cancer cells	Tang et al., 2006.
Fomitopsis nigra	Fomitoside-K	Induce apoptosis via ROS-dependent mitochondrial dysfunction	Bhattarai et al. 2012. Lee et al. 2012.

1.7 Research Goals

Canada and particularly British Columbia is fortunate with a wide range of basidiomycetes fungi that should be explored for their biological activity. The probability of finding novel immunomodulatory or growth-inhibitory compounds from Canadian wild mushrooms is very high. Mushrooms contain a wide range of small to large compounds, but the purification technique and strategy are to be used to isolate compounds will depend on its characteristic and chemical nature.

Following are the specific research goals of my MSc thesis:

(i) Genetic identification, chemical extraction and biological assessment (immuno-modulatory and growth-inhibitory activities) of six Canadian mushroom specimens.

(ii) Purification and characterization of small molecule growth-inhibitors from *Albatrellus flettii*

(iii) Purification and identification of small molecules from *Sarcodon scabripes*

Chapter 2: Evaluation of Canadian wild mushrooms for growth-inhibitory and immuno-modulatory activities

The immune system is known as body's defense system against pathogens. The exposure to the pathogens results in the activation of different immune-system markers: which could be either anti-inflammatory or immunostimulatory. Mushroom extracts could possess the potential to either stimulate TNF-α (immunostimulatory) or inhibit TNF-α (anti-inflammatory). Mushroom extracts could also be growth-inhibitory or cytotoxic in nature.

This chapter concerns the analysis of five mushroom species collected from British Columbia (BC) and one mushroom species collected from Quebec. The mushrooms were first genetically identified followed by chemical extractions to generate crude extracts. The crude extracts were then screened for growth-inhibitory and immuno-modulatory activities.

2.1 Materials and Methods

2.1.1 Mushroom Collection & Identification

The mushrooms used in this study were collected by the UNBC research team (Drs. Hugues Massicotte, Keith Egger, Chow Lee, Maggie Li and Ms. Linda Tackaberry) at different locations across north-central BC and Ste-Geneviève of Batiscan, in Quebec. The collected fungi were dried overnight in the hot air oven at 60 °C. The species were identified using morphological and genetical approaches. Morphological identification was based on different morphological parameters identified using the software "Matchmaker" (Gibson et al., 2010) and the reference guide Mushrooms Demystified (Arora, 1986).

To genetically identify mushroom samples, tissue sample from the cap flesh was collected and further processed for DNA extraction. After genomic DNA extraction, samples were sent for sequencing using the forward primer ITS3 (5'-GCATCGATGAAGAACGCAGC-3') and the reverse primer NLB4 (5'-GGATTCTCACCCTCTATGAC-3'). The minimum

concentration required to send for sequencing was 10.0 ng/µL. The sequences obtained from Macrogen Corporation were compared with sequences available in the National Center for Biotechnology Information (NCBI) internet database, GenBank, using the Basic Local Alignment Search Tool (BLAST) program. Specimens were considered to be tentatively identified if BLAST results indicated at least 97% similarity.

Table 2.1: Photographs of the mushroom specimens collected from different locations across Canada

	***Fomitopsis officinalis* (115)** **(also called *Laricifomes officinalis*)** **Collected on October 1st, 2015** **Location: Douglas-fir, Prince George, BC**
	***Sarcodon scabripes* (124)** **Collected on August 21, 2016** **Location: Twin Falls, Smithers, BC**

***Tricholoma vaccinum* (125)**

Collected on August 21, 2016

Location: Twin Falls, Smithers, BC

***Cerrena unicolor* (127)**

Collected on August 21, 2016

Location: Seeley Lake Provincial Park, BC

***Albatrellus flettii* (128)**

Collected on September 3, 2016

Location: Twin Falls, Smithers, BC

	***Trametes versicolor* (143)** **Collected on October 29, 2016** **Location: Rang des Forges, Ste-Geneviève de Batiscan, QC.**
	***Albatrellus flettii* (151)** **Collected on September 20, 2017** **Location: Twin Falls, Smithers, BC**

2.1.2 Genetic identification of the mushroom samples using ITS3 and NLB4 primers

Before determining the medicinal properties of collected mushrooms, their identity needs to be determined. In the past, mushrooms were primarily identified based on morphological characteristics of the fruiting body such as whether it was gilled or toothed, and then classified according to the system developed by Elias Fries (Binder & Hibbett, 2002), but often there was difficulty separating closely-related species due to similar morphological characteristics. One of the major advances in the past few decades in the field of taxonomy is the application of molecular genetic techniques to species identification.

The ITS regions have been found to have the greatest probability of correct identification for the greatest range of fungi as compared to other possible identification sequences. Researchers from previous literature have used either the ITS1, ITS2 or both regions to genetically identify unknown mushrooms samples (Martin & Rygiewicz, 2005). However, we

focused on the ITS2 region because the primer sets ITS3 and NLB4 extends into the 28S large subunit gene (Kowalczyk et al., 2015). The ITS2 region of the genomic DNA (gDNA) could be amplified using the forward primer ITS3 and the reverse primer NLB4. Thus, using these set of primers can aid in the identification of unknown mushroom samples.

2.1.3 DNA extraction procedures

The MoBio DNA PowerSoil Kit was used to extract genomic DNA from mushroom samples. The mushroom samples were emulsified using PowerBead™ tubes and then subjected to DNA extraction. Modifications made to the manufacturer's protocol include heating the mushroom samples to 95°C for 15 min in PowerBead tube solution as well as increasing the time vortexing the PowerBead tubes increased to 15-20 min. The process of gDNA extraction was performed for two samples only (143 and 151). The gDNA from other samples was extracted by Dr. Maggie Li. The extracted DNA was then quantified spectrophotometrically using a Nanodrop™ spectrophotometer (Table 2.2).

Table 2.2: Concentration of the genomic DNA and of the purified PCR product/Gel Extraction, using Nanodrop.

Sample	Concentration of gDNA (ng/µL)	Concentration after PCR purification (ng/µL) / gel Extraction
Mushroom 143	13.4	30.3
Mushroom 151	12.4	38.1

2.1.4 PCR amplification and purification procedure

The genomic DNA (gDNA) of mushroom samples (Table 2.2) were subjected to PCR using the conditions listed in Tables 2.3 and 2.4. The ITS2 region of the gDNA was amplified using the forward primer ITS3 (5'-GCATCGATGAAGAACGCAGC-3') and the reverse primer NLB4 (5'-GGATTCTCACCCTCTATGAC-3'). The efficiency of the PCR samples was assessed by agarose gel electrophoresis. Gel electrophoresis was performed at 140 V using a 1%

agarose gel, ethidium bromide and 0.5 x TBE Buffer. The gel ran for approximately 40 min at 140 V and was subsequently visualized under a UV transilluminator. In the case that no band was visualized, the amplification procedure was repeated except that a larger volume of gDNA was used (2-4 µL) and the source of TAQ polymerase and 10x thermopol buffer was changed. In the case where a faint band was observed, multiple PCR amplifications were done using higher amount of gDNA (2 µL) and after combining all amplified PCR products, PCR cleanup was performed using the QIAquick PCR kit. After purification, samples were sent to Macrogen Corporation for DNA sequencing using the forward primer ITS3 (5'-GCATCGATGAAGAACGCAGC-3') and the reverse primer NLB4 (5'-GGATTCTCACCCTCTATGAC-3'). The minimum concentration required to send for sequencing was 10.0 ng/µL.

Table 2.3: PCR reaction protocols required to amplify the extracted DNA from the mushroom species using both the forward (NLB4) and reverse (ITS3) primers.

Component	**Volume used (µL)**
H_2O	16
10x Thermo Pol Buffer	2.5
dNTPs (2.5 mM)	2.5
ITS3 (10 µM)	1
NLB4 (10 µM)	1
DNA template	1.5
TAQ polymerase	0.5

Table 2.4: PCR program, steps 2, 3, 4 are repeated 29 times in the cycle.

PCR Program		
Step	Temp	Time
1	95 °C	5min
2	95 °C	30sec
3	52 °C	30sec
4	72 °C	30sec
5	72 °C	10min
6	4 °C	10min

2.2 Chemical extraction of mushrooms

The choice of appropriate extraction technique solely depends on the compounds of interest and their chemical nature. Use of high temperature extraction technique becomes impossible if the bio-active compounds are thermolabile. To get the maximum quantity of desired bio-active compounds, the extraction must be based on the appropriative technique and pattern. Dr. Lee's lab recently adopted the use of Dionex speed extractor (ASE 350) in preparing extracts from mushrooms. Dionex Accelerated Solvent Extractor ASE 350 is an automated, safe and easy way for sequential extraction (80% ethanol, 50% methanol, and water) of bioactive compounds from solid and semisolid samples.

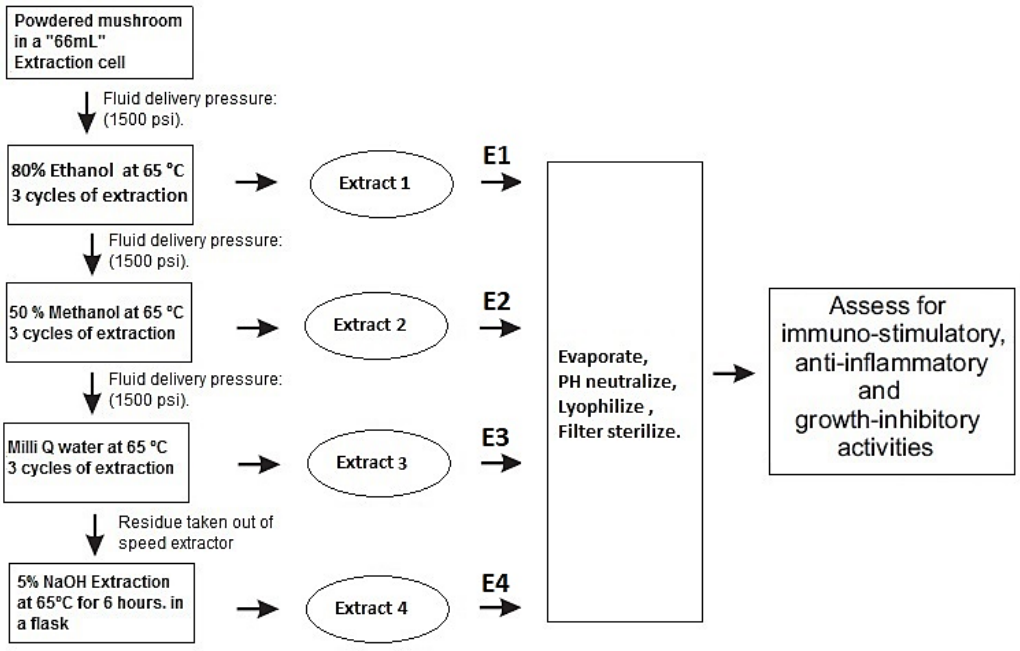

Figure 2. 1 Flowchart summarizing the chemical extraction protocol (Dionex ASE 350) (Graphics credit: Hasnain Yaqoob).

Traditional methods such as soxhlet and sonication are time consuming, difficult, labor intensive and require large amount of solvents. Dionex ASE 350 uses less solvent as compared to other extraction methods and allows simultaneous extraction of multiple samples. The concept

behind this technique is based on the use of elevated temperature to increase the extraction efficiency of analyte of interest from their matrix. Elevated nitrogen pressure is used to keep the solvents in a liquid state, the solubility of analyte is increased, and viscosity of the solvent is reduced, thereby increasing extraction efficiency and reducing extraction time (De Monte et al., 2014).

Using the Speed Dionex method, samples were initially placed in filter cell (thimble) and first extracted with 80% ethanol so that any low molecular weight compounds can be obtained. Samples were sequentially extracted with 50% methanol (for low molecular weight compounds) and then with water (for water-soluble polysaccharides). The 5% NaOH extraction step was then performed manually using a hotplate to extract water-insoluble polysaccharides. Several extraction parameters (temperature, time, cycle, nitrogen pressure) were considered, which can affect the stability and yield of the extracts (Liu et al., 2010).

2.2.1 Rotary evaporation, pH neutralization, snake skin dialysis, and lyophilization of the extracts

After successful extraction, the mushroom extracts were further processed for volume reduction to eliminate the excess amount of solvent. The process of evaporation was hastened with the help of rotary evaporator. Once the volume of the extracts was reduced to a required limit (if 90% solvent is removed), the extracts were subjected to pH neutralization. The pH range used as reference to neutralize the mushroom extracts was 6.90 to 7.10. For pH neutralization, either 2 M NaOH or 2 M HCl was used. To remove salts, the extracts were dialyzed using Thermo Scientific SnakeSkin Dialysis Tubing (3.5K MWCO) for 12 hours. The last step involved in the processing of extract was lyophilization. Extracts were first frozen in -80 ºC freezer and then lyophilized using Labconco Freeze dryer (0.008 bar vacuum pressure and -80

ºC). The amount of dried extracts was then determined so that the yield can be estimated and then used for biological assays.

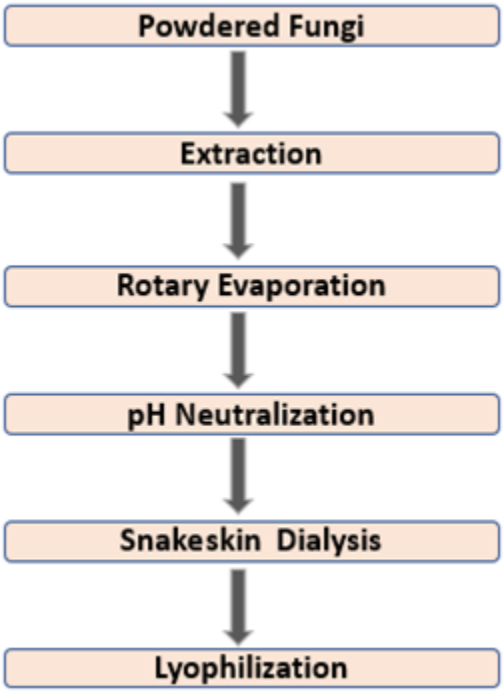

Figure 2. 2 Flowchart showing the scheme adopted to obtain dried extracts prior to cell treatment.

2.2.2 Stock solution and filter sterilization

Stock solution concentrations were made in consideration of the solubility of the extracts. Before making stock solutions, extracts were analyzed for their maximum solubility in an appropriate solvent. For extracts that were soluble in water, the stock solutions were prepared at 20 mg/mL. For extracts that were not soluble in water but soluble in methanol, the final concentration of stock solutions was prepared at 40 mg/mL. For example, E1 and E2 of *A. flettii* and *S. scabripes* were insoluble in water and were prepared in this manner.

After making the stock solution of the extracts, the next step was to filter-sterilize the solution. The process of filter-sterilization was carried out using 0.2 µm filter (Sarstedt,

Nümbrecht, Germany) to remove any precipitate or biological impurities (which can interfere with the results).

2.3 Assessment of Anti-proliferative and Immuno-Modulatory Activities (Immuno-stimulatory and Anti-inflammatory) of Mushroom Crude Extracts

2.3.1 Dose- and time-dependent MTT assay to determine the anti-proliferative activity of mushroom extracts on HeLa cell

The lyophilized mushroom extracts were reconstituted in their respective suitable solvents mentioned in Table 2.7. The stock concentration was 40 mg/mL for methanol-soluble extracts and 20 mg/mL for water-soluble extracts. For dose-dependent MTT assay, the stocks were further diluted using EMEM (Eagle's minimum essential media) supplemented with 10% FBS to make different doses of extracts. HeLa cells were first subjected to treatment with different concentrations (from 0.1 mg/mL to 1 mg/mL) of the extracts for 48 hours and MTT assay was performed. Based on the results from dose-dependent MTT assay, the time-dependent MTT assay was then performed. HeLa cells were subjected to treatment with selected concentration of active extracts for a specific period (1 to 7 days).

2.3.1.1 Dose-dependent MTT assay for assessment of growth-inhibitory activity of mushroom extracts

MTT [3-(4,5-dimethylthiazole-2-yl)-2,5-diphenyl tetrazolium bromide] assay is a colorimetric bioassay used to assess cell viability. The MTT assay can be used to determine the growth-inhibitory effect of mushroom extracts on human cancer cell lines. The mitochondrial NADPH-dependent reductase enzyme in viable cells reduces the water-soluble yellow tetrazole MTT dye to insoluble purple formazan crystals (Meerloo et al., 2011), which are accumulated in lipid droplets because of their lipophilic nature (Stockert et al., 2012).

Figure 2. 3 Mechanism involved in the reduction of MTT dye by mitochondrial reductase (indicator of cell redox activity)

The MTT dye readily penetrates viable cells (Riss et al., 2016). The mitochondria in viable cells has the enzyme that converts MTT into formazan. The concentration of the purple formazan makes it possible to estimate the number of viable cells. Dimethyl sulfoxide (DMSO) was then used to solubilize formazan crystals. After that, the absorbance from the formazan solution was determined using Synergy 2 multi-plate reader (BioTek®, USA). It is important to point out here that the MTT assay has some limitations regarding certain type of reductive chemicals and because of that, it can give an underestimation of the anti-proliferative activity of some chemicals (Wang et al., 2010).

2.3.2.2 Dose-dependent MTT assay protocol

Dose-dependent MTT assay was based on percent viability of HeLa (Henrietta Lacks cervical cancer cells) (ATCC®, Maryland US) after treatment with different concentrations of mushroom extracts. HeLa cells were propagated in a T-25 flask using Lonza Eagle's Minimum Essential Medium (EMEM by VWR ON, CA) supplemented with 10 v/v Fetal bovine serum (FBS). At 80% confluency, the growth media (EMEM+ 10% FBS) was removed from the flask. Cells were then washed with 3 mL of Dulbecco's Phosphate Buffer Saline (DPBS) (Lonza, Maryland) followed by trypsinization. Removal of adherent cell culture from T-25 flask surface

was carried out using 1 mL of Trypsin EDTA (0.25%) for 3 min. Cells were then quantified using a haemocytometer and further diluted to achieve the concentration of 15,000 cells/mL.

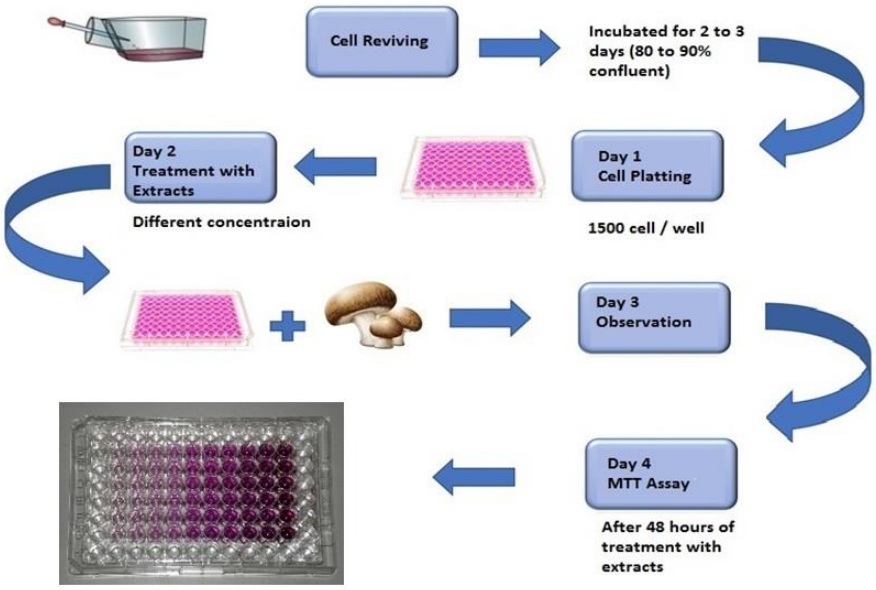

Figure 2. 4 Schematic representation of dose-dependent MTT assay protocol using HeLa Cells. (Graphics credit : Hasnain Yaqoob)

The 96-well plate was used to culture cells for treatment with different doses of extracts. The plated cells (1500 cells/100 µL/well) were incubated for 24 hours at 37°C in 5% CO_2. Twenty-four hours after plating, different doses (0.1, 0.25, 0.375, 0.5, 0.75 and 1 mg/mL) of mushroom extracts were made using EMEM with FBS and the respective solvents (Table 2.5). A stock of mushroom extracts was prepared based on their solubility in a suitable solvent. For extracts soluble in water, the stock concentration was 20 mg/mL. The stock concentration of methanol soluble extracts (E1 and E2 extracts of *A. flettii* and *S. scabripes*) was made at 40 mg/mL to reduce the final volume of methanol in well. The stock solutions were then filter-sterilized using 0.2 µm filter (Sarstedt, Nümbrecht, Germany) to remove any biological contamination or insoluble materials from the extracts or solvents.

Table 2.5: Representation of the different doses of mushroom extracts used for MTT assay.

		For One Well			For 6 Wells		
Final conc. (mg/mL) (in plate)	**Stock (mg/mL) (in tube)**	**Diluted water in MEM (µL)**	**Fraction at 4 mg/mL**	**MEM (µL)**	**Diluted water in MEM (µL)**	**Fraction at 4 mg/mL**	**MEM (µL)**
1	2	0	50	50	0	300	300
0.75	1.5	12.5	37.5	50	75	225	300
0.5	1	25	25	50	150	150	300
0.375	0.75	31.2	18.75	50	187.5	112.5	300
0.25	0.5	37.5	12.5	50	225	75	300
0.1	0.2	45	5	50	270	30	300
0	0	50	0	50	300	0	300
		Total Volume of 100 µL			Total Volume of 600 µL		

Figure 2. 5: Plate pattern (96-well) followed to screen different doses of extracts from selected mushroom samples, for their potential to exhibit anti-proliferative activity based on the MTT assay.

	1	2	3	4	5	6	7	8	9
A	water	water	water	water	water	water	water	water	water
B	water	1 mg/mL	0.75 mg/mL	0.50 mg/mL	0.375 mg/mL	0.25 mg/mL	0.1 mg/mL	Control	water
C	water	1 mg/mL	0.75 mg/mL	0.50 mg/mL	0.375 mg/mL	0.25 mg/mL	0.1 mg/mL	Control	water
D	water	1 mg/mL	0.75 mg/mL	0.50 mg/mL	0.375 mg/mL	0.25 mg/mL	0.1 mg/mL	Control	water
E	water	1 mg/mL	0.75 mg/mL	0.50 mg/mL	0.375 mg/mL	0.25 mg/mL	0.1 mg/mL	Control	water
F	water	1 mg/mL	0.75 mg/mL	0.50 mg/mL	0.375 mg/mL	0.25 mg/mL	0.1 mg/mL	Control	water
G	water	water	water	water	water	water	water	water	water

Cells were treated with 100 µL of the mushroom extract, making final concentration as planned. After treatment with different doses of mushroom extract and controls (water and methanol), cells were further incubated for 48 hours. On day 4, 50 µL of diluted MTT solution (1 mg/mL) was added to cells. Cells were further incubated for 3 hours allowing the live cells to take up the MTT dye and converting it to formazan crystals by mitochondrial reductase. To calculate cell viability, the supernatant was removed from each well and 150 µL of DMSO was

added to each well to dissolve the formazan crystals. The appearance of dark purple color was indication of cell high cell viability. The absorbance was read at 570 nm using Synergy 2 multi-plate reader.

2.3.2.3 Time-Dependent MTT assay for assessment of growth-inhibitory activity of mushroom extracts

Time-dependent MTT assay was also based on percent viability of HeLa (Henrietta Lacks cervical cancer cells) (ATCC®, Maryland US) cells after treatment with selected concentrations of mushroom extracts. HeLa cells were propagated the same way as in the case of dose-dependent MTT assay. Cells (750 cells/100 µL/well) were incubated for 24 hours at 37°C in 5% CO_2 allowing them to adhere to the surface of wells.

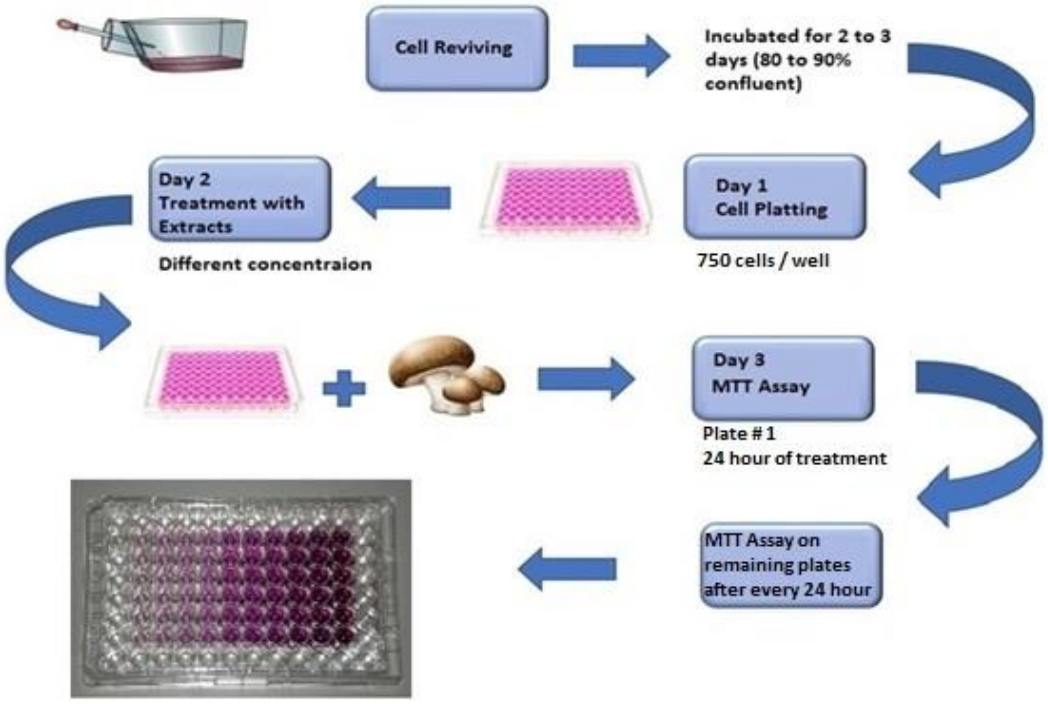

Figure 2. 6: Schematic representation of time-dependent MTT assay protocol using HeLa Cells. (Graphics credit : Hasnain Yaqoob)

Twenty-four hours after plating, mushroom extracts were added to the cells at selected concentrations for several days (24, 48, 72, 96, 120, 144, 168 hours). There was a total of eight

96-well plates used which include one for zero time period, where cells had no treatment. MTT assay was performed on a daily basis as described above for the dose-dependent MTT assay. The data obtained from Synergy 2 was further processed using Microsoft excel and Kaleidagraph.

2.3.2 Assessing TNF- α production by RAW 264.7 cells as an indication of immuno-stimulation

The stimulation of TNF-α production was conducted using mouse macrophage RAW 264.7 cells purchased from the American Type Culture Collection (ATCC® Maryland). Macrophages were cultured in 96-well plates using DMEM without 10% FBS and incubated at 37°C with 5% CO_2 for 18 hours. The number of cells plated per well were 100,000 cells/200 µL. After 18 hours of incubation, the medium (200 µL DMEM without FBS) was removed from the wells and cells were washed with 200 µL Dulbecco's Phosphate Buffer Saline (DPBS) (Lonza, Walkersville, Maryland). Plated RAW 264.7 cells were supplemented with 100 µL DMEM without FBS each well.

The mushroom extracts at 1 mg/mL (in DMEM without FBS) final concentration (in the well) were introduced (100 µL). Lipopolysaccharide (500 ng/mL) was used as a positive control while DMEM (Gibco's) without FBS and the solvents (used in the reconstitution of extract e.g., methanol, and water) were used as negative controls. The supernatant was collected (150 µL) after a 6-hour exposure period. The collected supernatant was stored at -80°C prior to performing ELISA for quantification of TNF-α production.

2.3.2.1 Enzyme-Linked Immunosorbent Assay (ELISA)

The collected supernatant was subjected to enzyme-linked immunosorbent assay (ELISA) for the quantification of TNF-α production by RAW 264.7 cells. The concentration of TNF-α in supernatant was determined using TNF-α ELISA kit as per manufacturer's protocol (BD OptEIA™ Mouse TNF (Mono/Mono) ELISA Set BD Biosciences, USA). The resulting

ELISA plate was coated with a capture antibody, diluted (1:250) in a coating buffer (pH 6.5) for 16 hours at 4°C. Next, the plate was washed using washing buffer (diluted 20 times) and blocked with assay diluent (200 µL) for 1 hour. Afterwards, plate was treated with a solution (100 µL of 1:9 collected supernatants in assay diluent) for 2 hours at room temperature. TNF-α standard dilutions (1000, 500, 250, 125, 62.5, 31.25 and 15.625 pg/mL) were prepared and added in duplicate to the last two columns of plate (100 µL/well).

The plate was washed (5 times) again then instilled with biotinylated mouse TNF-α monoclonal antibodies as well as the enzyme reagent for 1 hour. Subsequently, the substrate solution (100 µL) was added to the wells after washing the plate a total of 7 times and incubated in dark for 30 min before 50 µL of stop solution was added. The concentration of macrophage TNF-α was calculated through optical density readings using Synergy 2 multi-plate reader at 450 and 570 nm. The data obtained was further processed using Graph prism 6 and the standard curve of mouse recombinant TNF-α was used for quantification of TNF-α in samples.

2.3.3 Assessing inhibition of TNF-α production in RAW 264.7 cells as an indication of anti-inflammatory activity

The cell plating work for anti-inflammatory assay was performed in a similar manner as for the immuno-stimulatory assay but with slight modification in the cell treatment part: cells were treated with LPS first and later with mushroom extracts. As in immuno-stimulatory assay, the number of cells plated per well were 100,000 cells/200 µL.

Macrophage cells (RAW 264.7) were plated in 96 well plates using Dulbecco's Modified Eagle Medium by life technologies (DMEM without 10% FBS) and incubated at 37°C with 5% CO_2 for 18 hours. After 18 hours of incubation, the medium (200 µL DMEM without FBS) was removed from the wells and cells were washed with 200 µL Dulbecco's Phosphate Buffer Saline

(DPBS) (Lonza, Walkersville, Maryland). Each well of plated RAW 264.7 cell was supplemented with 100 µL LPS (250 ng/mL) in DMEM without FBS. The mushroom extracts at 1 mg/mL (in DMEM without FBS) final concentration (in the well) were introduced (100 µL). Polymyxin-B (200 units/well) was used as a positive control, while DMEM (Gibco's) without FBS and the solvents (used in the reconstitution of extract e.g. methanol, and water) were used as negative controls. The supernatant was collected (around 150 µL) from wells after a 6-hour incubation period. The supernatant was stored at -80°C prior to performing ELISA for the quantification of TNF-α production.

2.4 Results and Discussion

2.4.1 Genetic Identification of mushroom specimens 143 and 151.

Figure 2.7 represents the bands for the PCR products from mushroom # 143 and 151. The DNA bands of both samples are visible in between 500 and 600 base pair range of the ladder, which confirms the DNA of mushroom samples being pure. The DNA sequences obtained for the forward primer ITS3 and the reverse primer NLB4 were compared with sequences available in the National Center for Biotechnology Information (NCBI) internet database, GenBank, using the Basic Local Alignment Search Tool (BLAST) program. Specimens are considered tentatively identified (subject to confirmation of correct GenBank information) if BLAST results showed a greater than or equal to 97% similarity.

Table 2.6: The identification of mushroom species using BLAST searches, along with the percent of matching bases between the unknown sample and the closest match.

Identity	Collected By	Best GenBank Match (% similarity/ % coverage)
Fomitopsis officinalis (115)	Dr. Roy Rea	EU854436.1 (99% / 79%)
Sarcodon scabripes (124)	Dr. Chow Lee	JN135191.1 (99% / 78%)
Tricholoma vaccinum (125)	Dr. Chow Lee	FJ845444.1 (99% / 99%)
Cerrena unicolor (127)	Dr. Chow Lee	KC176316.1 (99% / 100%)
Albatrellus flettii (128)	Dr. Chow Lee	JF899544.1 (97% / 99%)
Albatrellus flettii (151)	Dr. Chow Lee	JF899544.1 (97% / 99%)
Trametes versicolor (143)	Drs. Keith Egger & Hugues Massicotte	KC581354.1 (93% / 97%)

Figure 2. 7: Agarose gel (1%) consisting of PCR product of mushroom # 151 and 1 kb DNA ladder. ITS3 and NLB4 were used as the primers for amplification.

The percent match of identification for *A. flettii* mushroom specimens (151) was 97 % and for mushroom 143 (*T. versicolor*), it was only 93 % . A match of less than 97% could be an indication that the isolate does not belong to any entry in the database and could possibly be an undiscovered species, as seen in the case of mushroom 143 (*T. versicolor*) the percent similarity was only 93%. It could also be an indication that the sequence obtained needs further sequencing and editing to eliminate ambiguous or incorrect base calls.

2.4.2 Chemical extraction of Canadian wild mushrooms

The collected mushrooms were extracted using Dionex ASE 350 speed extractor for extract E1, E2, and E3 only. The extraction for E4 was done manually using a hotplate. The summary of extraction results is provided in Table 2.7.

The higher yields were obtained for Extract E4 of all mushroom samples. The lower yields were obtained mostly for E1 extracts. The highest yield (78.77%) among all extracts was exhibited by E4 of *T. versicolor*, while the lowest yield (0.79%) was exhibited by E1 of *C. unicolor.* The physical properties of these extracts were also quite distinctive from each other. All four extracts from *S. scabripes* and *T. vaccinum* were coarse in nature. E2 and E3 extracts of mushroom sample 115, 127 and 143 were fluffy in nature. The extract E1 and E2 of *S. scabripes* and *A. flettii* were only soluble in methanol, indicative of the hydrophobic nature of bioactive compounds within them.

Table 2.7: Summary of the fungal extracts obtained through successive extraction process using Dionex ASE-350 speed extractor.

Extraction sample (grams)	Extract type	Solvent System used for extraction	Extract weight (gm)	Extract Yield (%)	Physical appearance	Solvent used for reconstitution
***Fomitopsis officinalis* (115)**						
5.690	E1	80% Ethanol	0.329	5.50	Coarse powder	Water
	E2	50% Methanol	0.226	3.97	Fluffy (Cotton like)	Water
	E3	Water	0.205	3.60	Fluffy (Cotton like)	Water
	E4	5% NaOH	4.219	74.15	Chunky powder	Water
***Sarcodon scabripes* (124)**						
8.820	E1	80% Ethanol	0.120	1.36	Coarse powder	Methanol
	E2	50% Methanol	0.514	5.82	Coarse powder	Methanol
	E3	Water	0.866	9.82	Coarse powder	Water
	E4	5% NaOH	3.474	39.39	Coarse powder	Water
***Tricholoma vaccinum* (125)**						
14.420	E1	80% Ethanol	0.246	1.71	Coarse powder	Water
	E2	50% Methanol	0.448	3.11	Coarse powder	Water
	E3	Water	0.927	6.43	Coarse powder	Water
	E4	5% NaOH	2.813	19.51	Coarse powder	Water
***Cerrena unicolor* (127)**						
10.552	E1	80% Ethanol	0.083	0.79	Coarse powder	Water
	E2	50% Methanol	0.127	1.21	Fluffy (Cotton like)	Water
	E3	Water	0.194	1.84	Fluffy (Cotton like)	Water
	E4	5% NaoH	4.137	39.21	Chunky powder	Water
***Albatrellus flettii* (128)**						
9.820	E1	80% Ethanol	0.236	2.40	Sticky paste	Methanol
	E2	50% Methanol	0.392	3.99	Sticky paste	Methanol
	E3	Water	0.489	4.98	Coarse powder	Water
	E4	5% NaOH	1.758	17.90	Coarse powder	Water
***Trametes versicolor* (143)**						
7.506	E1	80% Ethanol	0.061	0.82	Coarse Powder	Water
	E2	50% Methanol	0.117	1.56	Fluffy (Cotton like)	Water
	E3	Water	0.158	2.11	Fluffy (Cotton like)	Water
	E4	5% NaOH	5.913	78.77	Chunky powder	Water

2.4.3 Dose- and time-dependent anti-proliferative assessment of mushroom extracts using HeLa cells

2.4.3.1 *Fomitopsis officinalis*

The results obtained from dose-dependent MTT assay performed using four extracts (E1-E4) from *F. officinalis* are shown in Figure 2.8. The dose-dependent MTT results show that extract E1 and E2 reduced the cell viability by more than 90% at as low as 0.375 mg/mL. On the other hand, E3 only showed 40% reduction when treated at 0.75 and 1 mg/mL. No anti-proliferative activity was observed using E4 extract. Hence, HeLa cells were subjected to time-dependent MTT assay using selected doses of E1 and E2 extract.

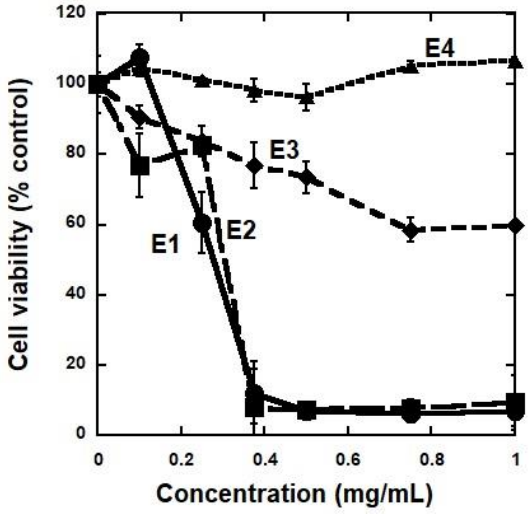

Figure 2. 8: Dose-dependent assessment of anti-proliferative activity of the four crude extracts isolated from *F. officinalis*. Several concentrations of crude extracts E1 (80% ethanol), E2 (50% methanol), E3 (water) and E4 (5% NaOH) were added to HeLa for 48 hours followed by assessment of cell viability using MTT assay. The result shown is a representative from two biological replicates (n=2). Error bars are standard deviation.

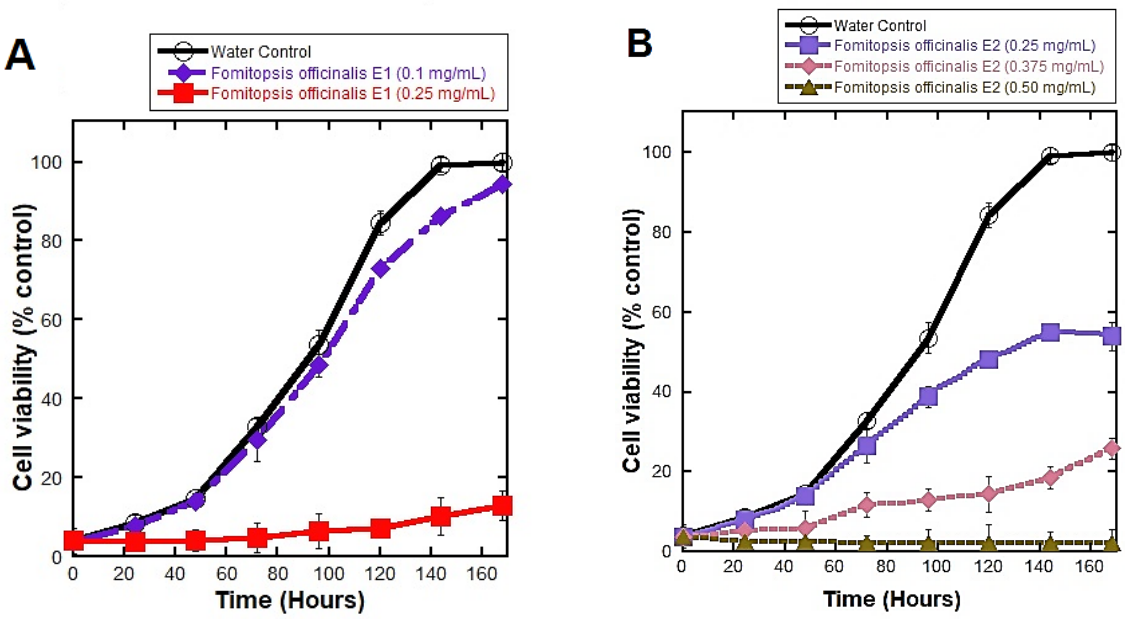

Figure 2. 9: Time-dependent assessment of anti-proliferative activity of E1 and E2 extracts from *F. officinalis*. (A) The time-dependent MTT assay of E1 extract at 0.1 and 0.25 mg/mL. (B) Time-dependent assay of E2 at 0.25, 0.375 and 0.5 mg/mL. Error bars are standard deviation.

Results in Fig 2.9 (left panel) show that cells treated with extract E1 at 0.25 mg/mL resulted in cell viability of less than 20% by Day 3 and this persisted until at least Day 7. At 0.1 mg/mL, E1 had little effect on cell viability. At 0.5 mg/mL, E2 extract significantly reduced cell viability to 10% by Day 1 and the effect persisted up to Day 7 (Figure 2.9, right panel). The cell viability after treatment with 0.25 mg/mL of E2 was less than 30 percent after 7 days of incubation. The time-dependent anti-proliferative effect exhibited by extract E2 at 0.25 mg/mL was moderate resulting in cell viability of more than 50% after 7 days of treatment.

2.4.3.2 *Trametes versicolor*

Figure 2.10 shows the result from the dose-dependent MTT assay of *T. versicolor*. The results show that Extract E1 (at 1 mg/mL) suppressed the cell viability down to only 50%. Extract E2 showed weak growth-inhibitory activity by suppressing cell viability only by 30%. Since the very weak anti-proliferative activity exhibited by other extracts (E3 and E4) was considered negligible (less than 20%), time-dependent MTT assay was not performed on any of the extracts from *T. versicolor.*

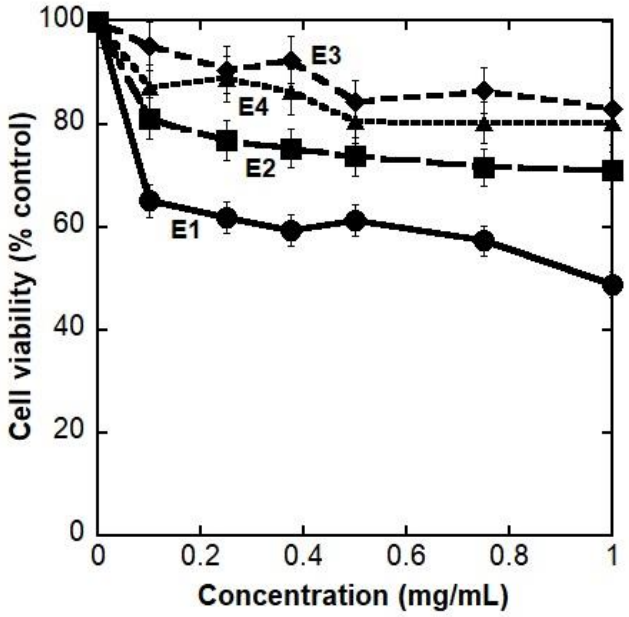

Figure 2. 10: Dose-dependent assessment of anti-proliferative activity of the four crude extracts isolated from *T. versicolor*. The result shown is a representative from two different biological replicates (n=2). Error bars are standard deviation.

2.4.3.3 *Cerrena unicolor*

Dose-dependent MTT assay on extracts from *C. unicolor* revealed that only extract E4 had moderate anti-proliferative activity, reducing cell viability down to 54%. In contrast, the anti-proliferative activity shown by Extract E2 and E3 was close to negligible even at high doses

i.e., 1 mg/mL. The extract E1 showed very weak anti-proliferative activity by reducing cell viability by only 18% as compared to the control.

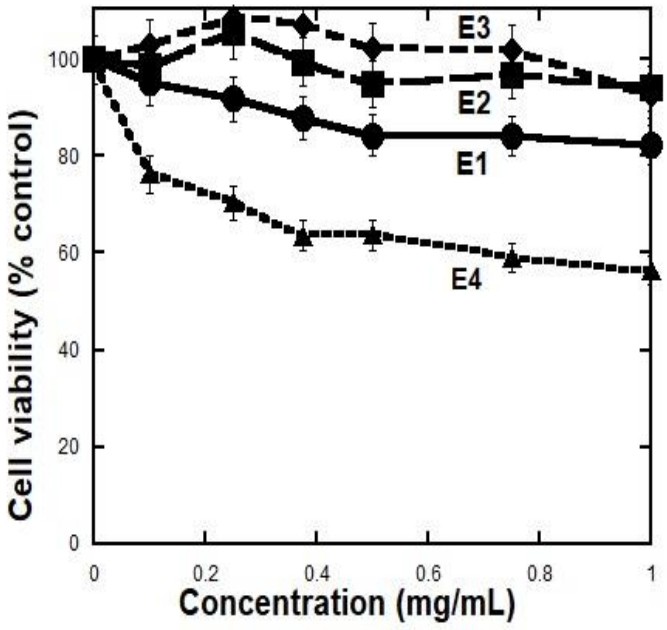

Figure 2. 11: Dose-dependent assessment of anti-proliferative activity of the four crude extracts isolated from *C. unicolor*. The result shown is a representative of two biological replicates (n=2). Error bars are standard deviation.

2.4.3.4 *Tricholoma vaccinum*

The dose-dependent MTT assay on *T. vaccinum* showed that only extract E4 exhibited moderate anti-proliferative activity by reducing cell viability down to 54%. The effects by extracts E1, E2 and E3 were very similar. All three extracts exhibited weak anti-proliferative activity by reducing cell viability only by 30% as compared to the control.

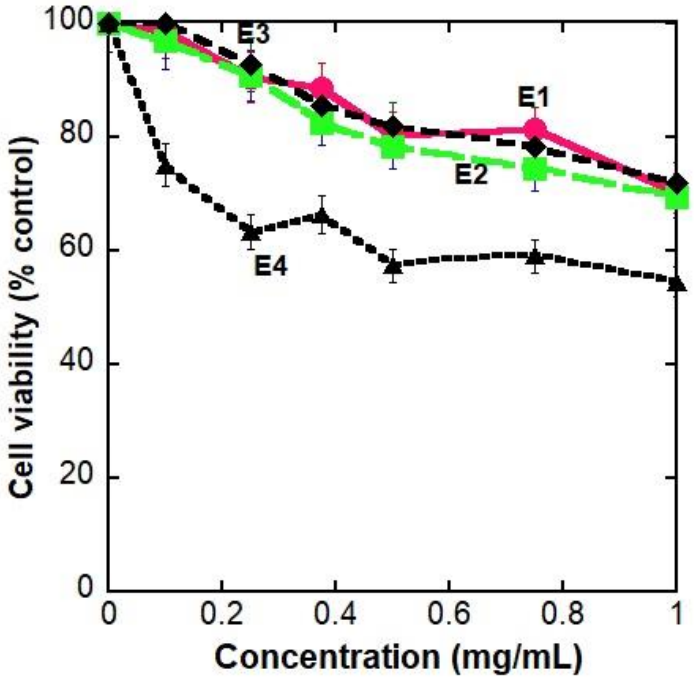

Figure 2. 12: Dose-dependent assessment of anti-proliferative activity of the four crude extracts isolated from *T. vaccinum*. The result shown is a representative from two biological replicates (n=2). Error bars are standard deviation.

2.4.3.5 *Sarcodon scabripes*

Results obtained from the dose-dependent MTT assay using four extracts (E1-E4) of *S. scabripes* are shown in Figure 2.13. The dose-dependent MTT results show that extract E1, E2 and E3 reduced the cell viability by more than 75% at 1.0 mg/mL. Extracts E1 and E2 were the most potent because the cell viability was inhibited to less than 20% when cells were treated at 0.375 mg/mL.

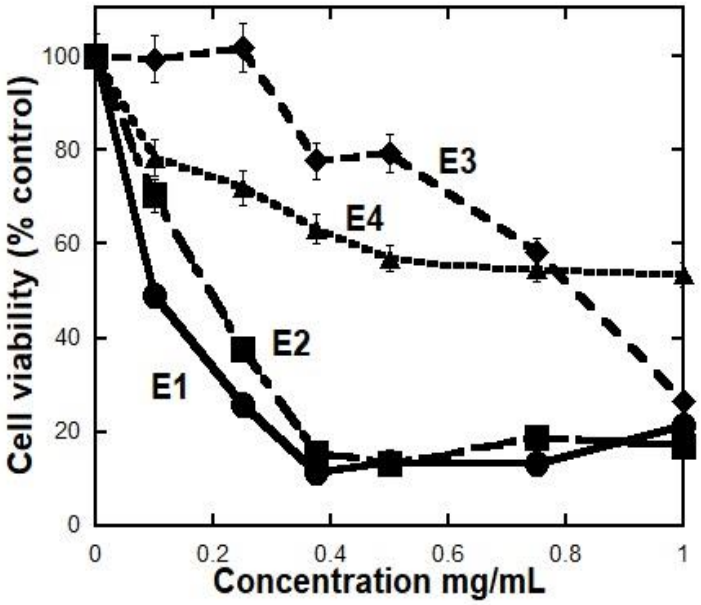

Figure 2. 13: Dose-dependent assessment of anti-proliferative activity of the four crude extracts isolated from *S. scabripes*. The result shown is a representative from two biological replicates (n=2). Error bars are standard deviation.

The anti-proliferative activity exhibited by extract E4 was moderate, reducing HeLa cell viability only by 50% at 1 mg/mL. Given the high potency of E1 and E2 in inhibiting growth, I next tested their effect on time-dependent MTT assay. Figure 2.14 (A) shows that, at 0.1 mg/mL, extracts E1 significantly reduced cell viability by Day 1 and this activity persisted up to Day 3. Figure 2.14 (B) shows that, at 0.375 mg/mL, both extracts E1 and E2 significantly reduced cell viability by Day 1 and this persisted up to Day 7. The time-dependent MTT assay results revealed that extract E1 was slightly more potent than E2 at 0.1 mg/mL after Day 3. However, the anti-proliferative activity was the same for both extracts at 0.375 mg/mL.

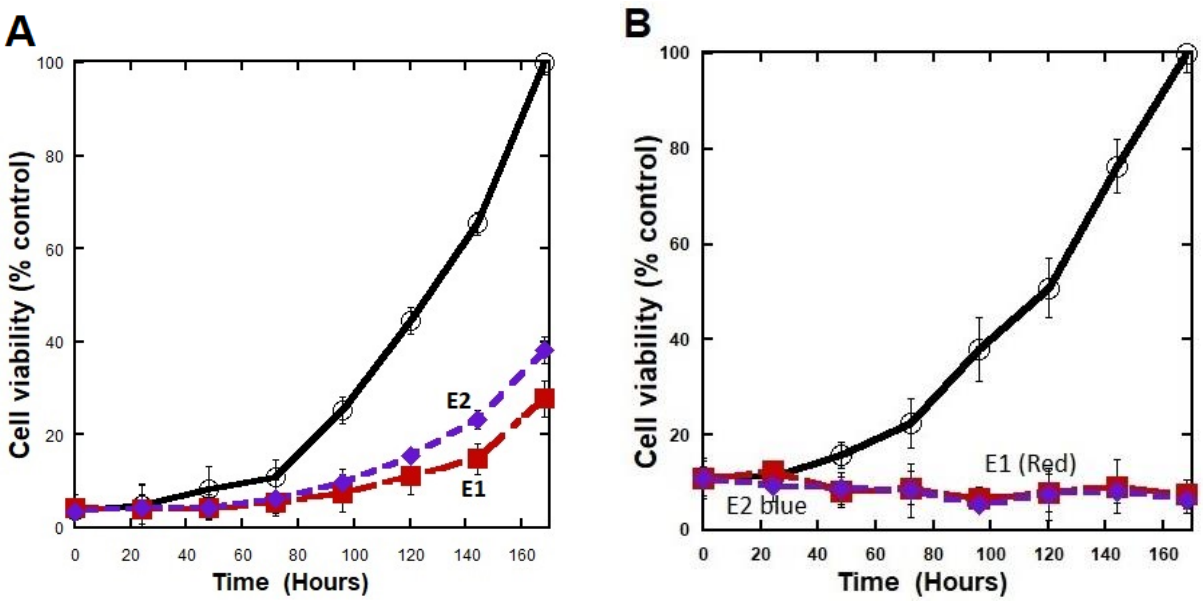

Figure 2. 14: Time-dependent assessment of anti-proliferative activity of E1 and E2 extracts isolated from *S. scabripes*. (A) At 0.1 mg/mL, E1 and E2 were added to HeLa cells for the duration shown on the graph. (B) At 0.375 mg/mL, E1 and E2 were added to HeLa cells. Results shown are representative from two biological replicates (n=2). Error bars are standard deviation.

2.4.3.6 *Albatrellus flettii*

The dose-dependent MTT assay results based on four crude extracts from *A. flettii* show that extracts E1 and E2 had strong anti-proliferative activity (Figure 2.15). It is interesting to note that there was a slight increase in cell viability as the concentrations of E1 and E2 increases. This had also been observed in Dr. Lee's lab with a small number of crude extracts from other mushrooms. The most possible explanation is that compound(s) present in some crude extracts reacted with MTT to give rise to colored reagents and hence detected as false negative in the MTT assay. Extracts E3 and E4 showed very weak anti-proliferative activity even at high doses 1 mg/mL (Figure 2.15). The cell viability after treatment with 1 mg/mL of both E3 and E4 extracts was more than 70%. Based on the results from dose-dependent MTT assay, HeLa cells were subjected to time-dependent MTT assay with selected concentrations of E1 and E2 extracts. The time-dependent MTT assay results shown in figure 2.16 revealed no difference between the

activity of extract E1 and E2 at two different concentrations: 0.1 and 0.5 mg/mL. These results confirmed the presence of highly potent growth-inhibitory compounds in E1 and E2 of *A. flettii*.

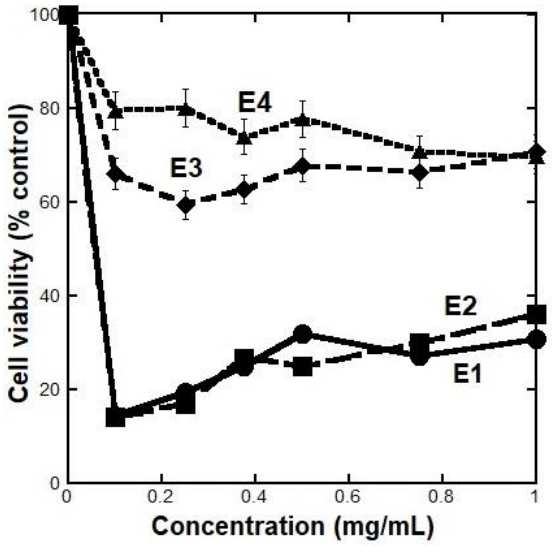

Figure 2. 15: Dose-dependent assessment of anti-proliferative activity of the four crude extracts isolated from *A. flettii*. The result shown is a representative from two biological replicates (n=2). Error bars are standard deviation.

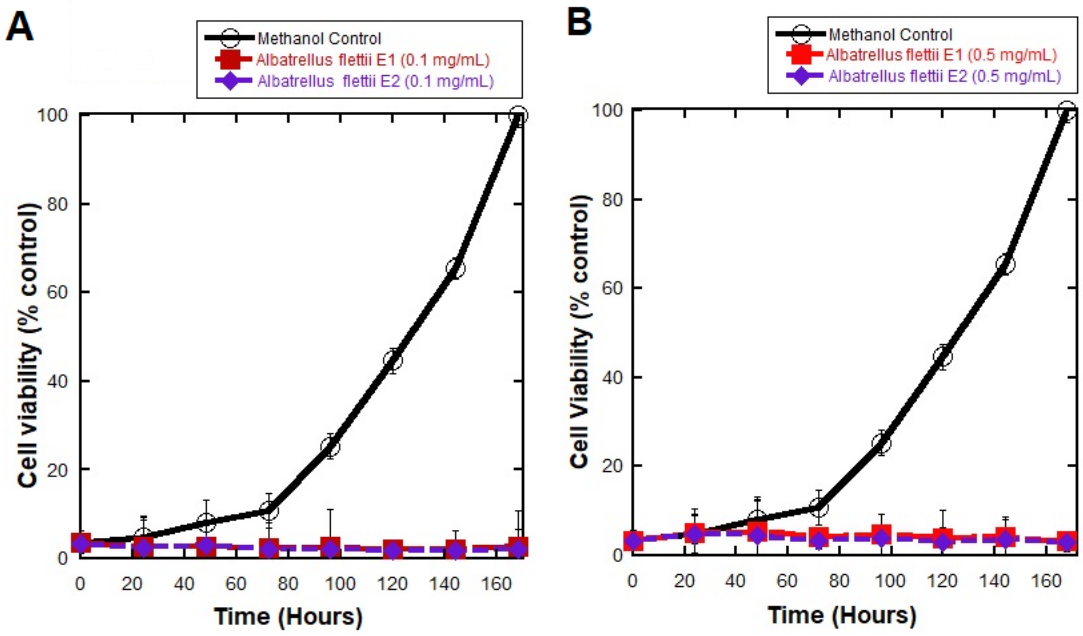

Figure 2. 16: Time-dependent assessment of anti-proliferative activity of E1 and E2 extracts isolated from *A. flettii*. (E1 and E2 extracts at 0.1 mg/mL (A) or 0.5 mg/mL (B) were added to HeLa cells for the duration shown on the graph. Results shown are representative from two biological replicates (n=2). Error bars are standard deviation.

2.4.4 Stimulation of TNF-alpha production in RAW 264.7 cells after treatment with mushroom extracts

All twenty-four extracts from six fungal specimens were assessed for immuno-stimulatory potential by measuring TNF-α production in RAW 264.7 cells. The standard dose of each extract used to determine immuno-stimulatory potential was 1 mg/mL. LPS was used as the positive control and DMEM (without 10% FBS), water and methanol were used as negative controls.

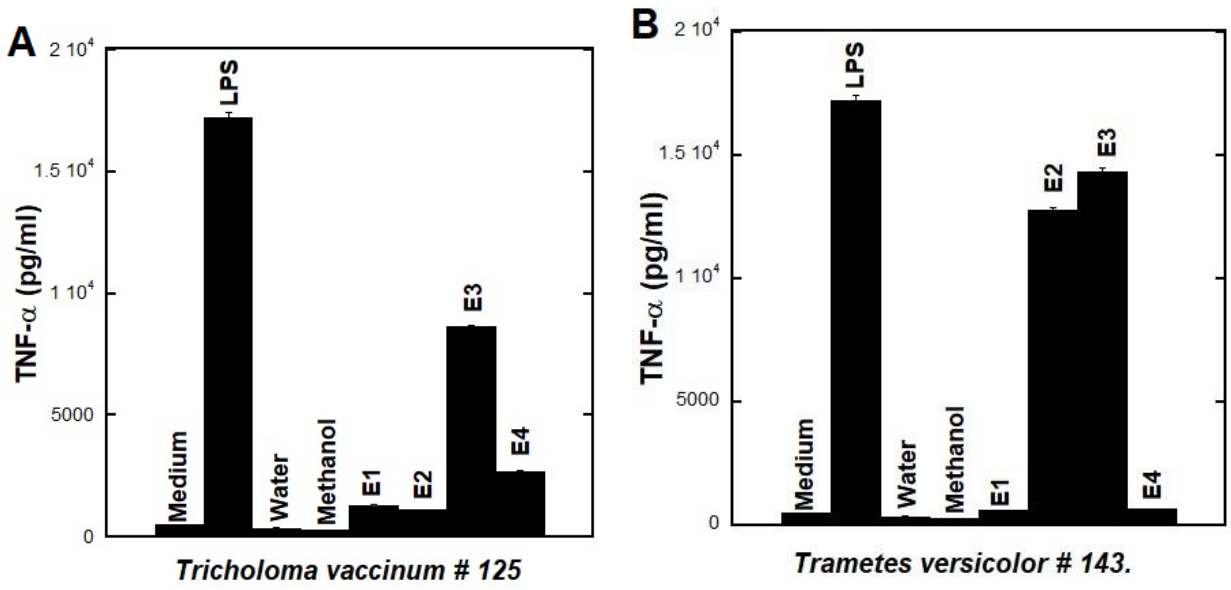

Figure 2. 17: Assessing the immuno-stimulatory activity of the four crude extracts isolated from *T. vaccinum* (A) and *T. versicolor* (B). RAW 264.7 macrophage cells in 96-well plates were treated with reagents as described in the Materials and Methods. LPS (500 ng/mL) was used as a positive control. Media, water and methanol were used as negative controls. Cell were treated with 1 mg/mL of crude extracts from *T. vaccinum* (A) or *T. versicolor* (B). Results shown are representative of two biological replicates (n=2). Error bars are standard deviation.

Figure 2.17 (A) shows that only extract E3 from *T. vaccinum* had moderate immuno-stimulatory activity by inducing TNF-α levels to 8646.8 pg/mL. The immuno-stimulatory potential shown by E1 and E2 extracts was insignificant compared to the controls. Extracts E1, E2 and E4 induced TNF-α levels to 1306.0, 1116.1, 2702.1 pg/mL respectively. TNF-α

production by the positive control LPS was 17197 pg/mL. The negative controls Media, water and methanol induced TNF-α level to only 503.91, 359.98 and 261.20 pg/mL respectively.

Extracts E2 and E3 from *T. versicolor* showed strong immuno-stimulatory activity by inducing TNF-α production to 12773 and 14344 pg/mL respectively. On the other hand, extracts E1 and E4 showed no immuno-stimulatory activity as the TNF-α production was close to the ones treated with media only. Media, water and methanol serving as a negative control induced TNF-α to 503.91, 359.98 and 261.20 pg/mL respectively, suggesting that negative controls had no effect on RAW 264.7 cells.

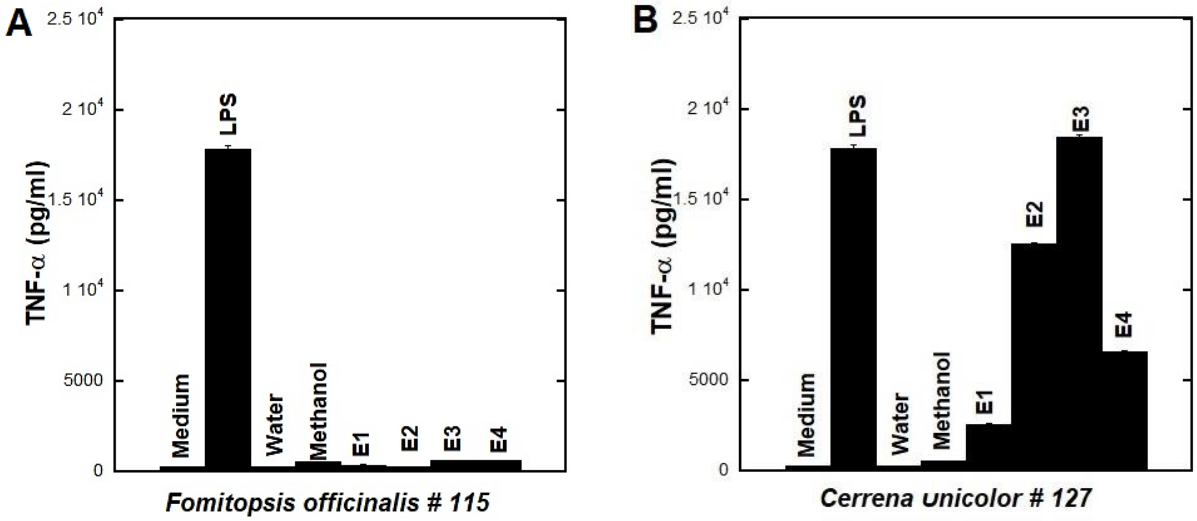

Figure 2. 18: Assessing immuno-stimulatory activity of the four crude extracts isolated from *F. officinalis* (A) and *C. unicolor* (B). RAW 264.7 cells were treated with 1 mg/mL of crude extracts from *F. officinalis* (A) or *C. unicolor* (B). Results shown are representative of two biological replicates (n=2). Error bars are standard deviation.

As seen the Figure 2.18(A), no immuno-stimulatory activity was seen with all four extracts from *F. officinalis* at a concentration of 1 mg/mL. The TNF-α production by E1, E2, E3 and E4 extracts of *F. officinalis* was 382.58, 279.54, 636.09 and 636.80 pg/mL respectively, which was very close to the negative controls. TNF-α production by positive control (LPS) was

17840 pg/mL. Media, water and methanol serving as a negative control induced TNF-α to 251.61, 304.16 and 570.00 respectively.

As shown in Figure 2.18(B), all four extracts from *C. unicolor* exhibited immuno-stimulatory activity. Extract E1 induced TNF-α level to approximately 2584.2 pg/mL making it the weakest of all the four extracts. On other hand, extract E2 exhibited a strong immuno-stimulatory activity by inducing TNF-α levels over 12580 pg/mL. Strongest immuno-stimulatory activity was exhibited by extract E3 where the TNF-α level was induced to a level slightly higher than the positive control: 18499 pg/mL. Extract E4 had moderate effect on RAW 264.7 cells with TNF-α level induced to 6615.0 pg/mL.

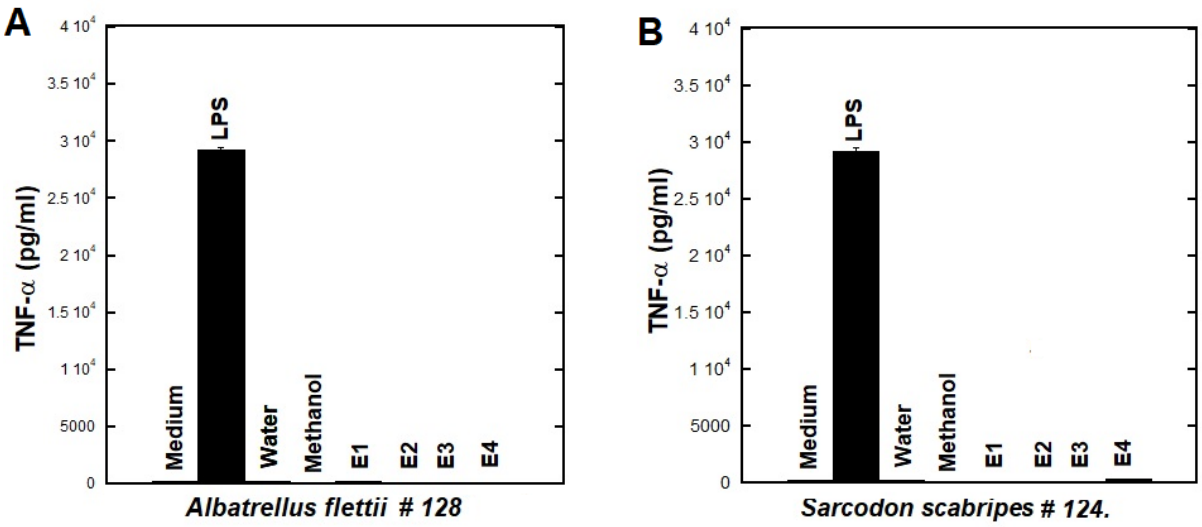

Figure 2. 19: Assessing the immuno-stimulatory activity of the four crude extracts isolated from *A. flettii* (A) and *S. scabripes* (B). RAW 264.7 cells were treated with 1 mg/mL of crude extracts from *A. flettii* (A) or *S. scabripes* (B). Results shown are representative of two biological replicates (n=2). Error bars are standard deviation.

No immuno-stimulatory activity was shown by any of the four extracts from *A. flettii* and *S. scabripes* (Figure 2.19). TNF-α production by E1, E2, E3 and E4 extracts of *A. flettii* was 178.15, 62.687, 85.967, and 144.97 pg/mL respectively, which were very close to negative controls. Extracts E1, E2, E3 and E4 from *S. scabripes* induced the TNF-α production to 47.565,

124.50, 125.02 and 357.99 pg/mL respectively, which were also close to negative controls. The dark color of the E1 and E2 extracts of both mushrooms hindered the microscopic observation of RAW 264.7 cells morphology.

2.4.5 Inhibition of TNF-alpha production in LPS-induced RAW 264.7 cells

Selective extracts that were not active for immuno-stimulation was further assessed for their ability to inhibit LPS-induced TNF-α production in RAW 264.7 cells. This is an *in-vitro* measure of anti-inflammation (Smith et al., 2017). The standard dose of each extract used to determine such anti-inflammatory potential was 1 mg/mL. Polymyxin-B (200 units/well) was used as the positive control and DMEM (without 10% FBS) and water served as negative controls.

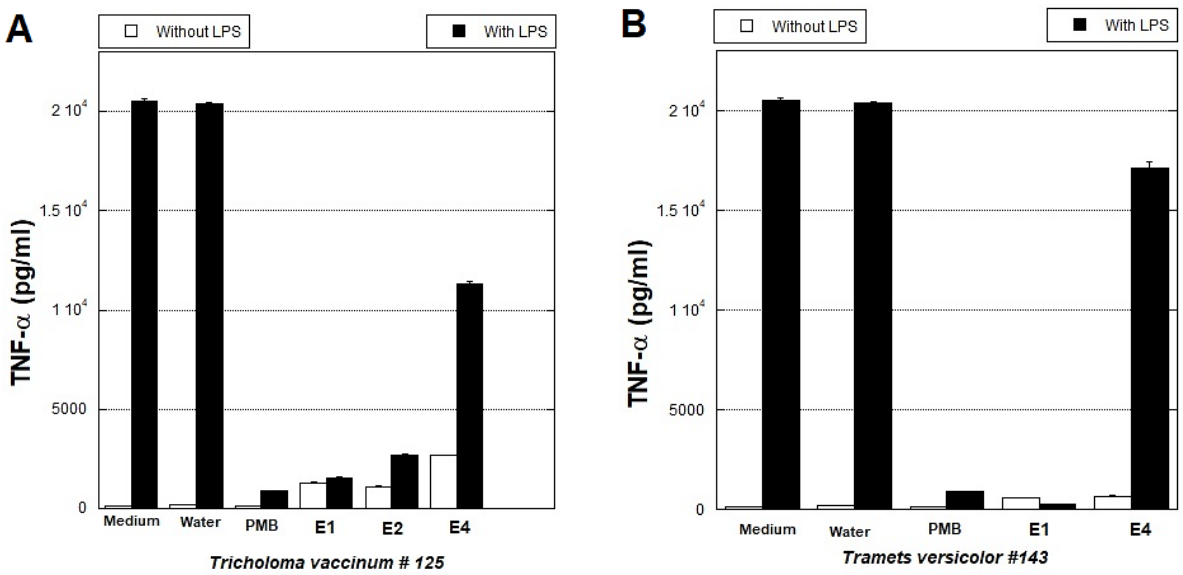

Figure 2. 20: Assessing the anti-inflammatory activity of crude extracts isolated from *T. vaccinum* (A) and *T. versicolor* (B). RAW 264.7 cells in 96-well plates were treated with test reagents in the presence or absence of LPS as described in Materials and Methods. Polymyxin-B (200 units/well) was used as a positive control. Media and water were used as negative controls. One mg/mL of crude extracts from *T. vaccinum* (A) and *T. versicolor* (B) were used. Results shown are representative of two biological replicates (n=2). Error bars are standard deviation.

Extract E1, E2 and E4 from *T. vaccinum* were assessed for their anti-inflammatory potential and the results are shown in Figure 2.20A. E1 extract has strong anti-inflammatory activity as compared to E2 and E4. The treatment with extract E1 resulted in very low level of TNF-α 1562.2 pg/mL**.** This is evident of anti-inflammatory compound(s) present in E1 extract. Extract E2 also exhibited strong anti-inflammatory activity by inhibiting the TNF-α production down to 2669.5 pg/mL. Extract E4 showed weak but significant anti-inflammatory activity by inhibiting TNF-α level to 11337 pg/mL. TNF-α levels, after 6 hours of treatment with Media and water, were 20485 and 20367 pg/mL respectively. Polymyxin-B (200 units/well), after six hours of treatment, inhibited the production of TNF-α levels down to 873 pg/mL.

Only two extracts from *T. versicolor* were assessed for anti-inflammatory activity. Extract E1 exhibited the potent anti-inflammatory activity by inhibiting the TNF-α level production down to 236.74 pg/mL which is even lower than positive control (PMB) at 873 pg/mL. This indicates the presence of potent anti-inflammatory compound(s) in this extract. Extract E4 exhibited very weak anti-inflammatory activity, which was close to negligible. TNF-α production after 6 hours treatment with 1 mg/mL concentration of E4 was 17122 pg/mL.

All four extracts of *F. officinalis* (E1, E2, E3 and E4) were assessed for their ability to inhibit the TNF-α production in RAW 264.7 cells (Figure 2.21 A). Extracts E1 and E2 showed the strongest anti-inflammatory activity by reducing the TNF-α production down to 89.446 and 183.62 pg/mL respectively, which were even lower than positive control Polymyxin-B i.e. 873.00 pg/mL. No significant anti-inflammatory activity was seen in Extract E3 and E4.

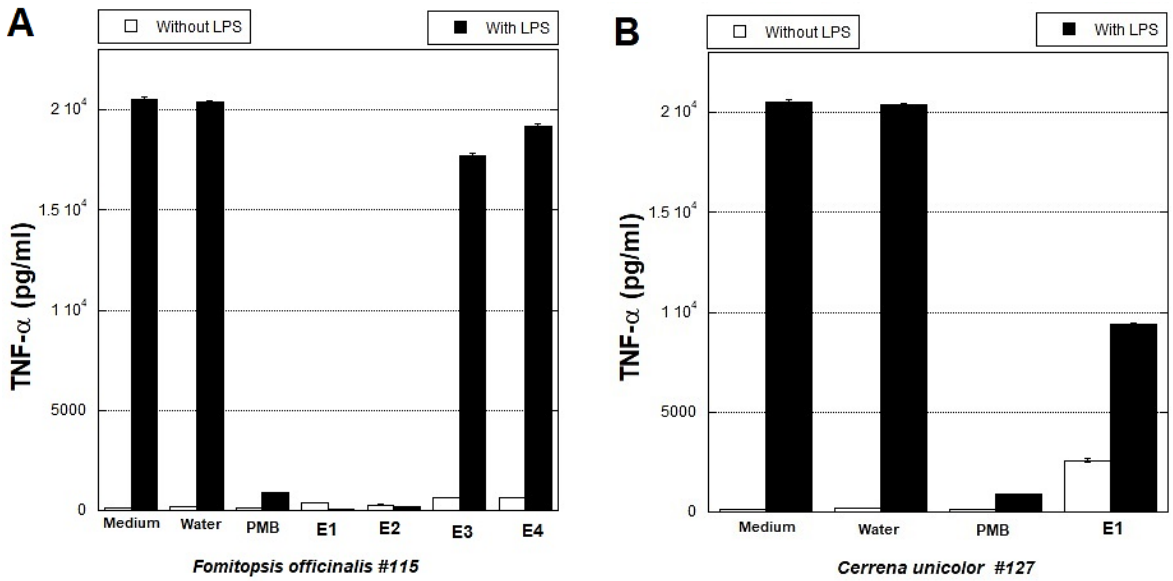

Figure 2. 21: Assessing the anti-inflammatory activity of crude extracts isolated from *F. officinalis* (A) and *C. unicolor* (B). Cells were treated with test reagents in the presence or absence of LPS. Polymyxin-B (200 units/well) was used as a positive control. Media, water and methanol were used as negative controls. One mg/mL of crude extracts from *F. officinalis* (A) and *C. unicolor* (B) were used. Results shown are representative of two biological replicates (n=2). Error bars are standard deviation.

The only extract from *C. unicolor* tested for its anti-inflammatory potential was E1. TNF-α levels after 6 hours of treatment were close to 9407.3 pg/mL, indicating a weak but significant anti-inflammatory activity. This could either be due to the presence of anti-inflammatory compound in very low quantity or very weak in nature. TNF-α levels after 6 hours of treatment with Media and water were 20485 and 20367 pg/mL respectively.

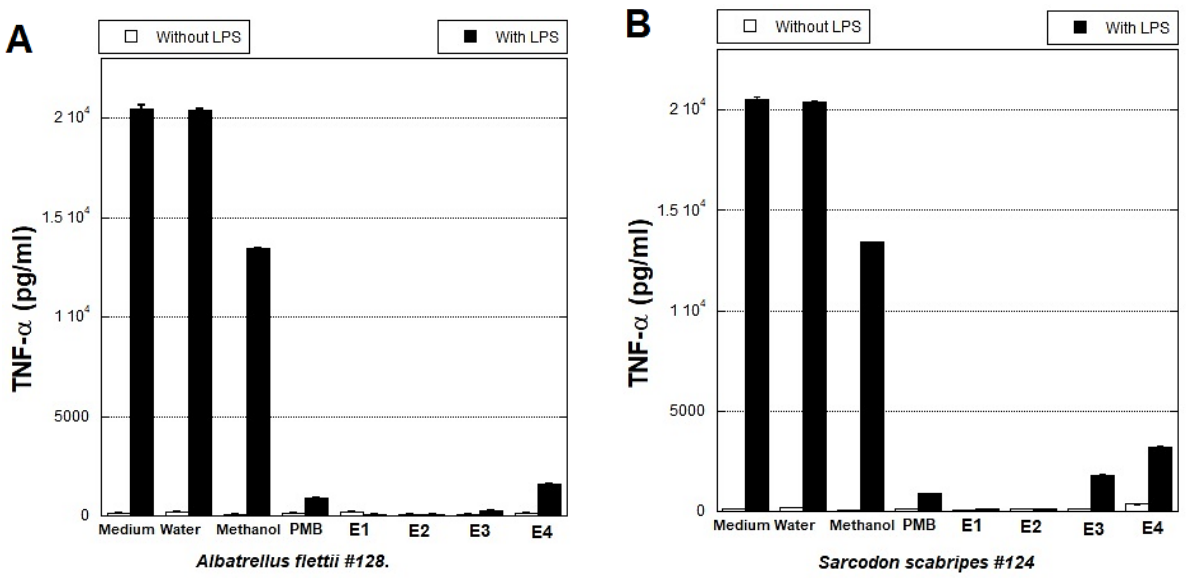

Figure 2. 22: Assessing the anti-inflammatory activity of crude extracts isolated from *A. flettii* (A) and *S. scabripes* (B) RAW 264.7 cells were treated with test reagents in the presence or absence of LPS. Polymyxin-B (200 units/well) was used as a positive control. Media, water and methanol were used as negative controls. One mg/mL of crude extracts from *A. flettii* (A) and *S. scabripes* (B) were used. Results shown are representative of two biological replicates (n=2). Error bars are standard deviation.

Furthermore, very interesting anti-inflammatory results were observed upon treatment with *A. flettii* and *S. scabripes.* A point to note is that the dark colored E1 and E2 extracts from both mushrooms made it hard to observe the post-treatment morphology of RAW 264.7 cells. All four extracts from both mushrooms showed strong anti-inflammatory activity, suggesting the presence of potent small and large anti-inflammatory molecules in these extracts. TNF-α levels, after 6 hours of treatment with media (EMEM), water and methanol were 20485, 20367 and 13442 pg/mL respectively. Polymyxin-B (200 units/well) after six hours of treatment inhibited the production of TNF-α levels down to 873 pg/mL.

TNF-α levels, after 6 hours of treatment with E1, E2, E3 and E4 extracts of *A. flettii,* were 77, 72, 281 and 1583 pg/mL respectively. Similar trend was observed after treatment with *S. scabripes,* The TNF-α levels, after 6 hours of treatment with E1, E2, E3 and E4 extracts of *S.*

scabripes, were 126.74, 106.18, 1772.5 and 3187.0 pg/mL respectively. These results suggested that both *A. flettii* and *S. scabripes* contain strong anti-inflammatory compounds.

2.5 Discussion

In the study described in this chapter, I chemically extracted 4 crude extracts representing small molecules (Extracts 1 and 2) and large molecules (Extracts 3 and 4), from 6 mushroom species. These crude extracts were screened for growth-inhibitory, immuno-stimulatory and anti-inflammatory activities. I provide below, for each fungus, a critical assessment of the current knowledge as it pertains to the 3 biological activities.

Fomitopsis officinalis, also known as quinine conk due to its extremely bitter taste, causes a brown heart rot on conifers (Ginns, 2017). In the current study, none of the extracts from *F. officinalis* showed immuno-stimulatory activity, while only Extract E1 and E2 showed potent anti-inflammatory activity. *Fomitopsis officinalis* polysaccharides (FOPS), at doses of 20, 40, and 80 mg/kg, have the ability to potentiate the humoral immune response (Wuliya & Li, 2003). Likewise, Hu et al. (2013) observed the effects of *F. officinalis* polysaccharides (FOPS), a hot water extract of *F. officinalis,* on S180 tumor bearing mice model and found remarkable growth-inhibitory and immuno-stimulatory effects. These *in vivo* findings do not seem to correlate with our *in vitro* study. It is possible that immune cells other than macrophage were responsive to *F. officinalis* as demonstrated in the two animal studies. Another possible reason could be due to the low content of FOPS present in E3 and E4 extracts in BC's *F. officinalis* sample # 115.

In this study, the E1 and E2 extracts of *F. officinalis* showed potent growth-inhibitory and anti-inflammatory activity, which is supported by previously reported studies. The investigation of chemical constituents of *F. officinalis* led to isolation of eight small molecules including (1)

4,6,8(14),22(23)-tetraen-3-one-ergos-tane, (2) ergosta-7,22,dien-3β-ol, (3) 3-ketodehydrosulfurenic acid, (4) dehydroeburiconic acid, (5) 4,6,8(14),22(23)-tetraen-3-one-ergostane, (6) fomefficinic acid A, (7) fomefficinic acid B and (8) fomefficinic acid C. Due to their higher abundance, compounds 3, 4, 6 and 8 were further screened for their growth-inhibitory potential against human cancer cells. Compound 3, 6 and 8 were found to be active against MCF-7 cell line, while only two compounds (6 and 8) were able to inhibit proliferation in SMMC-7721 cells (Chi & Bao 2014).

Han et al. (2016) isolated eight lanostane triterpenes named officimalonic acids A to H from the methanolic extracts of *F. officinalis*. Screening of these compounds for their ability to inhibit nitric oxide production in LPS-induced RAW 264.7 cells revealed that only officimalonic acids D, E, G, H, and fomitopsin A were potent for their anti-inflammatory activity. Lanostane triterpenes from *F. officinalis* have also been evaluated for their trypanocidal activity against *Trypanosoma congolense.* Five out of eight purified lanostane terpenoids exhibited trypanocidal activity with IC_{50} less than 27.1μM (Naranmandakh et al., 2018).

In the current study, only extract E4 (5% NaOH) of *C. unicolor* (also known as the mossy maze polypore) exhibited the moderate growth-inhibitory activity in HeLa cells. Extract E2, E3 and E4 showed immuno-stimulatory activity in RAW 264.7 macrophages. All these findings are in good agreement with the existing literature. A copper-containing enzyme laccase (molecular weight 57 kDa) responsible to degrade lignin has been isolated from *C. unicolor* (Kim et al., 2002). Crude endopolysaccharide, extracellular laccase and a subfraction of low molecular-weight secondary metabolites, isolated from *C. unicolor*, have shown antioxidant and antibacterial properties (Jaszek et al., 2013). These three compounds have cytotoxic activity against mouse melanoma B16-F10 cells. The crude endopolysaccharide also has the ability to

modulate the immune system (Statkiewicz et al., 2017). Two of these compounds (extracellular laccase 250 μg/ml and low molecular-weight secondary metabolites 10 μg/ml) have been studied further for their growth-inhibitory potential in cervical carcinoma. Laccase have also been found to have antiviral activity against different strains of viruses, specific to life cycle stages (Mizerska-Dudka et al., 2015). Chemical modifications to introduce both hydrophobic and hydrophilic characteristics in laccase resulted in more pH and thermostability as well as activity (Kucharzyk et al., 2012).

In this study, E2 and E3 extracts of *T. versicolor* resulted in strong stimulation of TNF-α in RAW 264.7 macrophages, thus supporting the previous findings. *Trametes versicolor,* also known as *Coriolus versicolor* because of its morphological characteristics, is also referred to as Turkey tail. *T. versicolor* is a well-known mushroom for its two proteoglycans Krestin (PSK) and PSP (Kidd, 2002). Krestin (PSK) is a complex of proteoglycan molecules with molecular weights ranging from 94,000 to 100,000 kDa and is active if administered orally; it has the ability to activate T-cells based immune response and the overexpression of cytokines IL-1, IL-2, IL-6 and IL-8 TNF-α, and IFN-γ (Enshasy & Hatti-Kaul, 2014). Studies based on toxicological profile assessment have indicated that Krestin (PSK) has low toxicity, with no indications of abnormalities during clinical trials (Standish et al., 2008). Japan is the pioneer to study clinical trials based on *T. versicolor.* Based on the vast clinical research data available, Krestin (PSK) has been successfully used as an adjuvant for chemotherapy for cancer treatments, particularly in gastrointestinal types of cancer (Kobayashi et al., 1995). Studies based on the *in vitro* data, clinical and animal models have endorsed the idea that these two proteoglycans can be used as adjuvants in cancer therapy or may serve as a comprehensive cancer treatment (Fisher & Yang, 2002).

In our study, extracts E1 and E2 of *A. flettii* showed strong growth-inhibitory and anti-inflammatory activities. There has been no report on the bioactive compounds from *A. flettii* responsible for these activities. *A. flettii* is found in British Columbia, mainly in Haida Gwaii and Hazelton/Smithers area. The mushroom has a characteristic blue color which is mainly due to the presence of albatrellin and its 16-hydroxy and 16-oxo derivatives. In addition to these pigments, *A. flettii* also contains two colorless cytotoxic compounds, grifolin and neogrifolin (Koch & Steglich 2007). Liu et al. (2010) studied the anti-bacterial profile (against *B. cereus and E. faecalis*) of the bioactive compounds isolated from *A. flettii* and documented the presence of a third antibacterial compound (confluentin) along with grifolin and neogrifolin.

The current study has also revealed the novel growth-inhibitory and anti-inflammatory activities of *S. scabripes*. All four extracts of *S. scabripes* possess anti-inflammatory activity while growth-inhibitory activity was only exhibited by extracts E1 and E2. Although many small molecules have been isolated from other *Sarcodon* species, there has been no study on bioactivities from *S. scabripes*. No study has been reported on anti-inflammatory activity of E1 and E2 extracts of *T. vaccinum* which makes it a potential candidate for exploration of novel anti-inflammatory compound(s). Due to the limited sample of *T. vaccinum* and no genetic identification of *S. scabripes* (at that time), it was deemed logical to first proceed with further studies on *A. flettii*, as described in Chapter 3.

2.6 Conclusion

The primary screening highlighted very interesting results in regard to the therapeutic potentials of extracts from the six Canadian wild mushrooms studied here. These mushrooms could be developed into a future drug with potential therapeutic benefits. The main challenge is

the purification and structural elucidation of the bioactive compounds from a selected mushroom. Chapter 3 of this thesis will describe in detail the purification, characterization and structural elucidation of the anti-proliferative small molecules from E1 extract of *A. flettii*. The rationale for selecting *A. flettii* for further studies is because no prior studies have been reported on its anti-cancer activity. The summary of the primary screening of the six Canadian wild mushrooms used in the current study (growth-inhibitory, immuno-stimulatory and anti-inflammatory potential) are presented in Table 2.8 and 2.9.

Table 2.8: Summary of bio-activity of Canadian wild mushrooms

Mushroom specimen	Extract	Immuno-stimulatory activity[1] (% stimulation of TNF-α w.r.t control) at 1 mg/mL	Anti-inflammatory activity[2] (% inhibition of TNF-α w.r.t control) at 1 mg/mL	Anti-proliferative activity (% viability at 1 mg/mL)
Fomitopsis officinalis (115)	E1 (80% ethanol)	2.10	99.5	6.74
	E2 (50% methanol)	1.56	99.10	9.31
	E3 (water)	3.50	6.0	59.80
	E4 (5% NaoH)	3.50	11.0	106.5
Sarcodon scabripes (124)	E1 (80% ethanol)	0.16	99.38	21.33
	E2 (50% methanol)	0.42	99.48	16.85
	E3 (water)	0.43	91.35	26.65
	E4 (5% NaoH)	1.22	84.44	53.61
Tricholoma vaccinum (125)	E1 (80% ethanol)	50.28	92	48.85
	E2 (50% methanol)	7.50	87	71.11
	E3 (water)	6.49	-	83.13
	E4 (5% NaoH)	15.71	44.0	80.19
Cerrena unicolor (127)	E1 (80% ethanol)	14.48	54.0	82.22
	E2 (50% methanol)	70.50	-	94.02
	E3 (water)	103	-	92.63
	E4 (5% NaoH)	37.0	-	56.54
Albatrellus flettii (128)	E1 (80% ethanol)	0.60	99.60	30.96
	E2 (50% methanol)	0.20	99.65	36.05
	E3 (water)	0.29	98.0	70.80
	E4 (5% NaoH)	0.49	92.27	69.60
Trametes versicolor (143)	E1 (80% ethanol)	2.90	98.8	70.19
	E2 (50% methanol)	74.27	-	69.33
	E3 (water)	83.41	-	72.07
	E4 (5% NaoH)	3.10	16.41	54.58

[1]Percent stimulation of TNF-α relative to LPS.
[2]Percent inhibition of LPS induced TNF-α relative to DMEM.
[3]Percent viability of HeLa cells as compared to control.

Table 2.9: Summary of bioactivity of Canadian wild mushrooms and their known activities.

Mushroom sample	**Immuno-stimulatory activity[1]**	**Anti-inflammatory activity[2]**	**Growth-inhibitory activity[3]**	**Known activity**	**Reference**
Fomitopsis officinalis (115)	+ (E1, E2, E3, E4)	+++ (E1, E2) + (E3, E4)	+++ (E1, E2) ++ (E3) + (E4)	Anti-inflammatory and growth-inhibitory	(Han et al., 2016) (Chi & Bao, 2014)
Sarcodon scabripes (124)	+ (E1, E2, E3, E4)	+++ (E1, E2, E3, E4)	+++ (E1, E2) ++ (E3, E4)	No activity	-
Tricholoma vaccinum (125)	++ (E1) + (E2, E3, E4)	+++ (E1, E2) ++ (E4)	++ (E1) + (E2, E3, E4)	No-activity	-
Cerrena unicolor (127)	+++ (E3) ++ (E2) + (E1, E4)	++ (E1)	++ (E4) + (E1, E2, E3)	Immuno-stimulatory, growth-inhibitory	Mizerska-Dudka et al., 2015
Albatrellus flettii (128)	+ (E1, E2, E3, E4)	+++ (E1, E2, E3, E4)	+++ (E1, E2) + (E3, E4)	Antibacterial Only.	Liu et al., 2010
Trametes versicolor (143)	+++ (E3) ++ (E2) + (E1, E4)	+++ (E1) + (E4)	++ (E4) +(E1, E2, E3)	Immunomodulatory and growth-inhibitory	Fisher & yang, 2002.

(+++); Greater than 80% of TnF-α stimulation[1] in RAW 264.7 cells; greater than 80% of TnF-α inhibition in RAW 264.7 cells; greater than 80% growth-inhibition in HeLa cells[3] or complete inhibition[2,3]
(++); 40-80% stimulation[1] of TnF-α stimulation[1] in RAW 264.7 cells; 40-80% of TnF-α inhibition[2]; 40-80% growth-inhibition in HeLa cells[3]
(+); 10-40% stimulation[1] of TnF-α stimulation[1] in RAW 264.7 cells or no stimulation; 10-40% of TnF-α inhibition[2] or no inhibition; 10-40% growth-inhibition in HeLa cells[3] or no inhibition.

Chapter 3: Purification, Identification and Characterization of Growth-inhibitory Compounds from *Albatrellus flettii*

This chapter focuses on the purification, characterization and structural elucidation of growth-inhibitory compounds from the E1 (80% ethanol) extract of *A. flettii*.

3.1 Introduction

3.1.1 Purification and characterization strategies

Mushrooms are popular folk medicines, owing to their nutritional and medicinal values. Recently, mushrooms have attracted considerable attention because of their demonstrated efficient antitumor and immunomodulatory activities. Modern research also endorses the idea of therapeutic effects of traditionally used species. Mushrooms are rich in a wide range of therapeutic compounds, which could be small or large molecules. The isolation and purification strategies for bio-active compounds is dependent on the nature of the compound; the liquid - liquid extraction, based on the polarity of compounds, is a first adequate step for compounds isolation. Using two immiscible liquids, liquid-liquid extraction can be carried out efficiently. Once the chemical nature of the compounds of interest is determined, it becomes easy to decide the subsequent steps of purification. Extensive studies along with advances in purification approaches have made analytical chemistry much easier in recent years. Purification techniques like size-exclusion chromatography (e.g., Sephadex-LH20), ion-exchange chromatography (e.g., DEAE), and high-pressure liquid chromatography (HPLC) are usually employed. The structure of compounds is then characterized using analytical tools such as LC-MS (Liquid chromatography-Mass Spectrometry), GC-MS (Gas chromatography-Mass Spectrometry), Fourier transform infrared spectroscopy (FTIR) and NMR (Nuclear Magnetic Resonance).

One of the best initial step approaches to separate the compounds based on the molecular masses is Sephadex™ LH-20. The compounds with the higher molecular masses elute early due

to less interaction with the resin, while the smaller molecular mass compounds elute later, due to higher interaction with the resin. After the size-exclusion chromatography, compounds can be further purified using high-resolution HPLC.

The HPLC method could be either normal phase (NP-HPLC) or reverse phase (RP-HPLC). The optimal separation of compounds is dependent on the nature of the compounds, the choice of stationary phase (column) and mobile phase (solvent system). HPLC method becomes very approachable, if the nature of the compounds of interest has been determined by Liquid-Liquid extraction. If compounds are hydrophobic in nature, the C-18 column could be a good choice to proceed. The weakly polar end capped silica column can be used if the compound has both polar and non-polar components. HILIC (hydrophilic interaction) columns could be a good starting point if compounds are highly polar or have Zwitter ions. The solvent system could either be isocratic or gradient; this also depends on sample mixture as well as interaction of the compounds with column-packing material. To get a good separation, solvent system can be manipulated to obtain good peak shape and optimal separation of peaks as observed on HPLC spectra. By doing this, the collection of compounds also become feasible. The method development can be initiated on analytical columns.

To increase the productivity, separation method can be scaled up to semi-preparative or preparative column. Combination of mass spectroscopy (MS) with HPLC provides the information about the molecular mass of the compounds of interest. Mass spectrophotometer works by ionizing the compounds and by sorting them based on their mass to charge (*m/z*) ratios. Quadrupole mass detectors use oscillating electrical fields to detect the ionized compounds. Only the ions within a selected scan range of mass to charge (*m/z*) ratio are detected through the quadrupole system.

Nuclear magnetic resonance (NMR), also known as magnetic resonance spectroscopy (MRS), is a technique that provides the detailed structural information of compounds. Combination of 1D and 2D spectrum provides in depth information on linkages and neighboring atoms. Only deprotonated solvents can be used for NMR analysis. Combination of one dimensional ^{13}C and ^{1}H spectra with two-dimensional spectra (HSQC and COSY) reveals the resonance for different functional groups and their positions in the structure.

3.1.2 *Albatrellus flettii*

In western North America*, A. flettii* (blue knight) is more common than *A. confluens*. Growing on the ground in coniferous forests (Arora 1986), it was first described by Elizabeth Eaton Morse as *Polyporus flettii* (Morse, 1941). Later, Zdeněk and Pouzar re-named it to the genus *Albatrellus* (Pouzar, 1973). Since no study has been reported on the growth-inhibitory activity of this mushroom, extract E1 (80% ethanol), which exhibited potent growth-inhibitory activity as described in Chapter 2, was selected for purification and characterization studies.

3.1.3 Compounds already reported in *Albatrellus flettii*

The fleshy polypore has a characteristic blue color which is mainly due to presence of a pigment named albatrellin and its 16-hydroxy and 16-oxo derivatives. Along with these pigments, *A. flettii* is also known to contain two colorless cytotoxic compounds, grifolin and neogrifolin (Koch & Steglich 2007). Liu et al. (2010) studied the anti-bacterial activity (against *Bacillus cereus* and *Enterococcus faecalis*) of the bio-active compounds isolated from *A. flettii* and claimed the presence of a third antibacterial compound confluentin along with grifolin and neogrifolin. To date, there has been no report on growth-inhibitory activity of *A. flettii* on mammalian cells. Grifolin and neogrifolin, in synthetic form or purified from the species *A. confluens*, had been studied in detail for their anti-proliferative biochemical pathways in

mammalian cells. In contrast, the mechanism for growth-inhibition by confluentin has not been studied

3.1.3.1 Grifolin

Grifolin was first screened in 2005 for its anti-cancer properties after more than 50 years of its discovery from *A. confluens* (Ye et al., 2005). The ability of grifolin to inhibit tumor growth in cell lines (CNE1, HeLa, MCF7, SW480, K562, Raji and B95-8) is by induction of apoptosis through the pathway involving Bcl-2 family members and cytochrome c (Ye et al., 2005). Monitoring the health of the mitochondrial membrane is one way to detect apoptosis. In general, the loss of mitochondrial membrane potential indicates cell apoptosis (Perry et al., 2011). Cytochrome c also has an intermediate role in apoptosis, in response to damage to DNA. In a study by Yang et al. (2016), the release of cytochrome c from mitochondria to cytosol was investigated in two gastric cancer cell lines after treatment with grifolin.

Grifolin downregulates the expression of mitogen activated protein kinases related genes and thus could induce apoptosis in many types of cancer cell lines (Jin et al., 2007). The cell-cycle regulator, cyclin-dependent kinase 4 inhibitor2D (CDKN2D), was significantly upregulat-ed, which suggests that grifolin might affect the cell-cycle by upregulating the expression of CDKN2D (Yang et al., 2016). Western blot analysis revealed another underlying mechanism involved in the arrest of tumor cells at G1 phase, mainly due to inhibition of cyclin D, Cyclin E and CDK 4 of the ERK1/2 or the ERK5 pathway (Ye et al., 2007).

Researchers have found that the inhibition of Akt/mTOR/S6K pathway is associated with autophagy in human melanoma cells (Zhao et al., 2016). Grifolin could also induce autophagic cell death in ovarian cancer cell lines (A2780 and SKOV3), by inhibiting the activity of Akt/mTOR/S6K pathway (Che et al., 2016). Grifolin treatment resulted in reduced

phosphorylation of Akt, FOXO transcription factor and GSK3, which contributed to suppressed proliferation of osteosarcoma (Jin et al., 2007). Grifolin also induced apoptosis in osteosarcoma cells by down-regulating the expression of the IAP (inhibitor of apoptosis protein) and induction of caspases (Jin et al., 2007).

Grifolin may serve as a promising anticancer compound because of its ability to directly target ERK1/2-Elk1-DNMT1 signaling pathway to suppress cancer cell metastasis, migration and invasion (Luo et al., 2015). Luo et al. (2016) studied the suppression of underlying mechanism responsible for adhesion and migration of highly metastatic 5-8F and MGC803 cells, using wound healing assay. It has been concluded that grifolin has the ability to cause reduction of reactive oxidative species by 40% and it also interferes with the interplay between PGC1α and Fra-1/LSF-MMP2/CD44 axes. Other important mechanism of grifolin to induce apoptotic effect on nasopharyngeal carcinoma cell CNE1 involved upregulation of DAPK1 via the p53–DAPK1 pathway (Luo et al., 2011).

3.1.3.2 Neogrifolin

Neogrifolin is an isomer of grifolin, with the same molecular formula and mass, but with a slightly different structural conformation of the aromatic ring. Like grifolin, neogrifolin has also proven ability to inhibit tyrosinase (Dembitsky & Kilimnik, 2016). Neogrifolin, isolated from *A. confluens,* induced apoptosis in the aggressive cancerous neoplasm (osteosarcoma) (Chen et al., 2015). The underlying mechanism involved was found to be based on the induction of cytochrome c release, activation of caspases and cleavage of PARP (Chen et al., 2015). Furthermore, neogrifolin affected the AKT signaling pathway through the same mechanism as grifolin. Phosphorylated AKT level, FOXO transcription factor, and glycogen synthase kinase 3 (GSK3) levels were found to be downregulated. Neogrifolin has the ability to induce apoptosis in

osteosarcoma cells by down-regulating the expression of the IAP (inhibitor of apoptosis protein) and induction of caspases (Chen et al., 2015).

3.2 Materials and methods

3.2.1 Large scale chemical extraction & confirmation of growth-inhibitory activity

Two fresh collections of *A. flettii* sporocarps were gathered on September 3, 2016 (70 grams of sample 128) and September 20, 2017 (35 grams of sample 151) from the Twin Falls trail, in Smithers B.C. The samples were morphologically and genetically identified (see Chapter 2). Subsequently, mushroom sample (128) was finely powdered using a blender, and large-scale extraction of extract E1 (80% ethanol) and E2 (50% methanol) was performed using the Dionex speed extractor ASE 350. Only the first two extractions (i.e. 80% ethanol and 50% methanol) were performed and the residue after two extractions was saved. The extracts were lyophilized using a Labconco freeze dryer and stored at -80°C.

The E1 (80% ethanol) extract was then utilized for further biological cell assays and purification. E1 (80% ethanol) extract from new batch (151) of *A. flettii* was also tested on HeLa cells for growth-inhibitory activity.

3.2.2 Liquid-liquid extraction (phase separation)

Liquid–liquid extraction or phase separation is a method to separate compounds based on their chemical nature using two different immiscible liquids. To separate the compounds based on their solubility, water (polar) and chloroform (non-polar) were used. To carry out liquid-liquid extraction, a glass test tube was used.

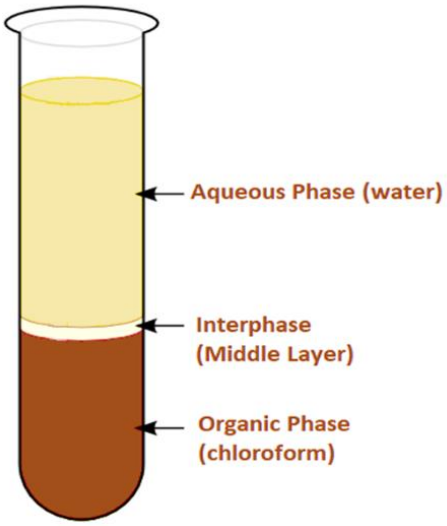

Figure 3. 1 Illustration of the Liquid-Liquid extraction technique. (Graphics credit : Hasnain Yaqoob)

First, a solution (4mL) of 20 mg/mL of E1 extract (80% ethanol) was prepared using chloroform as a primary solvent. Later, water was added in the equal volume (4mL) to make sure that separation of compounds between two layers was maximum. After adding the secondary solvent (water), the solution was vortexed for 2-3 minutes. Solution was chocolate brown in color after vortexed. The last step involved separation of the immiscible layers by centrifugation. The process of centrifugation was performed using Allegra X-15R benchtop centrifuge (Beckman coulter) at the speed of 100 RCF for 5 min.

After centrifugation, three layers were observed in the test tube (Figure 3.1). All three layers were collected into different clean test tubes using Pasteur pipettes. The lower layer (chloroform layer) was dried using a hot-plate at 65 °C. The top and middle layers were lyophilized using Labconco Freeze dryer (0.008 bar vacuum pressure and -80 ºC). Yield was calculated, based on the portions of E1 extract (80% ethanol) recovered from each layer. All three layers were further screened for their ability to exhibit growth-inhibitory activity using MTT assay.

3.2.3 Sephadex™ LH-20 (molecular sieve chromatography)

Sephadex™ LH-20 column separates the compounds based on their molecular masses. Any larger size bioactive compound should be eluted in earlier fractions. In contrast, smaller molecules should be eluted in later fractions. Based on this separation technique, small and large molecules should be easily separated.

Figure 3. 2 Photograph of the Sephadex™ LH-20 size exclusion technique using a large C26/100 column (GE Healthcare) and the mobile phase (degassed methanol)

For all molecular sieve (size exclusion) chromatographic runs, the mobile phase used was 100% methanol. The stationary phase utilized for this type of chromatographic technique was Sephadex™ LH-20 (swelled in methanol). Initial trial of compounds separation was done using a small 22 mL column (gravity drip) of Sephadex™ LH-20. This size-based elution technique was further scaled up to 100 mL column using a C16/70 glass column (GE Healthcare). The mobile phase (degassed methanol) flow rate was set at 1 mL/min using an automated pump (Pharmacia).

Fractions were collected using an automated fraction collector and the final volume of each fraction was 3 mL. This chromatographic technique was further scaled up to 400 mL (Figure 3.2), using a larger C26/100 column (GE Healthcare) and the mobile phase (degassed methanol) flow rate was set at 2 mL/min. The final volume of each fraction collected from C26/100 column was 12 mL.

3.2.3.1 Sephadex™ LH-20 resin swelling and column Packing

The Sephadex™ LH-20 resin was first swelled in methanol which was used as mobile phase. The mobile phase (methanol) was chosen based on the nature of active compounds (chloroform layer). Methanol was degassed for 4-5 hours to make sure that the mobile phase was free from any dissolved gases. The swelling ratio of Sephadex™ LH-20 resin to methanol was 1:4; for each gram of dry Sephadex™ LH-20 resin, 4 mL degassed methanol was required. The Sephadex™ LH-20 resin was swelled overnight in excess volume of degassed methanol. After the resin was completely swelled, the excessive volume of methanol was discarded from the slurry.

To pack a small gravity drip 22 mL sized column, a 25 mL serological pipette (Sarstedt, Germany) was utilized. A cotton plug was used to support the resin at the opening of the pipette. To ensure that cotton plug has allowed the right flow of mobile phase (methanol), the column was first packed with only 2 mL of the resin. Next, full column (22 mL) was packed slowly under the influence of gravity (no external pressure or flow rate was applied), carefully to avoid air entrapment. To pack, 100 mL (C16/70) and 400 mL (C26/100) (GE Healthcare) glass columns were utilized. The top and lower adapters were used to support the resin in the glass column. The column was packed and washed at a flow rate of 2 mL/min. The column was equilibrated with degassed methanol for at least two column volumes between every run.

3.2.3.2 Sample loading and fractions collection

Sample was prepared using the dried material from the lower layer (chloroform layer) of liquid-liquid extraction. Methanol (100%) was used to reconstitute the sample because of its complete solubility. The final concentration of loading sample was 80 mg/mL. The sample was filtered using a 0.2 µm filter (Sarstedt, Germany) before loading onto the column. Because of 100% solubility of sample in methanol, percent loss due to filtration was negligible. For a 22 mL column, the sample was loaded onto the column with the help of a micropipette (Thermo Fisher Scientific, USA). Final volume of the sample (organic layer) loaded was 2% (440 µL) of the packed column volume. Fraction collection was based solely on gravity. The final volume of each collected fraction was 1 mL. The sample (2% of column volume) was introduced into the large (100 mL and 400 mL) (GE Healthcare) columns with the help of a syringe and three-way switch. The mobile phase flow rate for C16/70 (100 mL) and C26/100 columns was at 1 mL/min and 2 mL/min respectively. The volume of the collected fractions was 3 mL and 12 mL respectively. Fractions were collected using an automated fraction collector. After collection, the fractions were stored in a cold room (4°C) before assessment of their growth-inhibitory activity.

3.2.3.3 Sephadex™ LH-20 Column clean-up, unpacking and storage

After each run or between two runs, columns were washed with degassed mobile phase (100% methanol) at 1.5 times of the actual flow rate, and with mobile phase volume twice the column bed volume. This was to ensure the long shelf life and reusability of resin. After the column was washed, the resin was removed from the column in a way that there is minimal contact with air. The recovered resin was then stored at 4°C in degassed 100% methanol to prevent any microbial contamination of the resin.

3.2.4 Nanodrop analysis

A nanodrop spectrophotometer (Thermo Fisher Scientific, SA) was utilized to determine the λ_{max} of bioactive fractions 20 and 21 from Sephadex LH20 (22 mL column). After calibration with water, the spectrophotometer was blanked with HPLC grade methanol. Sample peddle was rinsed with the autoclaved milliQ water before analyzing the sample. A sample of 2 µL was used to determine λ_{max} of fractions 20 and 21. The λ_{max} for both fractions (20 and 21) was read at 279 nm, which was later used in HPLC analysis of the active fractions.

3.2.5 High performance liquid chromatography (HPLC-UV) analysis

To efficiently and accurately separate bioactive compounds collected from Sephadex-LH20 fractions, high performance liquid chromatography (HPLC) technique was utilized. The separation of each components of the mixture depends on three factors:(1) chemical nature of compounds, (2) stationary phase (column) and (3) mobile phase composition. Based on the results from liquid-liquid extraction experiments, bioactive compounds were found to be hydrophobic because of their presence in chloroform layer. Therefore, it was decided that the best option was a Phenomenex Aqua® 5 µm C18 125 Å (250 x 4.6 mm) column, for better resolution of hydrophobic small compounds and biomolecules.

The wavelength (nm) used to visualize UV signal of bioactive compounds was 279 nm (based on reading from nanodrop spectrophotometer). All HPLC-MS analyses were performed using Agilent 1260 Infinity Systems (HPLC) and Agilent 6120 quadrupole mass spectrophotometer.

The reverse phase (RP-HPLC) separation method was first developed using the non-polar analytical column Phenomenex Aqua® 5 µm C18 125 Å (250 x 4.6 mm). Mobile phase was based on two solvents, water and acetonitrile. To separate small molecules efficiently and

accurately, a gradient solvent system was used, starting with 40/60% water to acetonitrile at time zero and acetonitrile being increased constantly during run. The mobile phase after 15 min was not changed, i.e., isocratic with 10:90% water to acetonitrile. HPLC grade solvents were used for the separation of bioactive compounds. The solvents were automatically degassed through the degasser part of HPLC before entering the quaternary pump. The quaternary pump controls the flow rate as well as the gradient of the solvent system. The flow rate for gradient mobile phase was set at 1.0 mL/min.

Samples were filtered using a 0.2 μm filter (Sarstedt, Germany) before injecting into the column using auto-sampler. The needle of the auto-sampler was programmed to wash every time before sample injection to prevent any cross contamination. Before injecting the sample into the column, the column was washed with solvent system for at-least 10 column volumes. The sample volume loaded onto the column was 5 μL (20 mg/mL). It took 30 min in total to better separate and elute all the peaks out of the column. The fraction collection was done based on the HPLC-UV. The wavelength value used to operate variable wavelength recorder (Agilent infinity Lab 1260) was the same as obtained from nanodrop spectrophotometer, i.e., at 279 nm. The fractions were collected using a fraction collector (Agilent infinity Lab 1260). The vials used for fraction collection were 1.5 mL size. The fractions were collected based on the retention times of the compounds in UV spectra.

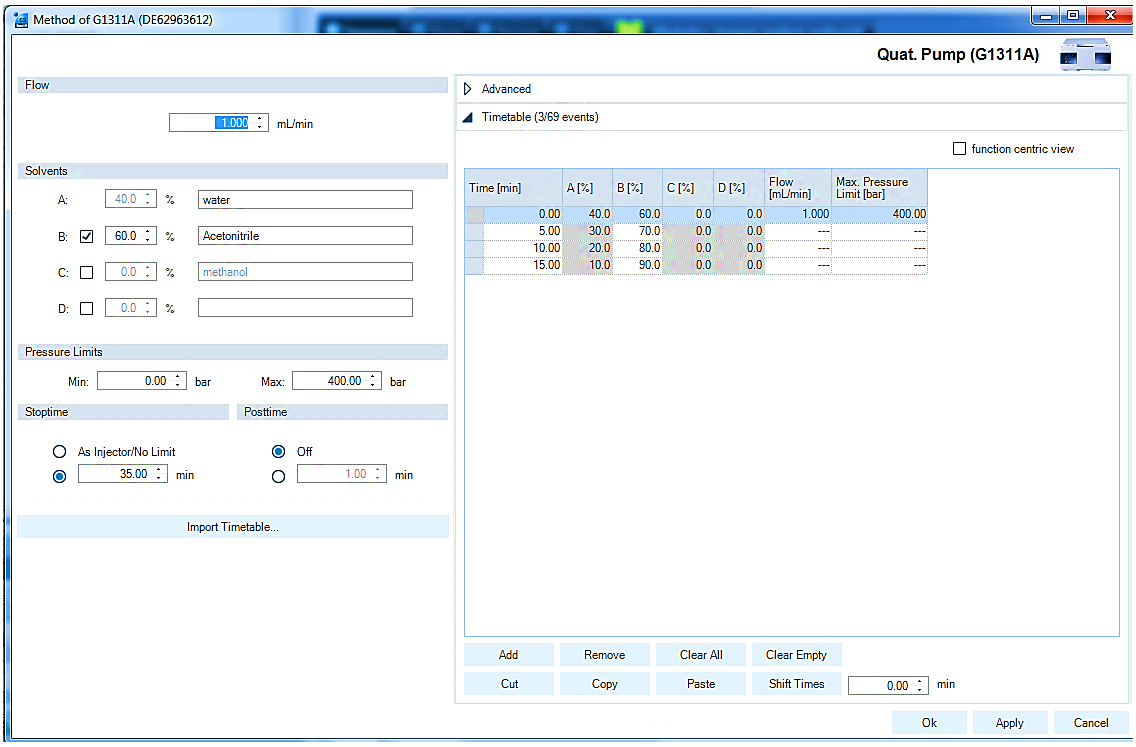

Figure 3. 3 Illustration of the gradient solvent system (Solvent A: water, solvent B: acetonitrile) adopted using the non-polar analytical column Phenomenex Aqua® 5 µm C18 125 Å (250 x 4.6 mm).

3.2.5.1 Semi-preparative HPLC

To purify enough quantity of compounds for chemical and biological analyses, HPLC purification was scaled up using a semi-preparative column. The hydrophobic semi-preparative column used for this purpose was an Agilent Zorbax Eclipse XBD-C18 5 µm (9.4 mm x 250 mm). The Solvent system used in semi-preparative HPLC was isocratic, consisting of 90% acetonitrile and 10% water. HPLC grade acetonitrile (VWR USA) and milliQ water were degassed before entering the quaternary pump and semi-preparative column. The isocratic mobile phase flow rate was set at 2 mL/min. Due to an increase in column size, the sample loading capacity was also increased, so the final volume of sample loaded on semi-preparative column was 20 µL. The sample was filtered using a 0.2 µm filter (Sarstedt, Germany) before loading it into auto-sampler and column. The compounds were collected by fraction collector

based on their retention times on UV signal. The wavelength value used was the same (279 nm) for the semi-preparative column as used previously for the analytical column. It took 25 min in total to elute all the compounds with best possible separation. Fractions were collected in 8 mL collection vials. The percent purity of the collected peaks/compounds was determined by re-running the sample on the same column under same analytical conditions.

3.2.5.2 HPLC-MS analysis

A hydrophobic analytical column (Agilent Zorbax Eclipse XBD-C18, 4.6 mm x150 mm) was used to perform MS analysis of the purified compounds. Due to poor ionization of the bioactive compounds, the active splitter was removed from the assembly line and all the output of column was injected directly into the mass spectrophotometer. By doing this, the mass spectrophotometer signal shape was improved, and the abundance of the ions was also increased. The analysis condition for HPLC-MS was based on isocratic mobile phase (75% acetonitrile and 25% water). The flow rate for isocratic mobile phase was set at 0.700 mL/min. The maximum limit for column pressure was set at 150 bar, considering the limitation for the guard column cartridge.

3.2.6 Nuclear magnetic resonance (NMR) analysis

After the successful purification, the compounds were subjected to nuclear magnetic resonance (NMR) analysis. The structural elucidation of the compounds was done using a Bruker 300 MHz NMR spectrophotometer. 1D and 2D NMR spectra were recorded on a Bruker 300 spectrometer with a 5 mm Fourier easy probe.

To reduce the chances of the errors, the magnets of the Bruker 300 MHz NMR spectrophotometer were shimmed properly before analysis of each sample. Topspin 2.1 software was used to shim the magnets and operate the Bruker 300 MHz NMR spectrophotometer for sample analysis. Approximately 30 mg of the sample was solubilized using deuterated

chloroform $CDCl_3$ (99.96 % chloroform-d and 0.3% TMS) (Sigma Aldrich) and transferred directly into 5 mm NMR tube (Kimble, USA). The final volume of the sample in NMR tube was approximately 1 mL.

One-dimensional ^{13}C spectrum was obtained using C_{13}CPD mode of Topspin 2.1 software. The number of scans performed for P5 (grifolin) was 1024, enough to get adequate information for C_{13}CPD spectra. The number of scans performed to obtain HSQC2D spectra was also 1024. Heteronuclear Single-Quantum Correlation (HSQC) is a 2D spectrum that provided information about the directly-bonded protons to the carbons at different shifts. HSQC2D spectra offers the high sensitivity and detailed information of the structure as compared to conventional ^{13}C spectrum. 1H-NMR Spectrum provided clear information for each proton, even at 64 scans. Further, COSY scan was performed on samples to get the information related to neighboring protons. COSY is a homonuclear correlation spectroscopy, which provides information about spin-spin coupling of the protons. The tip angle used for COSY was 90 degrees. After getting good resolution, the 1D spectra were further integrated to calculate the exact number of carbons and protons. The 2D spectra provided more detailed information about the relationships between carbons and protons. Together, 1D and 2D spectrum integration provided clear information about the structure of compounds. Same methodology was followed for sample P6 (neogrifolin) and P8 (confluentin) to obtain spectra for structural elucidation. The numbers of scans used for confluentin (P8) to get ^{13}C spectrum were 4096.

3.2.7 Fluorescent polarization

We used a fluorescent polarization method to study the physical interaction between an RNA-binding protein called IMP-1 and KRas RNA (Wang C, 2016). The method employs a recombinant IMP-1 protein and a fluorescently-labeled KRas RNA. The fluorescent polarization

experiments described in this thesis were performed by Mr. Victor Liu. Recombinant full-length wild-type IMP-1 protein and truncated IMP-1 protein KH34 (containing only KH3 and KH4 domains) were used. The following were mixed in a Thermo Scientific micro-Fluor 384-well microplate: 8 µL protein, 3 µL Thermo Scientific 45 nt fluorescein labeled K-Ras Probe (5'AUGGAGAAACCUGUCUCUUGGAUAUUCUCGACACAGCAGGUCAU-6-FL-3') and 4 µL binding buffer (50 mM Tris-Cl pH 7.4, 12.5 mM EDTA pH 8, 25% glycerol, 0.01% Triton-X and ddH2O). The final concentration of protein (IMP-1) and probe (KRas) was 300 nM and 10 nM respectively. To each well, 4 µL of inhibitor was added for a final concentration of 10 µM, 20 µM, 40 µM, 80 µM or 100 µM. DMSO (5%) was used as a control. The plate was incubated at 37ºC for 30 min prior to analysis on the Bio-Tek Synergy 2 plate reader.

3.2.8 Western blot analysis

3.2.8.1 Cell plating and lysate collection.

Around 0.6 million (6 x 10^5) HT-29 cells/2 mL/well were plated into 6-well culture plate. Twenty-four hours after plating, cells were treated with different concentration of purified compounds as well as the control (2% DMSO). The cells were incubated further for 48 hours with purified compounds. On day 4, the cells were observed microscopically and washed with 1 mL DPBS (Lonza) twice. Lysates were collected using ice cold lysis buffer (300 µL/well). To get lysates completely, scrapers were used to scrape off the cells from the bottom of the wells. Cell lysates were mixed in Eppendorf tube with acetone to cause complete precipitation of proteins (1:4 ratio). The cell lysates were stored at -80 ^{0}C to avoid any degradation of proteins.

Next day, cell lysates in Eppendorf tube were spun at 16000 rpm at 4^{0}C for 10 min. Supernatant was removed and the pellet was air dried. Twenty µL of autoclaved MilliQ water was used to resuspend the pellet and solubilize the proteins. The protein solution in Eppendorf

tube was centrifuged again at same conditions and supernatant containing proteins was collected in a separate Eppendorf and saved at -80^{o}C for western blot.

3.2.8.2 Protein quantification

The amount of protein in cell lysates were quantified using Pierce BCA protein assay kit (Thermo Fisher Scientific). Plate (96-well) was read using Synergy 2 spectrophotometer at 652 nm wavelength.

3.2.8.3 Gel preparation and sample introduction

Polyacrylamide gel (12%) was prepared for Western blot analysis. The upper layer (stacking layer) had a slightly different composition than the lower layer (resolving layer).

Table 3. 1 Recipe of the upper (stacking) gel mix and lower (resolving) gel mix.

Recipe	Upper Gel mix	Lower Gel mix
30% polyacrylamide	3.33 mL	0.48 mL
Gel Buffer (upper or lower)	2 mL	0.75 mL
Water	2.67 mL	1.77 mL
20% APS	4.8 µL	3 µL
TEMED	16 µL	7.5 µL

Approximately 30 µg of proteins in cell lysates were loaded onto sodium dodecyl sulfate-polyacrylamide gel (SDS-PAGE), along with 3 µL of the 5x dye containing 5% β-mercaptoethanol. MilliQ water was used to make the final volume (15 µL). Before loading onto the membrane, the proteins were boiled at 95^{o}C for 5 min. BLUelf pre-stained protein ladder (7 µL) was used as a reference. Gel was resolved at 120 volts until fully resolved. SDS (1 x) running buffer was used to run the gel.

3.2.8.4 Bands transfer to nitrocellulose

Transfer buffer (1x) containing 20% methanol was used to transfer the proteins from the gel to nitrocellulose membrane. The voltage during the transfer was kept to the lowest possible point (100 amp) to make sure the transfer was good as well as proteins are intact. A cold pack

was used in the transfer assembly to keep the temperature constant during the transfer of proteins.

3.2.8.5 Blocking, antibodies treatment and developing

Once transferred, the membrane was blocked overnight with 5% skimmed milk in 1 x TBST at 4ºC. The membrane was further incubated with primary antibody for KRas (EMD Millipore, Germany) (1:500 in 1% skimmed milk in 1 x TBST) for one hour at room temperature. The membrane was washed three times with 1 x TBST (10 min each) on a rocker. Subsequently, the membrane was incubated with secondary antibody (anti-mouse antibody) for KRas (diluted 1: 4000 in 1% skimmed milk in 1 x TBST). The membrane was developed using a West pico chemiluminescent solution (Thermo Fisher Scientific) and chemiluminescence on the blot was imaged using a Flourchem Imager. GAPDH was used as the housekeeping gene. The same technique was applied for GAPDH except the dilution ratio for primary antibody was (1:10000).

3.2.9 Flow Cytometry

Around 0.6 million (6 x 10^5) SW480 cells/2 mL/well were plated into 6-well culture plate. Twenty-four hours after plating, cells were treated with 50 µM of confluentin as well as the negative control (2% DMSO). The cells were incubated further for 48 hours after treatment with confluentin. On day 4, the cells were observed microscopically and washed with 1 mL DPBS (Lonza) twice. Cells were trypsinized and counted using a haemocytometer. After counting, cells were centrifuged in an Eppendorf tube for 5 min at 400 x g. Cells were washed twice with cold PBS and then resuspended in 1 x binding buffer at a concentration of 1x 10^6 cells /mL. One hundred µL of cells (1x 10^5 cells) were filtered into a 5 mL polystyrene round bottom culture tube with a strainer cap. For assessing apoptosis, BD Pharmingen™ PE annexin V Apoptosis Detection Kit-I (Cat # 559763) was used. BD FACSMelody™ flow cytometer was

used to perform the apoptosis assay. For cell cycle analysis, BD cycletest plus DNA reagent kit (ref # 340242) was utilized.

3.3 Results

3.3.1 Large scale chemical extraction and confirmation of growth-inhibitory activity

Large scale chemical extraction to isolate extracts E1 and E2 was performed on both collections (samples 128 & 151) of *A. flettii.* The extract yield from both collections was very similar. For sample # 128, the yield for Extract E1 (80% ethanol) was 10.212% and the yield for Extract E2 (80% ethanol) was 9.074%. The yield for E1 and E2 extracts from sample # 151 was 9.77% and 9.362% respectively. After large scale extraction, solubility of the extracts was re-confirmed.

Table 3. 2 Yield of two extracts (E1 and E2) from two different samples of *A. flettii*.

Sample no.	Mass of sample (g)	Mass of extract E1 (g)	Yield (%)	Mass of Extract E2 (g)	Yield (%)
Sample 128	70	7.1489	10.212	6.3522	9.074
Sample 151	35	3.4213	9.77	3.2767	9.362

As shown in Figure 3.4, both E1 and E2 extracts (from sample 151) exhibited dose-dependent growth-inhibitory activity against HeLa cells, consistent with earlier results (Chapter 2). It is important to point out that the increase in cell viability, due to increase in colored solution, by E2 at above 0.5 mg/mL, was most likely due to the interaction between compounds in E2 and MTT. This is because complete cell killing by E2 was microscopically observed at concentrations above 0.5 mg/mL.

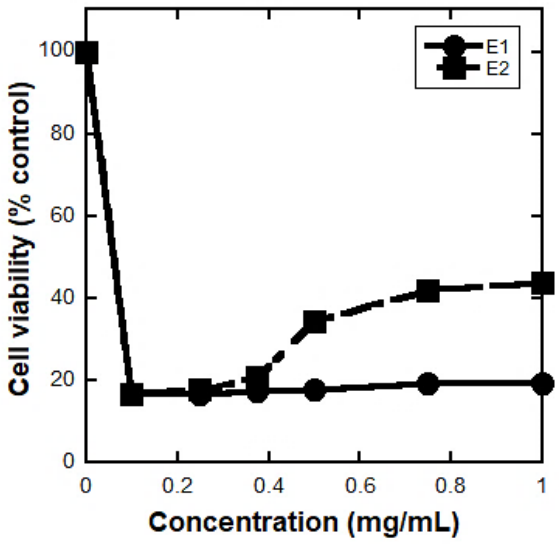

Figure 3. 4 Dose-dependent assessment of anti-proliferative activity of E1 and E2 extracts from *A. flettii* (#151).

3.3.2 Phase separation (liquid-liquid extraction)

Liquid-liquid extraction performed on Extract E1 (7.1489 grams) of *A. flettii* resulted in three distinct layers. The lower layer was chloroform and the top layer was water. The color of the lower chloroform layer was dark brown, and it had 44-50% yield (Table 3.3). Compounds present in the chloroform were most likely to be non-polar in nature. Interphase (middle-layer) was white in color and it contained the lowest yield, i.e., only 22% of the total mass (Table 3.3). Polar compounds were recovered from top water layer which was cream in color. The yield from the top water layer was 33.50% (Table 3.3). Furthermore, solubility of the compounds in both layers was determined in order to perform growth-inhibitory assay. Compounds from top-layer (water layer) were soluble in water. Compounds from interphase (middle layer) and lower layer (chloroform layer) were soluble in methanol. After determining the solubility, the layers were further screened for their growth-inhibitory potential.

Table 3. 3 Yield of three layers based on liquid-liquid extraction (Phase separation) of E1 (80% ethanol) extract of *A. flettii*.

Layer of Liquid-Liquid extraction	Color of the layer	Mass (mg) out of 20mg	Mass %	Growth inhibitory Activity	Solubility
Top Layer (Aqueous Phase)	Cream	6.70	33.50%	No	Water
Interphase (middle layer)	White	4.40	22.00%	No	Methanol
Lower Layer (Chloroform phase)	Dark Brown	8.90	44.50%	Yes	Methanol

3.3.3 Growth-inhibitory activity of the liquid-liquid extracted layers

Dose-dependent MTT assay was performed on lyophilized samples from all three layers of the liquid-liquid extraction; HeLa cells plating, and doses used were as described in Chapter 2. The final concentration of the methanol was less than 2% in each well. The range of the doses tested on HeLa cells was from 0.1 to 1 mg/mL.

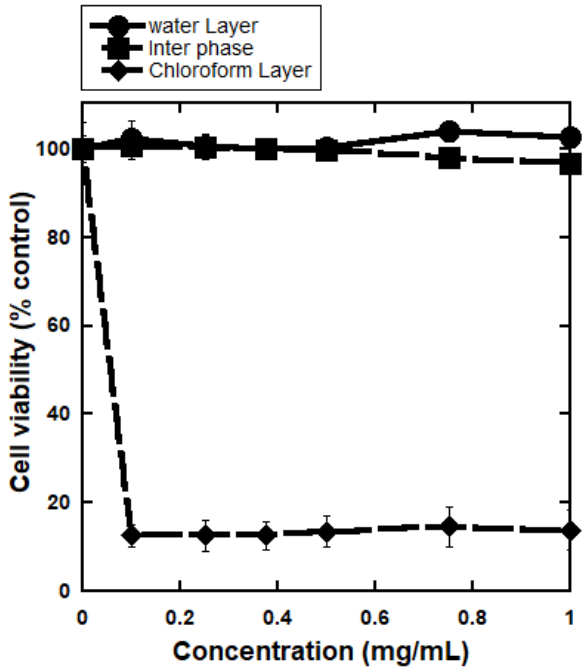

Figure 3. 5 Dose-dependent assessment of anti-proliferative activity of three layers from liquid-liquid extraction of E1 (80% ethanol) extract.

As shown in Figure 3.5, strong growth-inhibitory activity was observed from the lower chloroform layer. The cell viability was less than 20% at each dose and results were consistent

with all doses. However, no growth-inhibitory activity was observed from the middle or lower layer. Based on the MTT results, it was decided to proceed with purification of bioactive compounds from the lower chloroform layer.

3.3.4 Assessment of bio-activity of post-Sephadex™ LH-20 fractions collected from a 22 mL column

Fractions from a 22 mL Sephadex LH-20 column were collected in 1.5 mL Eppendorf tubes and the final volume of each fraction was 1 mL. Fractions 1-11 & 22-30 were colorless while fractions 12-21 were pale yellow in color, suggesting presence of most compounds in the latter fractions.

Results from the MTT assay (1500 cells/well), performed using the post-Sephadex™ LH-20 (22 mL) fractions are shown in Figure 3.6. Fractions (1 mL each) were collected by running 8.8 mg of the E1 (80% ethanol extract) chloroform layer of *A. flettii*.

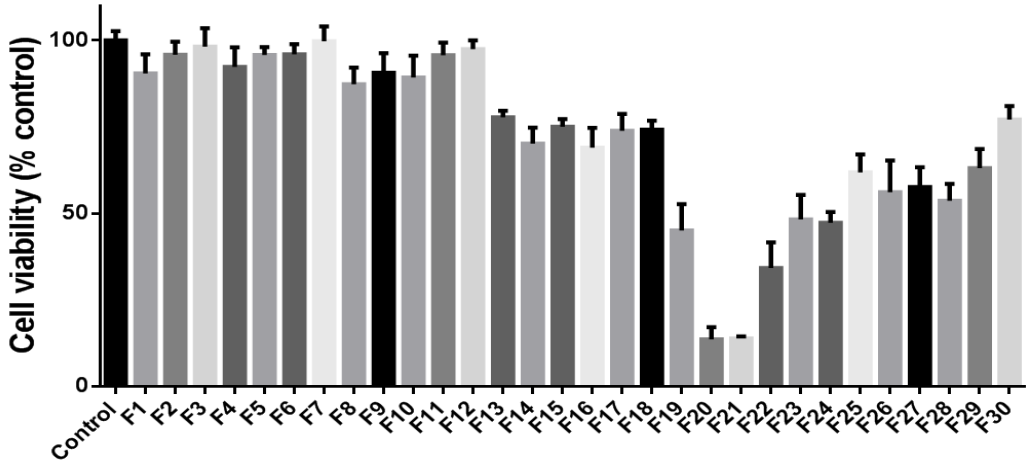

Figure 3. 6 Assessing anti-proliferative activity of fractions collected from 22-ml size Sephadex™ LH-20 column.

Results showed that fractions 20 and 21 reduced the HeLa cell viability to even less than 20% as compared to the control. Weak growth-inhibitory activity was observed for Fractions 19 and 22, suggesting the presence of bioactive compounds in these fractions as well, which could be either low in quantity or different in nature. The cell viability after treatment with these

fractions was close to 50%. MTT assay was based on HeLa cells (1500 cells/well) after 24 hours of incubation and cells were treated with 2 µL of the fraction volume + 98 µL of EMEM with 10% FBS. The final concentration of methanol in well was only 1% which was non-toxic to cells. MTT assay was performed on treated cells after 48 hours of incubation. Given that the inhibitory activity was observed in later eluting fractions, it is likely that the bioactive compounds are small.

3.3.5 Assessment of growth-inhibitory activity of post-Sephadex™ LH-20 fractions from a 100 mL column

After bioactivity was detected in specific fractions collected from the small Sephadex column (22 mL), the technique was scaled up to a 100 mL using a C16/70 (GE Healthcare, Quebec) column. MTT assay (1500 cells/well) was performed on fractions (3 mL each) obtained by running a total 40 mg of the E1 (80% ethanol extract) chloroform layer of *A. flettii*. The results of the MTT assay of the fractions are shown in Figure 3.7.

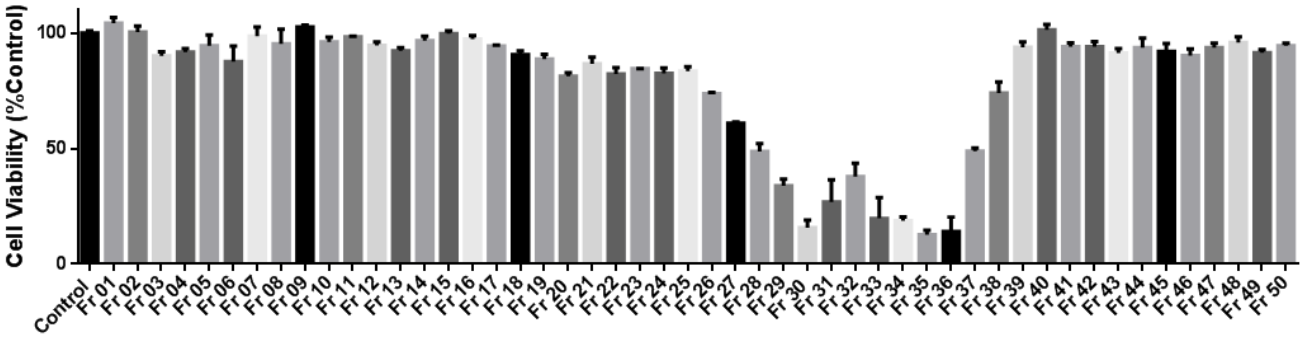

Figure 3. 7 Assessing anti-proliferative activity of fractions collected from a 100-ml size Sephadex™ LH-20 column.

Results showed that fractions 30, 34, 35 and 36 reduced the HeLa cell viability to less than 20% as compared to the control. Weak growth-inhibitory activity was exhibited by Fractions 29 and 37, suggesting the presence of bioactive compounds in these fractions, but possibly in low quantity. Although the cell viability after treatment with fractions 31 and 32 was

close to 50%, the microscopic observation of the wells treated with fractions 31 and 32 revealed 90% killing of HeLa cells. Based on microscopic observation of the cells treated with fractions 31 and 32, the intrinsic reduction potential of these active compounds at high doses was discovered. In summary, results from 100 mL Sephadex LH20 column were consistent with the results from 22 mL columns. The active fractions from the 100 mL column were further analyzed using analytical HPLC.

3.3.6 Assessing methanol for growth-inhibitory effect

To assess the effects of methanol concentration on two different batches of HeLa cell cultures, dose-dependent MTT assay was performed (Figure 3.8). New cells were the ones which had not been split or propagated, while the cells which had propagated more than 15 times were labelled as old cells.

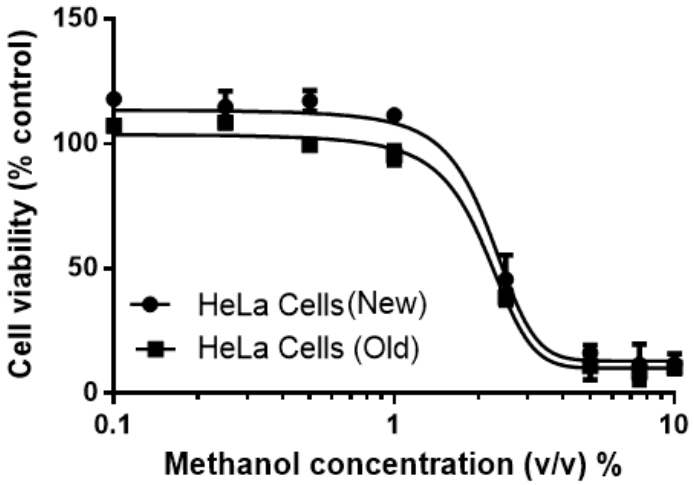

Figure 3. 8 Effects of methanol on the growth of HeLa cells

Final concentrations of methanol in wells were 0.1%, 0.25%, 0.50%, 1%, 2.5%, 5%, 7.5%, & 10%. The safe limit of methanol concentration was determined to be 1%. Above 1% of methanol, cytotoxicity was observed in both HeLa cell types. The response of both HeLa cells cultures was quite similar towards each concentration of methanol.

3.3.7 Assessing fractions collected from Sephadex LH-20 for anti-inflammatory activity

Anti-inflammatory assay was performed using the post-Sephadex™ LH-20 (100 mL) fractions. Anti-inflammatory assay was based on RAW 264.7 cells (100,000 Cells/well) and after 16 hours of incubation, cells were treated with LPS (250 ng/mL) and 2 µL of the fraction volume + 98 µL of DMEM without 10% FBS for 6 hours. The final concentration of methanol in well was only 1% (within safe limits).

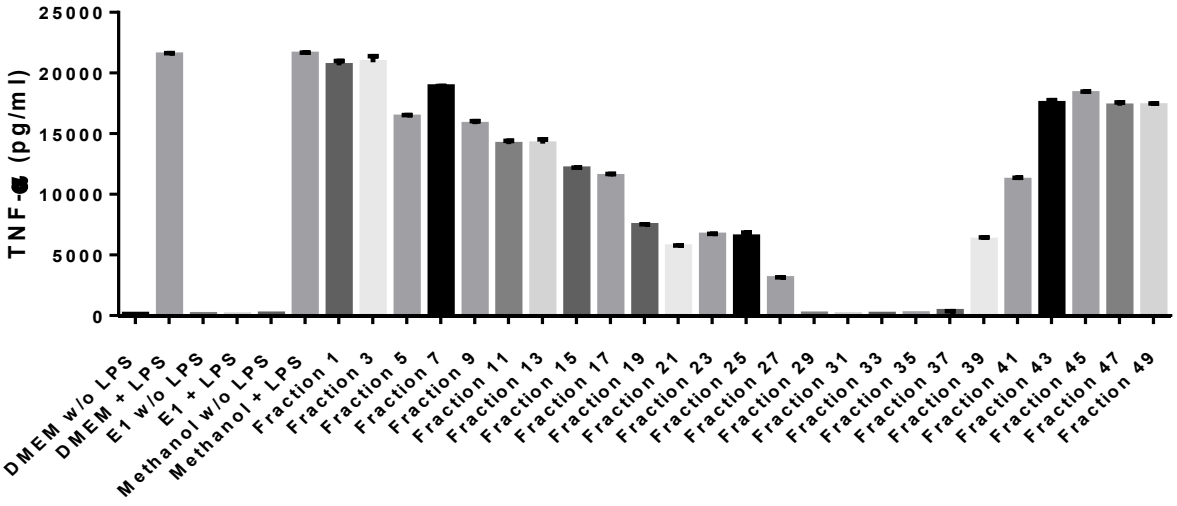

Figure 3. 9 Assessing anti-inflammatory activity of fractions collected from a 100-ml size Sephadex™ LH-20 column.

Only odd numbered fractions were assessed for their anti-inflammatory activity. Results in Figure 3.9 show that fractions 29 to 37 inhibited the LPS-induced TNF-α production at ≥ 95% in RAW 264.7 cells. The compounds present in these fractions were found to be cytotoxic, based on microscopic observation of the cells. The cell morphology after treatment with these fractions was different than normal macrophages. Given that the 'anti-inflammatory activity' could be the result of growth-inhibition by the fractions, the anti-inflammatory activity was not pursued further.

3.3.8 HPLC results

3.3.8.1 Analytical

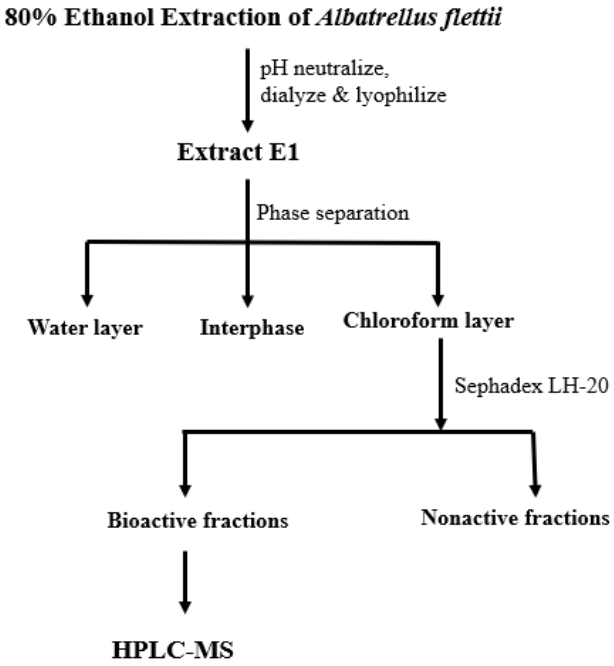

Figure 3. 10 Flow chart diagram representing the method of compounds purification from E1 (80% ethanol) extract of *A. flettii.*

The resolution based on analytical HPLC conditions was excellent: each peak was distinct and very well separated. It took 30 min for all the compounds to be eluted. The retention times for peak 5 (later confirmed to be grifolin), peak 6 (later confirmed to be neogrifolin) and peak 8 (later confirmed to be confluentin) were 14.324 min, 16.669 min and 20.077 min respectively (Figure 3.11). The retention time of the last peak was 28.720 minutes. The percent abundance based on UV spectra for peak 5 (later confirmed as grifolin), peak 6 (later confirmed as neogrifolin) and peak 8 (later confirmed as confluentin) were 32.62%, 51.97% and 8.12% respectively. The highest abundance was peak 6.

Fractions 30 to 36 of the Sephadex LH-20 column were analyzed for the presence of the bioactive compounds. All six spectra were analyzed further by laying over to make a final

spectrum (Fig 3.11). Peaks 5, 6 and 8 were found to be most abundant in all of the spectra. Based on the spectra, 10 most abundant peaks were collected and further analyzed for growth-inhibitory activity.

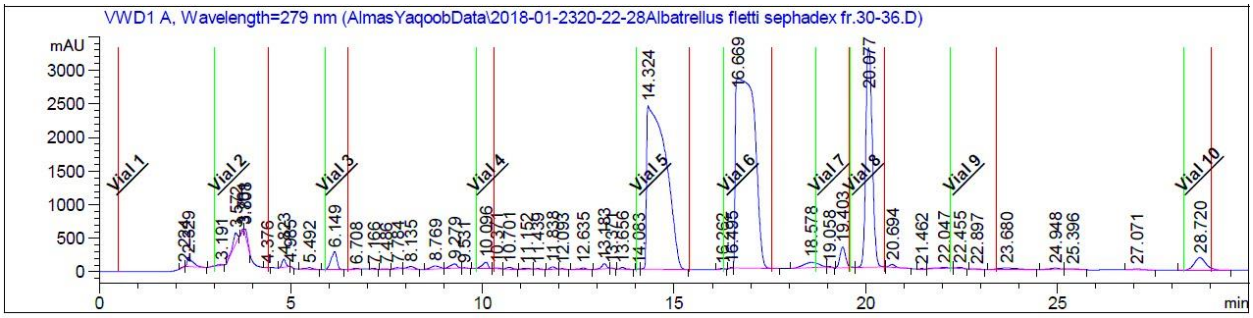

Figure 3. 11 Illustration of HPLC-UV (Phenomenex aqua C-18 column) chromatogram at 279 nm. Ten different peaks were collected at different retention times.

The chromatograms from all six active Sephadex fractions (30-36) were overlayed. This was done to compare the pattern of similar peaks that were most abundant based on UV spectrum of all six fractions. Peaks 5, 6 and 8 were found to be most abundant in all of the UV spectra (Figure 3.12).

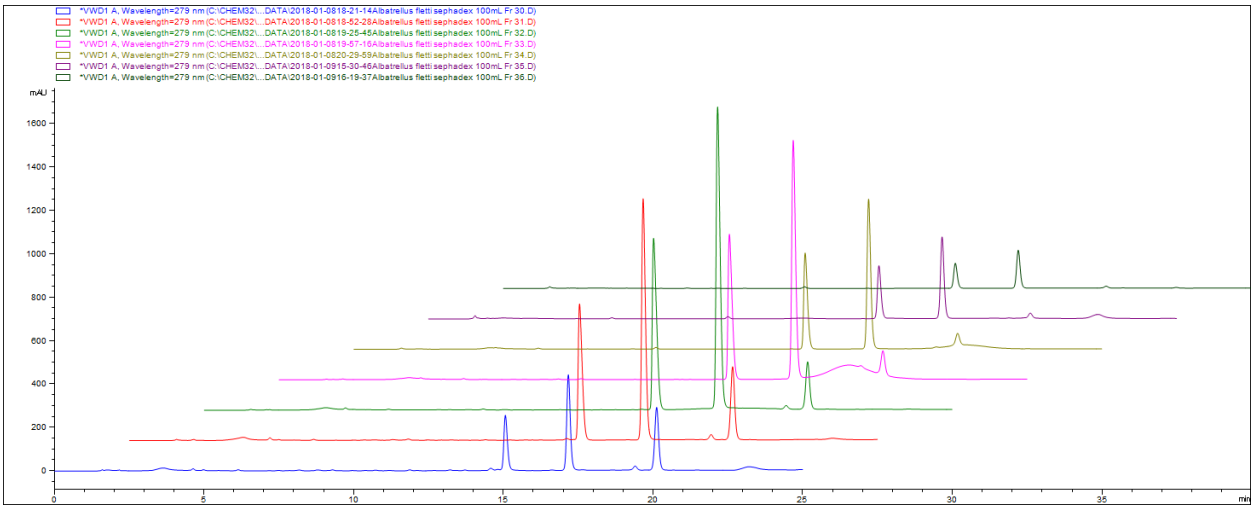

Figure 3. 12 Illustration of layover UV spectrum representing Sephadex LH-20 fractions 30-36.

3.3.8.2 Growth-inhibitory assessment of the peaks collected from analytical HPLC column.

The sample (5 µL each) from Sephadex LH-20 active fraction was run ten times on the analytical HPLC column, and the ten distinct peaks were collected. The collected peaks volume was dried (no mass determination was done) and reconstituted in methanol (100µL) . To determine the growth-inhibitory activity of the different peaks, MTT assay was performed as before. The final concentration was 1% v/v (2 µL of peak solution+ 98 µL of EMEM supplemented with 10% FBS). The final concentration of methanol was also in the range where it had no toxic effects on cells.

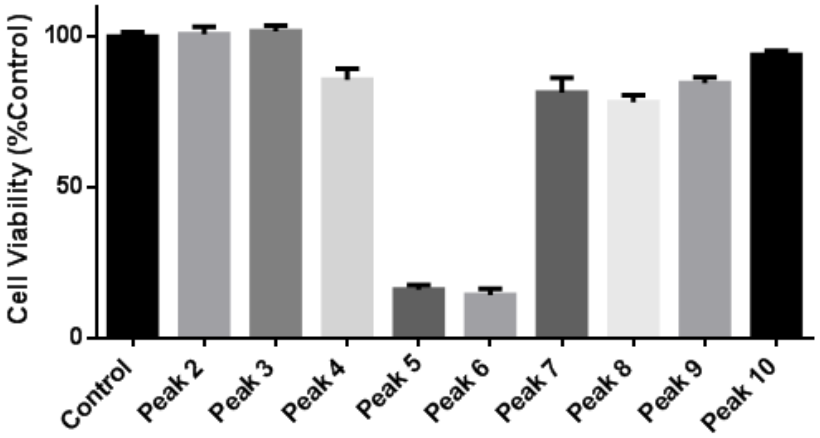

Figure 3. 13 Effect of HPLC-based collected peaks of E1 extract from *A. flettii* on HeLa cell viability: Cells were treated with Peak solution for 48 hours; 2% methanol in EMEM was used as the negative control. Error bars represent standard deviation for four biological replicates.

As shown in Figure 3.13, compound(s) present in peak 5 and peak 6 showed growth inhibition. Due to insufficient samples, quantification of the compound(s) present in the peaks could not be done. So, it was decided to collect all three major peaks using a semi-preparative HPLC column (Peaks 5, 6 and 8).

3.3.8.3 Anti-inflammatory assessment of the peaks collected from HPLC analytical column (Phenomenex aqua C-18)

The peaks collected using analytical column (Phenomenex aqua C-18) were assessed for potential anti-inflammatory activity using RAW 264.7 cells as described in Chapter 2. The

volume of each peak used was 2 µL. DMEM with LPS was used as the negative control, while the crude extract, at 1 mg/mL, was used as a positive control in LPS-activated RAW 264.7 cells.

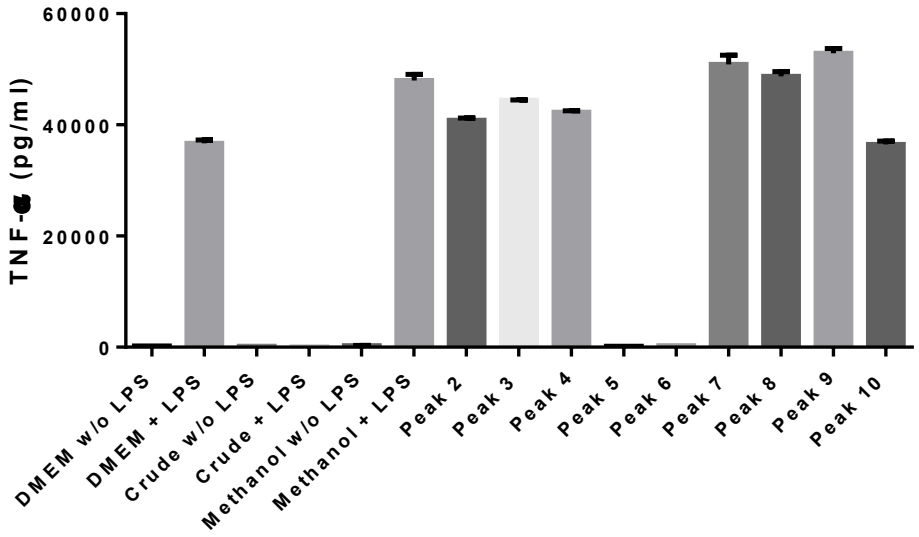

Figure 3. 14 Assessing HPLC based collected peaks of E1 extract from *A. flettii* for anti-inflammatory activity: Cells were treated with Peak solution for 6 hours; 2% methanol in EMEM was used as the negative control. Error bars represent standard deviation for four biological replicates.

The cell morphology after treatment with Peaks 5 and 6 was found to be abnormal, suggesting cytotoxicity of these compounds toward RAW 264.7 cells. Given that there was no quantification of Peak 5 and 6 compound(s), it was proposed that toxicity could be due to high doses of the compounds. In contrast, no marked difference in anti-inflammatory activity was observed with Peaks 2-4 and 7-10 and the negative control (Figure 3.14).

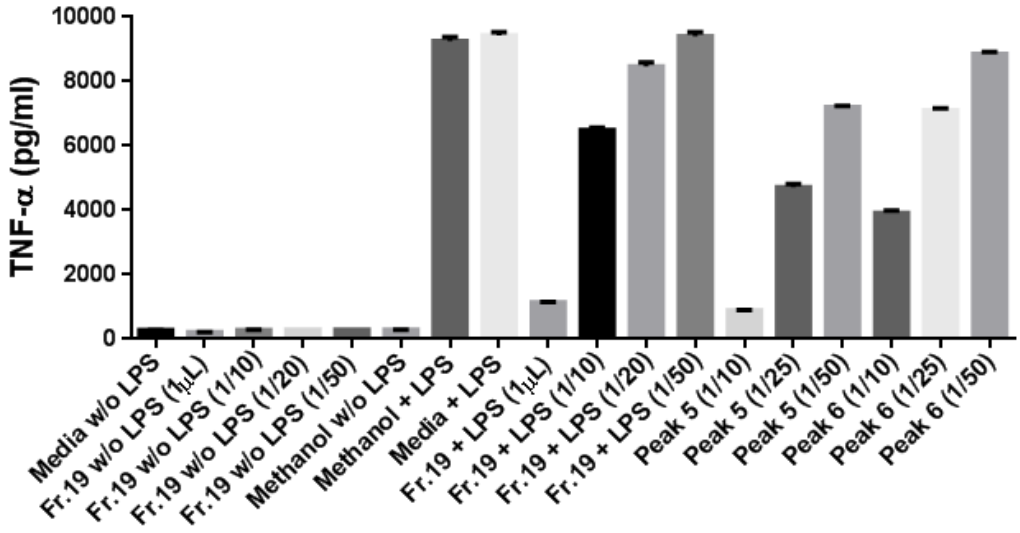

Figure 3. 15 Results of Anti-inflammatory assay of HPLC based collected peaks of E1 extract of *A. flettii.* Cells were treated with Peak solution for 6 hours; 2% methanol in EMEM was used as the negative control. Error bars represent standard deviation for four biological replicates.

After determining the cytotoxicity of the two peaks in the macrophage cells, dilutions were made on the peak solutions. The dilutions were made 1 in 10, 1 in 25 and 1 in 50. The bioactive Fraction 19 collected from Sephadex LH-20 was also diluted in the similar manner using methanol. Anti-inflammatory assay was performed using each dilution. The purpose of making dilution was to see if there was any anti-inflammatory activity without toxicity being observed. The microscopic observation indicated toxicity of RAW 264.7 cells at each dilution except for 1:50 dilution (Figure 3.15). At this point, it was still inconclusive to decide whether compounds are cytotoxic or anti-inflammatory in nature. A proper quantification of compounds and a detailed anti-inflammatory analysis based on the quantified dose should be able to address this issue.

3.3.8.4 Assessing the three compounds purified from HPLC semi-preparative column for anti-inflammatory activity

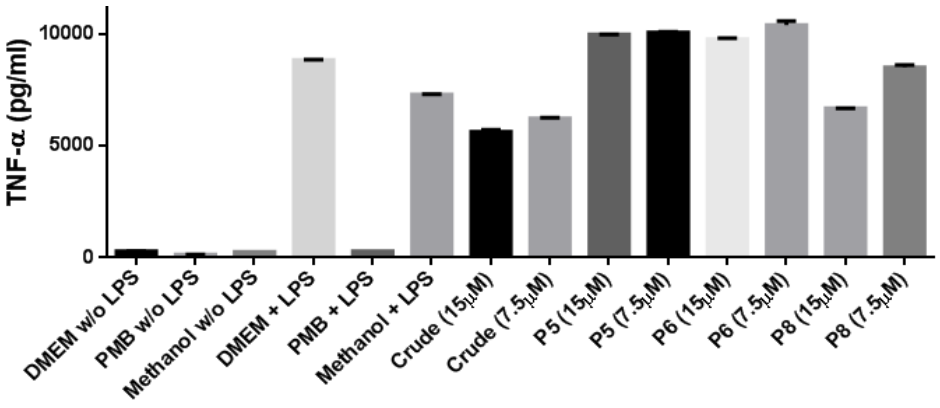

Figure 3. 16 Assessing HPLC based collected peaks of E1 extract from *A. flettii* for anti-inflammatory activity: Cells were treated with Peak solution for 6 hours. 2% methanol in EMEM was used as the negative control. Error bars represent standard deviation.

The potential anti-inflammatory activity of peak 5 (later confirmed as grifolin), 6 (later confirmed as neogrifolin) and 8 (later confirmed as confluentin) was performed as described previously. The lowest possible concentrations made were 0.005 mg/mL (15 μM) and 0.0025 mg/mL (7.5 μM). The compounds were resuspended in methanol. DMEM w/o FBS and 1% methanol were used as negative controls while polymyxin-B (PMB) was used as a positive control.

As shown in Figure 3.16, no anti-inflammatory activity was observed at these doses. Microscopic observation revealed the fact that these compounds are cytotoxic in nature rather than anti-inflammatory. Therefore, it is concluded that the reduced levels of TNF-α after treatment with these compounds described previously were due to cell killing and not because of anti-inflammatory activity.

3.3.8.5 Semi-preparative HPLC

To obtain a larger quantity of compound(s) in Peaks 5, 6 and 8, a semi-preparative HPLC column was used. A chromatogram obtained using the semi-preparative column is shown in

Figure 3.17. The peak separation pattern was similar to the pattern obtained using the analytical column. Three major peaks holding around 92% of the total mass of the bioactive Sephadex LH-20 fractions, were observed in the UV signal.

The retention time for peak 5 was at 10.821 min on UV visible chromatogram and percent abundance was like the analytical column. The UV visible retention time for P6 was at 14.582 min and the percent abundance was the highest, at around 52%. Like the results of analytical HPLC, P8 was among the later eluting peak that was visible at 21.438 min with abundance at around 8.12%. It took 29.981 min for the last peaks to elute out of the column. So, the total run time was set at 32 min.

Many less abundant hydrophobic small molecule peaks were also observed in the UV spectra (Figure 3.17). The collection and further processing of these hydrophobic compounds was practically impossible due to limited quantity of sample and lower yields.

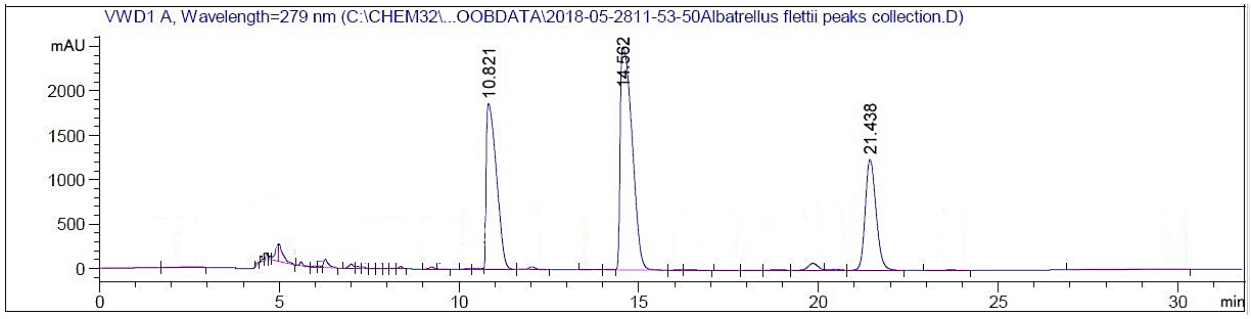

Figure 3. 17 UV spectrum representing the relative abundance and retention time of the three major peaks using λ_{max} 279 nm (using semi-preparative column and Sephadex LH-20 fraction sample).

It took more than 500 runs in total to purify the required amount of peak 5, peak 6 and peak 8; enough to perform biochemical studies.

The purity of the collected compounds was further confirmed by running the collected "pure peaks" again under the same HPLC conditions. The retention time for all three purified

compounds was the same as the peaks observed using semi-crude sample. The percent purity for all three compounds was 100% (Figure 3.18-3.20). The structures of purified compounds were determined by NMR Spectroscopy.

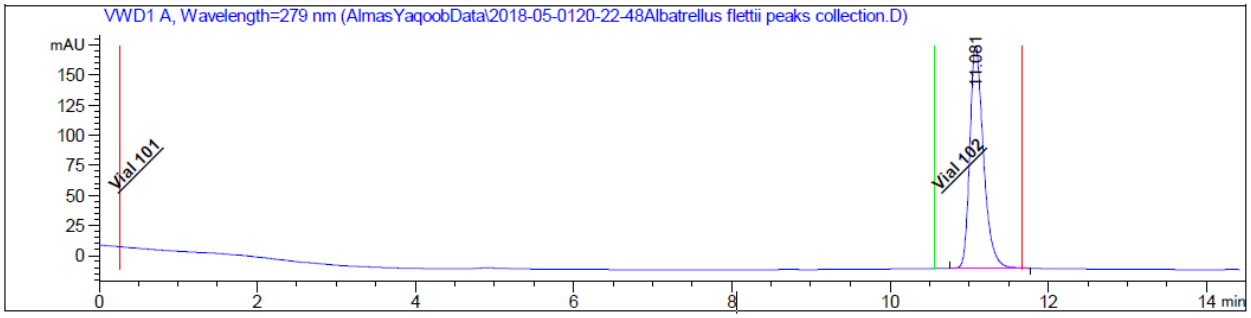

Figure 3. 18 UV signal confirming the 100% purity of the compound in peak 5 (later confirmed as grifolin).

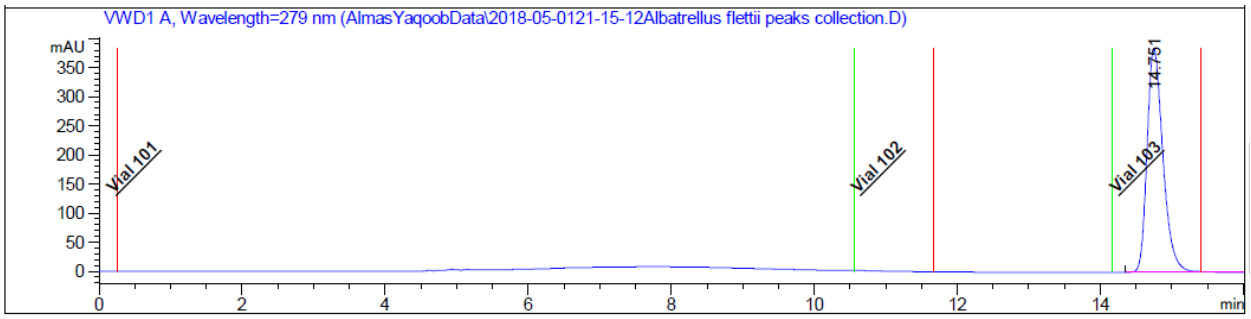

Figure 3. 19 UV signal confirming the 100% purity of the compound in peak 6 (later confirmed as neogrifolin).

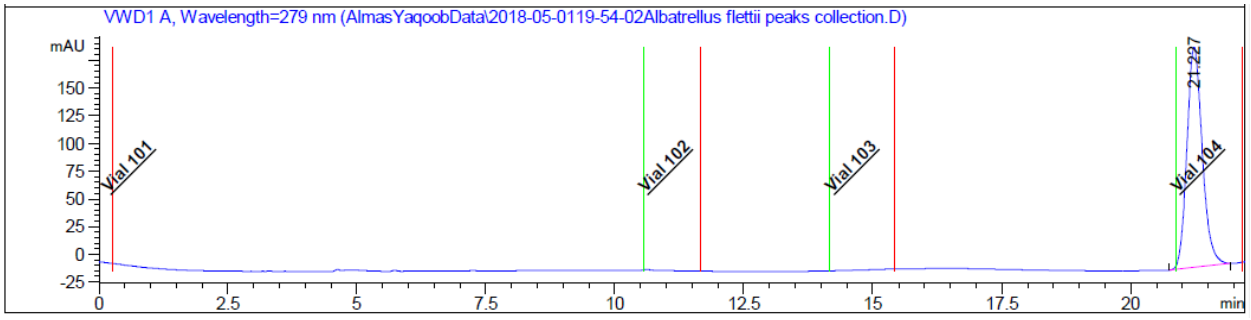

Figure 3. 20 UV signal confirming the 100% purity of the compound in peak 8 (later confirmed as confluentin).

3.3.8.6 Yield of purified compounds from *A. flettii*

The final yield of P5 (later confirmed as grifolin), P6 (later confirmed as neogrifolin) and P8 (later confirmed as confluentin) from 70 g of *A. flettii* # 128 was 0.26, 0.16 and 0.025% respectively. Table 3.4 shows the yield at each step of the purification.

Table 3. 4 Techniques followed and yield of compounds from E1 (80% ethanol) extract of *A. flettii*

Technique	Yield (in mass)	% yield based on technique
Powdered fungi sample # 128	70 g	-
E1 (80% Ethanol) Fraction weight	7.1489 g	10.21
Liquid-liquid extraction yield.	3.1813 g	4.54
Loaded on Sephadex™ LH-20 (400 mL) (Total 5 columns)	= 640 mg/run (8 ml of 80 mg/mL each).	-
Active fractions obtained from Sephadex™ LH-20 (400 mL)	~178 mg/run. (Total around 800 mg from 5 columns)	1.14
Sample purified by HPLC-UV	~400 mg (active fractions Post LH-20 Sephadex®)	-
Purified compounds from HPLC-UV	~350 mg	-
P5 (Later confirmed as grifolin)	182.5 mg	0.26
P6 (Later confirmed as neogrifolin)	114.2 mg	0.16
P8 (Later confirmed as confluentin)	17.5 mg	0.025

3.3.8.7 Mass spectroscopy (MS) analysis

The purified compounds were protonated with the aid of 0.1% formic acid isocratic solution. Figure 3.21 represents the UV spectrum showing three abundant peaks with their respective retention times.

The molar mass of the protonated purified Peaks 5 and 6 was the same (m/z = 329.3) (Figure 3.24 and 3.27), suggesting that they may be isomers. Spectra shown in Figure 3.22 and

3.23 represent the SIM and scan signal of peak 5 respectively, while Figure 3.25 and 3.26 represent the SIM and scan spectra of peak 6 respectively.

However, the molar mass of the purified compound (peak 8) was determined to be ESIMS = 327.3 *m/z* (Figure 3.30). Spectra shown in Figure 3.28 and 3.29 represent the SIM and scan signal of peak 8 respectively.

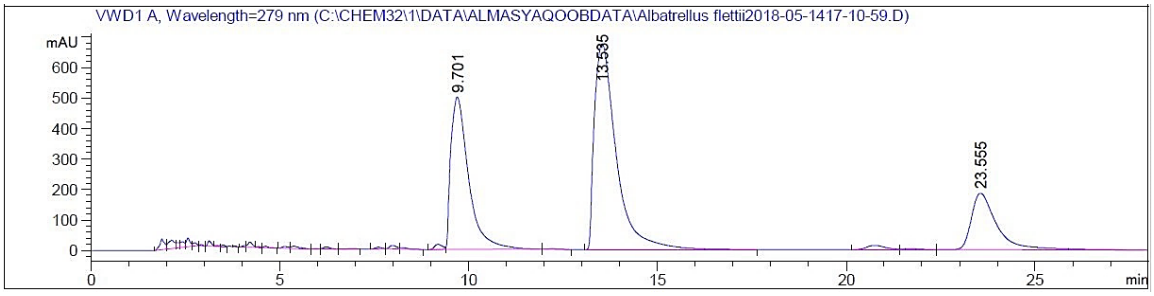

Figure 3. 21 UV spectrum representing the relative abundance and retention time of peaks at λ_{max} 279nm (using analytical column and Sephadex LH20 active fraction sample).

3.3.8.7.1 Peak 5 (Later confirmed as grifolin)

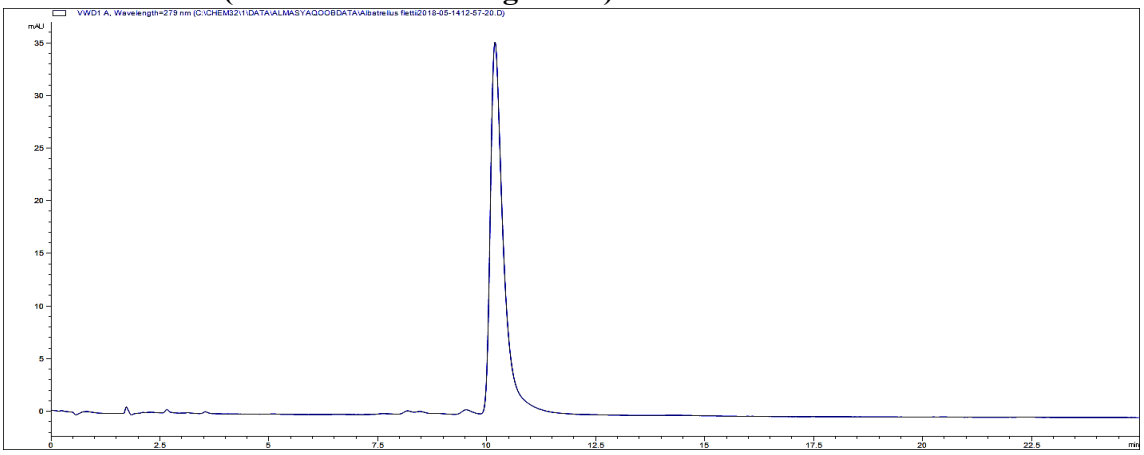

Figure 3. 22 UV spectrum confirming the purity of the compound $[M+H]^+$ *m/z* 329.3 detected at 10.226 min through ESI (Electrospray ionization) chamber. The type of column utilized was Agilent C-18 analytical column and the sample was 5 µL of purified compound from Peak 5.

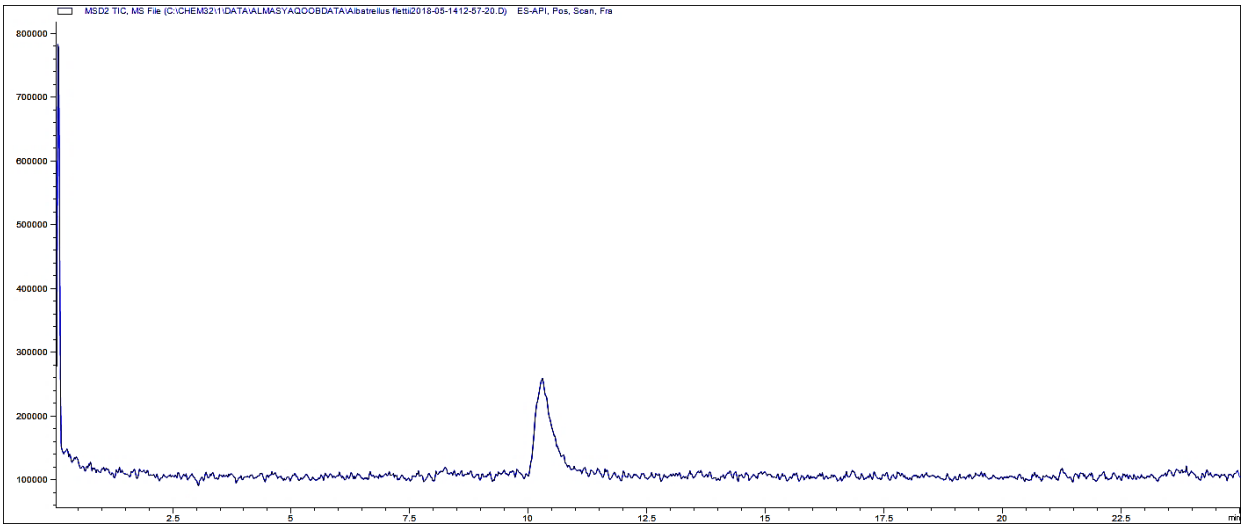

Figure 3. 23 MS Scan spectrum representing the relative abundance and retention time of the compound with $[M+H]^+$ *m/z* 329.3 detected at 10.226 min through ESI (Electrospray ionization) chamber. The type of column utilized was Agilent C-18 analytical column and the sample was 5 µL of purified compound from Peak 5.

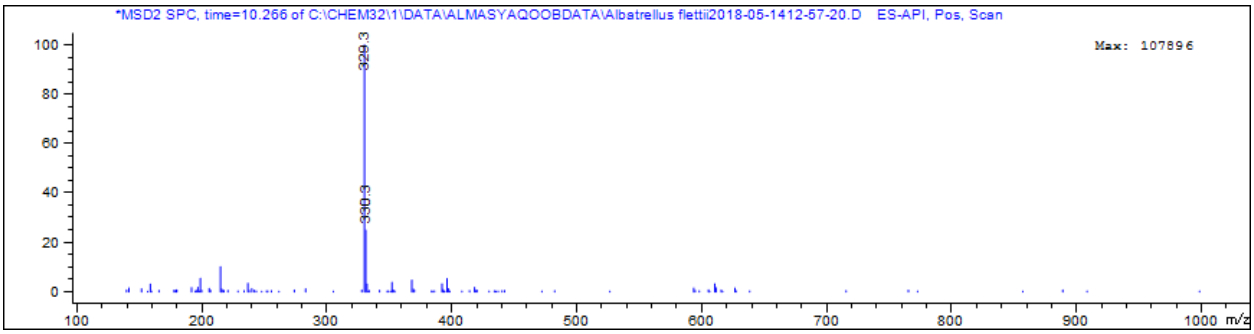

Figure 3. 24 Integration of MS Scan spectrum indicating the presence and abundance of compound Peak 5 with $[M+H]^+$ *m/z* 329.3 visible at 10.266 min.

3.3.8.7.2 Peak 6 (later confirmed as neogrifolin)

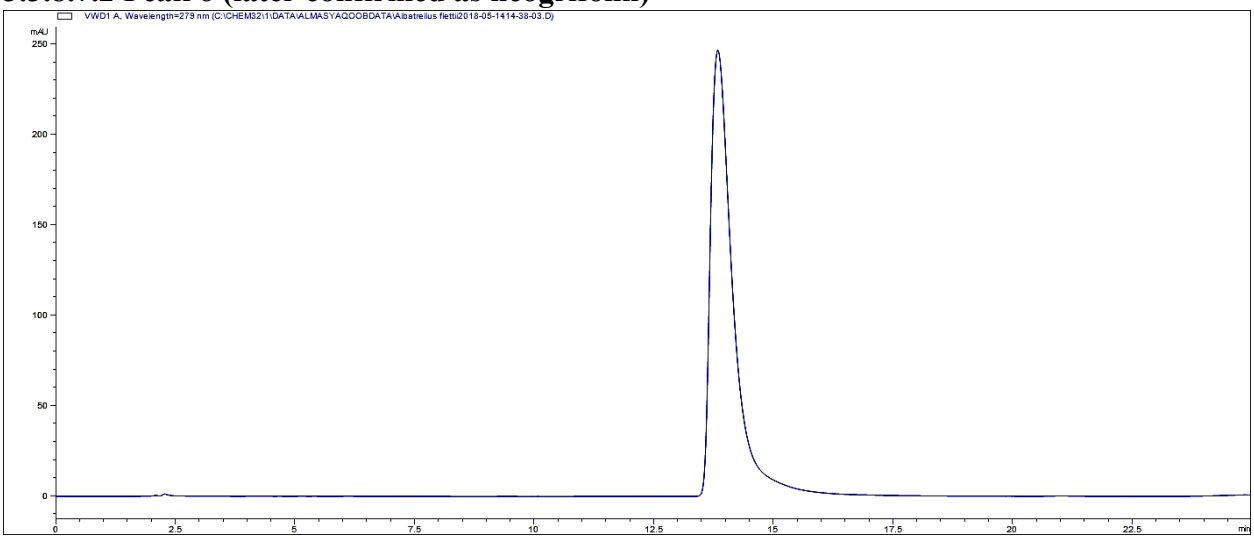

Figure 3. 25 UV spectrum confirming the purity of the compound with $[M+H]^+$ *m/z* 329.3 detected at 13.987 min through ESI (Electrospray ionization) chamber. The type of column utilized was Agilent C-18 analytical column and the sample was 5 µL of purified compound from Peak 6.

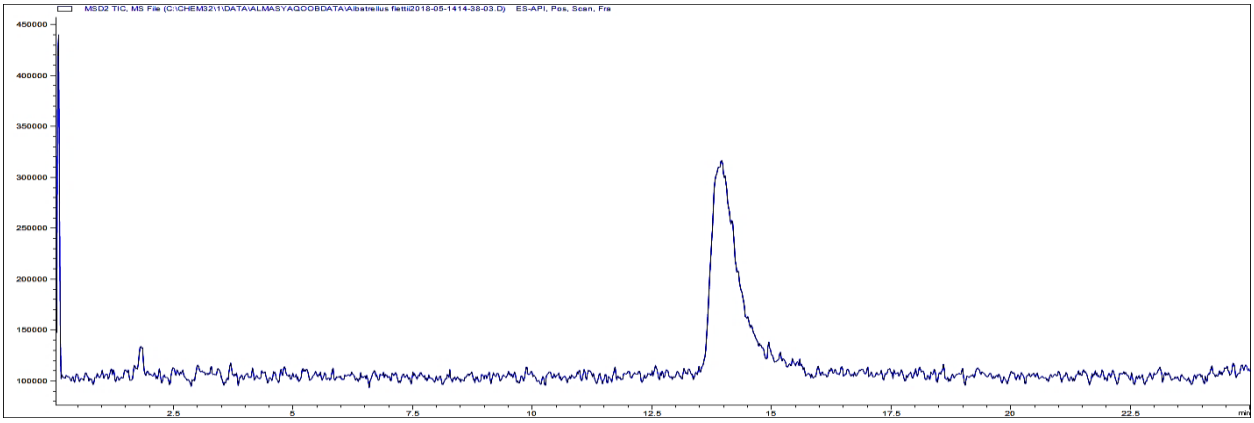

Figure 3. 26 MS scan spectrum representing the relative abundance and retention time of the compound with $[M+H]^+$ *m/z* 329.3 detected at 13.987 min through ESI (Electrospray ionization) chamber. The type of column utilized was Agilent C-18 analytical column and the sample was 5 µL of purified compound from Peak 6.

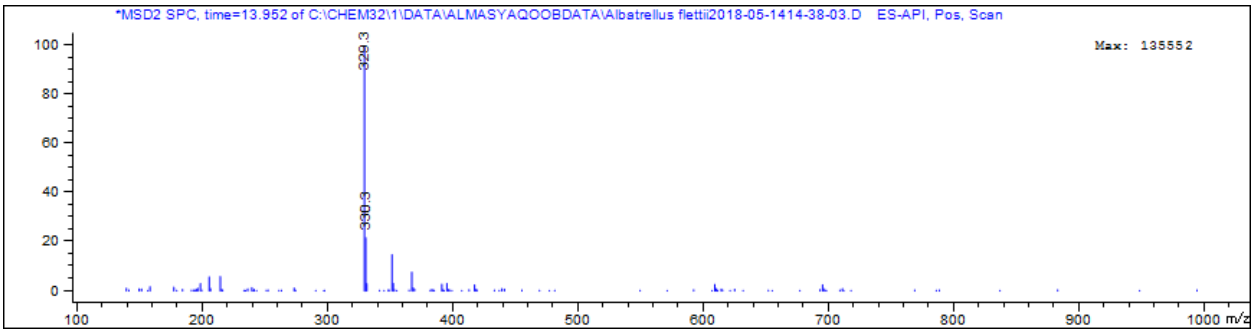

Figure 3. 27 Integration of MS Scan spectrum indicating the presence and abundance of compound Peak 6 with $[M+H]^+$ *m/z* 329.3 visible at 13.952 min.

3.3.8.7.3 Peak 8 (later confirmed as confluentin)

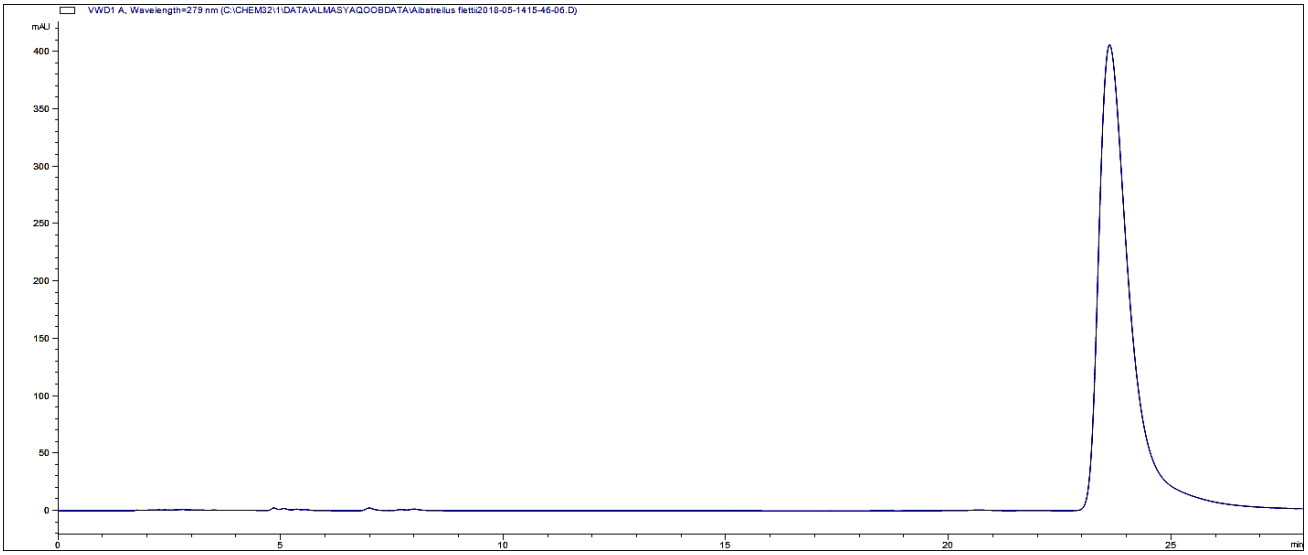

Figure 3. 28 UV spectrum confirming the purity of the compound $[M+H]^+$ *m/z* 327.3 detected at 23.555min through ESI (Electrospray ionization) chamber. The type of column utilized was Agilent C-18 analytical column and the sample was 5 µL of purified compound from Peak 8.

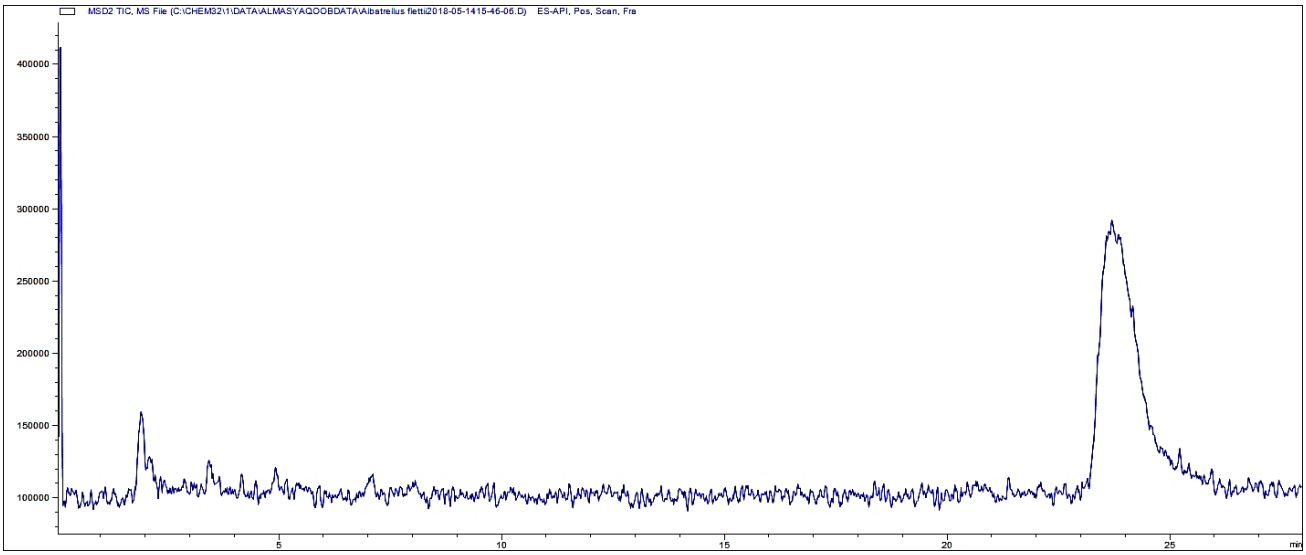

Figure 3. 29 MS scan spectrum representing the relative abundance and retention time of the compound with $[M+H]^+$ *m/z* 327.3 detected at 23.555min through ESI (Electrospray ionization) chamber. The type of column utilized was Agilent C-18 analytical column and the sample was 5 µL of purified compound from Peak 8.

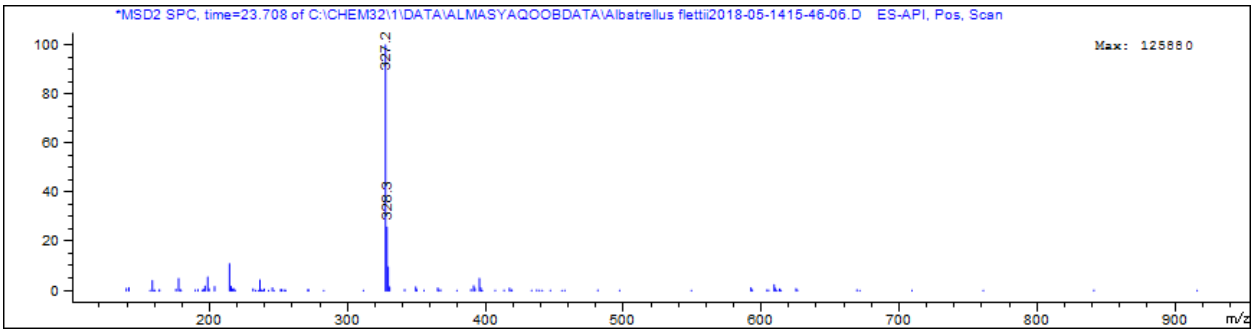

Figure 3. 30 Integration of MS Scan spectrum indicating the presence and abundance of compound Peak 8 with $[M+H]^+$ *m/z* 327.3 visible at 23.708 min.

3.3.9 Nuclear Magnetic Resonance (NMR) analysis

In the course of investigation on growth-inhibitory constituents of the *A. flettii*, three previously reported compounds (grifolin, neogrifolin and confluentin) were isolated and structurally elucidated by comparing their NMR spectra (Table 3.5-3.6) with already published NMR data (Ishii et al., 1988[1] : Iwata et al., 2004[2]: Liu & Woggon, 2010[3]). Compounds in peaks 5, 6 and 8 of HPLC UV spectra were identified as grifolin, neogrifolin and confluentin respectively.

Table 3. 5 ^{13}C NMR spectral data of purified compounds (grifolin, neogrifolin and confluentin) obtained using Bruker Fourier A-300 NMR.

Carbon	Grifolin	Grifolin[1]	Neogrifolin	Neogrifolin[1]	Confluentin	Confluentin[2]
C-1	109.1	109.3 *(d)*	109.7	109.9 *(d)*		
C-2	137.5	137.2 *(s)*	154.1	154.1 *(s)*	78.2	78.2 *(s)*
C-3	109.1	109.3 *(d)*	101.1	101.2 *(s)*	127.2	127.2 *(d)*
C-4	154.8	154.6 *(s)*	155.4	155.2 *(s)*	116.7	116.7 *(d)*
C-4a					106.7	106.8 *(s)*
C-5	110.4	111 *(s)*	117.9	118.4 *(s)*	151.0	151.0 *(s)*
C-6	154.8	154.6 *(s)*	138.5	138.7 *(s)*	108.4	108.3 *(d)*
C-7					139.5	139.5 *(s)*
C-8	21.0	21 *(q)*	20.2	20.2 *(q)*	109.8	109.3 *(d)*
C-8a					154.1	154.1 *(s)*
C-1’	22.2	22.3 *(t)*	25.1	25.2 *(t)*	41.0	41.0 *(t)*
C-2’	121.6	122 *(d)*	122	122.3 *(d)*	22.6	22.6 *(t)*
C-3’	139.1	138.4 *(s)*	137.7	137.3 *(s)*	124.0	124.0 *(d)*
C-4’	39.7	39.7 *(t)*	39.7	39.8 *(t)*	135.3	135.3 *(s)*
C-5’	26.7	26.7 *(t)*	26.4	26.6 *(t)*	39.7	39.7 *(t)*
C-6’	123.6	123.7 *(d)*	123.8	123.9 *(d)*	26.7	26.7 *(t)*
C-7’	135.6	135.4 *(s)*	135.5	135.4 *(s)*	124.4	124.4 *(d)*
C-8’	39.7	39.7 *(t)*	39.7	39.8 *(t)*	131.3	131.3 *(s)*
C-9’	26.7	26.7 *(t)*	26.7	26.8 *(t)*	25.7	25.7 *(q)*
C-10’	124.4	124.5 *(d)*	124.4	124.5 *(d)*	17.7	17.7 *(q)*
C-11’	131.3	131 *(s)*	131.4	131.4 *(s)*	15.9	16.0 *(q)*
C-12’	25.7	25.7 *(q)*	25.7	25.8 *(q)*	26.3	26.3 *(q)*
C-13’	17.7	17.7 *(q)*	17.7	17.8 *(q)*	21.5	21.5 *(q)*
C-14’	16.2	16.1 *(q)*	16.3	16.4 *(q)*		
C-15’	16.0	16 *(q)*	16.2	16.2 *(q)*		

Table 3. 6 ^{1}H NMR spectral data of purified compounds (grifolin, neogrifolin and confluentin) obtained using Bruker Fourier A-300 MHz NMR.

Hydrogen	Grifolin	Grifolin[1]	Neogrifolin	Neogrifolin[1]	Confluentin	Confluentin[3]
H-1	6.23 (s)	6.20 (s)	6.25 (d, 3.0 Hz)	6.23 (d, 3.0 Hz)		
H-2						
H-3	6.23 (s)	6.20 (s)	6.21 (d, 3.0 Hz)	6.18 (d, 3.0 Hz)	5.48 (d, 10 Hz)	5.49 (d, 10 Hz)
H-4					6.59 (d, 10 Hz)	6.60 (d, 10 Hz)
H-6					6.11 (s)	6.11 (s)
H-8	2.21 (s)	2.21 (s)	2.22 (s)	2.21 (s)	6.24 (s)	6.24 (s)
H-1’	3.37 (d, 7.0 Hz)	3.37 (d, 7.0 Hz)	3.27 (d, 7.0 Hz)	3.27 (d, 7.0 Hz)	1.67 – 1.78 (m)	1.65-1.78 (m)
H-2’	5.23 (t, 7.0 Hz)	5.26 (t, 7.0 Hz)	5.11 (t, 7.0)	5.11 (t, 7.0)	2.03-2.12 (m)	2.01-2.13 (m)
H-3’					5.08 (m)	5.06 (m)
H-4’	1.96-2.12 (m)	1.9-2.10 (m)	1.84-2.04 (m)	1.84-2.04 (m)		
H-5’	1.96-2.12 (m)	1.9-2.10 (m)	1.84-2.04 (m)	1.84-2.04 (m)	1.95 (m)	1.95 (m)
H-6’	5.05 (m)	5.06 (m)	5.04 (m)	5.04 (m)	2.03-2.12 (m)	2.01-2.13 (m)
H-7’					5.11 (m)	5.11 (m)
H-8’	1.96-2.12 (m)	1.9-2.10 (m)	1.84-2.04 (m)	1.84-2.04 (m)		
H-9’	1.96-2.12 (m)	1.9-2.10 (m)	1.84-2.04 (m)	1.84-2.04 (m)	1.67 (s)	1.67 (s)
H-10’	5.05 (m)	5.06 (m)	5.04 (m)	5.04 (m)	1.59 (s)	1.59 (s)
H-11’					1.57 (s)	1.57 (s)
H-12’	1.67 (s)	1.66 (s)	1.67 (s)	1.66 (s)	1.37 (s)	1.37 (s)
H-13’	1.59 (s)	1.57 (s)	1.58 (s)	1.58 (s)	2.20 (s)	2.20 (s)
H-14’	1.58 (s)	1.57 (s)	1.58 (s)	1.58 (s)		
H-15’	1.81 (s)	1.80 (s)	1.79 (s)	1.80 (s)		

3.3.9.1 Grifolin

The signals observed for ^{13}C NMR spectra of grifolin indicated the presence of twenty-two carbons in the structure. The signals for non-proton bearing carbons of grifolin (C-3’, C-7’ and C-11’) were observed with shifts in the range 131.33-139.50 ppm. The downfield signal at 154.81 ppm in the ^{13}C NMR spectrum of grifolin was observed for aromatic carbons (C-4 & C-

6) having hydroxyl groups attached to them. The ^{13}C shifts at 25.74, 17.72, 16.23, 16.06 ppm were observed for side chain methyl carbons at positions C-12', C-13', C-14' and C-15' respectively. Side chain carbons C-4' and C-8' were observed as overlapping signal at 39.70 ppm. This overlap is due to C-4' and C-8' existing in similar chemical environment. The signals at 121.62, 123.62 and 124.43 ppm correspond to the methine carbons at positions C-2', C-6' and C-10' respectively. The signals for aromatic carbons (C-1 and C-3) were observed at 109.3 ppm, because C-1 and C-3 exist in identical chemical environment. The signal at 21.0 ppm is due to an aromatic methyl group (C-8). Grifolin structure is terpenoid in nature having an isoprene skeleton side chain.

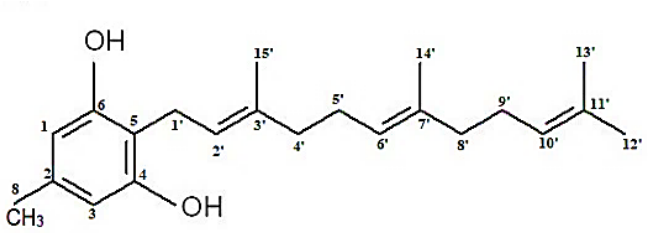

Figure 3. 31 Chemical structure of grifolin.

The ^{1}H NMR spectrum of grifolin (Table 3.6) exhibited four singlets for methyl groups at 1.584 (3H, H-14'), 1.594 (3H, H-13'), 1.672 (3H, H-12'), 1.812 ppm (3H, H-15'). A singlet at 2.205 ppm (3H, H-8) corresponds to an aromatic methyl group at C-8. A multiplet at 5.046 ppm corresponds to two hydroxyls (H-4 and H-6) and two methines (H6' and H-10').

The signals for H-1 and H-3 appeared as singlet at 6.234 ppm. The multiplet at 1.962-2.120 ppm was integrated to eight protons containing the signals for methylene groups at H-4', H-5' H-8' and H-9'. The signal for (-CH_2-) methylene group at H-1' was observed as a doublet

at 3.376 (J = 7.0 Hz). The signals for methine protons (H-6' and H-10') were observed in the range of 5.046 - 5.23 ppm.

On comparison using the ^{1}H-NMR spectra of grifolin and neogrifolin, a prominent shift difference was observed for protons attached to carbon C-1 and C-3. The chemical environment for protons (H-1 & H-3) is equal in grifolin, due to symmetry of the neighbor substituents attached to aromatic ring. The singlet having two protons (H-1 & H-3) was observed for grifolin at 6.234 (s) ppm. A signal at 6.214 (d, 3.0 Hz) ppm was observed for neogrifolin aromatic protons (H-1 & H-3), indicating meta coupling of these protons. This indicates that the protons (H-1 and H-3) in grifolin structure are equally de-shielded, while in neogrifolin H-3 is more de-shielded than H-1.

^{1}H-^{1}H COSY is a 2D method used for determining the signals arising from neighboring protons. The peaks that do not show up across diagonal are termed as cross peaks, which tell about coupled signals of neighboring protons. A cross peak was observed at 6.234 and 2.205 ppm for aromatic protons at carbon (C-1 and C-3) and methyl group protons (H-8') attached to aromatic ring, indicating them being neighbors. The presence of two aromatic hydroxyl group (H-4 and H-6) was confirmed by a cross peak at 5.046 and 2.205 ppm, indicating two hydroxyl group in close environment of the aromatic methyl group. The proton pair (H-1') at carbon (C-1') displayed a cross-peak with H-15' protons at 3.376 and 1.812 ppm.

Heteronuclear single quantum correlation (HSQC), is used in NMR spectroscopy of organic molecules. HSQC is a two-dimensional spectrum having two axis, one axis for proton (^{1}H NMR) and other for ^{13}C spectrum. HSQC provides in detail information about protons and heteronuclear atoms (C or N), to which those protons are linked. The HQSC spectrum of grifolin revealed resonances for four methyl groups [1.584 (H-14'), 1.594 (H-13'), 1.672 (H-12'), and

1.812 ppm (H-15')] and one aromatic methyl group at 2.205 ppm (H-8), three methines [5.046 (H-6'), 5.046 (H-10'), 5.230 (H-2')], and five methylenes (-CH_2-) groups at 3.376 ppm (j=7.0 Hz, H-1'), 1.962-2.120 ppm (H-4', H-5', H-8' and H-9'). The carbons at position C-3', C-7' and C-11, displayed no resonance signals with ^{1}H signal indicating quaternary carbons.

3.3.9.2 Neogrifolin

The signals observed for ^{13}C NMR spectra of neogrifolin indicated the presence of twenty-two carbons in the structure. The signals for non-proton bearing carbons of neogrifolin (C-3', C-7' and C-11') were observed downfield at 137.72 , 135.47 and 131.36 ppm respectively. Two distinct upfield signals were observed for aromatic carbons (C-1 and C-3) at 109.69 and 101.05ppm respectively, making neogrifolin distinct from grifolin. The carbon signal trend for neogrifolin side chain primary carbons (C-12', C-13', C-14' and C-15') was the same as observed in grifolin spectra. The signals for C-12', C-13', C-14' and C-15' were observed at 25.74, 17.72, 16.27 and 16.21 ppm respectively. Side chain carbons C-4' and C-8' exhibited signal at 39.68 ppm. The carbons C-4' and C-8' exist in similar chemical environment. The two downfield signals at 154.15 and 155.39 ppm on ^{13}C NMR spectra was observed for aromatic carbons (C-2 & C-4) having hydroxyl groups attached to them. Neogrifolin structure is terpenoid in nature having an isoprene skeleton side chain.

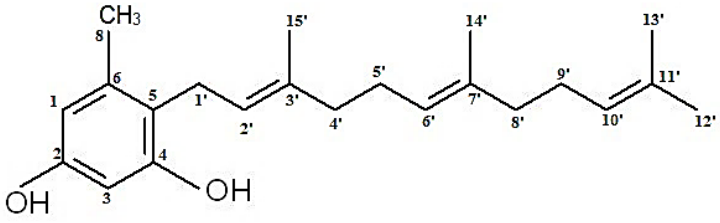

Figure 3. 32 Chemical structure of neogrifolin.

The ^{1}H NMR spectrum of neogrifolin (Table 3.6) exhibited four singlets for methyl protons attached to side chain primary carbons at 1.580 (3H, H-14'), 1.580 (3H, H-13'), 1.67 (3H, H-12'), 1.790 (3H, H-15') . A singlet at 2.226 ppm (3H, H-8) is characteristic of an aromatic methyl group. A multiplet signal at 5.049- 5.11 ppm represents five protons, mainly two from aromatic hydroxyl groups (H-2 and H-4) showed overlapping signals with side chain hydrogens attached to methines at positions H2, H6' and H-10'. The signals for eight protons from four (-CH_2-) methylene groups at H-4', H-5' H-8' and H-9' were observed as a multiplet at 1.84-2.04 ppm. A doublet at 3.273 ppm (J=7.0 Hz) is due to the presence of two protons (H-1') on (-CH_2-) methylene carbon (C-1').

A cross peak indicating a hydroxyl group (C-2) close to the methyl group (C-8) of aromatic structure was observed at 5.049 and 2.226 ppm in neogrifolin ^{1}H-^{1}H COSY spectrum. Methylene (-CH_2-) protons at position H-1' displayed a cross peak at 3.273 and 5.11 ppm with protons at position H-2', indicating them being neighbors. A cross peak was observed at 5.049 and 1.84-2.04 ppm due to coupling of protons H-6' and H-5'.

The HQSC spectrum of neogrifolin revealed resonances for four methyl groups [1.580 (H-13'& H-14'), 1.67 (H-12'), 1.790 ppm (H-15')] and one aromatic methyl group 2.226 (H-8) ppm, three methines [5.049 (H-6'), 5.049 (H-10'), 5.11 ppm (H-2')], and five methylenes (-CH_2-) groups 3.273 (j=7.0 Hz, H-1'), 1.84-2.04 ppm (H-4', H-5',H-8'and H-9'). The carbons at position C-3', C-7' and C-11, displayed no resonance signals with the ^{1}H spectrum indicating quaternary carbons.

3.3.9.3 Confluentin

The signals observed for ^{13}C NMR spectra of confluentin indicated the presence of twenty-two carbons in the structure. The structure of confluentin contains an oxygen containing

hetero cycle. The signals for the cyclic carbons bounded directly to the oxygen of the heterocycle (C-2 & C-8a) were observed at 78.21 and 154.10 ppm. ^{13}C NMR spectrum corresponded the presence of five non-proton-bearing cyclic carbons (C-2, C-5, C-7,C-4a and C-8a) exhibiting their signals at 78.21, 151.02, 139.55, 106.74 and 154.1 ppm respectively. The signals for non-proton bearing side chain quaternary carbons (C-4' and C-8') were observed at 135.27 & 131.36 ppm respectively.

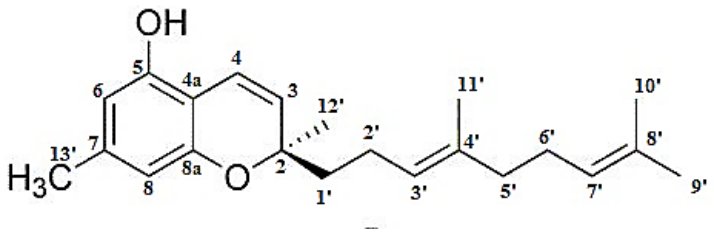

Figure 3. 33 Chemical structure of confluentin

The chemical shift at 151.02 ppm, is representative of aromatic carbon (C-5) having a hydroxyl group substitution. The signals for methine carbon C-3' and C-7' were very close to each other (124.06 & 124.38 ppm). The signals for side chain (-CH_2-) methylene groups (C-1', C-2', C-5' and C-6') were visible at 41.06, 22.61, 39.68 and 26.68 ppm respectively. Confluentin structure is terpenoid in nature having an isoprene skeleton side chain.

For ^{1}H-NMR spectrum, two doublets were observed at 5.478 (j= 10 Hz) and 6.593 (j= 10 Hz) ppm representing H-3 and H-4 respectively. Two singlets visible at 6.116 and 6.241 ppm represents the protons H-6 and H-8 respectively. A multiplet at 5.082 ppm (j= 7.0 Hz) ppm indicates the presence of two protons attached to methine carbons (H-3' and H-7'). A singlet at 2.201 ppm was corresponds to protons of methyl group (H-13') attached to the aromatic ring. The signal for the methyl protons (H-9', H-10', H-11' and H-12') attached to the side chain

primary carbons were observed as singlets at 1.670, 1.587 and 1.575 and 1.374 ppm respectively. The signals for the protons bound to the methylene (-CH_2-) carbons (C-1', C-2', C-5' and C-6') were visible as multiplets from 1.740 to 2.120 ppm.

In COSY spectrum, cross peak at 5.478 (j= 10 Hz) and 6.593 ppm (j= 10 Hz) are due to two neighboring aromatic protons (H-3 and H-4). Cross peaks were observed for the H-5' and H-6' at 1.949 ppm and 2.031 ppm. Protons at H-1' and H-2' showed a cross peak at 1.670 and 2.031 ppm. The HQSC spectrum of the confluentin revealed resonances for three methyl groups at 1.670 ppm (H-9'), 1.587 ppm (H-10'), 1.575 ppm (H-11') and two aromatic methyl group at 1.374 ppm (H-12') and 2.201ppm (H-13'). The carbons at position C-2, C-4' and C-8', displayed no resonance signals with ^{1}H signal indicating quaternary carbons. Due to the unavailability of a chiral column (HPLC), it was not possible confirm the stereochemistry of the purified compound.

Grifolin and confluentin are structurally relatable to each other. Either grifolin can be a precursor in confluentin formation or vice versa. Confluentin has a pyran ring in its structure, which could possibly be formed due to the bonding between aromatic hydroxyl (at C-4) and carbon (C-3') of the side chain of grifolin. Or, it is also possible that grifolin could have been formed by the breakage of bond between oxygen and carbon-2 of pyran ring of confluentin.

3.3.10 NMR Spectrum of the compounds purified from *A. flettii*

3.3.10.1 Grifolin ($C_{22}H_{32}O_2$)

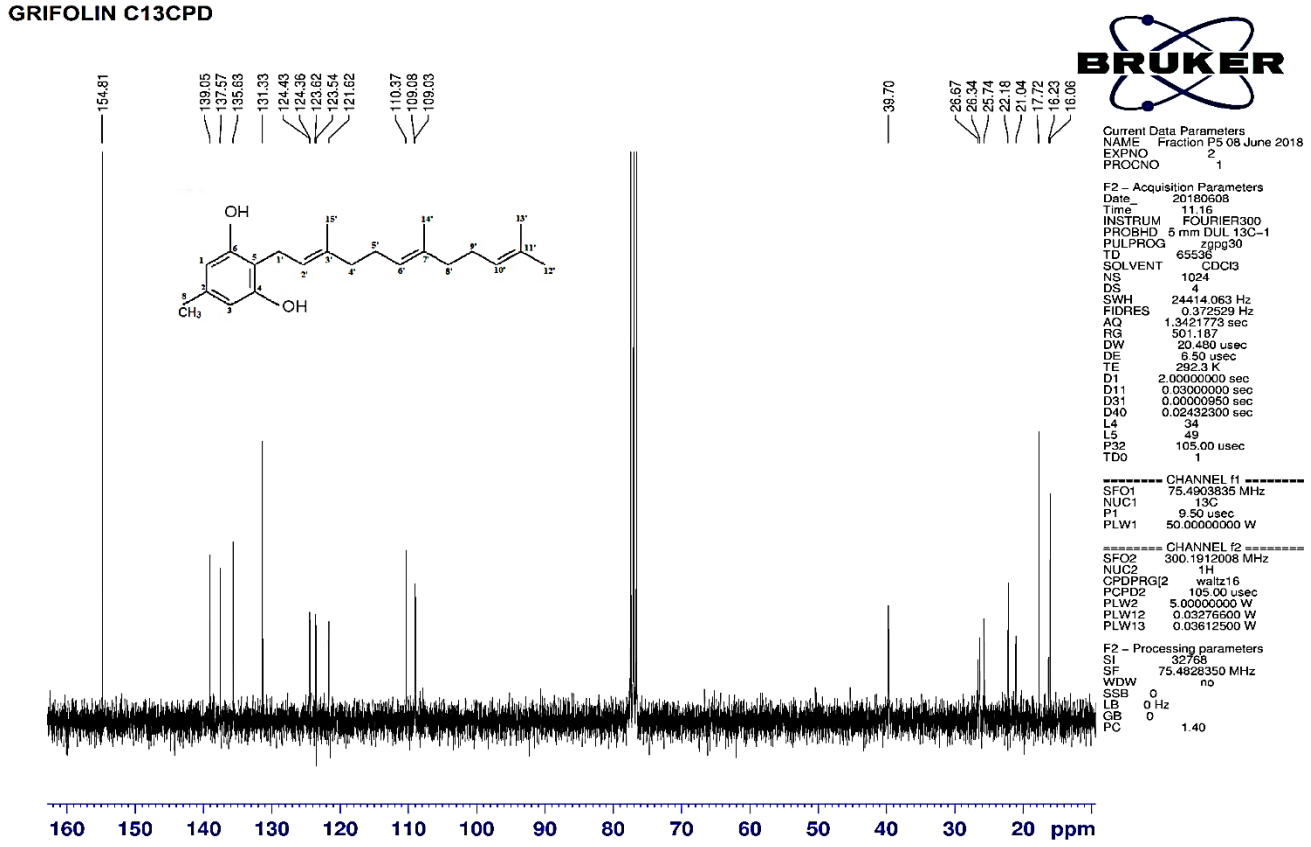

Figure 3. 34 ^{13}C-NMR spectrum of grifolin in $CDCl_3$ containing 0.3% TMS.

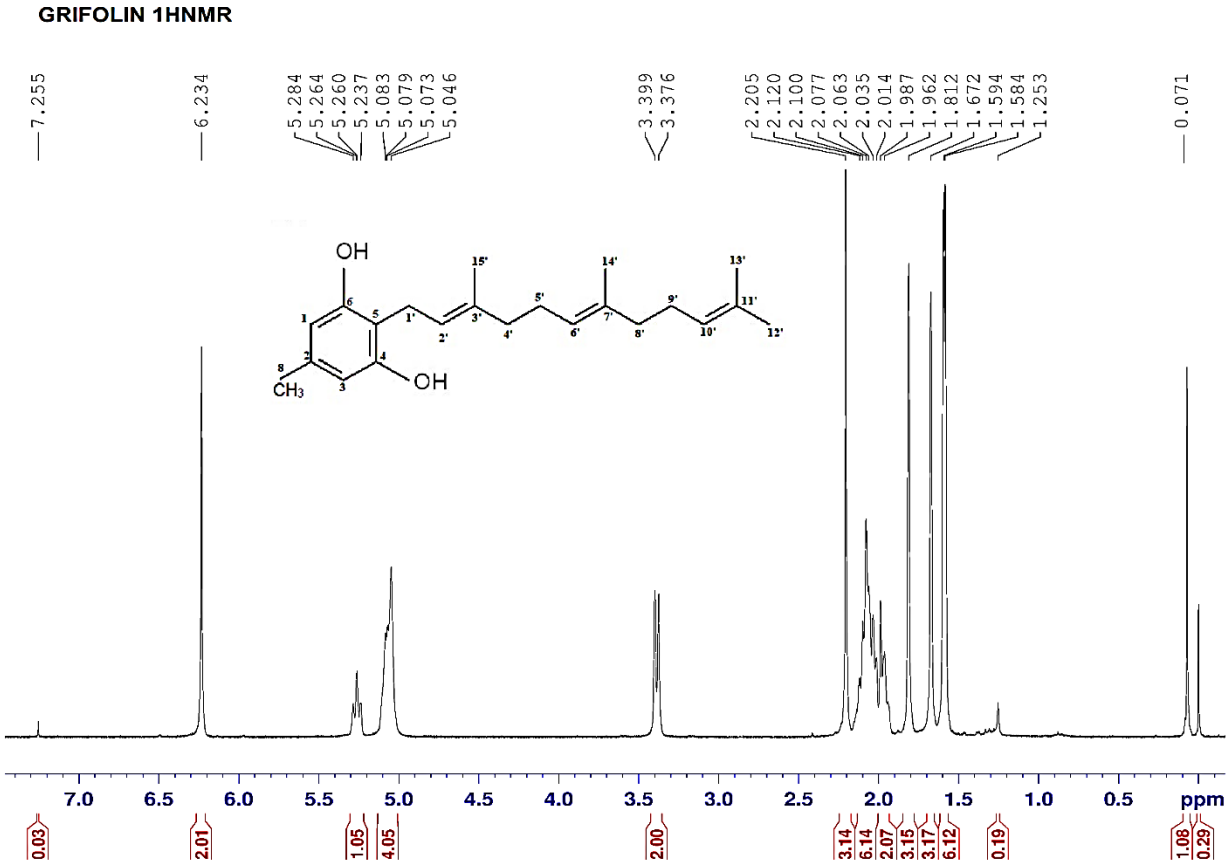

Figure 3. 35 ^{1}H-NMR spectrum of grifolin in $CDCl_3$ containing 0.3% TMS.

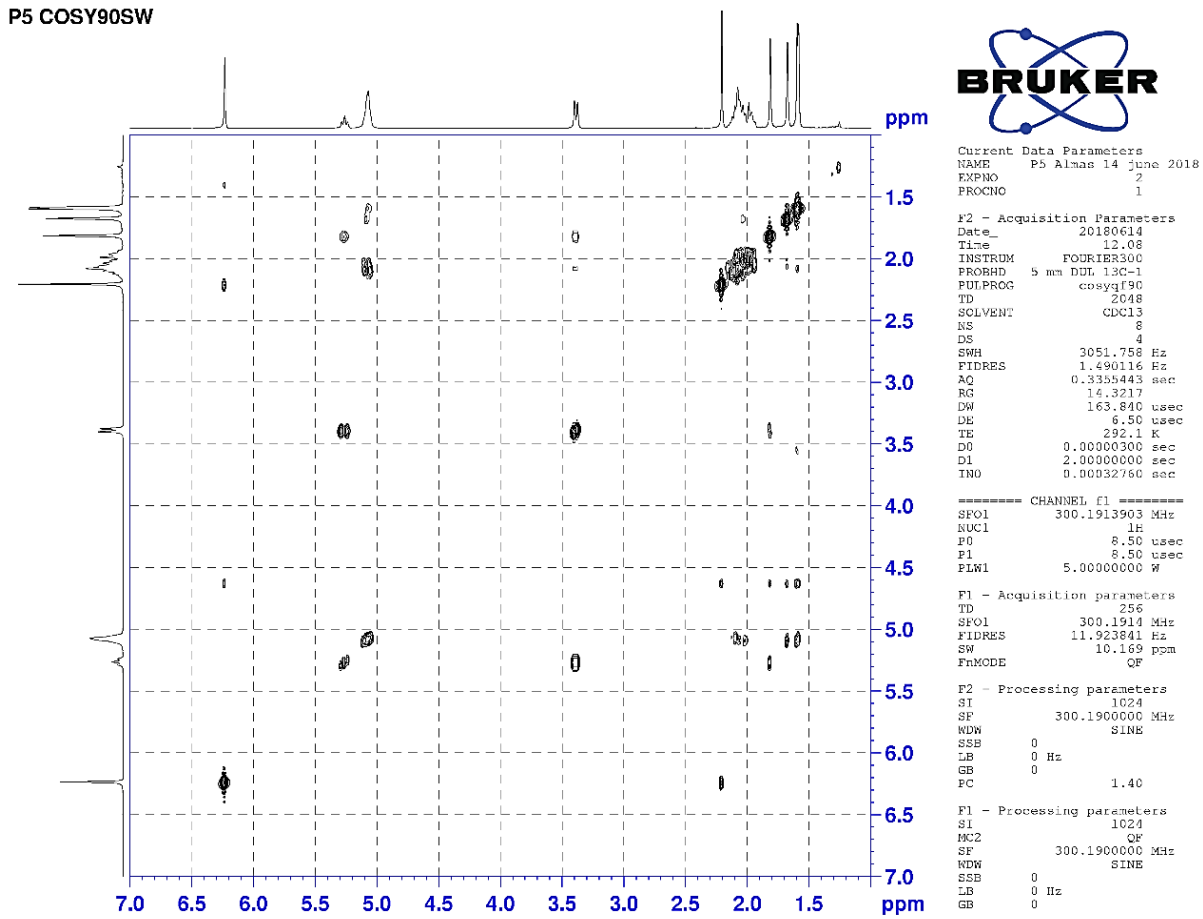

Figure 3. 36 ^{1}H- ^{1}H NMR correlation spectroscopy (COSY) 2D spectrum of grifolin in $CDCl_3$ containing 0.3% TMS.

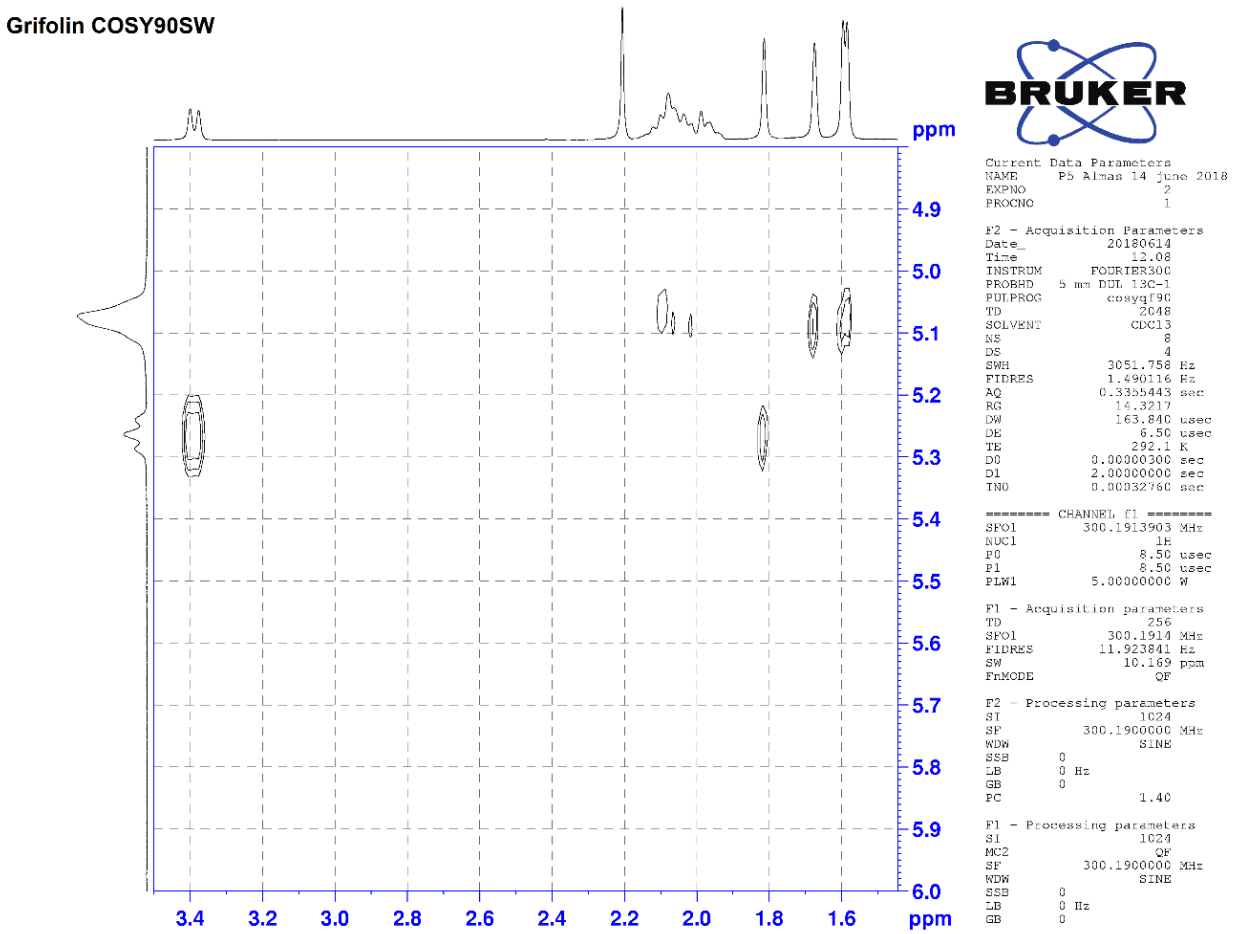

Figure 3. 37 ^{1}H- ^{1}H NMR correlation spectroscopy (COSY) 2D spectrum of grifolin (expanded).

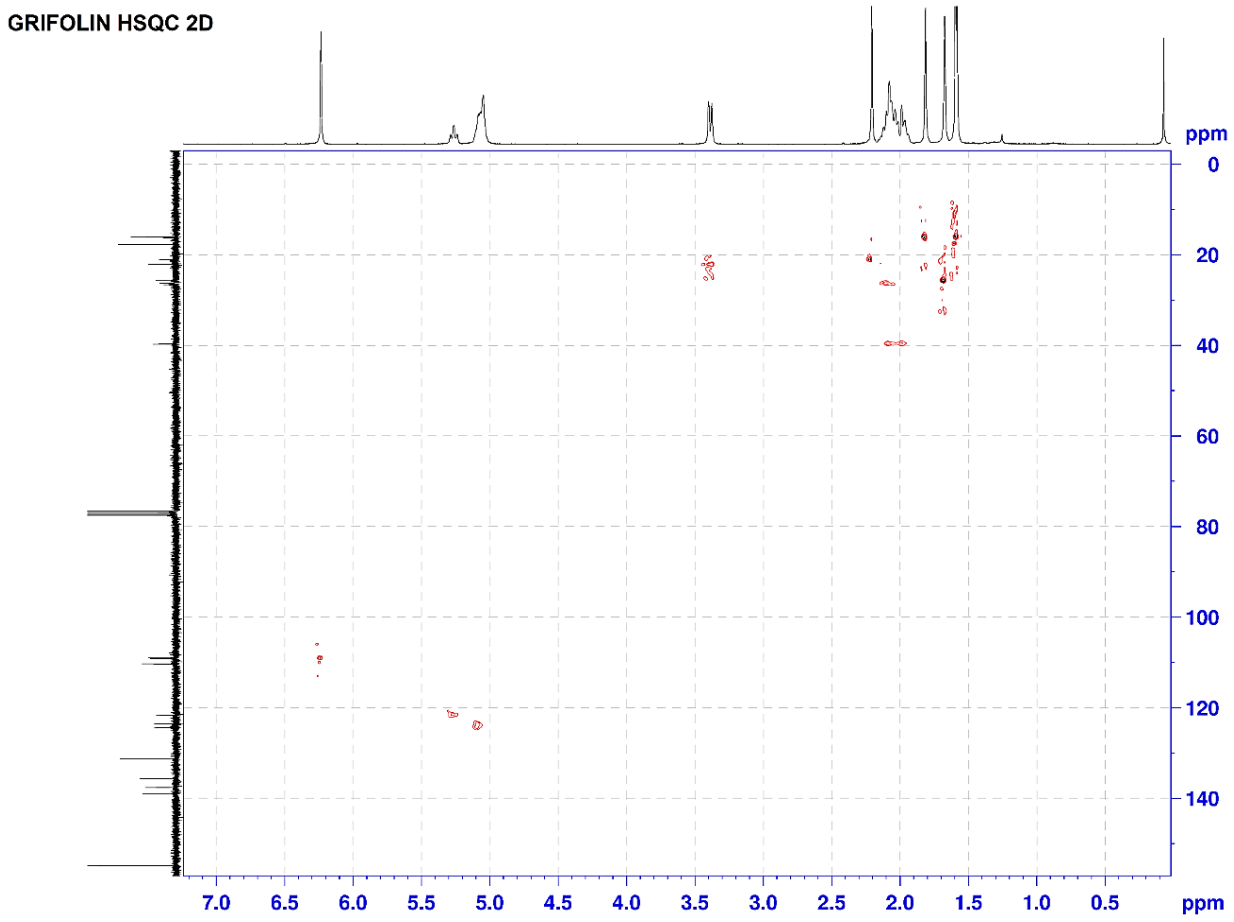

Figure 3. 38 HSQC-NMR-2D (^{13}C-^{1}H-NMR) spectrum of grifolin in $CDCl_3$ containing 0.3% TMS.

3.3.10.2 Neogrifolin ($C_{22}H_{32}O_2$)

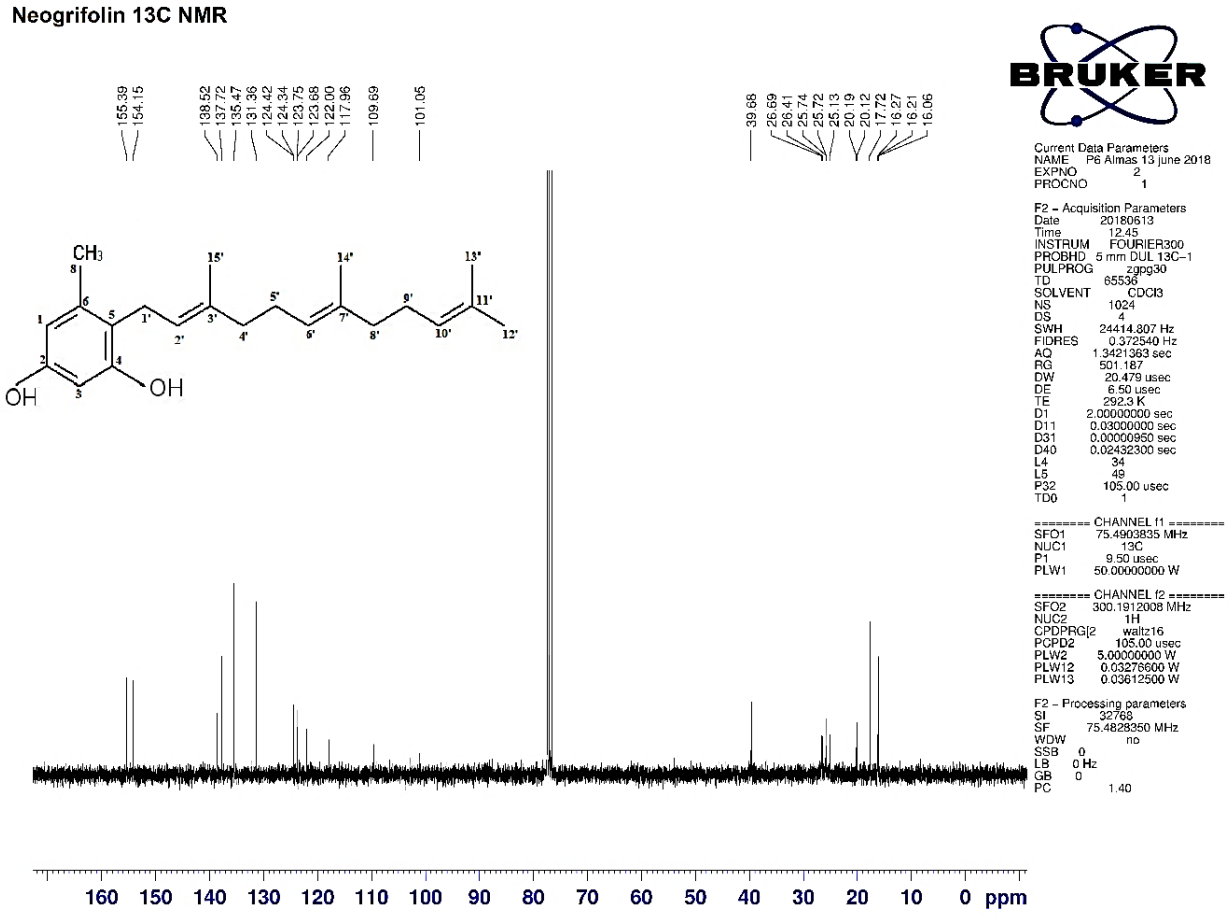

Figure 3. 39 ^{13}C-NMR spectrum of neogrifolin in $CDCl_3$ containing 0.3% TMS.

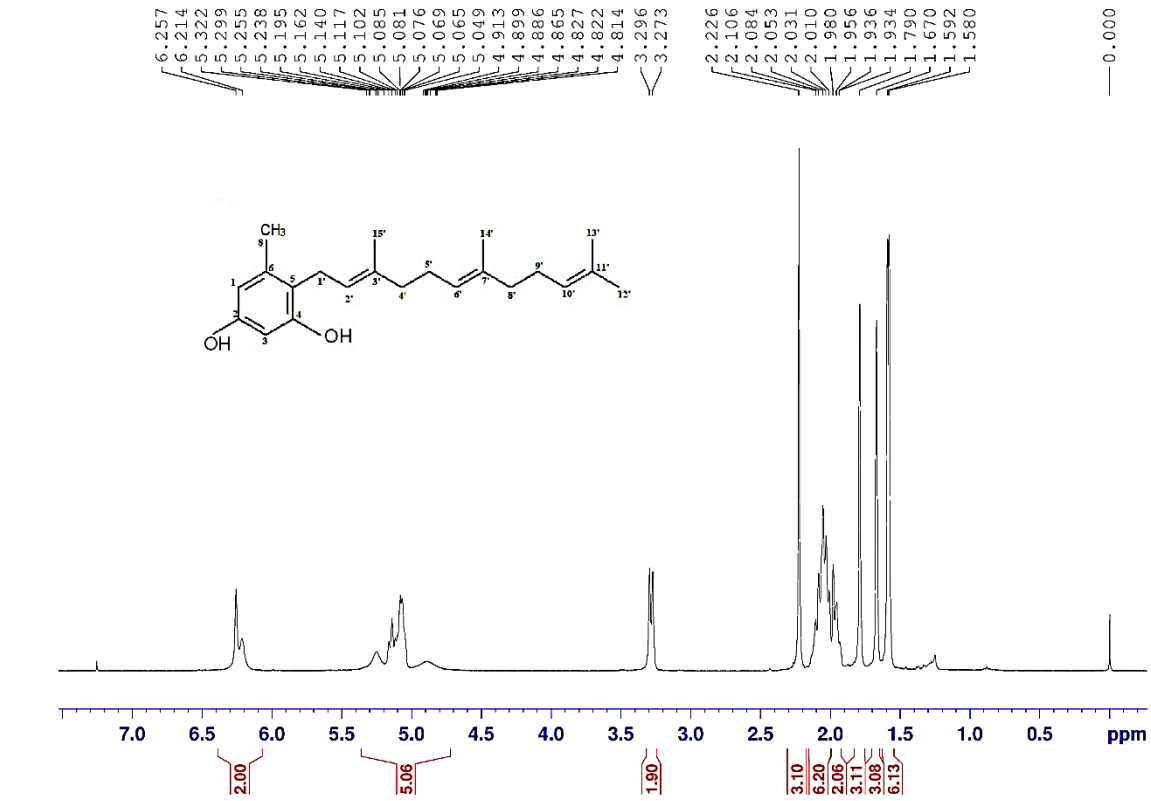

Figure 3. 40 ^{1}H-NMR spectrum of neogrifolin in $CDCl_3$ containing 0.3% TMS.

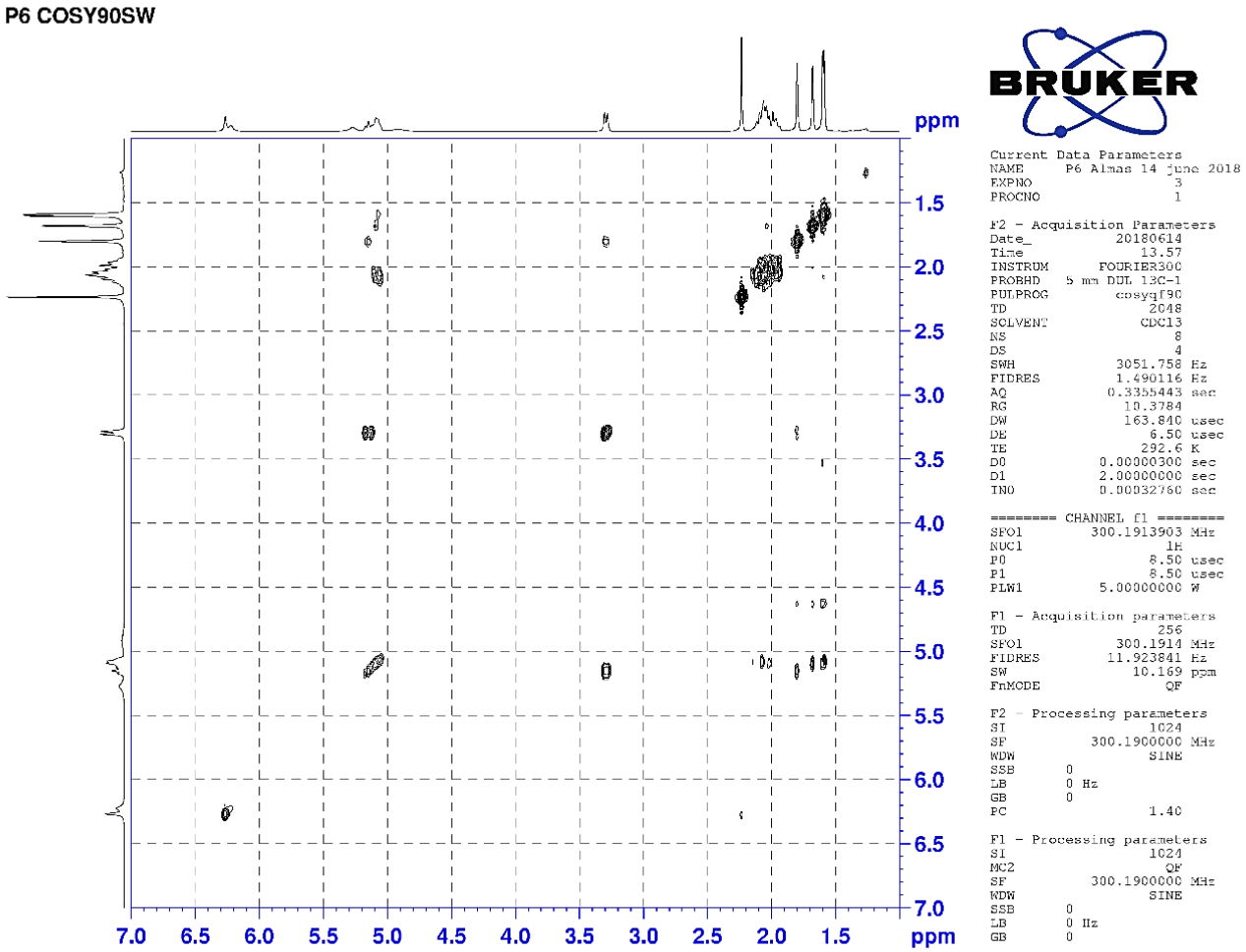

Figure 3. 41 ^{1}H- ^{1}H NMR correlation spectroscopy (COSY) 2D spectrum of neogrifolin in $CDCl_3$ containing 0.3% TMS.

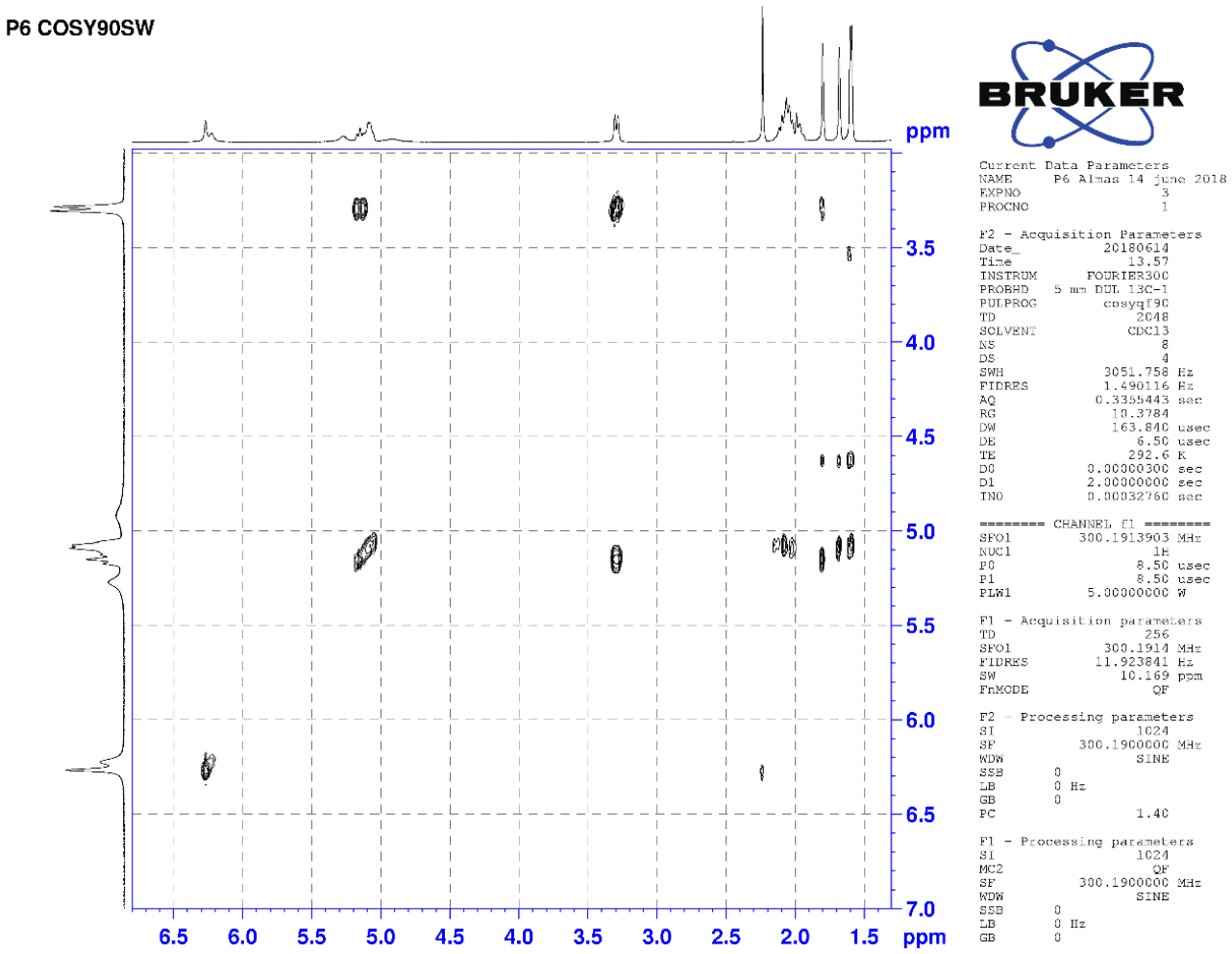

Figure 3. 42 ^{1}H- ^{1}H NMR correlation spectroscopy (COSY) 2D spectrum of neogrifolin (expanded).

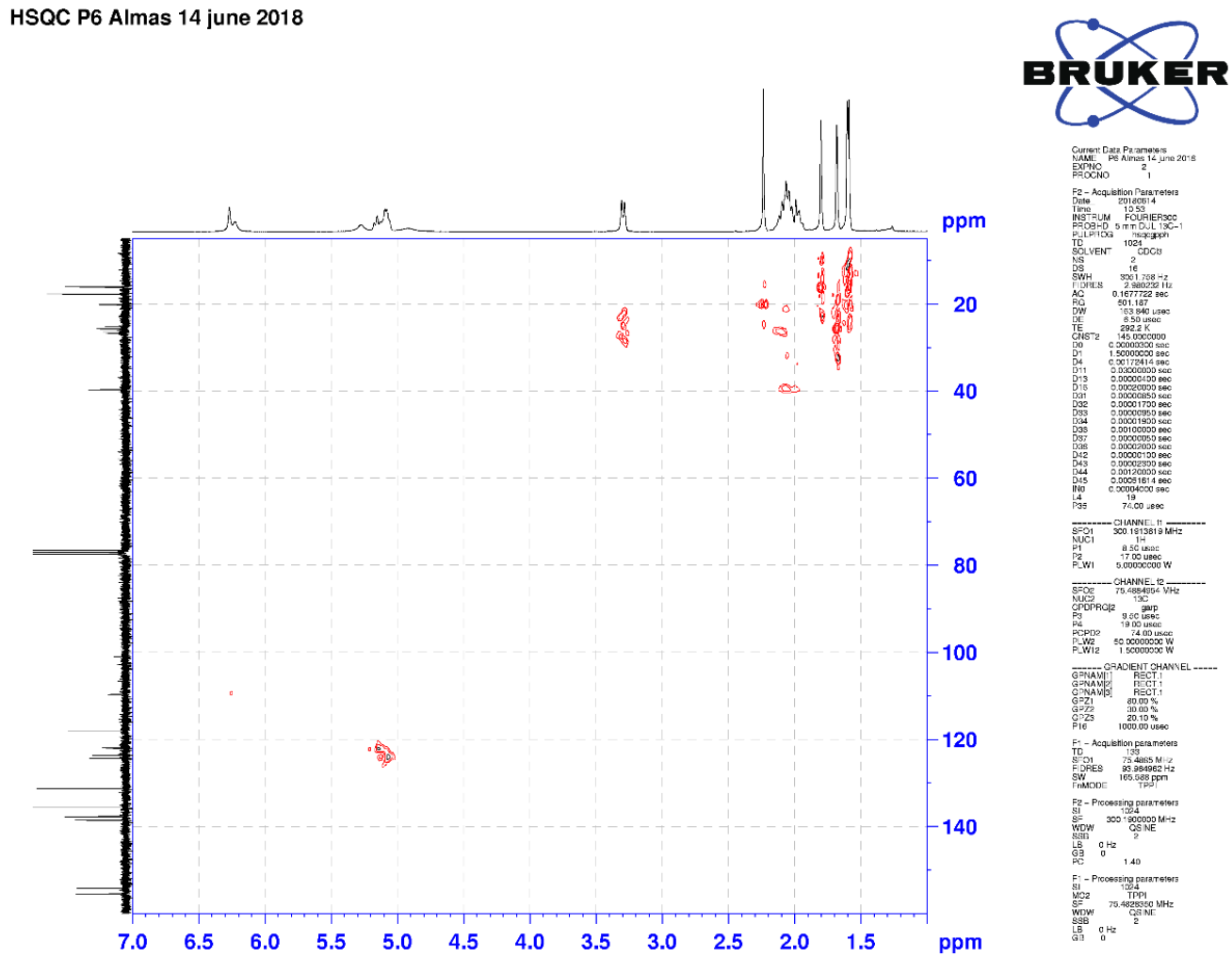

Figure 3. 43 HSQC-NMR-2D (^{13}C-^{1}H-NMR) spectrum of neogrifolin in $CDCl_3$ containing 0.3% TMS.

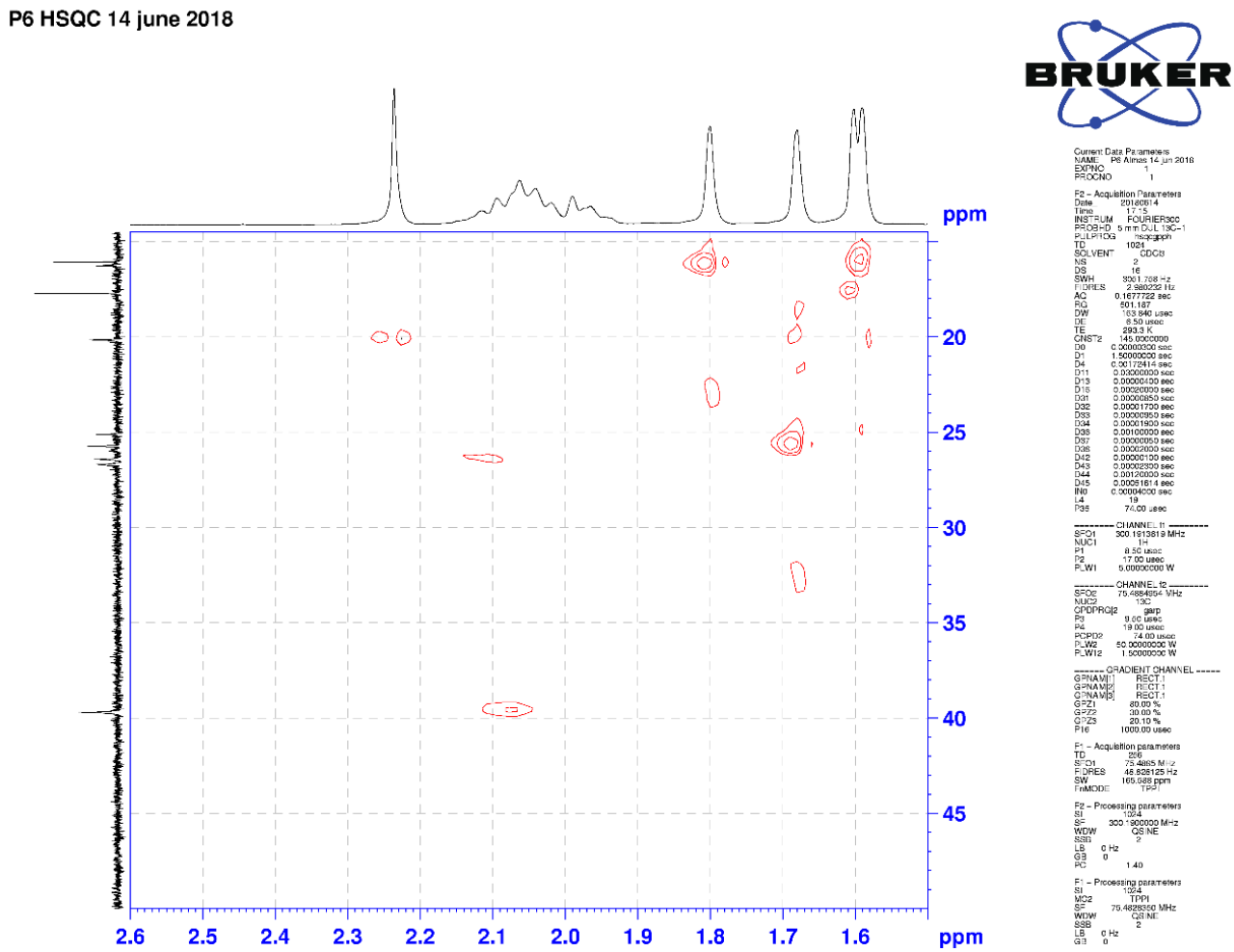

Figure 3. 44 HSQC-NMR-2D (^{13}C-^{1}H-NMR) spectrum of neogrifolin (expanded).

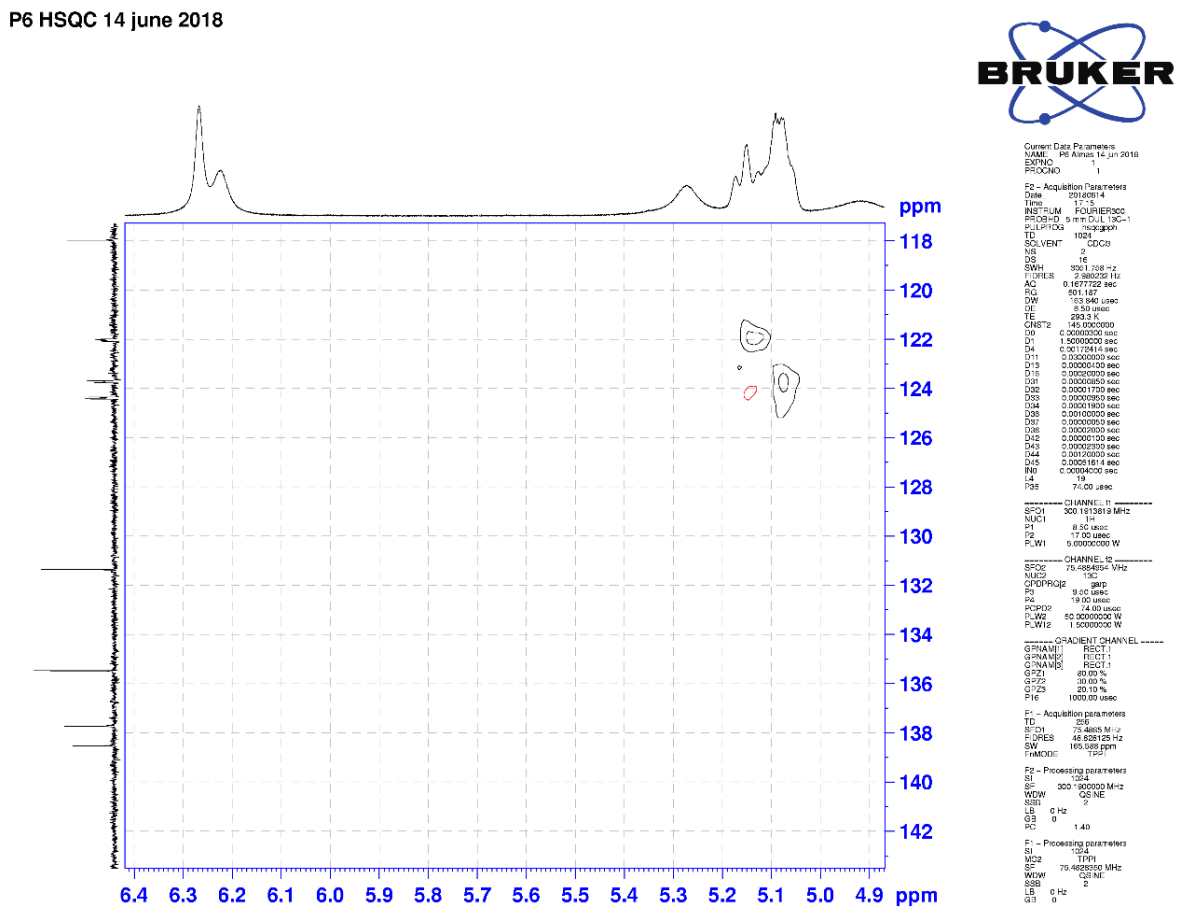

Figure 3. 45 HSQC-NMR-2D (^{13}C-^{1}H-NMR) spectrum of neogrifolin (expanded).

3.3.10.3 Confluentin ($C_{22}H_{30}O_2$)

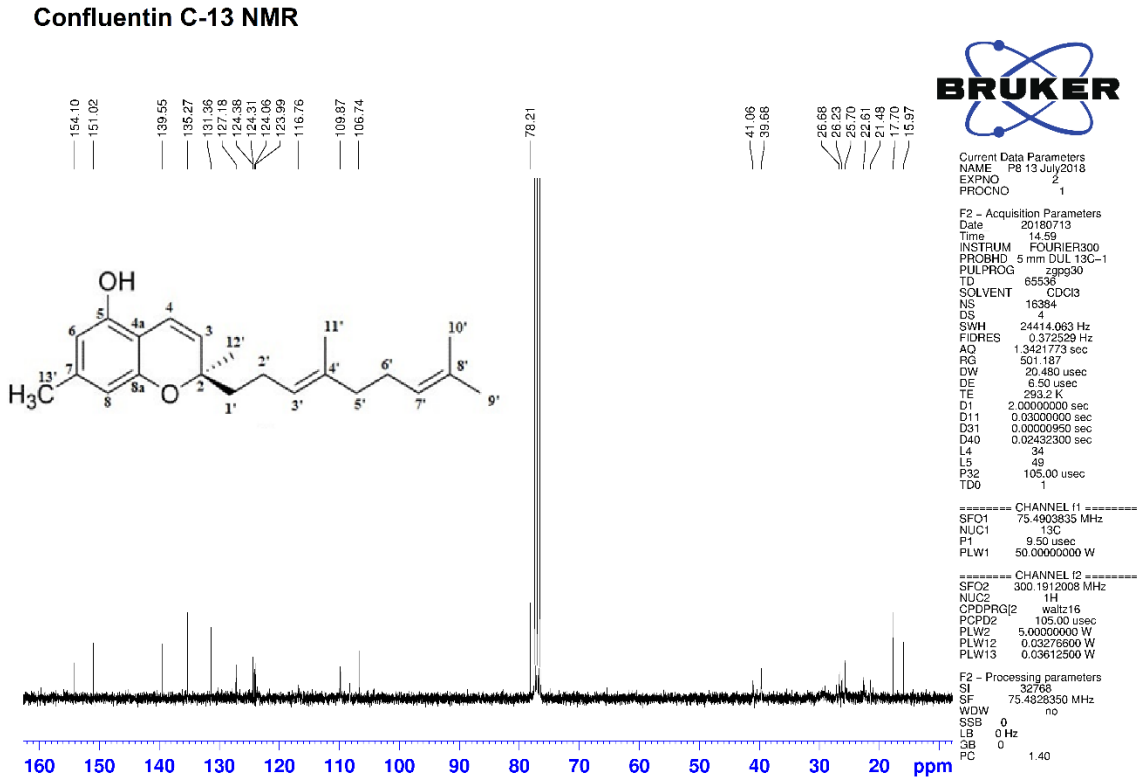

Figure 3. 46 ^{13}C-NMR spectrum of confluentin in $CDCl_3$ containing 0.3% TMS.

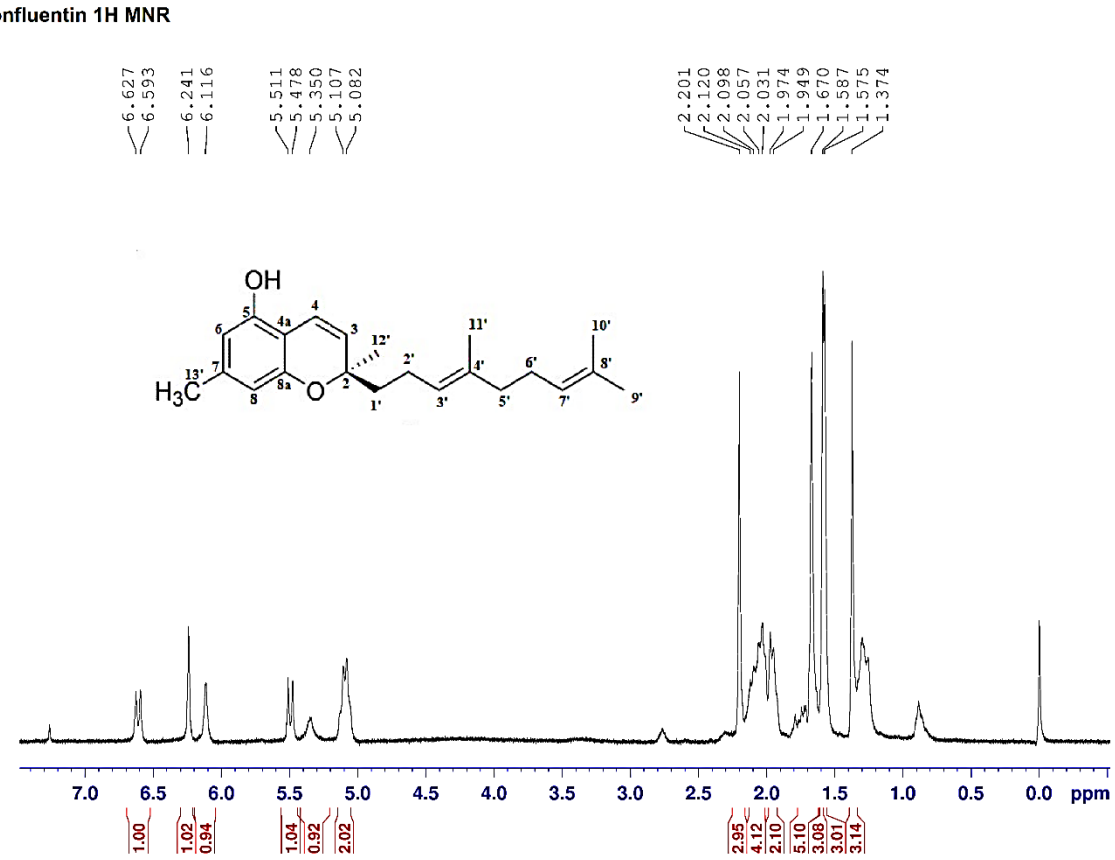

Figure 3. 47 ^{1}H-NMR spectrum of confluentin in $CDCl_3$ containing 0.3% TMS.

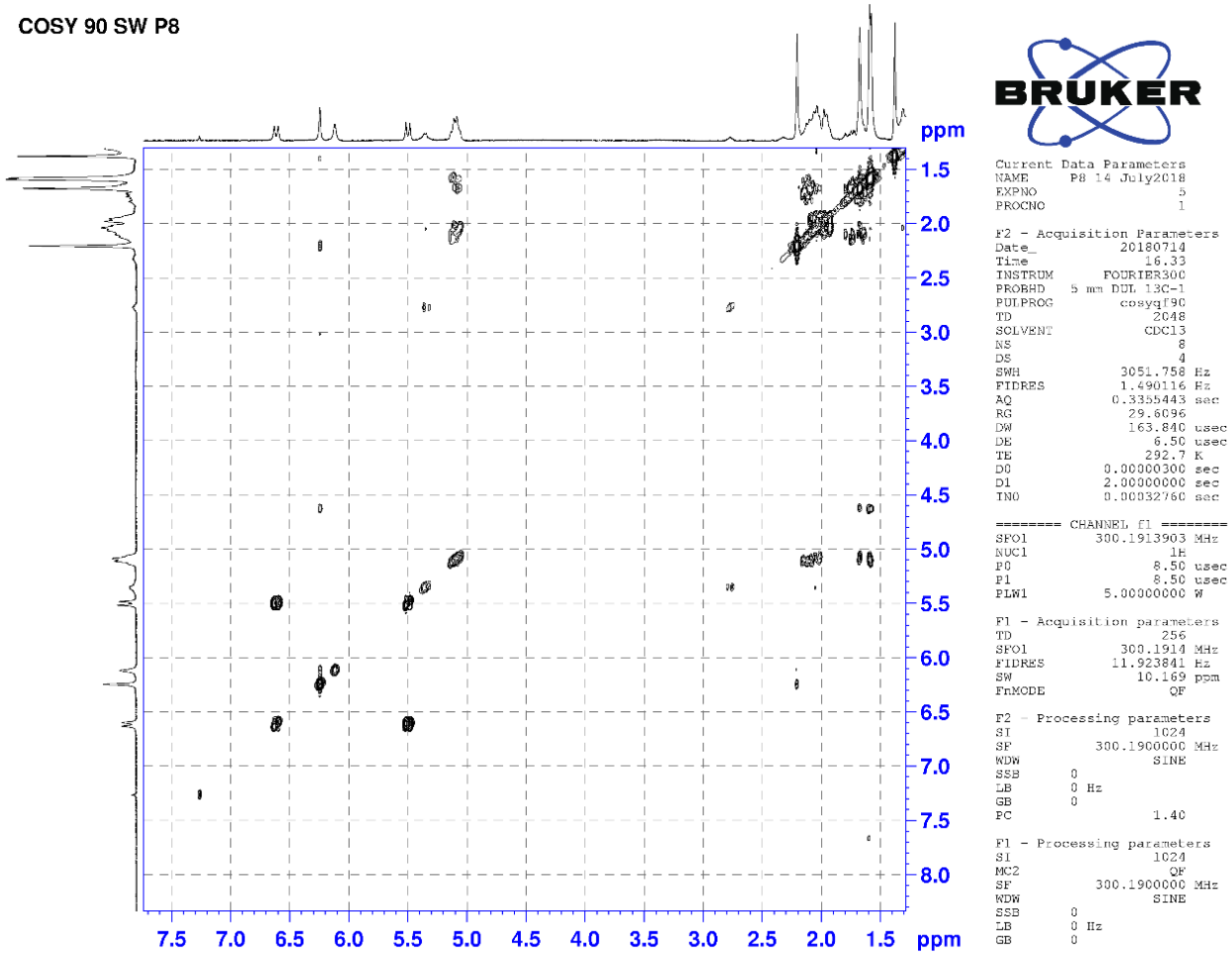

Figure 3. 48 ^{1}H- ^{1}H NMR correlation spectroscopy (COSY) 2D spectrum of confluentin in $CDCl_3$ containing 0.3% TMS.

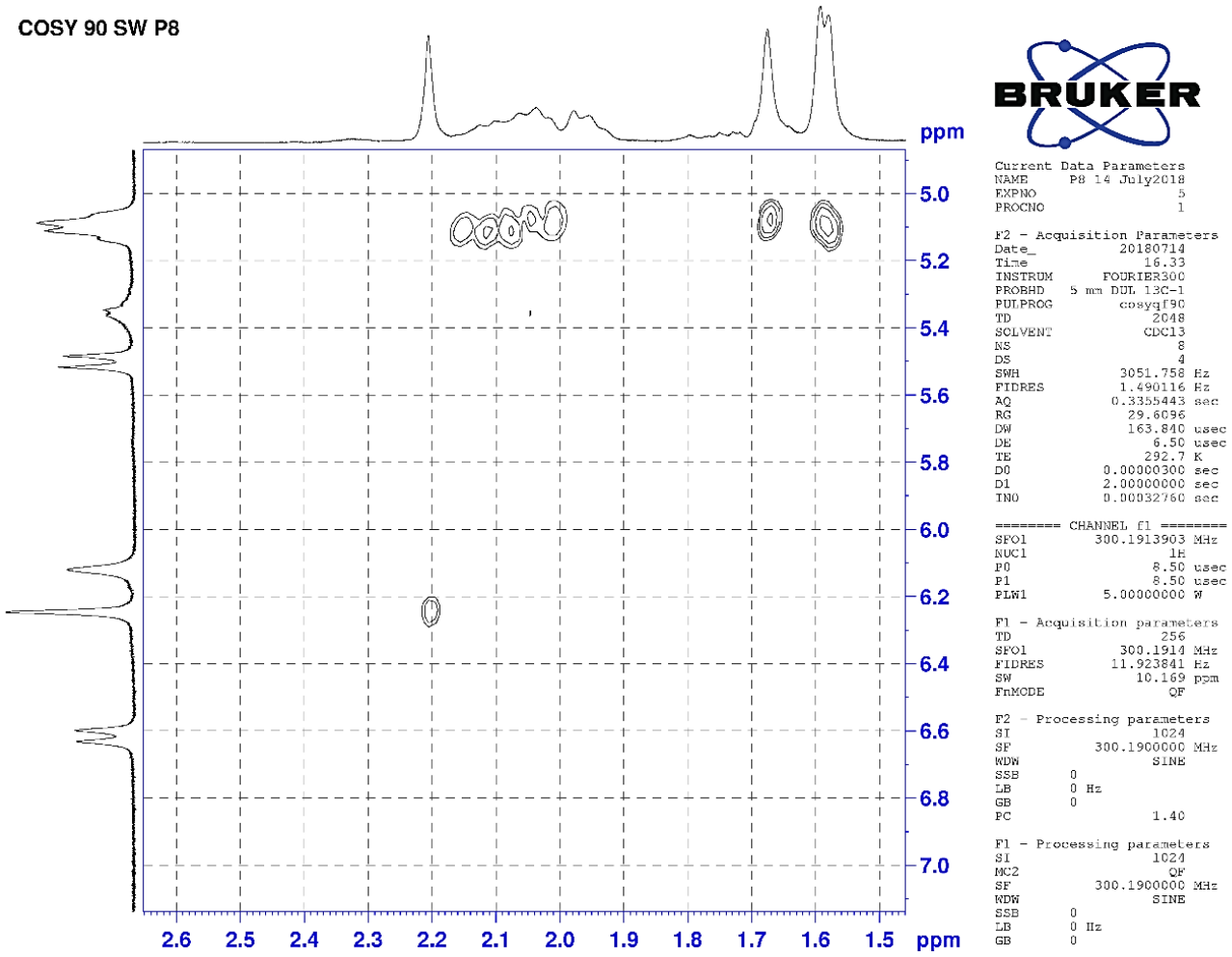

Figure 3. 49 ^{1}H- ^{1}H NMR correlation spectroscopy (COSY) 2D spectrum of confluentin (expanded).

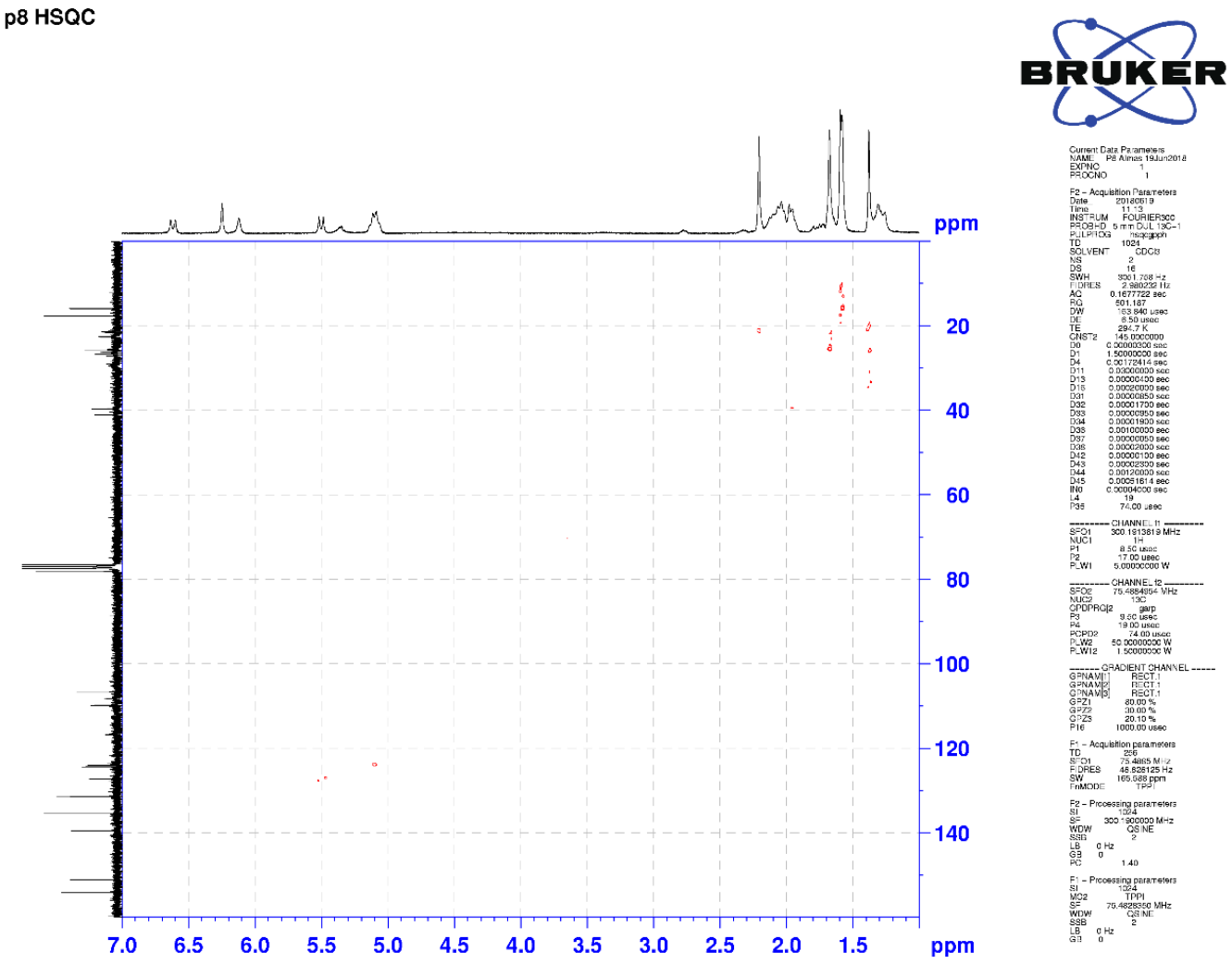

Figure 3. 50 HSQC-NMR-2D (^{13}C-^{1}H-NMR) spectrum of confluentin in $CDCl_3$ containing 0.3% TMS.

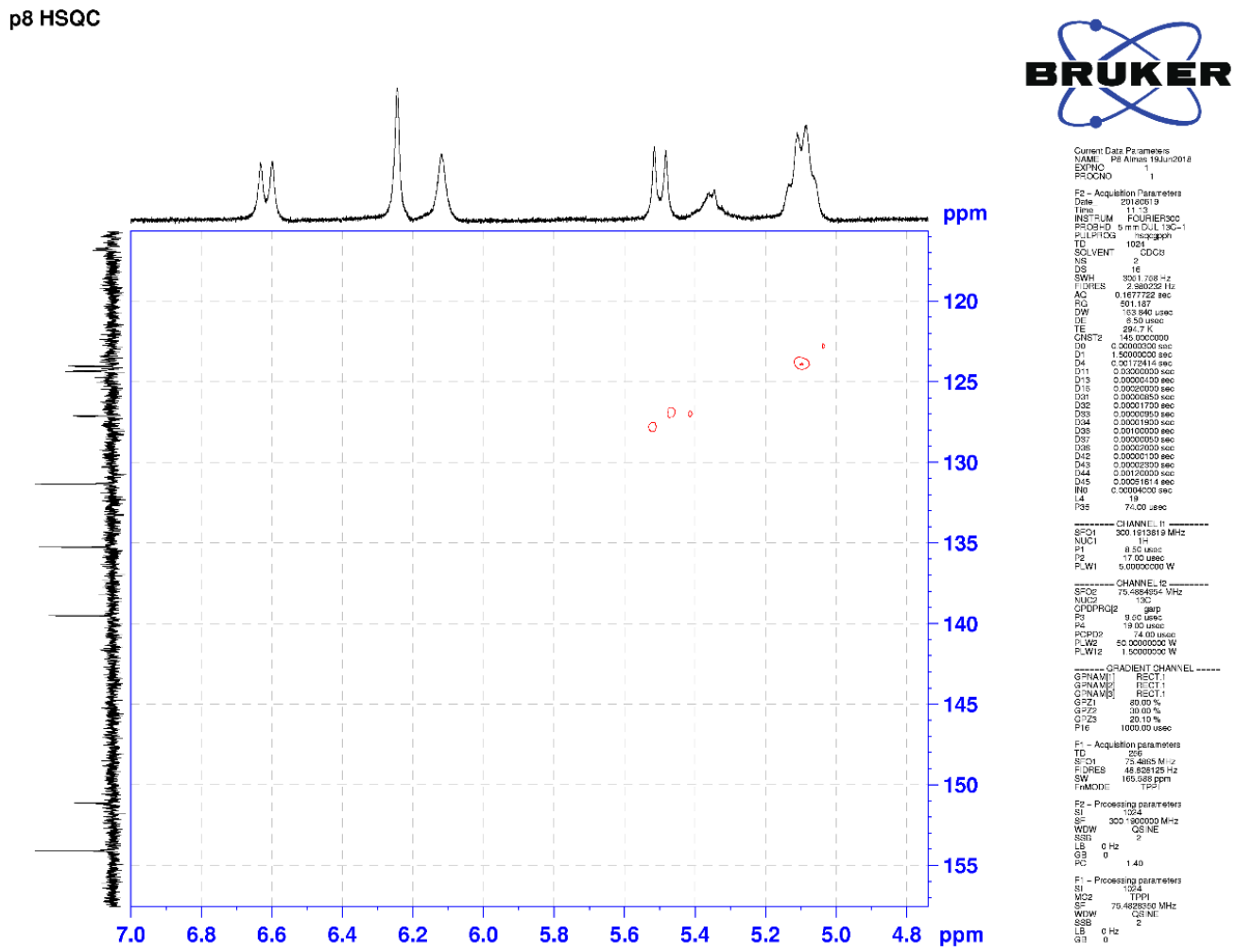

Figure 3. 51 HSQC-NMR-2D (^{13}C-^{1}H-NMR) spectrum of confluentin (expanded).

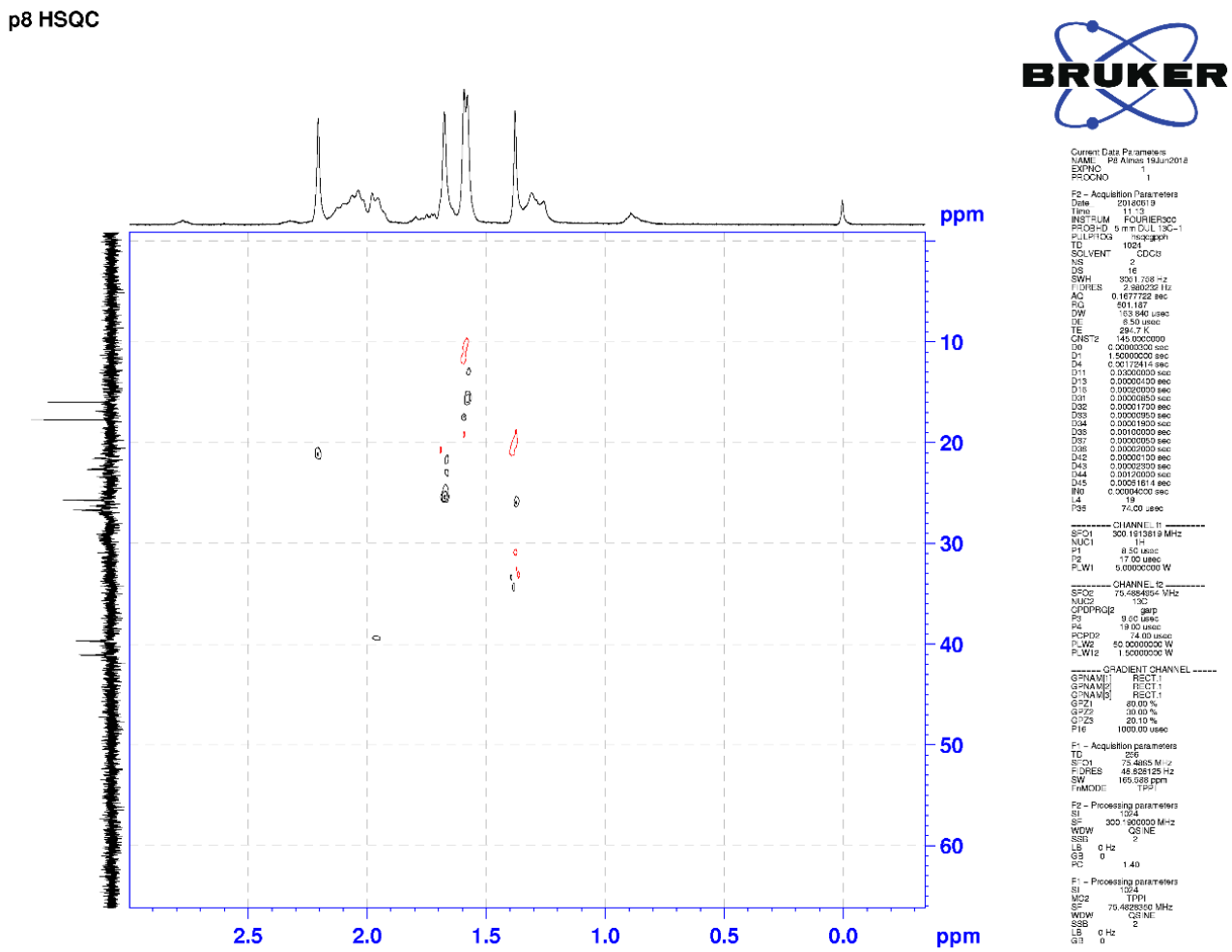

Figure 3. 52 HSQC-NMR-2D (^{13}C-^{1}H-NMR) spectrum of confluentin (expanded).

3.3.10.4 Physical properties of the purified compounds from *A. flettii*

The three major compounds (Peak 5, Peak 6 and Peak 8), purified using HPLC, were lyophilized. All three compounds had very distinctive physical characteristics. Compound Peak 5 (grifolin) was cream color fluffy (needle shaped) powder, while compound Peak 6 (neogrifolin) was oily in nature and yellowish brown in color. The physical appearance of compound Peak 8 (confluentin) was completely different from the previous two pure compounds (grifolin and neogrifolin): it was light brown sticky paste (Figure 3.53).

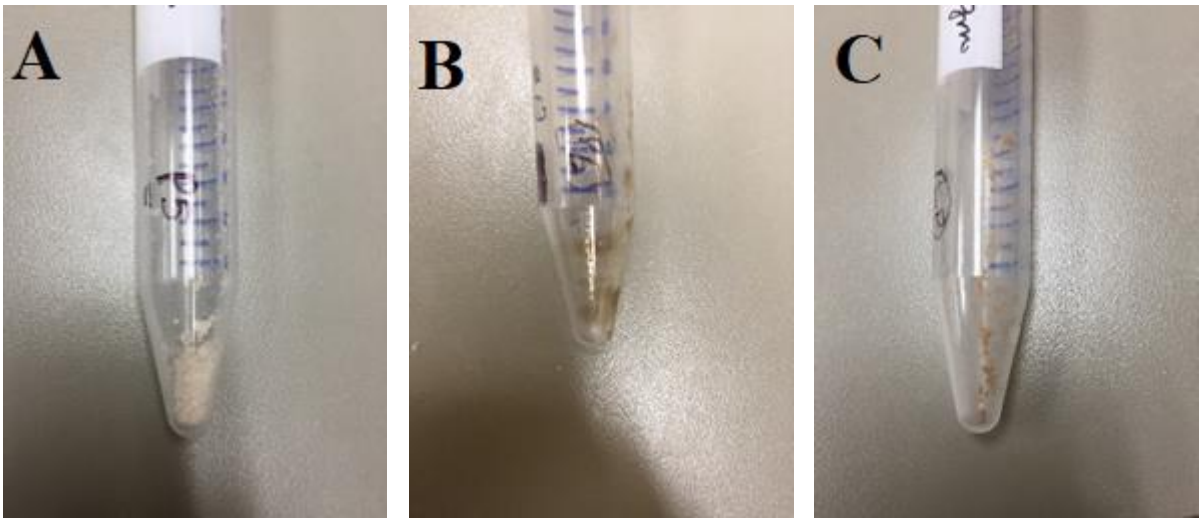

Figure 3. 53 Photographs of three purified compounds from *A. flettii*.

(A) Grifolin: Cream color (needle) powder: **(B)** Neogrifolin: Brownish colored oil: **(C)** Confluentin: Brownish colored sticky compound

3.3.11 Intrinsic reductive potential of purified compounds in cell-based and cell-free environment

Anti-oxidant compounds can directly reduce the MTT dye (yellow) to formazan crystals (purple). Because of this intrinsic reduction potential of plant extracts, phytoestrogens and anti-oxidants, MTT tetrazolium assay may lead to false negative growth-inhibitory results (Bruggisser et al., 2002). Grifolin has been shown to possess antioxidant properties (Jing et al.,

2017). Therefore, grifolin has an intrinsic reduction potential toward MTT dye. Neogrifolin could also be anti-oxidant in nature, because of its structural similarity with grifolin and interaction with MTT dye.

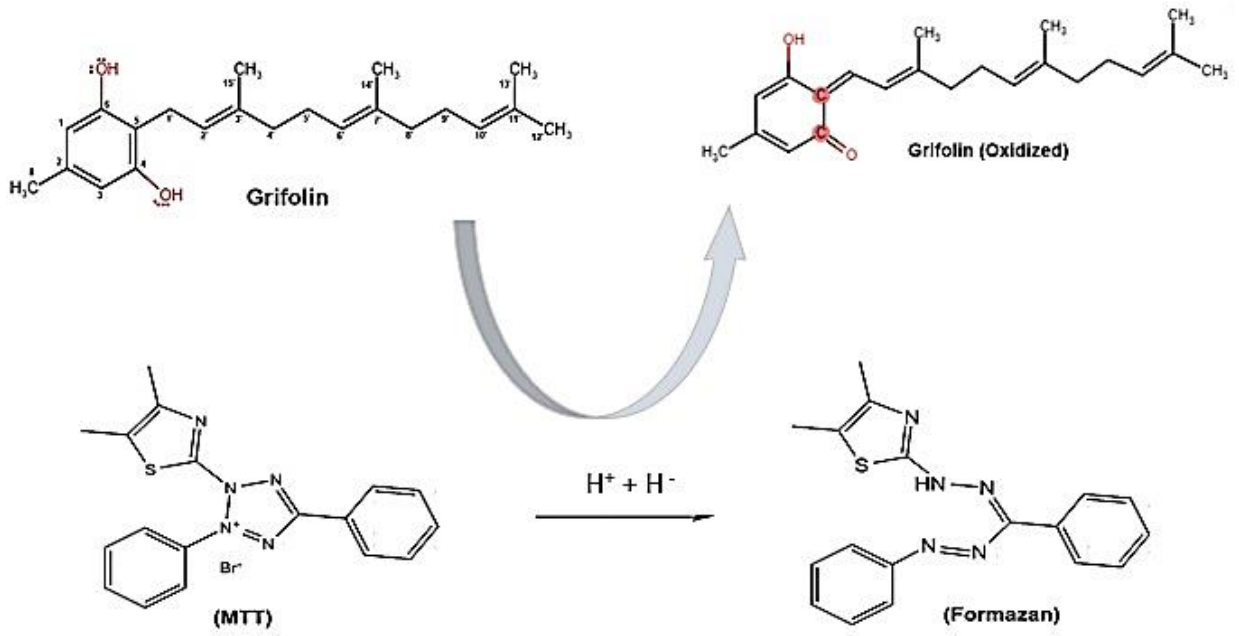

Figure 3. 54 Illustration of proposed mechanism of MTT dye reduction by grifolin.

Treatment of HeLa cells with higher doses of the purified compounds resulted in false negative growth-inhibitory results. Although HeLa cell numbers were decreased (observed microscopically), interestingly formation of formazan (purple color) also increased, suggesting a direct interaction of these purified bioactive compounds with the MTT reagent.

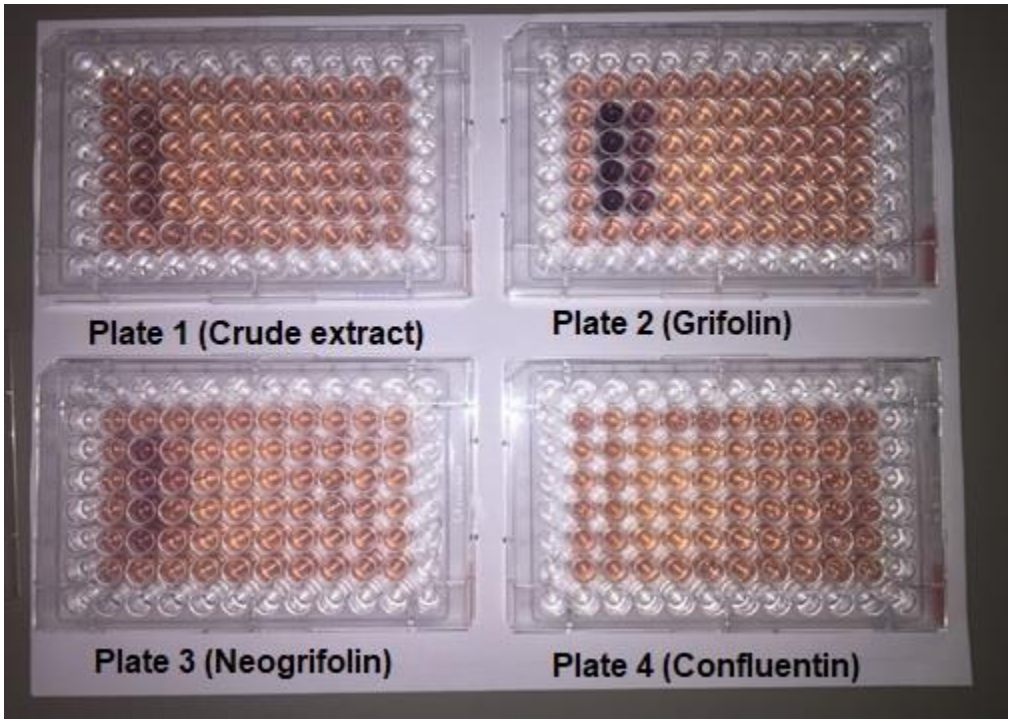

Figure 3. 55a Reductive potential of *A. flettii* crude extract (top left); P5 (grifolin: top right), P6 (neogrifolin: lower left) and P8 (confluentin: Lower right) at different doses. (Plate columns from left to right represent were Negative control, 0.25 mg/mL, 0.1 mg/mL, 0.075 mg/mL, 0.05 mg/mL, 0.035 mg/mL, 0.025 mg/mL, 0.010 mg/mL, 0.005 mg/mL and Negative control)

The interaction of purified compounds with MTT solution can clearly be seen in Figure 3.55a. Plates 1, 2, 3 and 4 are representative of crude extract, grifolin, neogrifolin and confluentin respectively. Grifolin exhibited the strongest interaction (at 0.25 and 0.1 mg/mL) with MTT solution as compared to the crude extract and neogrifolin. Confluentin showed no interaction with MTT tetrazolium dye. This interesting observation indicates the possibility of false negative growth-inhibitory results using natural compounds with intrinsic reduction potential towards MTT tetrazolium bromide reagent. Neogrifolin and crude extract showed interaction at 0.25 mg/mL only.

The reduction potential of grifolin and neogrifolin towards MTT dye was reconfirmed in a cell-free environment. Figure 3.55b represents the reduction of MTT (5 mg/mL) into formazan after incubation with equal volume of grifolin and neogrifolin solution (1 mg/mL). Figure 3.47 illustrates the proposed mechanism behind reduction of MTT dye by grifolin.

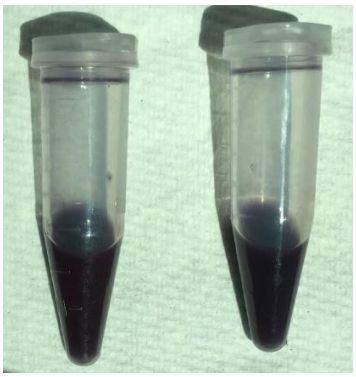

Figure 3.55b Intrinsic reductive potential of grifolin (left) and neogrifolin (right) in a cell free system. MTT tetrazolium bromide (5 mg/mL) and Purified compounds (1 mg/mL) were mixed in equal quantity (300 µL each) in an Eppendorf and incubated for 3 hours at 37 °C.

3.3.12 IC_{50} determination of purified compounds on HeLa cells

Dose-dependent MTT assays of grifolin, neogrifolin and confluentin on HeLa cells were performed. The concentration range tested was from 7.6 to 228 µM. As shown in Figure 3.56, grifolin and neogrifolin were the most potent growth inhibitors in HeLa cells. The IC_{50} of grifolin and neogrifolin on HeLa cells was 29.85 and 23.22 µM respectively. On the other hand, the IC_{50} of confluentin on HeLa cells was determined to be 50.47 µM, making it the least potent. The cell viability (% of control) of HeLa cells treated with 76.10 µM concentration of grifolin, neogrifolin and confluentin was 11.44, 10.50 and 12.76 respectively. No cytotoxicity was observed in HeLa cells with confluentin at the lowest dose 7.6 µM.

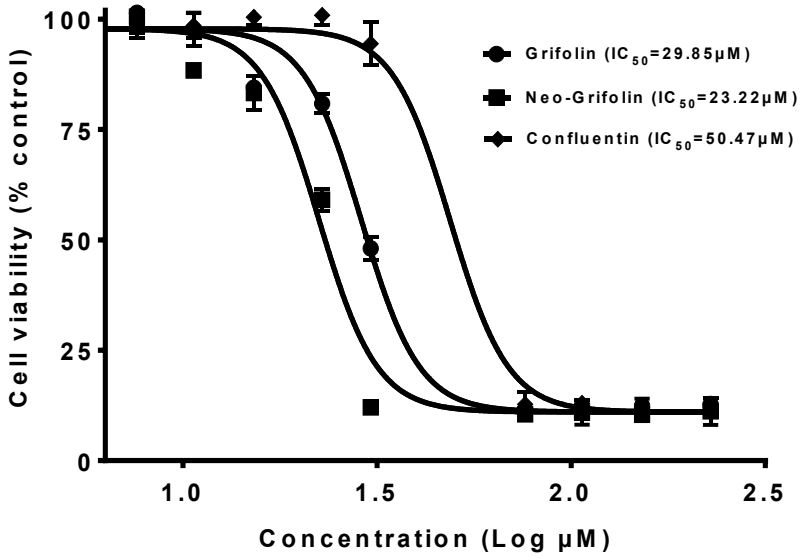

Figure 3. 56 Dose-dependent growth-inhibitory effect of grifolin, neogrifolin and confluentin on HeLa cells. The graph is representative of results from two biological replicates (n=2). Error bars are standard deviation.

3.3.13 IC_{50} determination of purified compounds on human colon cancer cells lines

Similar dose-dependent MTT assay experiment was performed on human colon cancer cell lines SW480 and HT29 cells. Different wells containing 1500 cells each were treated with different final concentrations of grifolin and neogrifolin. The control used was 2% DMSO because the compounds were dissolved in DMSO.

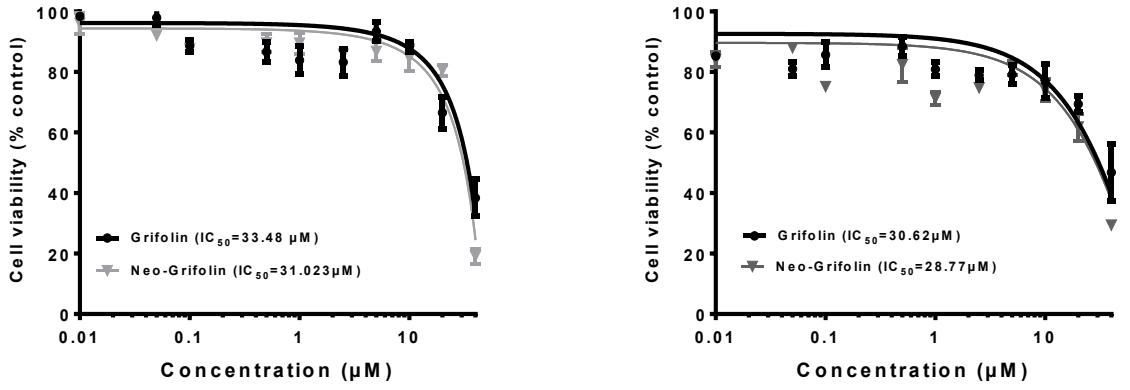

Figure 3. 57 Dose-dependent growth-inhibitory effect of grifolin and neogrifolin human colon cancer cell lines, SW-480 (left) and HT-29 (right)

As shown in Figure 3.57, both compounds appear to have similar effect on SW480 and HT29 cells. The IC_{50} of grifolin on HT-29 cells was 30.62 µM and 33.48 µM on SW-480 cells. However, neogrifolin was slightly more potent than grifolin. The IC_{50} of neogrifolin on SW-480 and HT-29 was 31.023 and 28.77 µM respectively.

3.3.14 Assessing grifolin and neogrifolin on IMP1-KRas RNA interaction using fluorescent polarization method

The fluorescent polarization experiments described here were performed by Mr. Victor Liu. Different concentrations were utilized to determine the potential inhibitory effects of the grifolin and neogrifolin on the interaction between and KRas RNA and IMP1. For IMP1 protein, both the full-length recombinant wild-type IMP1 protein and truncated IMP1 KH34 protein containing only the KH3 and KH4 domains were used.

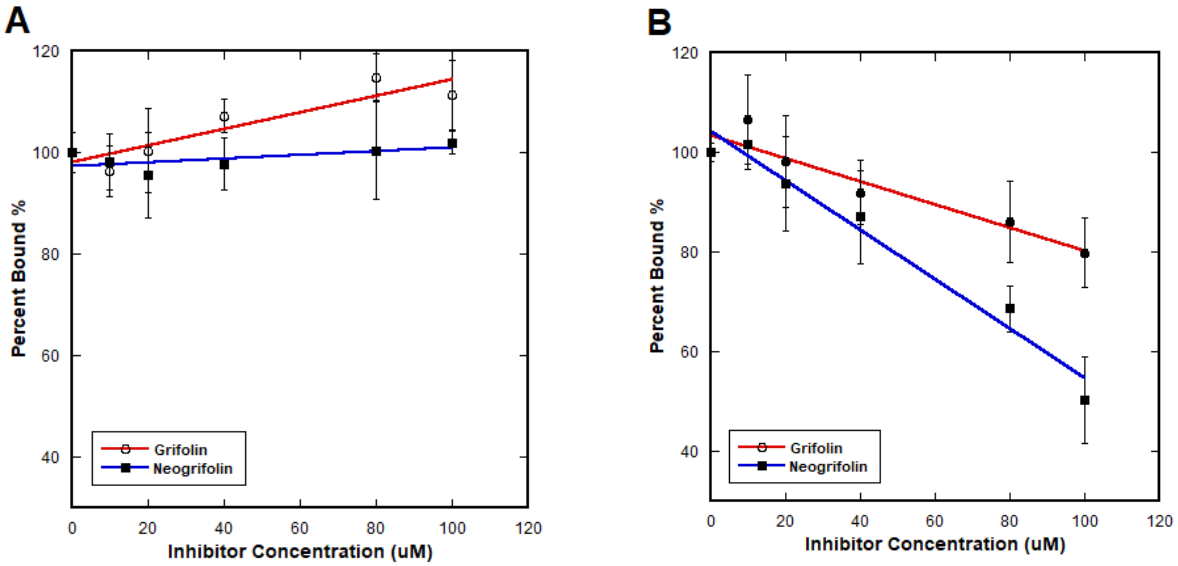

Figure 3. 58 Assessing grifolin and neogrifolin for their ability to disrupt IMP1 and KRas RNA interaction using fluorescent polarization. (A) Dose-dependent effect of grifolin and neogrifolin on the interaction between IMP1 KH34 (300 nM) and fluorescently labeled KRas RNA (10 nM). **(B)** Effect of grifolin and neogrifolin on the interaction between full-length IMP1 (300 nM) and fluorescently labeled KRas RNA (10 nM)

As shown in Figure 3.58A, no inhibitory effect was observed at any concentrations of the grifolin and neogrifolin. In contrast, when the full-length IMP1 protein was used (Figure 3.58B), both grifolin and neogrifolin dose-dependently inhibited IMP1 and KRas RNA interaction.

3.3.15 Assessing grifolin, neogrifolin and confluentin on KRas expression using Western blot analysis

Based on the results from fluorescent polarization experiments, it was deemed logical to assess the purified growth-inhibitory compounds (grifolin, neogrifolin and confluentin) from *A. flettii* on KRas expression in colon cancer cells. K-Ras4a and K-Ras4b are two splice variants of KRAS. Although both isoforms have a lot of similarities, there are also major differences. The major difference is based on their disordered C-terminal hypervariable region and four catalytic domain residues (G151R/D153E/K165Q/H166Y). They also differ based on the hypervariable region charge; K-Ras4b (+9e) has more charge hypervariable region than K-Ras4a (+6e). (Chakrabarti et al., 2016).

Treatment with three purified compounds (grifolin, neogrifolin and confluentin) elicited growth-inhibitory effect in a concentration-dependent manner in SW480 and HT-29 human colon adenocarcinoma cells (Figure 3.57). To determine whether the purified compounds (grifolin, neogrifolin and confluentin) have any effects on KRas expression, SW480 and HT-29 cell lines were treated with 20 μM of grifolin, neogrifolin and confluentin for 24 hours. The results are described below.

3.3.15.1 HT-29 Cells

HT-29 cells were treated with 20 μM concentration grifolin, neogrifolin and confluentin. After 48 hours of treatment, the KRas-4b levels were found to be down-regulated by grifolin, neogrifolin and confluentin to 48.25, 51.84 and 54.04% respectively (Figure 3.59).

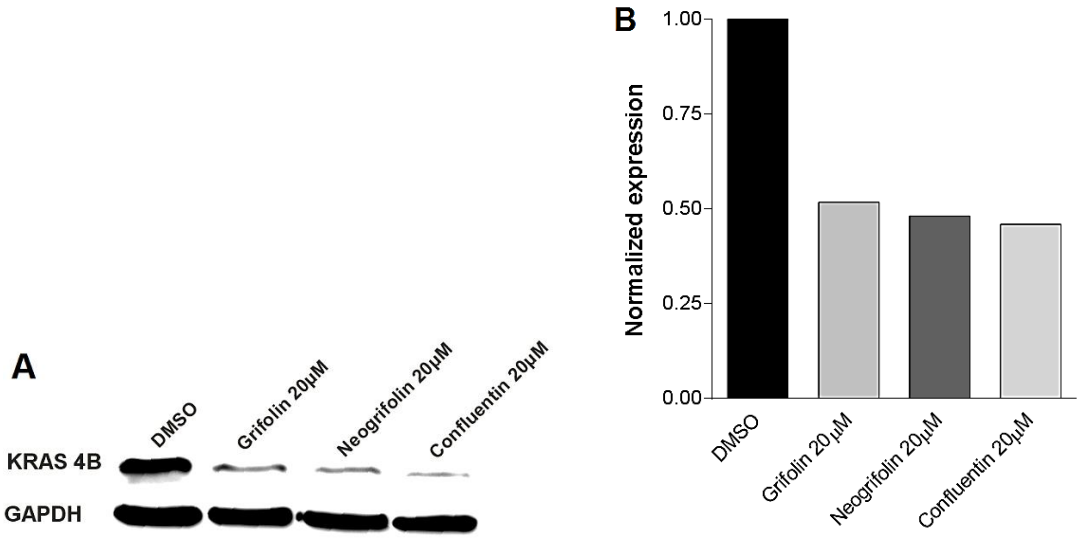

Figure 3. 59 Effects of grifolin, neogrifolin and confluentin on Kras-4b expression in HT29 Colon adenocarcinoma cells. (A) Cells were treated with 20 µM of drugs for 48 hours. Lysates from cells were isolated and subjected to Western blot analysis. **(B)** The Kras-4b band in (A) was normalized to the house-keeping gene GAPDH and expressed relative to the control, DMSO, taken as 1.0.

Lysates from another biological replicates confirmed the results shown in Figure 3.59. The KRas-4b expression levels after treatment with different (20 and 50 µM) concentrations of positive controls (AcQ and VLA9) and purified compounds from *A. flettii* (grifolin, neogrifolin and confluentin) are shown in Fig 3.60. The KRas-4b levels were down-regulated to 71.26 and 52.60% after treatment with 50 µM of grifolin and neogrifolin respectively. Treatment with the positive controls (20 µM) ACQ and VLA9 also down-regulated KRas-4b expression by 25.29% and 22.86% respectively. The KRas-4a levels were also down-regulated after treatment with different concentrations of these compounds.

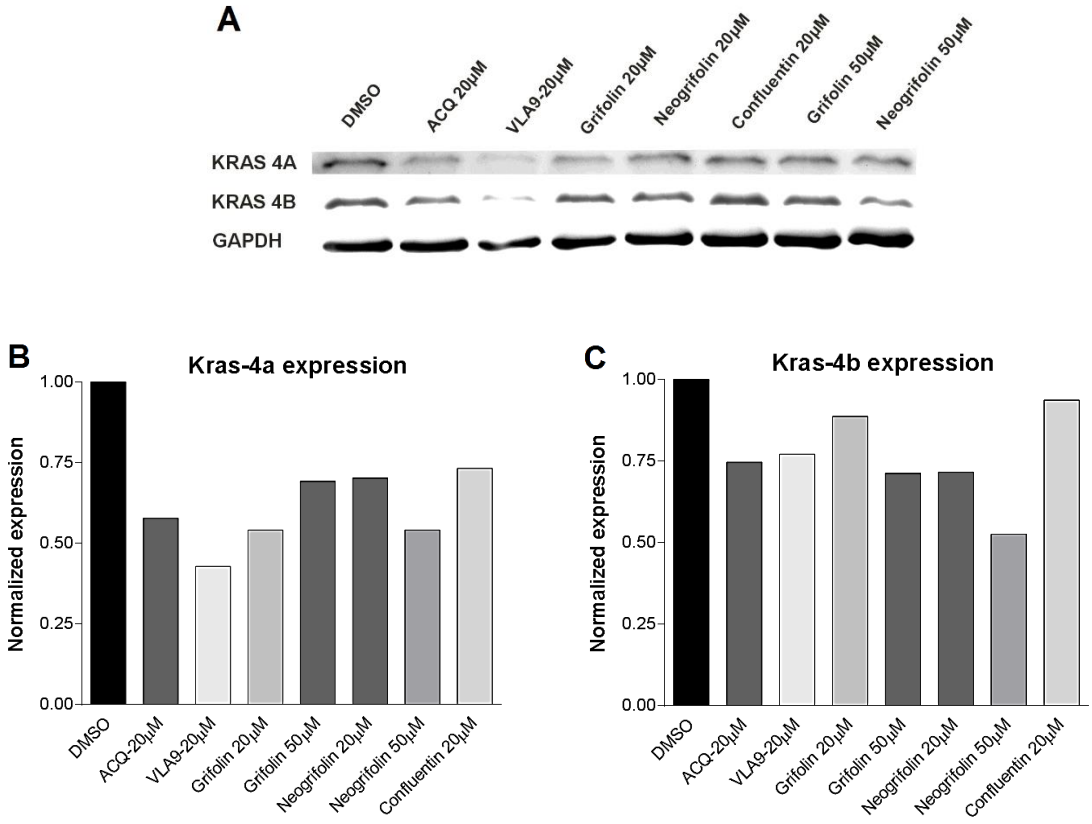

Figure 3. 60 Effects of grifolin, neogrifolin and confluentin on Kras-4a and Kras-4b expression in HT29 Colon adenocarcinoma cells. (A) HT29 Cells were treated with 20 and 50 μM of drugs for 48 hours. Lysates from cells were isolated and subjected to Western blot analysis. **(B)** The Kras-4a band in (A) was normalized to the house-keeping gene GAPDH and expressed relative to the control, DMSO, taken as 1.0. **(C)** The Kras-4b band in (A) was normalized to the house-keeping gene GAPDH and expressed relative to the control, DMSO, taken as 1.0.

Another technical replicate of the above experiment showed similar results (Fig 3.61). This further confirmed the reproducibility of the results for KRas expression. The only dose tested for confluentin was 20 μM; however, it proved to have very little effect on down-regulation of both forms of Kras.

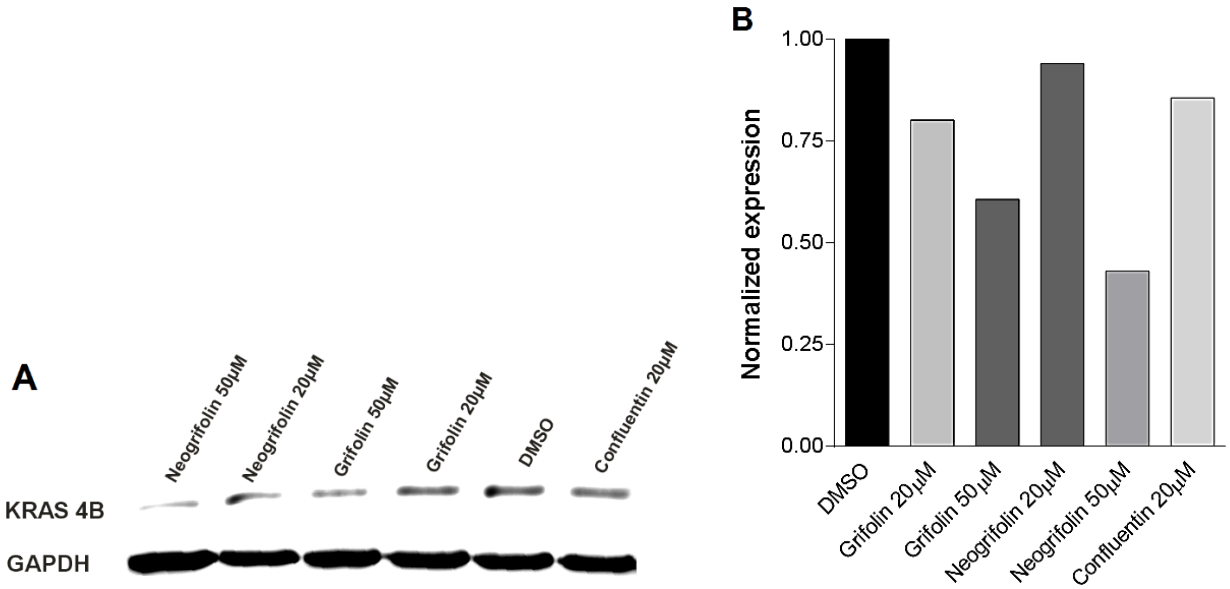

Figure 3. 61 Effects of grifolin, neogrifolin and confluentin on Kras-4b expression in HT29 Colon adenocarcinoma cells. (A) Cells were treated with 20 and 50 µM of drugs for 48 hours. Lysates from cells were isolated and subjected to Western blot analysis. **(B)** The Kras-4b band in (A) was normalized to the house-keeping gene GAPDH and expressed relative to the control, DMSO, taken as 1.0.

3.3.15.2 SW480 Cells

To determine whether Kras-4b expression in SW480 cells is also affected by the purified compounds, two experiments were performed using different doses of neogrifolin only. KRas-4b expression in SW480 cells, after treatment with 10 (Fig. 3.62B) and 50 µM (Fig. 3.62B) concentration of neogrifolin was downregulated to 85.72 and 34.10 % respectively. No effect on Kras-4b expression was observed after treatment with 5 µM of neogrifolin (Fig. 3.62B).

KRAS-4a levels were also found downregulated to 87.20% after treatment with 50 µM (Fig. 3.63B) concentration of neogrifolin. So, both KRas isoforms were also affected in SW480 cells after treatment with neogrifolin treatment.

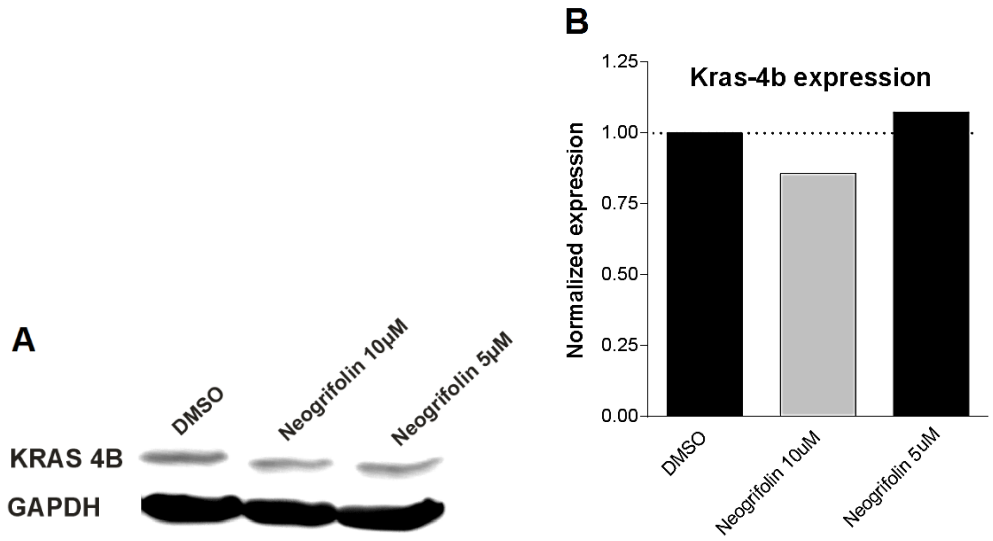

Figure 3. 62 Effects of neogrifolin treatment on Kras-4b expression in SW480 Colon adenocarcinoma cells. (A) Cells were treated with 5 and 10 μM of neogrifolin for 48 hours. Lysates from cells were isolated and subjected to Western blot analysis. **(B)** The Kras-4b band in (A) was normalized to the house-keeping gene GAPDH and expressed relative to the control, DMSO, taken as 1.0.

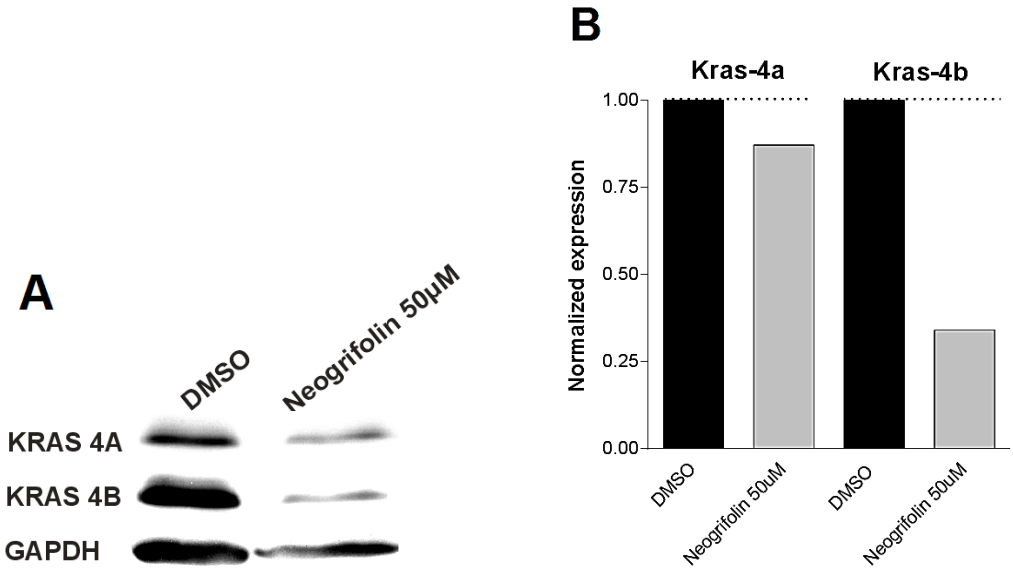

Figure 3. 63 Effects of neogrifolin treatment on Kras-4a and Kras-4b expression in SW480 Colon adenocarcinoma cells. (A) Cells were treated with 50 μM of neogrifolin for 48 hours. Lysates from cells were isolated and subjected to Western blot analysis. **(B)** The Kras-4a and Kras-4b bands in (A) were normalized to the house-keeping gene GAPDH and expressed relative to the control, DMSO, taken as 1.0.

The Kras-4b expression was determined in SW480 cells based on the time of treatment. Figure 3.64B represents the normalized expression of Kras-4b using housekeeping gene (GAPDH). Treatment of SW480 cells after 24 hours of treatment (50µM) with grifolin, neogrifolin and confluentin resulted in downregulation of Kras-4b to 72.59, 76.52 and 67.77% respectively (Figure 3.64B).

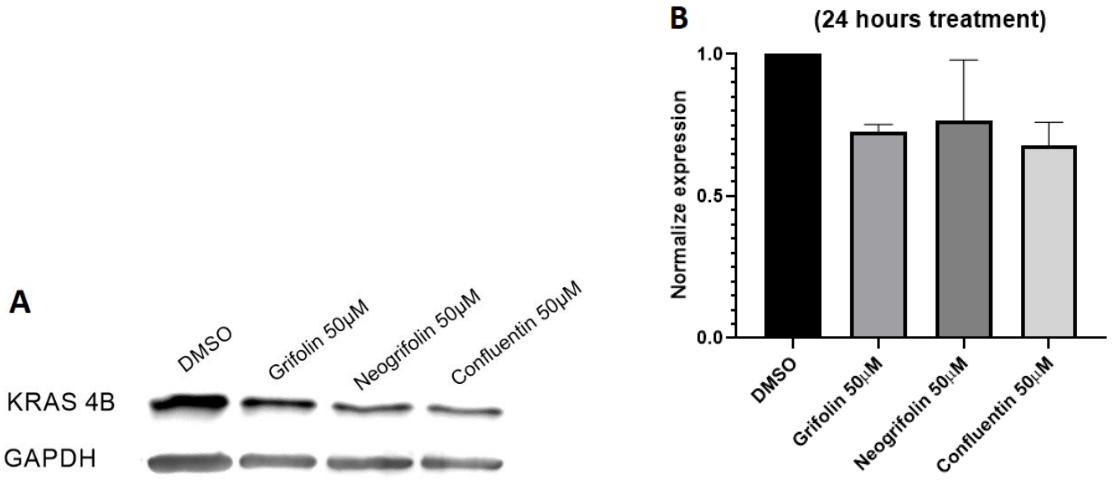

Figure 3. 64 Effects of grifolin, neogrifolin and confluentin treatment (50µM) on Kras-4b expression in SW480 Colon adenocarcinoma cells. (A) Cells were treated with 50 µM of grifolin, neogrifolin and confluentin for 24 hours. Lysates from cells were isolated and subjected to Western blot analysis. **(B)** The Kras-4b bands in (A) were normalized to the house-keeping gene GAPDH and expressed relative to the control, DMSO, taken as 1.0.

Figure 3.65A is the representative of Kras-4b expression after treatment (48hrs) with 50 µM of grifolin, neogrifolin and confluentin. Figure 3.65B represents the normalized expression of Kras-4b using housekeeping gene (GAPDH). The Kras-4b expression was downregulated to 72.03, 80.32 and 49.08 % after 48hrs treatment with grifolin , neogrifolin and confluentin respectively.

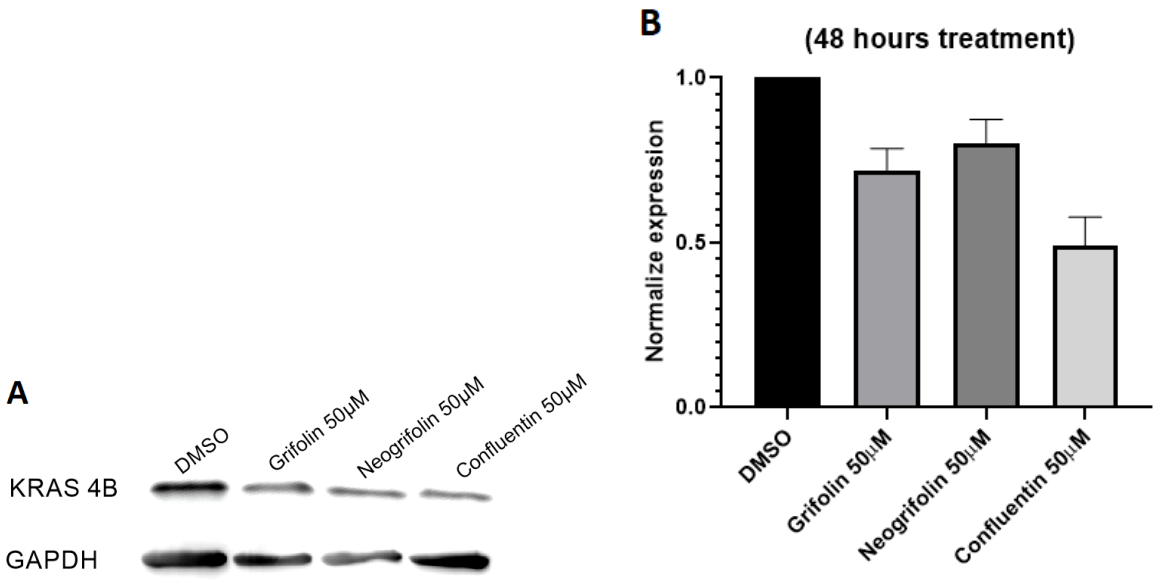

Figure 3. 65 Effects of grifolin, neogrifolin and confluentin treatment (50μM) on Kras-4b expression in SW480 Colon adenocarcinoma cells. (A) Cells were treated with 50 μM of grifolin, neogrifolin and confluentin for 48 hours. Lysates from cells were isolated and subjected to Western blot analysis. **(B)** The Kras-4b bands in (A) were normalized to the house-keeping gene GAPDH and expressed relative to the control, DMSO, taken as 1.0.

3.3.16 Apoptosis induction in SW480 cells

PE Annexin V was used to determine the percentage of cells undergoing apoptosis. To distinguish viable cells from non-viable cells a standard 7-AAd viability probe was used for flow cytometry. Only necrotic or dead cells are permeable to 7-AAd. Figure 3.66 (A) represents cells treated with the negative control 2% DMSO. While cells treated with 50 μM of confluentin are represented in Figure 3.66 (B). Figure 3.66 (A and B) bottom left panels Q4 (PE Annexin V and 7-AAD negative) indicated that the cells were viable and not undergoing apoptosis. The total number of events (population of cells) recorded for negative control (2% DMSO) and confluentin (50μM) were 13197 and 12090 respectively.

The population of cells undergoing apoptosis after confluentin treatment (3627 events) were higher than the control (1102 events). While there is also a huge population of cells (962 events) in panel Q1, indicating a large number of cells being necrotic or dead after 24 hours

treatment with 50 µM confluentin. The population of cells undergoing necrosis after treatment with negative control was only 68 events.

The percentage of the cells viable after treatment with 2% DMSO and confluentin 50 µM were 90.0% (11877 events) and 61.60% (7447 events) respectively. Panels Q3 and Q2 (PE Annexin V positive and 7-AAD negative) represent the early and late stage apoptosis respectively. The population of cells in Q3 and Q2 after treatment with the negative control was 156 and 1102 events respectively. On the other hand, the population of cells in Q3 and Q2 after treatment for 24 hours with 50 µM confluentin was 56 and 3627 events respectively. The cells in panel Q1 are considered dead /necrotic (PE Annexin V and 7-AAD positive). The population of cells undergoing necrosis after 24 hours treatment with 2% DMSO and confluentin 50 µM were 68 and 962 events respectively.

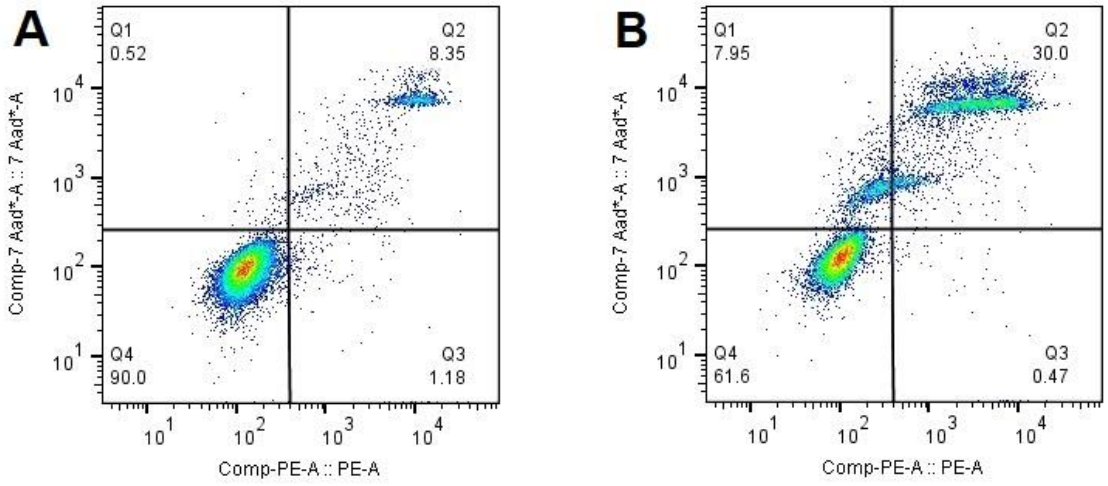

Figure 3. 66 Flow cytometry analysis of SW480 cells using PE annexin V in a buffer containing 7-Amino-Actinomycin (7-AAD) staining. **(A)** Cells after treatment for 24 hours with 2% DMSO. **(B)** Cells after treatment for 24 hours with 50 µM of confluentin. Bottom left panel Q4 (PE Annexin V and 7-AAD negative) in **(A)** and **(B)** indicated the cells were viable and not undergoing apoptosis. Cells undergoing apoptosis (PE Annexin V positive and 7-AAD negative) (Q3 Early stage apoptosis and Q2 Late apoptosis). Population of cells observed to be PE Annexin V and 7-AAD positive, indicating end stage apoptosis or already dead (Q1).

The flow cytometry assay on the effect of confluentin on apoptosis was done twice using different cell preparations. From this result it is clear, that confluentin induced apoptosis in SW480 cells.

Another experiment (treatment time 14 hours) (Figure 3.67) using the same cell line (SW480) revealed confluentin as being more a potent inducer of apoptosis than grifolin. After plating, SW480 cells were incubated for 60 hours and treated with 50 μM concentration of grifolin (Figure 3.67B) and confluentin (Figure 3.67C) for 14 hours. For negative control (Figure 3.67A), 13030 events (cell population) were recorded using FACSMelody. The population of cells in Q3 and Q2 after treatment with the negative control (2% DMSO) was 263 and 1915 events respectively. The population of cells undergoing necrosis was 185 only. The major population (visible in panel Q4) containing viable cells (not undergoing apoptosis or necrosis) was 10658 events (81.80%). The number of events recorded for SW480 cells after treatment with grifolin and confluentin (50 μM) were 10917 and 10884 respectively. The population of viable cells (panel Q4) were 8133 (74.50%) and 6008 (55.20%) respectively.

The population of cells undergoing necrosis or already dead were similar in grifolin- and confluentin-treated cells. The population of cells dead or necrotic after treatment with grifolin and confluentin (Panel Q1) were 608 (5.57%) and 1197 (11.0%) events respectively. A significant difference in cell population undergoing apoptosis can be seen after treatment with grifolin and confluentin. The population of SW480 cells in the late apoptosis stage was 1965 (18.0%) and 3534 (32.50%) respectively after grifolin and confluentin treatment.

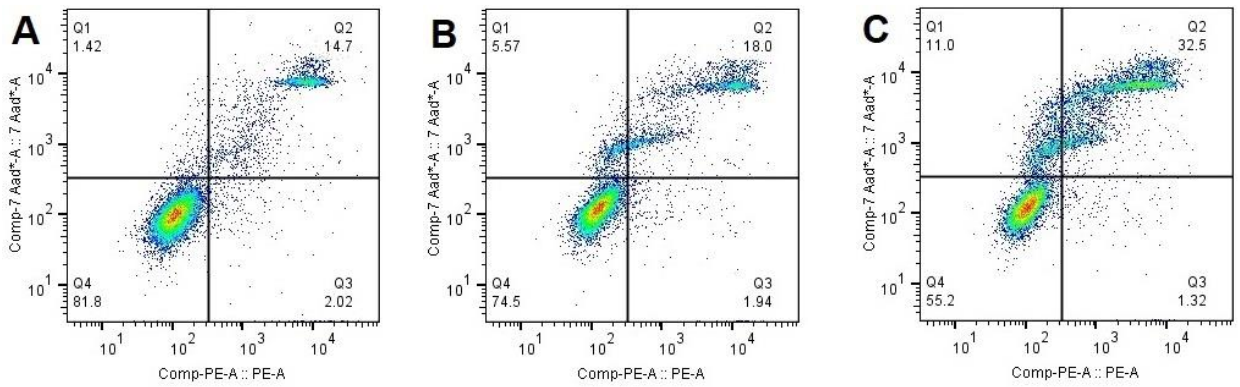

Figure 3. 67 Flow cytometry analysis of SW480 cells using PE annexin V in a buffer containing 7-Amino-Actinomycin (7-AAD) staining. **(A)** Cells after treatment for 14 hours with 2% DMSO. **(B)** Cells after treatment for 14 hours with 50 µM of grifolin. **(C)** Cells after treatment for 14 hours with 50 µM of confluentin. Bottom left panel Q4 (PE Annexin V and 7-AAD negative) in all panels indicated the cells were viable and not undergoing apoptosis. Cells undergoing apoptosis (PE Annexin V positive and 7-AAD negative) (Q3 Early stage apoptosis and Q2 Late apoptosis). Population of cells observed to be PE Annexin V and 7-AAD positive, indicating end stage apoptosis or already dead (Q1).

Treatment of SW480 cells with same concentration of confluentin revealed that confluentin has ability to induce apoptosis even within 6 hours (Figure 3.68). 15000 events were recorded for both negative control and confluentin (50µM) treated cells. The population of viable cells (panel Q4) after treatment with negative control and confluentin were 86 % (12900 events) and 70.3 (10545 events) respectively. The population of SW480 cells going under apoptosis after treatment with negative control (DMSO) and confluentin is 1385 events (9.23%) and 2895 events (19.3%) respectively. Population undergoing necrosis after treatment with 50 µM confluentin is 6.20% (Panel Q1).

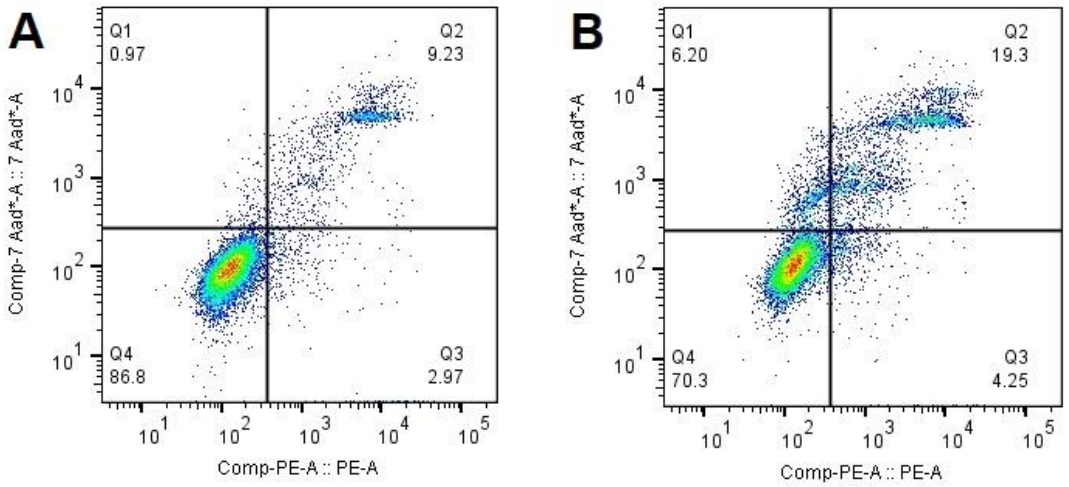

Figure 3. 68 Flow cytometry analysis of SW480 cells using PE annexin V in a buffer containing 7-Amino-Actinomycin (7-AAD) staining. **(A)** Cells after treatment for 6 hours with 2% DMSO. **(B)** Cells after treatment for 6 hours with 50 µM of confluentin. Bottom left panel Q4 (PE Annexin V and 7-AAD negative) in **(A)** and **(B)** indicated the cells were viable and not undergoing apoptosis. Cells undergoing apoptosis (PE Annexin V positive and 7-AAD negative) (Q3 Early stage apoptosis and Q2 Late apoptosis). Population of cells observed to be PE Annexin V and 7-AAD positive, indicating end stage apoptosis or already dead (Q1).

3.3.17 Cell cycle arrest at G_2/M phase

G2 phase of the cell cycle is the second sub-phase of interphase and is crucial for cell growth and protein synthesis. Figure 3.69A represents cell population after treatment with the negative control 2% DMSO. Figure 3.69B represents cell population after treatment with confluentin (50 µM). As shown, confluentin (50 µM) exhibited cycle arrest at G_2/M phase in SW480 cells. The percent population of cells at G_2/M phase after treatment for 24 hours with confluentin 50 µM and negative control (2% DMSO) was 11.40% and 0.42% respectively.

Table 3. 7 Representing relative percentage of SW480 cells in different phases of cell cycle.

Treatment	G_1 phase (%)	S phase (%)	G_2/M phase (%)
2% DMSO	79.4	17.6	0.42
Confluentin (50 µM)	83.3	4.12	11.40

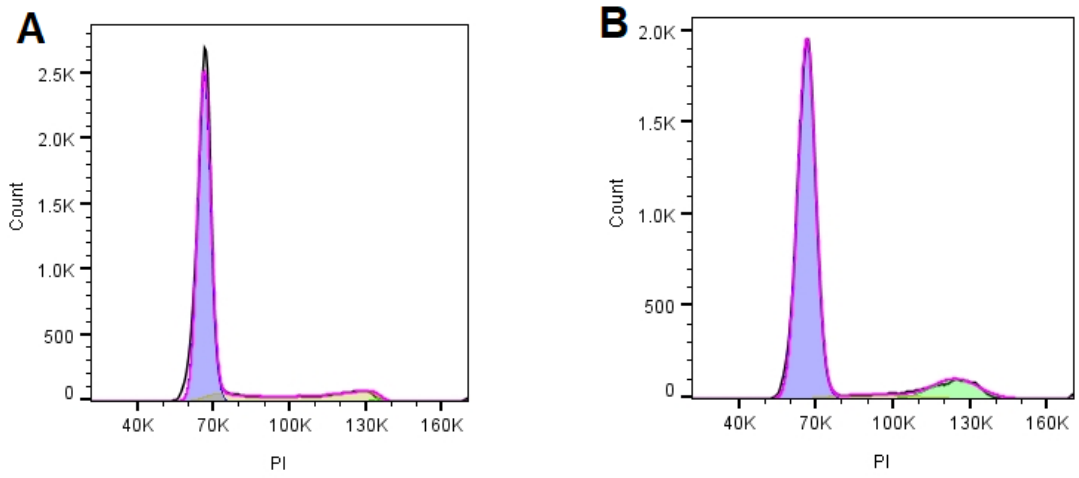

Figure 3. 69 Flow cytometry analysis of SW480 cells using propidium iodide staining. **(A)** Cells after treatment for 24 hours with 2% DMSO. **(B)** Cells after treatment for 24 hours with 50 µM of confluentin. G_1 phase is represented by blue color, S phase is represented by yellow and G_2/M phase is represented by green color.

3.4 Discussion

This chapter describes the successful purification, characterization, structural elucidation and molecular mechanistic studies of the three growth-inhibitory compounds from *A. flettii.* E1 (80% ethanol) and E2 (50% methanol) extracts of the *A. flettii* exhibited potent growth-inhibitory activity. HeLa cell viability after treatment with both extracts was less than 20%. For further studies, extract E1 was selected because of its potent growth-inhibitory activity. To obtain the bioactive compounds from *A. flettii* E1 extracts, a series of purification steps were developed (Figure 3.70).

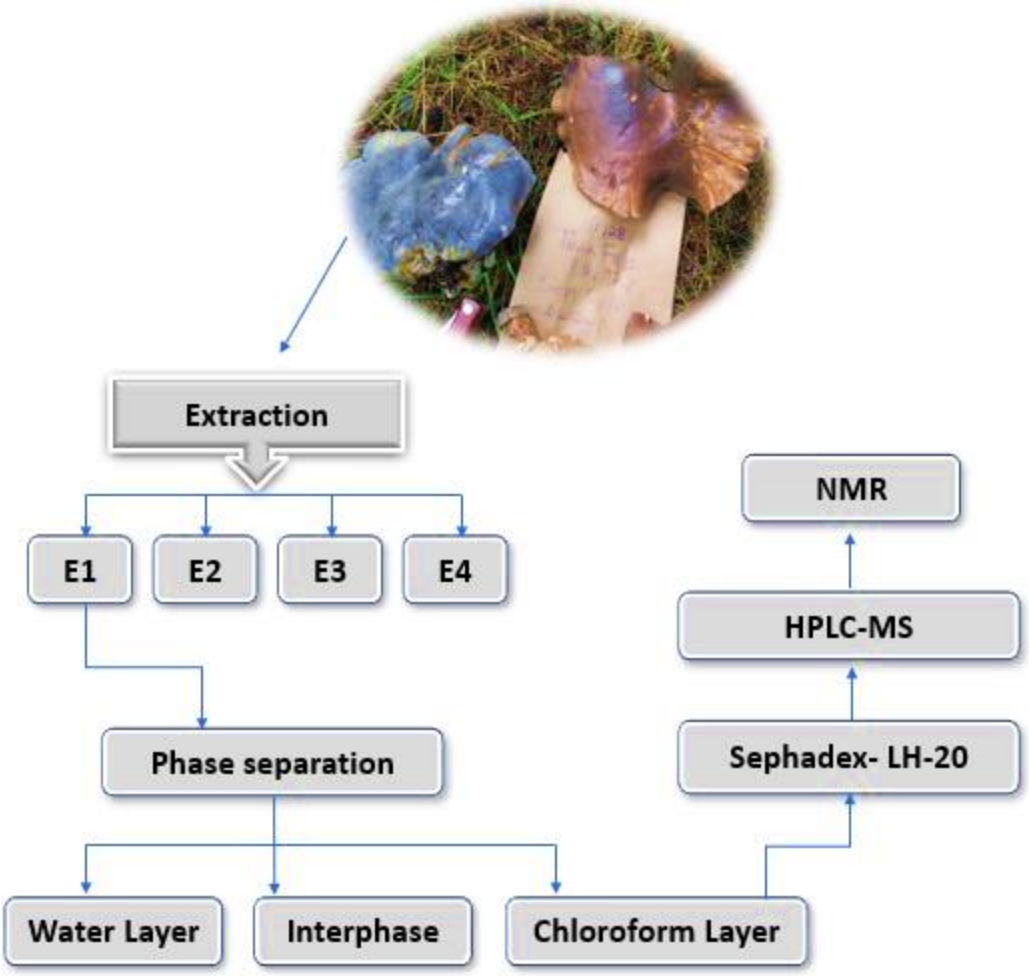

Figure 3. 70 Flow diagram representing the steps involved in the purification and structural elucidation of pure compounds from *A. flettii.*

The E1 extract was first subjected to phase separation of molecules based on the liquid-liquid extraction technique. This approach was based on two immiscible solvents (due to differences in polarity index). Separation of compounds was possible based on their polarity. Non-polar compounds were expected to move into the chloroform layer, while polar compounds were expected to solubilize and move into the water layer. An interphase was also observed which could be the degraded proteins not soluble in any of the solvents. Further screening for growth-inhibitory activity confirmed the presence of bioactive molecules in chloroform layer

(non-polar in nature). The yield of compounds in chloroform layer after liquid-liquid extraction was 44.50%.

Compounds from the chloroform layer were then subjected to Sephadex LH-20 size exclusion chromatography. The fractions collected from Sephadex LH-20 columns were further assessed for growth-inhibitory potential. Even at 1 µL, the fractions were capable to reduce the cell viability down to 20% as compared to the negative control (methanol). Since bioactive compounds were eluting in later fractions, it was proposed that compounds are smaller in size. This technique was further scaled up to 400 mL Sephadex LH-20 column. Sample introduced onto the column was 80 mg/mL of chloroform layer. Yield of active fractions from Sephadex LH-20 column was 27.813%.

The post Sephadex LH-20 bioactive fractions were subjected to a second purification step using high-resolution HPLC. Initially, a method was developed for optimal separation of compounds present in the bioactive post-Sephadex LH-20 fractions. The solvent system utilized for optimal separation of peaks was a gradient solvent system based on acetonitrile and water. Later, the HPLC technique was scaled up using Agilent Zorbax C-18 semi-preparative column and isocratic solvent system using 90% acetonitrile and 10% water. After multiple runs, three peaks were collected and lyophilized. After collection, the three major peaks were re-assessed for their purity as well as determination of the molar mass. The purity of all three peaks (Peak 5, 6 and 8) were determined to be 100%. The *m/z* $[M+H]^+$ of peak 5, 6 and 8 were determined to be 329.3, 329.3 and 327.3 respectively. All these three compounds were further tested for their growth-inhibitory and anti-inflammatory activities. It was concluded that all three compounds are cytotoxic in nature towards RAW 264.7 macrophages instead of being anti-inflammatory.

The three peaks (Peak 5, 6 and 8) collected based on semi-preparative HPLC were further lyophilized. Purified compound form Peak 5 was cream color fluffy needle-like powder while the compound purified from peak 6 was oily in nature. The physical appearance of the purified compound from peak 8 was sticky brownish paste. The yield of purified compounds from Peak 5, 6 and 8 based on semi-preparative HPLC was 52.14, 32.62 and 5.00 percent respectively. The overall yield of HPLC column was 89.77%.

For structural elucidation, the purified sample were further analyzed using Bruker NMR 300 MHz. Sample was prepared using deuterated chloroform $CDCl_3$ (99.96 % chloroform-d and 0.3% TMS) (Sigma Aldrich) directly in NMR sample tube. The information based on 1D (^{1}H-NMR and ^{13}C-NMR) and 2D (COSY and HSQC) revealed the purified compounds in Peak 5, 6 and 8 as grifolin, neogrifolin and confluentin respectively. The final yield of grifolin, neogrifolin and confluentin from 70 grams of *A. flettii* # 128 was 0.26, 0.16 and 0.025% respectively, showing that confluentin was the least abundant growth-inhibitory compound from *A. flettii*.

Experiments aimed at determining the potency of grifolin, neogrifolin and confluentin on HeLa cells revealed their IC_{50} to be 29.85, 23.22 and 50.47 μM respectively.

The purified compounds, especially grifolin and neogrifolin, were found to downregulate KRas expression in human colon cancer cell lines (HT-29 and SW480). The IC50s of these compounds on HT29 and SW480 cells were also determined. To my knowledge, this is the first study reporting the growth-inhibitory compound(s) on mammalian cells isolated from *A. flettii*. This is also the first study to show the ability of grifolin and neogrifolin to down-regulated KRas expression in cancer cells. However, the mechanism of action of these purified compounds (grifolin, neogrifolin and confluentin) on KRas expression is yet to be investigated in detail (whether it is affecting mRNA levels or not). At the outset of this study, grifolin and neogrifolin

had been extensively studied for their effect on the apoptosis and cell cycle pathways. In contrast, confluentin has not been investigated for its growth-inhibitory molecular mechanism. This study shows for the first time that confluentin can induce apoptosis and arrest cell cycle at G_2/M phase in SW480 human colon cancer cells.

Chapter 4: Purification and Characterization of Growth-Inhibitory Compounds from *Sarcodon scabripes*

This chapter focuses on the purification and characterization of growth-inhibitory compound(s) from the E1 (80% ethanol) extract of *Sarcodon scabripes*. There has been no prior study on bioactivity from *S. scabripes.* Therefore, this species is an ideal candidate for searching for potential novel growth-inhibitory compounds.

4.1 Materials and Methods

4.1.1 Manual extraction

Manual extraction was performed on 81 grams of pulverized mushroom sample. Only E1 (80% ethanol) and E2 (50% methanol) extraction was performed, and the residue was saved. The manual extraction was done using a hotplate at 65ºC for 6 hours. The extract was then filtered using Whatman filter paper on a Büchner funnel. The extracts were lyophilized using Labconco freeze dryer and stored in -80°C freezer. The E1 (80% ethanol) extract was then utilized for further biological cell assays and purification process.

4.1.2 Two-step sequential liquid-liquid extraction

The E1 (80% ethanol) extract of *S. scabripes* was first phase-separated using water (inorganic) and chloroform (organic). This technique was utilized to separate the compounds based on their polarity index. For that purpose, VWR glass culture tube was used. First, 20 mg/mL solution of E1 (80% ethanol) extract of *S. scabripes* was prepared in a glass culture tube using chloroform. Later, water was added in the equal volume to make sure that separation of compounds between the two layers was optimum. The solution was vortexed for 2-3 min and centrifuged. The process of centrifugation was carried out using Allegra X-15R benchtop centrifuge (Beckman Coulter) at the speed of 100 RCF for 5 min. Once a clear separation of three layers has been achieved, all the layers were separated in clean culture tubes. The water

layer was further re-extracted with ethyl acetate to further separate the compounds (present in the water layer) based on the weak polar nature. The color of each layer was distinct, suggesting the presence of different types of compounds in each layer. The color of the chloroform layer was dark brown, while the ethyl acetate and water layers were dark orange and green respectively. All layers were dried using a hotplate at 65ºC and stored at 4ºC.

4.1.3 Sephadex LH-20

In general, the procedures used to separate compounds in Sephadex LH-20 columns are essentially the same as those described in chapter 3 section 3.2.3. Briefly, compounds were separated from the chloroform layer of E1 extract usingSephadex-LH20 resin as the stationary phase and degassed 100% methanol was utilized as the mobile phase. Initial trial of compounds separation was done using a small 25 mL column (gravity drip) of Sephadex™ LH-20. This size-based elution technique was further scaled up to a 100 mL column using a C16/70 glass column (GE Healthcare). Fractions were collected using automated fraction collector and final volume of each fraction was 5 mL. Mobile phase (degassed 100% methanol) flow rate was set at 1 mL/min using an automated pump (Pharmacia).

The Sephadex-LH20 column-based purification was performed only for chloroform layer. The sample concentration of 80 mg/mL was prepared and only 2% of column volume was loaded onto the column (500 µL containing 40 mg of chloroform layer). For gravity drip 25 mL column, sample (500 µL) was loaded into the column using a micropipette. Sample was loaded into C16/70 glass column (GE Healthcare) with syringe using 3-ways valve. Collected fractions were stored at 4ºC.

4.1.4 Nanodrop Analysis

A nanodrop spectrophotometer (Thermo Fisher scientific, USA) was used to determine the λ_{max} of fraction 18 and 26 from Sephadex LH20 (gravity drip/small column). After calibration with water, the spectrophotometer was blanked with HPLC grade methanol. Sample peddle was rinsed with the autoclaved milliQ water before analyzing the sample. A sample of 2 µL was used to determine λ_{max} of fraction 18 and 26. The λ_{max} for both fractions (18 and 26) was observed at 262 nm, which was further used as a function of UV spectrophotometer in HPLC analysis of the Sephadex LH-20 active fractions.

4.1.6 HPLC-MS

4.1.6.1 Chloroform layer

The reverse phase (RP-HPLC) separation method was first developed using the non-polar analytical column (Zorbax eclipse, 5 µm C18, 150 x 4.6 mm) and gradient solvent system (Fig 4.1). Solvent A is water, solvent B is acetonitrile and solvent C is methanol. Gradient mobile phase was developed for the optimal peak separation and better peak shape in UV spectra.

Starting at (A: B: D) 60: 6: 34% at time zero, water was consistently reduced and organic content (acetonitrile and methanol) was increased. The solvent ratio after 8 min of HPLC sample run was (47: 8: 45%) and was kept consistent after 8 min until each compound elutes out of the column. HPLC grade solvents (VWR) were used for the separation of the bioactive compounds. The solvents were automatically degassed through the degasser part of the HPLC before entering the quaternary pump. The quaternary pump controls the flow rate as well as the gradient of the solvent system. Flow rate for gradient mobile phase was set at 0.7 mL/min. The amount of the sample injected into the HPLC analytical column was 2 µL. Fraction 24 of the Sephadex gravity drip column was analyzed using these conditions.

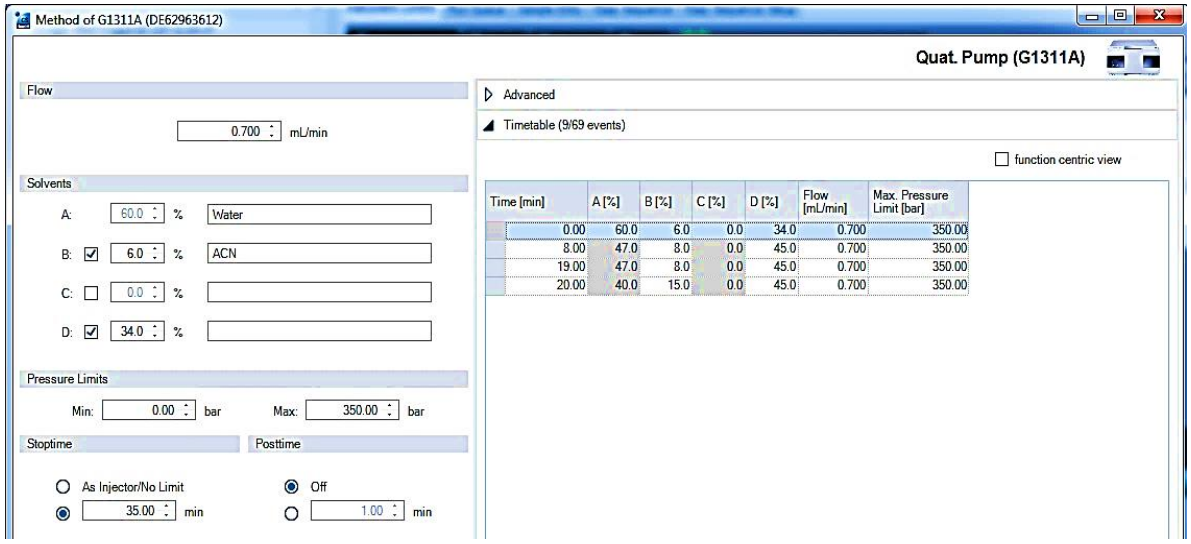

Figure 4. 1 Illustration of gradient solvent system utilized to resolve HPLC profile peaks generated from the chloroform layer.

Mass spectroscopy was performed using an active splitter. The active splitter ratio used was 1:66. Scan mode was performed first to determine the mass of ionized compounds in the peaks. Formic acid (0.1%) isocratic solution was utilized to ionize the compounds of sample. After determination of molecular masses, a second step confirmation was done using SIM mode. SIM mode only targets the masses for which the mass spectrophotometer has been programmed. It took 30 min in total to elute all the compounds out of the column.

4.1.6.2 Ethyl acetate layer (TEA)

HPLC analysis of the ethyl acetate layer was performed using Phenomenex phenyl-Hexyl column (4.6 x 250 mm) and isocratic solvent system (three solvent system). The Sephadex-LH-20 based size separation was not performed on this layer. The composition of isocratic mobile phase was based on water 50%, acetonitrile 40% and methanol 10%. Flow rate was set at 0.6 mL/min for optimal resolution of peaks. It took 15 min in total to elute all the compounds out of the column. Mass spectroscopy was performed using an active splitter. The active splitter ratio used was 1:66. Scan mode was performed first to determine the mass of ionized compounds in the peaks. Formic acid (0.1%) isocratic solution was utilized to ionize the

compounds of sample. After determination of molecular masses, a second step confirmation was done using SIM mode. SIM mode only targets the masses for which the mass spectrophotometer has been programmed.

4.1.6.3 Water layer (TW)

The method to resolve the water (TW) layer compounds was based on Phenomenex Phenyl-Hexyl 4.6*250 mm analytical column. Optimal flow rate for mobile phase was determined to be 0.6 mL/min. Isocratic mobile phase was developed based on 80% water, 10% acetonitrile and 10% methanol. It took 10 min in total to elute all peaks out of the column. The nature of the compounds present in water layer was highly polar and the column type used for this analysis was weakly polar. Due to this limitation, it was impossible to clearly separate the peaks from each other. The best possible separation was achieved based on the manipulation of solvent system.

4.1.7 Semi-preparative HPLC

HPLC technique was scaled up to a semi-preparative column, Agilent Zorbax Eclipse XBD-C18 5um (9.4 mm * 250 mm) for bioactive fractions collected from Sephadex LH-20 that originally derived from the chloroform layer. The optimal peak shape and separation was attained using isocratic mobile phase (water 43%, acetonitrile 12% and methanol 45%). Degassing of the solvents was carried out by the degasser part of the HPLC (Agilent technologies 1200 series). The sample was filtered using 0.2 μm filter (Thermo Fisher Scientific, USA) before loading into the column. A sample volume of 10 μL was injected through an auto-sampler. Based on these conditions, it took 50 min in total to elute all peaks out of the semi-preparative column. The peaks were collected using a fraction collector based on their retention times on UV signal. Fractions were collected in 8 mL collection vials.

4.2 Results

4.2.1 Yield from manual extraction

The yield of both extracts (E1 and E2) using manual extraction was higher than that obtained using the Dionex speed extractor. The yield for E1 and E2 extracts was 6.19 and 5.839 % respectively, when using manual extraction. The yield of E1 and E2 extracts using Dionex ASE speed extractor (as shown in Table 2.7) was 1.36 and 5.82% respectively. The color of both extracts was dark greenish brown. After a large-scale manual extraction, the solubility (Table 4.1) and growth-inhibitory activity of the extracts was re-confirmed (as shown in Figure 4.2). After treatment with 1 mg/mL final concentration of extracts E1 and E2, HeLa cell viability was 11.79 and 8.81 % respectively.

Table 4. 1 Representing the yield of two extracts (E1 and E2) from *S. scabripes*.

Mushroom	Mass of sample	Mass of Extract E1	Yield	Mass of Extract E2	Yield
Sample 128	81 g	5.02 g	6.19%	4.730 g	5.839 %

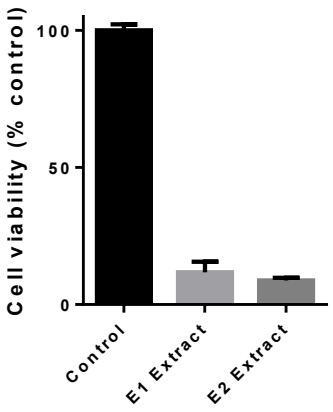

Figure 4. 2 Growth-inhibitory activity of extracts E1 and E2 from *S. scabripes.* One mg/mL of E1 and E2 was added to HeLa cells for 48 hours, after which MTT assay was performed. Error bars represent standard deviation of four biological replicates.

4.2.2 Liquid-liquid extraction/phase separation

Liquid-liquid extraction of E1 from *S. scabripes* resulted in three distinct layers. Non-polar compounds were present in the chloroform layer (CL), while polar and weak polar compounds were present in water layer (TW) and top ethyl acetate (TEA) respectively.

Table 4. 2 Yield of three layers, based on liquid-liquid extraction (phase separation) of E1 (80% ethanol) extract of *S. scabripes.*

Layer of liquid-liquid extraction	Color of the layer	Mass (mg) out of 20 mg	% Mass	Growth inhibitory Activity	Solubility
Top Layer (Aqueous Phase) (TW)	Green	5.20	26.00	Yes	Water
Lower Layer (Chloroform phase)	Dark Brown	6.94	34.70	Yes	Methanol
Ethyl acetate (TEA)	Dark orange	7.11	35.55	No	Methanol

The ethyl acetate layer (TEA) was dark orange in color containing the highest yield (35.55%). TEA was assumed to contain weak polar compounds due to nature of ethyl acetate. The water layer has the lowest yield (26%). Solvents from these layers were evaporated using a hotplate at 65^{o}C. The dried mass from all three layers was solubilized and then assessed for growth-inhibitory activity.

4.2.3 Assessing the three layers obtained from liquid-liquid extraction of E1 for growth-inhibitory activity

Dose-dependent MTT assay was performed on all three layers of the liquid-liquid extraction. The final concentration of the methanol was less than 2% in each well. The doses tested on HeLa cells were 0.5 and 1 mg/mL. At the high concentration of 1 mg/mL, both water (TW) and chloroform layer resulted in false negative results because colored solution was seen. This was presumably the results of chemical reaction between MTT and compounds present in the water and chloroform layers.

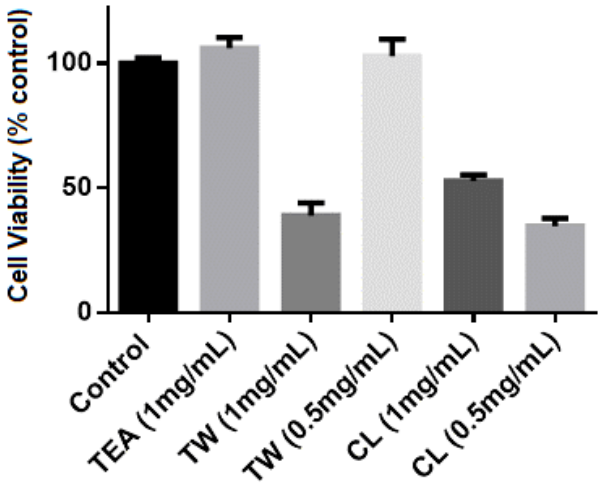

Figure 4. 3 Growth-inhibitory potential of the liquid-liquid extraction layers. CL represents Chloroform layer. TEA and TW are Top Ethyl acetate layer and Top water Layer respectively. Error bars represent standard deviation of four biological replicates.

However, as shown in Figure 4.3, strong growth-inhibitory activity was observed after treatment with 0.5 mg/mL of chloroform and 1 mg/mL of water layer. No growth-inhibitory activity was observed after treatment with the ethyl acetate (TEA) layer at 1 mg/mL. Based on the results, I decided to focus on the chloroform layer for the next step of purification using size-exclusion chromatography.

4.2.4 Assessing fractions collected from Sephadex LH-20 (25 mL) gravity drip column for growth-inhibitory activity.

The final volume of each fraction collected from gravity drip column (25 mL) was 1 mL. All the fractions were collected using 1.5 mL Eppendorf tubes. The color of all the collected fractions was quite distinct from each other.

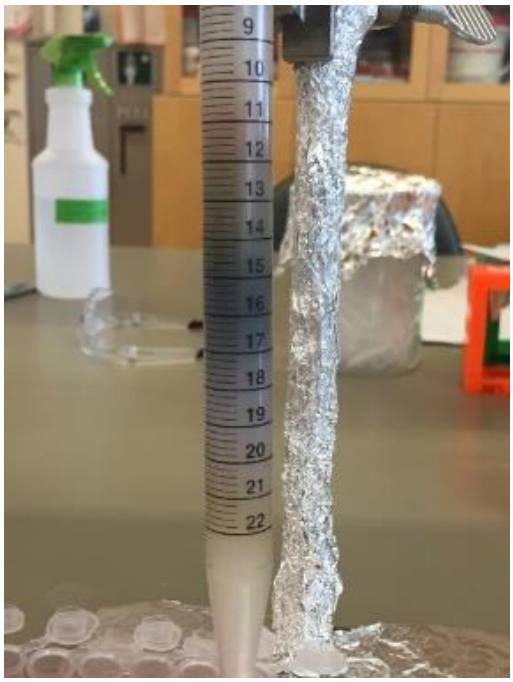

Figure 4. 4 Photograph of Sephadex LH-20 gravity drip column (25 mL). The final concentration of the sample (Chloroform Layer) loaded onto the column was 80 mg/mL.

The color of the fractions F14-F22 was pale yellow, while dark yellow color was observed for fraction 24. Dark grey color was observed for fractions F28-F30. No growth-inhibitory activity was shown by fractions F36 and F46, having pale green and red color respectively.

Table 4. 3 Representing the color and activity of Sephadex LH-20 (gravity drip, 25 mL) column fractions.

Fraction number	Color	Growth-inhibitory activity
F14-F22	Pale yellow	Yes
F24	Yellow	Yes
F28-F30	Dark grey	Yes
F36	Pale green	No
F46	Red	No

The fractions collected from gravity drip Sephadex-LH20 column were assessed for their growth-inhibitory activity using HeLa cells. The final volume of fraction added into each well was 2 µL with 98 µL of EMEM + 10% FBS. No activity was observed in the first attempt.

Consequently, the fractions volume was reduced from 1 mL to 200 µL and re-assessed for growth-inhibitory activity. Only even number fractions were tested for growth-inhibitory activity.

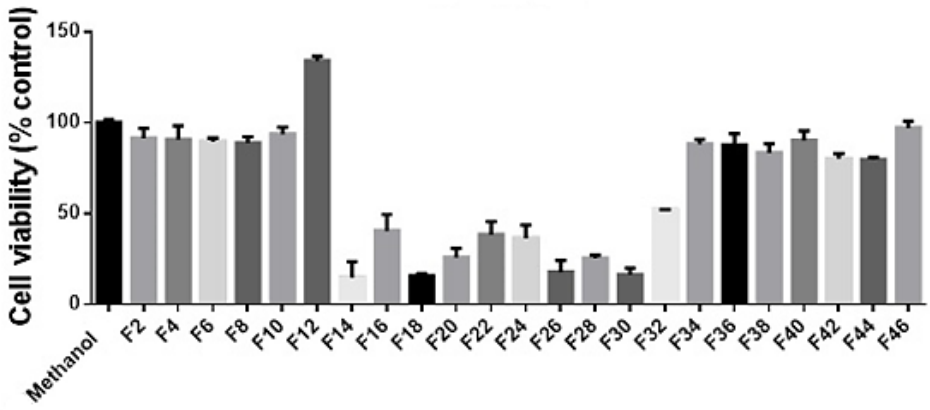

Figure 4. 5 Growth-inhibitory activity of fractions collected from 25-mL size Sephadex™ LH-20 column. HeLa cells were plated at 1500 cells/well. The final volume of fraction introduced in each well was 2 µL with 98 µL of EMEM + 10% FBS. HeLa cells were treated with the fractions for 48 hours. Error bars represent standard deviation for four biological replicates.

MTT assay results revealed that fractions 14-30 reduced HeLa cell viability to less than 50% compared to control (Figure 4.5). Some fractions (16 and 22) exhibited weaker growth-inhibitory activity, suggesting the presence of bioactive compounds in these fractions either in low quantity or different in nature. Due to the activity observed in later eluting fractions, it is likely that the bioactive compounds are small.

4.2.5 Assessing the fractions collected from Sephadex LH-20 (100 mL column) for growth-inhibitory activity

MTT assay results based on the fractions collected from Sephadex LH-20 (100 mL) column were more revealing than the 25 mL gravity drip column. Fractions 15 and 16 exhibited strong growth-inhibitory activity; the cell viability after treatment with these fractions was 26% and 31% respectively (Figure 4.6). Cell viability after treatment with fractions 17, 18 and 19 was

above 90%, indicating no growth-inhibitory potential of these fractions. Weaker growth-inhibitory activity was exhibited by fractions 20, 21, 22 and 24 (Figure 4.6). The cell viability after treatment with fractions 20, 21, 22 and 24 was 59%, 40%, 70% and 61% respectively. This weak activity of fractions could either be due to low abundance of cytotoxic compounds or less potent cytotoxic compounds in these fractions. Other than that, no fraction showed any growth-inhibitory activity on HeLa cells.

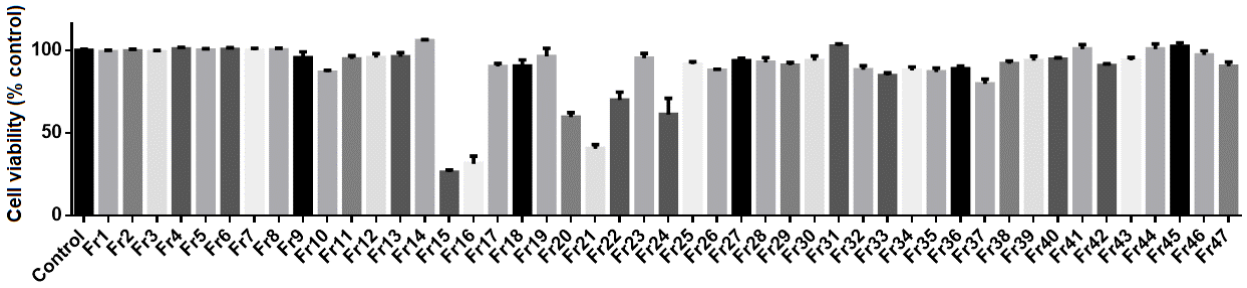

Figure 4. 6 Assessing fractions collected from 100-ml size Sephadex™ LH-20 column for growth-inhibitory activity. HeLa cells were plated 1500 cells/well. The final volume of fraction introduced in each well was 2 µL with 98 µL of EMEM + 10% FBS. HeLa cells were treated with the fractions for 48 48 hours. Error bars represent standard deviation for four biological replicates.

4.2.6 HPLC-MS

4.2.6.1 Chloroform layer (CL)

The optimal resolution of the peaks in UV spectra upon analysis of the chloroform layer indicated the ideal conditions of mobile and stationary phase. The most abundant peak on UV spectrum was observed at 16.672 min containing 58.66% of the sample mixture (Figure 4.7). The percent abundance of UV peak visible at 10.703 min was 12.9368%, making it the second most abundant peak on the spectrum. The percent abundance of the peaks at 8.610 and 3.080 min was 3.087% and 6.476% respectively. The molar mass $[M+H]^+$ of ionized compound present in the 8.610 min peak was determined to be 428.1 *m/z*. The signal of UV major peak for MS scan signal was observed for peak at 16.672 min. The *m/z* of ionized compounds present in the UV peaks at 16.672, 10.703 and 27.921 min were determined to be 484.1, 442.1, and 526.0

respectively. The MS signals are visible with slight delay time because of the travel time through the 24-inch line from UV spectrophotometer to the active splitter and then to the mass spectrophotometer.

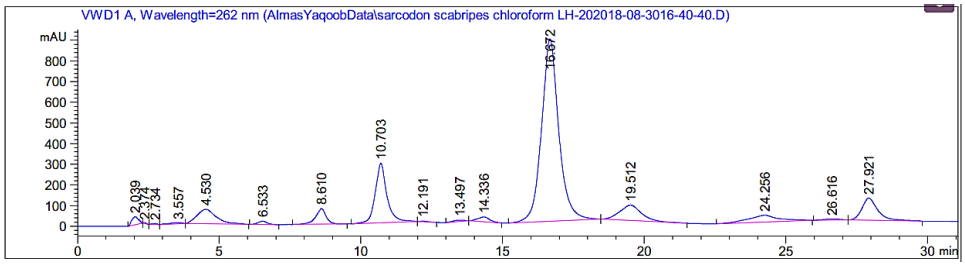

Figure 4. 7 UV spectrum representing the relative abundance and retention time of peaks at λ_{max} 262 nm (using analytical column and Sephadex LH-20 active fraction of Chloroform layer sample).

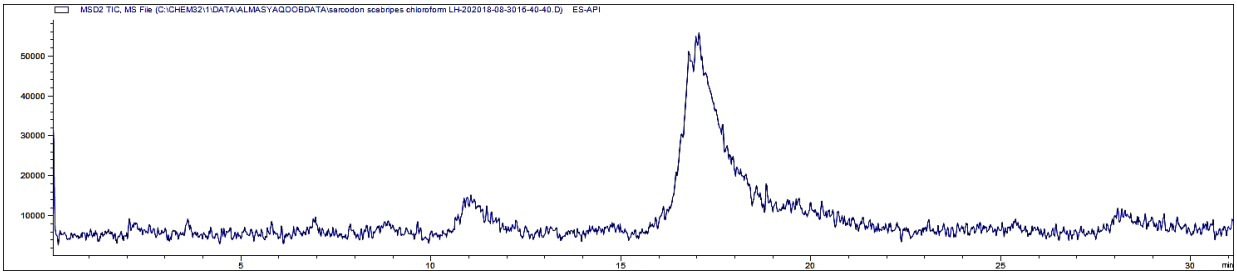

Figure 4. 8 MS Scan spectrum representing the relative abundance and retention time of the ionic compounds detected in ESI (Electrospray ionization) chamber. The type of column utilized was Agilent Zorbax analytical and sample was 1 µL of filtered Sephadex active fraction.

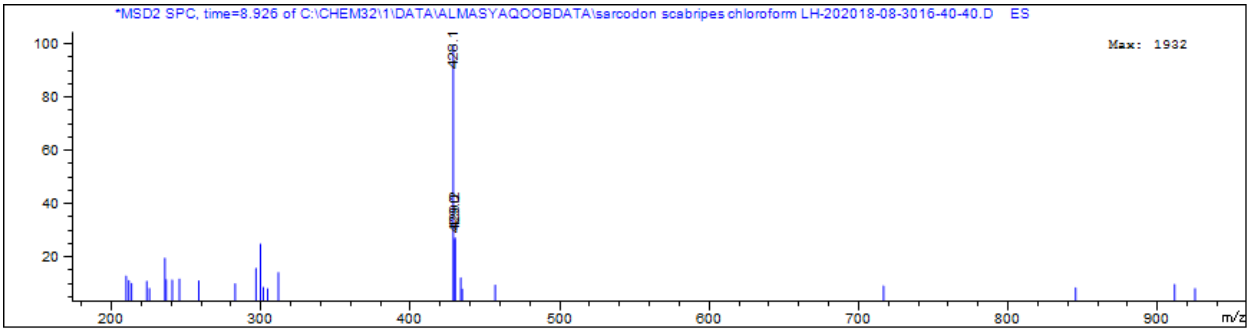

Figure 4. 9 Integration of MS scan spectrum revealing the presence and abundance of compound with *m/z* 428.1 in the peak visible at 8.926 min; representing peak at 8.610 min in UV signal shown in Figure 4.7.

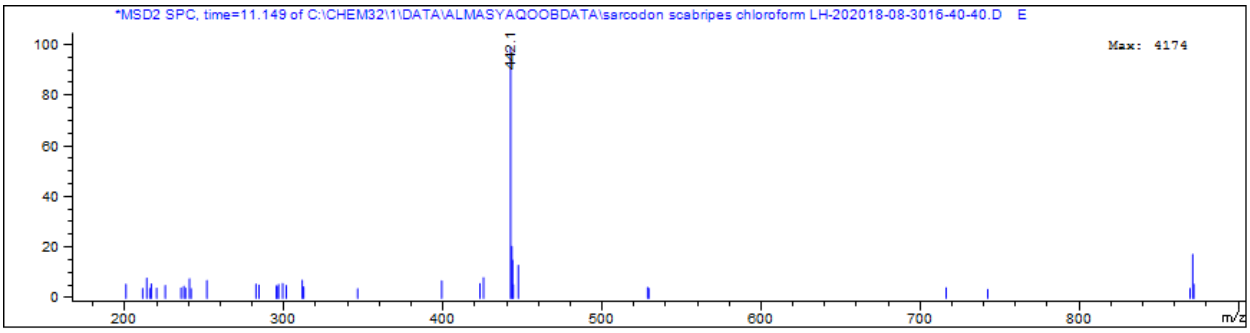

Figure 4. 10 Integration of MS scan spectrum revealing the presence and abundance of compound with *m/z* 442.1 in the peak visible at 11.149 min; representing peak at 10.703 min in UV signal shown in Figure 4.7.

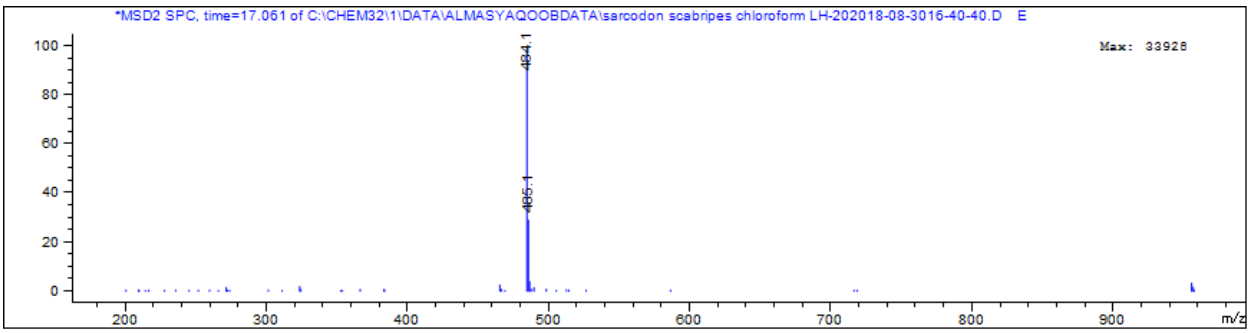

Figure 4. 11 Integration of MS scan spectrum revealing the presence and abundance of compound with *m/z* 484.1 in the peak visible at 17.061 min. (represents peak at 16.672 min in UV signal shown in Figure 4.7).

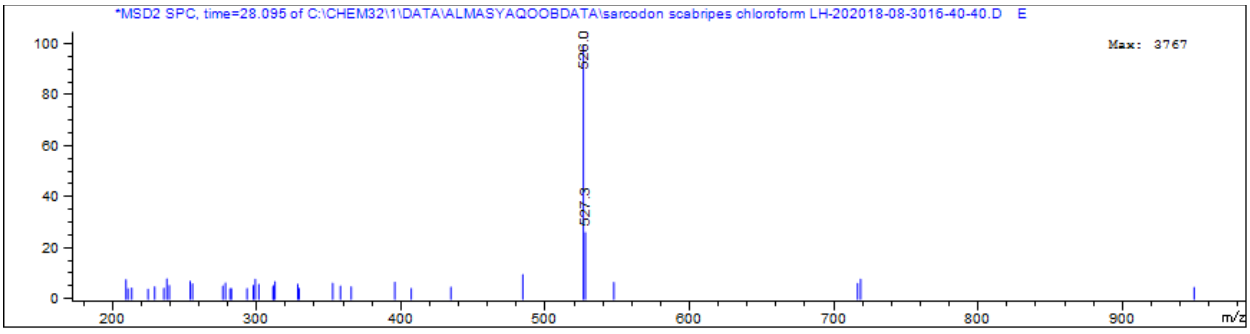

Figure 4. 12 Integration of MS scan spectrum revealing the presence and abundance of compound with *m/z* 526.0 in the peak visible at 28.095 min. (represents peak at 27.921 min in UV signal shown in Figure 4.7).

4.2.6.2 Second step confirmation using SIM mode and targeting the selected masses

A second step confirmation using SIM (selected ion mode) was performed on the same semi-crude sample. Molecular masses targeted are shown in Figure 4.15. The SIM mode signal (Fig 4.14) confirmed the presence of the target masses. The abundance of the targeted masses was also found to be higher in SIM mode than in the SCAN mode, confirming the presence of the compounds in the sample. The abundance of *m/z* = $[M+H]^+$ 484.1 ions in SIM mode was found to be three time higher than in the SCAN mode. The abundance of *m/z* = $[M+H]^+$ ions was also found to have increased for other SIM signals. Figure 4.13 shows the UV spectrum, the retention times and abundance for all the peaks that are quite similar to those seen in the UV spectrum in Figure 4.7. Figure 4.16 shows the integration of the peak visible at 8.902 min (visible at 8.610 min of UV signal), therefore confirming the presence as well as the abundance of compound with $[M+H]^+$ *m/z* = 428.0. Integration of MS SIM spectrum for ions with $[M+H]^+$ *m/z* = 442.0, 484.0 and 526.0 are illustrated in Figures 4.17, 4.18 and 4.19 respectively.

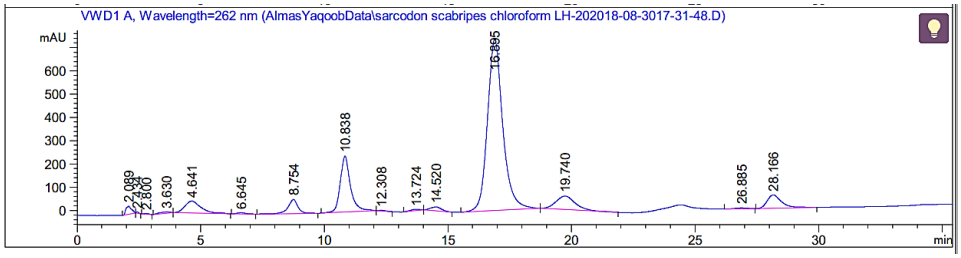

Figure 4. 13 UV spectrum representing the relative abundance and retention time of peaks at λ_{max} 262 nm (using analytical column and Sephadex LH-20 active fraction sample of chloroform layer).

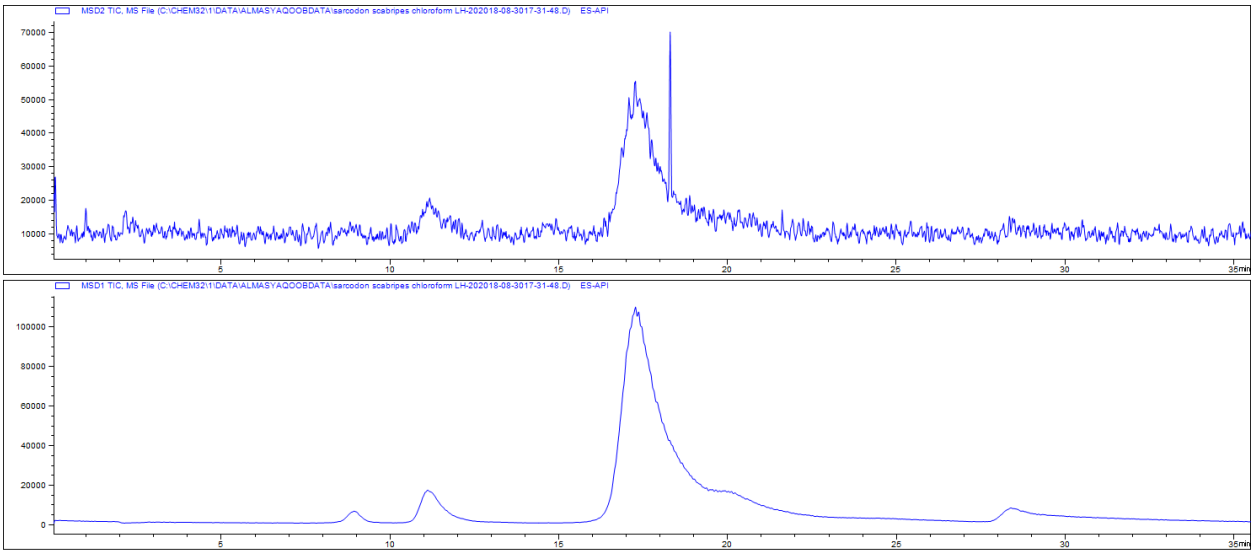

Figure 4. 14 MS SIM spectrum representing the relative abundance and retention time of the targeted masses, detected through ESI (Electrospray ionization) chamber. The type of column utilized was Agilent Zorbax analytical and the sample was 1 µL (20mg/mL) of filtered Sephadex active fraction.

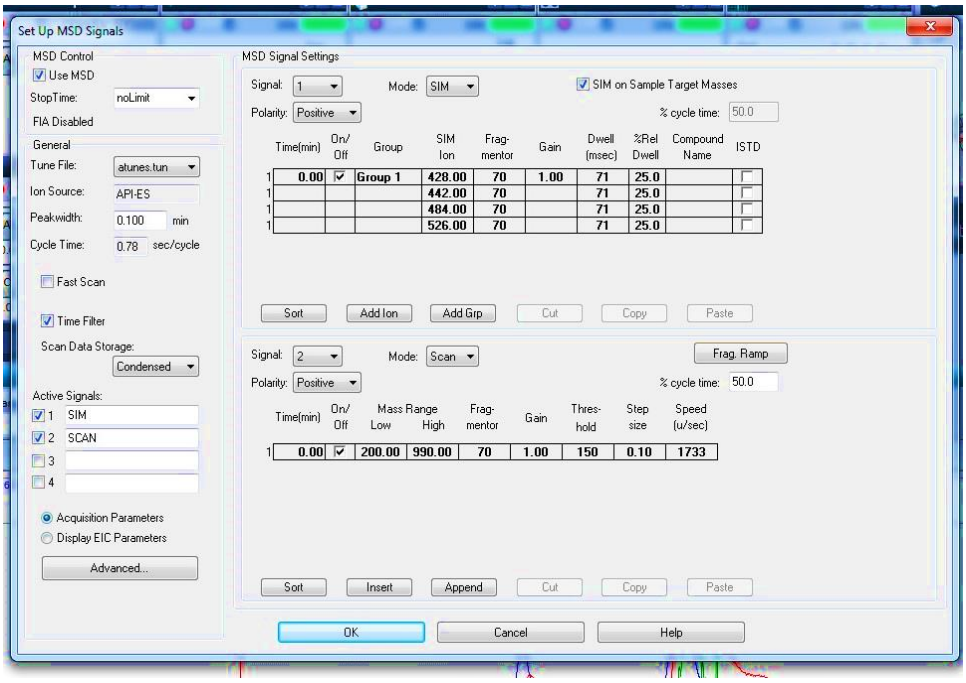

Figure 4. 15 Screen computer image showing the SIM mode targeted masses and the fragmented value as well as % relative dwell time for the targeted masses.

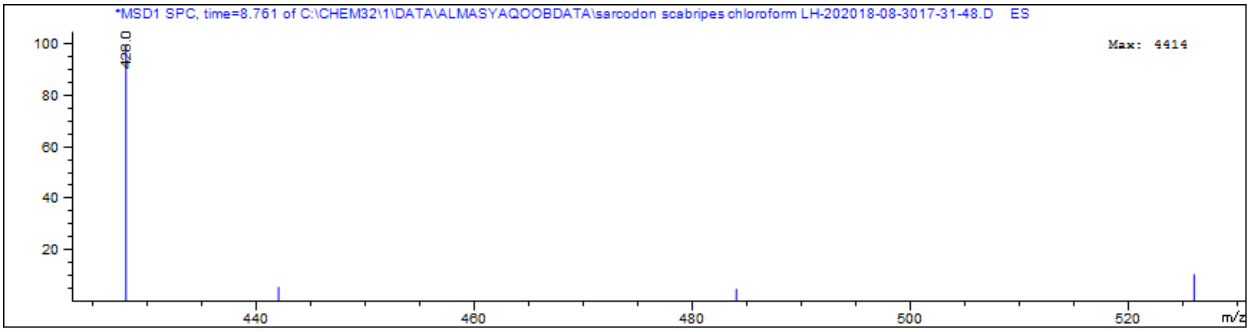

Figure 4. 16 Integration of MS SIM spectrum confirming the presence and abundance of compound with *m/z* 428.0 in the peak visible at 8.761 min. (represents peak at 8.610 min in UV signal shown in Figure 4.7).

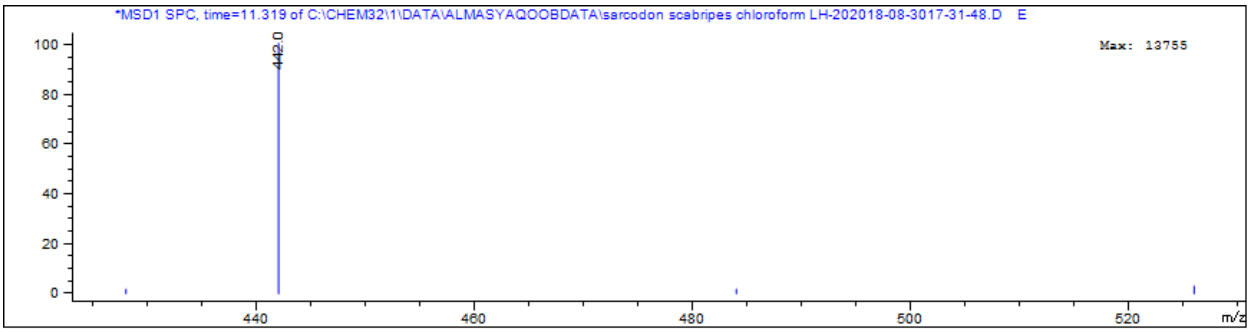

Figure 4. 17 Integration of MS SIM spectrum confirming the presence and abundance of compound with *m/z* 442.0 in the peak visible at 11.319 min. (Represents peak at 10.703 min in UV signal shown in Figure 4.7).

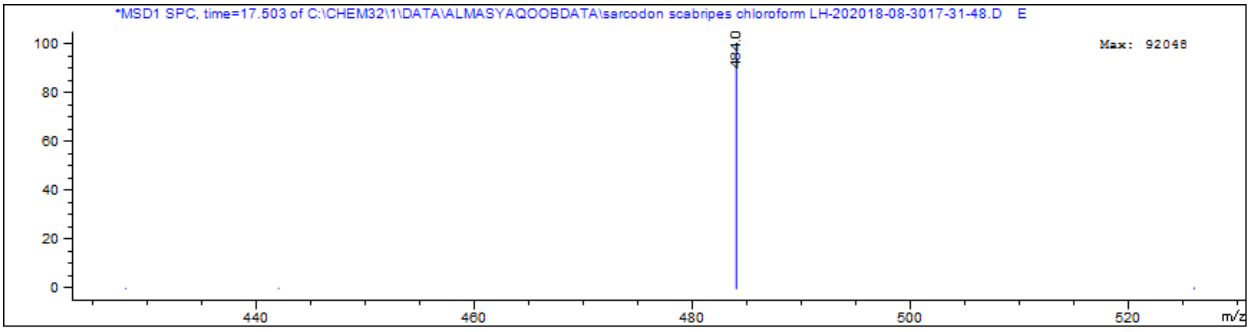

Figure 4. 18 Integration of MS SIM spectrum confirming the presence and abundance of compound with *m/z* 484.0 in the peak visible at 17.503 min. (Represents peak at 16.672 min in UV signal shown in Figure 4.7).

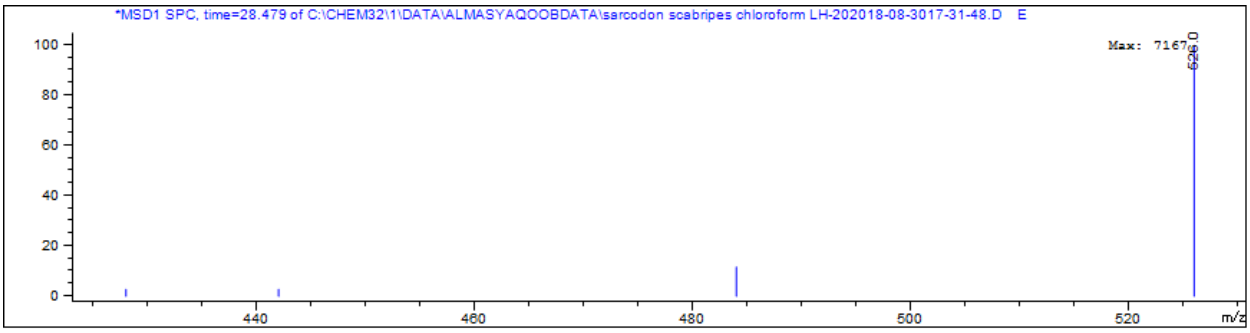

Figure 4. 19 Integration of MS SIM spectrum confirming the presence and abundance of compound with *m/z* 526.0 in the peak visible at 28.479 min. (Represents peak at 27.921 min in UV signal shown in Figure 4.7).

4.2.6.3 Top ethyl acetate layer (TEA)

The column used for the analysis of the top ethyl acetate layer was the weak polar Phenomenex Phenyl-Hexyl column (4.6 x 250 mm). The optimal resolution of the peaks in UV spectra indicated the ideal conditions of mobile and stationary phase. Two major peaks were observed at 4.963 and 7.738 min (Figure 4.20). The most abundant peak on UV spectrum was observed at 4.963 min, containing 48.38% of the sample mixture. The molar mass $[M+H]^+$ of ionized compound present in the peak at 4.963 min was determined to be 339.1 *m/z*. The percent abundance of UV peak visible at 7.738 min was 34.81%, making it the second most abundant peak on the spectrum. A small peak was observed at 6.646 min with an abundance of 8.27%. The molar mass *m/z* = $[M+H]^+$ of ionized compound present in peaks at 6.464 and 7.738 min was 444.1 and 442.1 respectively. Figure 4.21 represents the MS scan spectrum of TEA sample. while Figures 4.22, 4.23 and 4.24 show the presence and abundance of compound with *m/z* 339.1, 44.1 and 442.1 respectively.

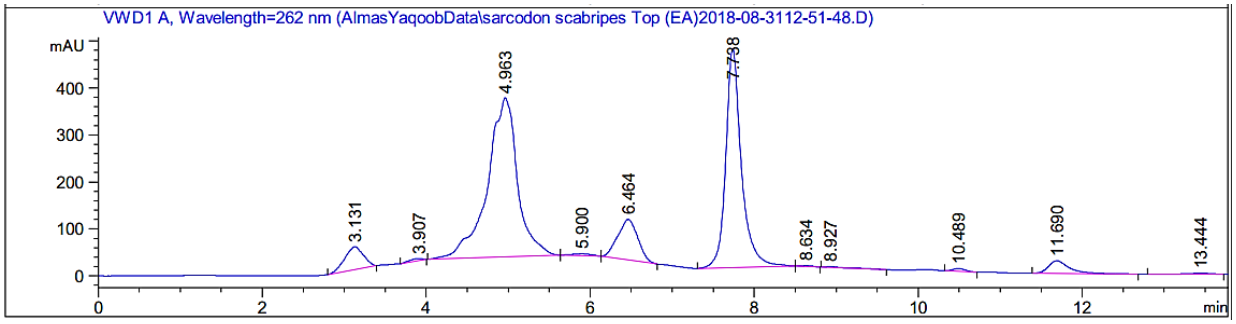

Figure 4. 20 UV spectrum representing the relative abundance and retention time of peaks at λ_{max} 262 nm (using analytical column and TEA Top ethyl acetate layer sample).

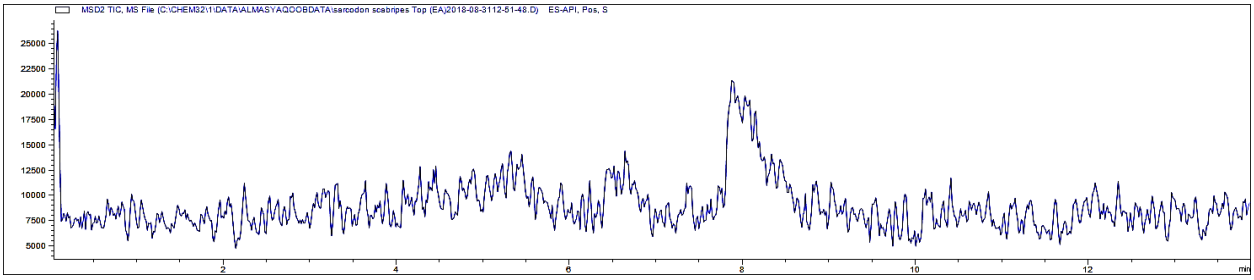

Figure 4. 21 MS Scan spectrum representing the relative abundance and retention time of the ionic compounds detected in ESI (Electrospray ionization) chamber. The type of column utilized was Phenomenex phenyl-hexyl column and the sample was 1 µL (20mg/mL) of top ethyl acetate layer.

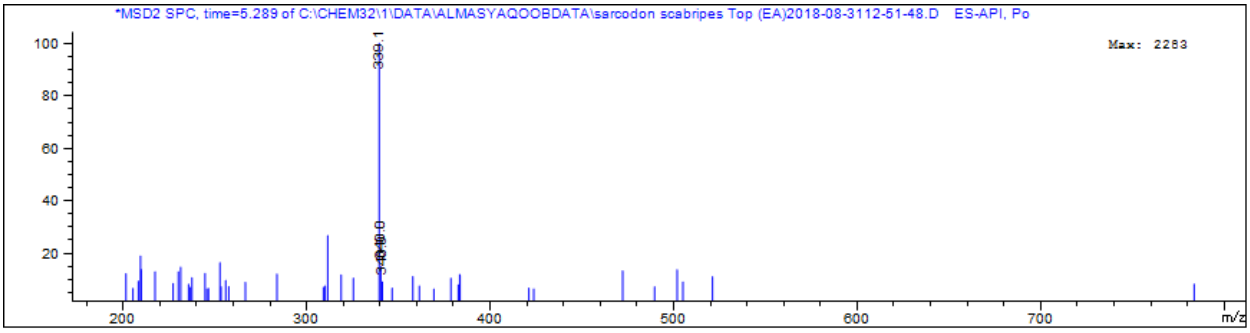

Figure 4. 22 Integration of MS Scan spectrum indicating the presence and abundance of compound with *m/z* 339.1 in the peak visible at 5.289 min. (Represents peak at 4.963 min in UV signal shown in Figure 4.20).

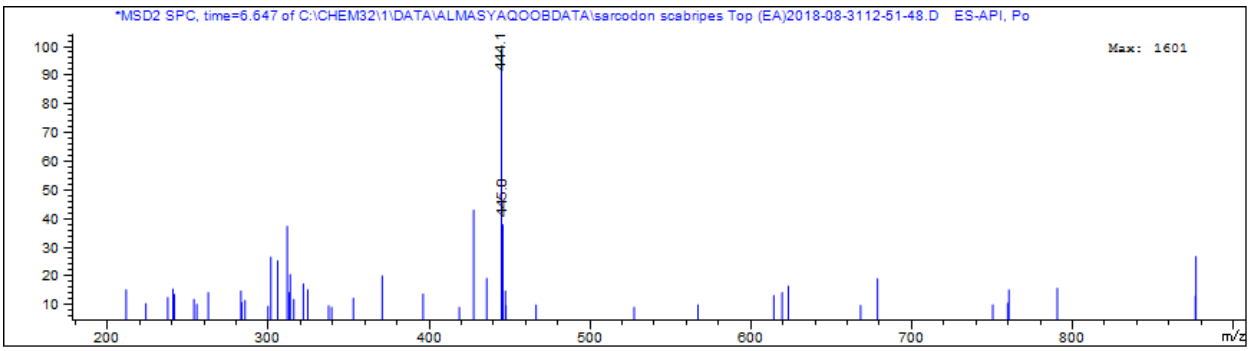

Figure 4. 23 Integration of MS scan spectrum indicating the presence and abundance of compound with *m/z* 444.1 in the peak visible at 6.647 min. (Represents peak at 6.646 min in UV signal shown in Figure 4.20).

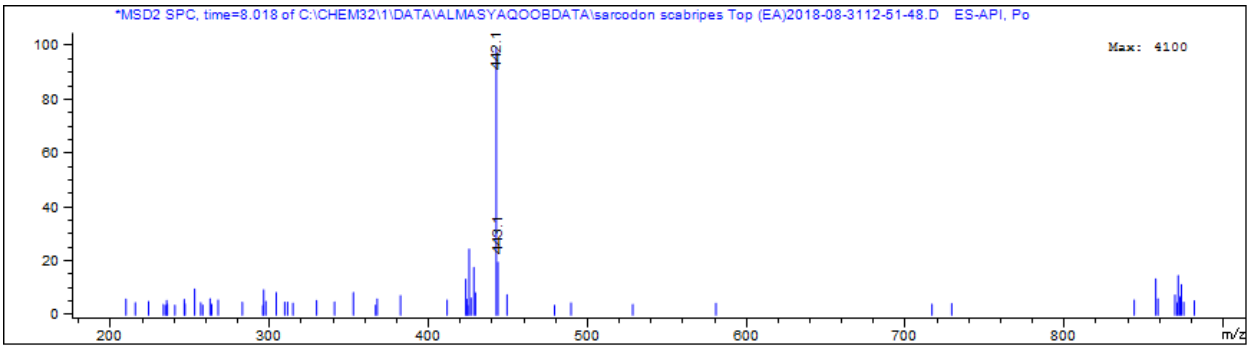

Figure 4. 24 Integration of MS scan spectrum indicating the presence and abundance of compound with *m/z* 442.1 in the peak visible at 8.018 min. (Represents peak at 7.738 min in UV signal shown in Figure 4.20).

4.2.6.4 Second step confirmation using SIM mode by targeting the selected masses

A second step confirmation using SIM (selected ion mode) was performed on the same semi-purified sample. The SIM mode signal (Figure 4.25) confirmed the presence of the target masses. The abundance of the targeted masses was also found to be higher in the SIM mode than in the SCAN mode, confirming the presence of compounds in the sample. The abundance of all compounds (*m/z* = $[M+H]^+$ in SIM mode) was found to be three time higher than the SCAN mode. Since the ethyl acetate layer did not exhibit any growth-inhibitory activity,

it was considered of less priority for purification purposes. Figures 4.26, 4.27 and 4.28 confirm the presence and abundance of compound with *m/z* 338.9, 44.1 and 442.1 respectively.

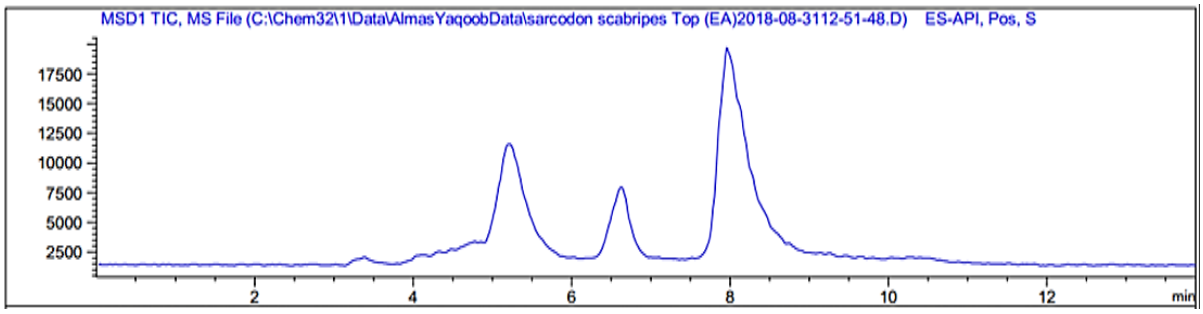

Figure 4. 25 MS SIM spectrum representing the relative abundance and retention time of the targeted masses, detected through ESI (Electrospray ionization) chamber. The type of column utilized was Phenomenex phenyl-hexyl column and sample was 1 µL (20mg/mL) of top ethyl acetate layer.

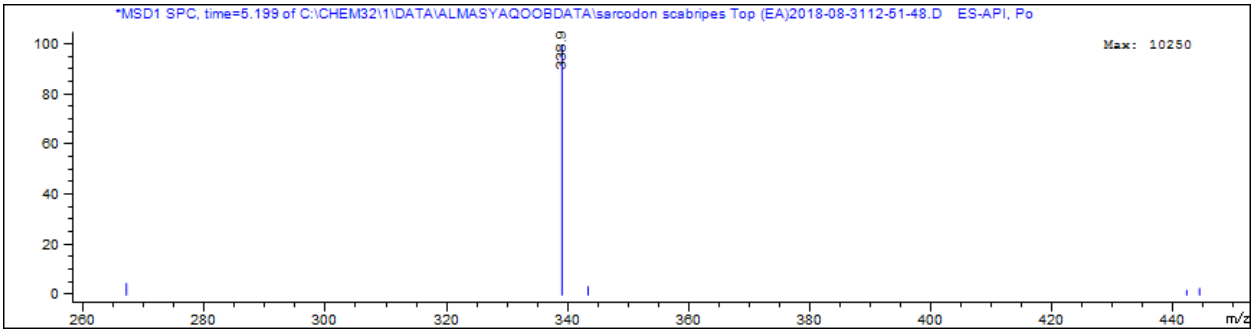

Figure 4. 26 Integration of MS SIM spectrum confirming the presence and abundance of compound with *m/z* 338.9 in the peak visible at 5.199 min. (Represents peak at 4.963 min in UV signal Figure 4.20).

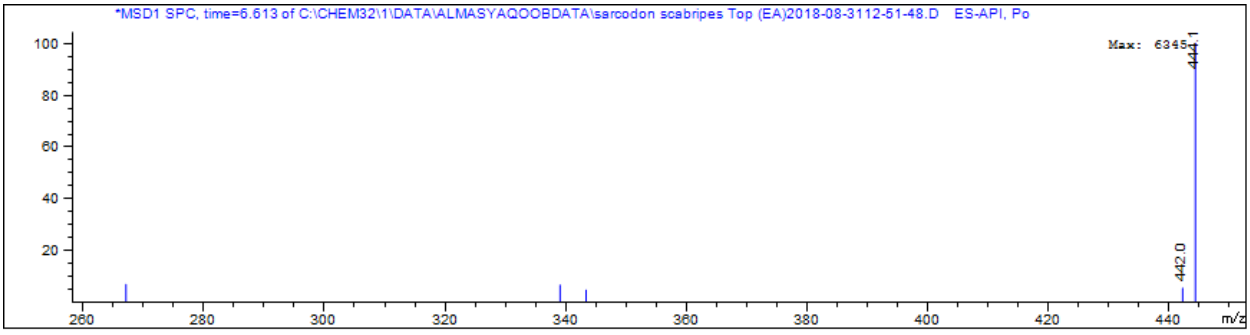

Figure 4. 27 Integration of MS SIM spectrum confirming the presence and abundance of compound with *m/z* 440.1 in the peak visible at 6.613 min. (Represents peak at 6.464 min in UV signal Figure 4.20).

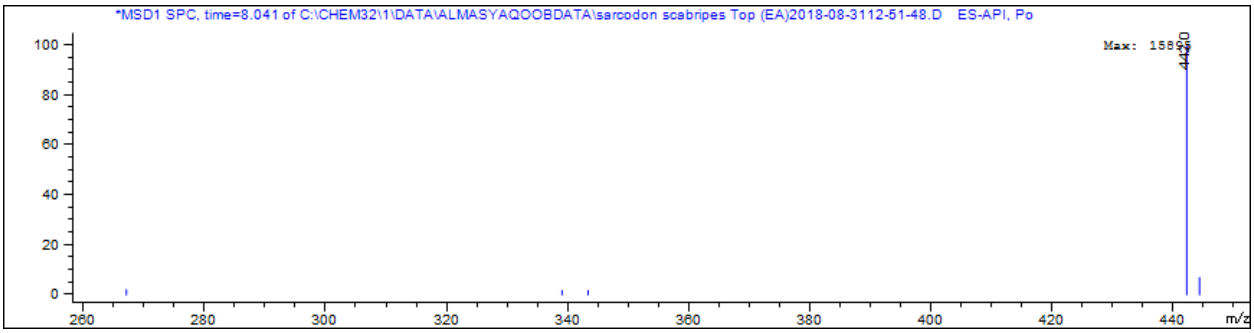

Figure 4. 28 Integration of MS SIM spectrum confirming the presence and abundance of compound with *m/z* 442.0 in the peak visible at 8.041 min. (Represents peak at 7.738 min in UV signal Figure 4.20).

4.2.6.5 Top water layer (TW)

Due to the limited range of HPLC columns available for separating polar compounds, it was difficult to obtain optimal separation of compounds using the currently available columns. Also, the UV Spectrum (Figure 4.29) peaks obtained using phenyl-Hexyl column did not correlate with the mass spectrophotometer signals. The mass spectrophotometer signals had a totally different retention time than the UV signals. This suggests the presence of carbohydrates in the sample (which needs to be separated using Sephadex column) or the compounds were not quite visible at this UV wavelength. Since this water layer exhibited a strong growth-inhibitory activity (Figure 4.3), future studies by other lab members should focus on using an appropriate HPLC column to purify the bioactive compound(s).

MS scan mode (Figure 4.30) indicated the presence of two small molecules with *m/z* values of 360.2 and 258.1 at 4.89 and 4.727 min respectively. While there was no peak in UV signal visible with these retention times, SIM mode mass spectrometry (by targeting these two compounds) revealed the two distinct signals at 4.923 and 6.243 min. The SIM signal at 4.932 min represents the compound with 360.2 *m/z* and 77992 abundance. Figures 4.31 and 4.32 are the integration of the scan spectrum showing the presence and abundance of compound with *m/z*

360.2 and 358.1 respectively. Figure 4.34 shows integration of MS-SIM spectrum at 4.391 min to confirm the presence of the compound with *m/z* 360.0.

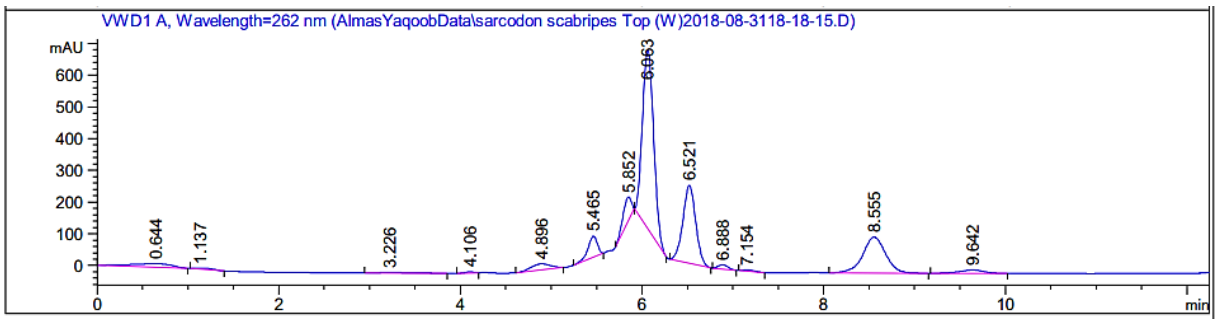

Figure 4. 29 UV spectrum representing the relative abundance and retention time of peaks at λ_{max} 262 nm (using analytical column and Top water layer).

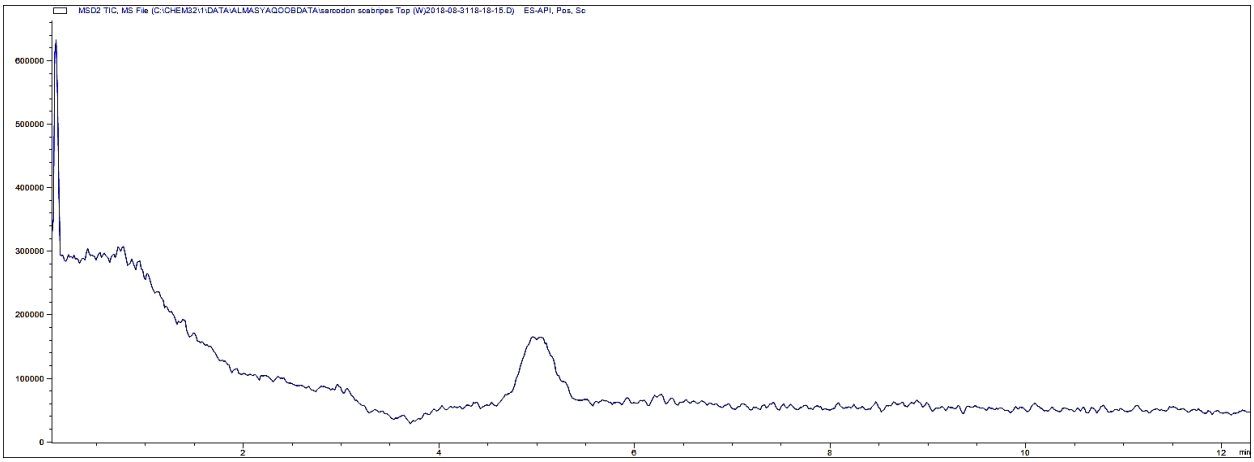

Figure 4. 30 MS scan spectrum representing the relative abundance and retention time of the compounds detected through ESI (Electrospray ionization) chamber. The type of column utilized was Phenomenex phenyl-hexyl column and sample was 1 µL of top water layer.

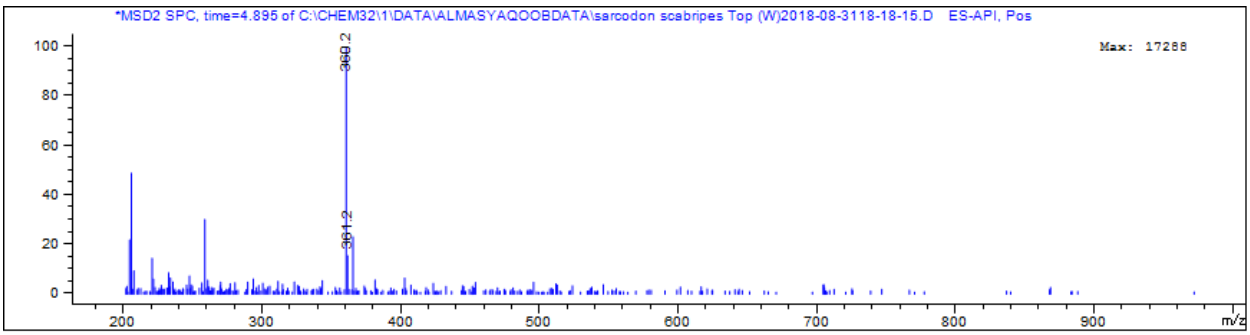

Figure 4. 31 Integration of MS Scan spectrum indicating the presence and abundance of compound with *m/z* 360.2 visible at 4.895 min.

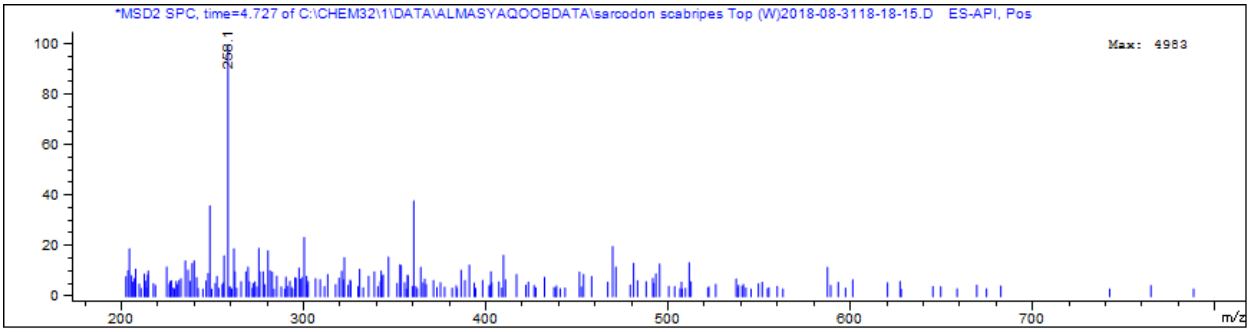

Figure 4. 32 Integration of MS Scan spectrum indicating the presence and abundance of compound with *m/z* 258.1 visible at 4.727 min.

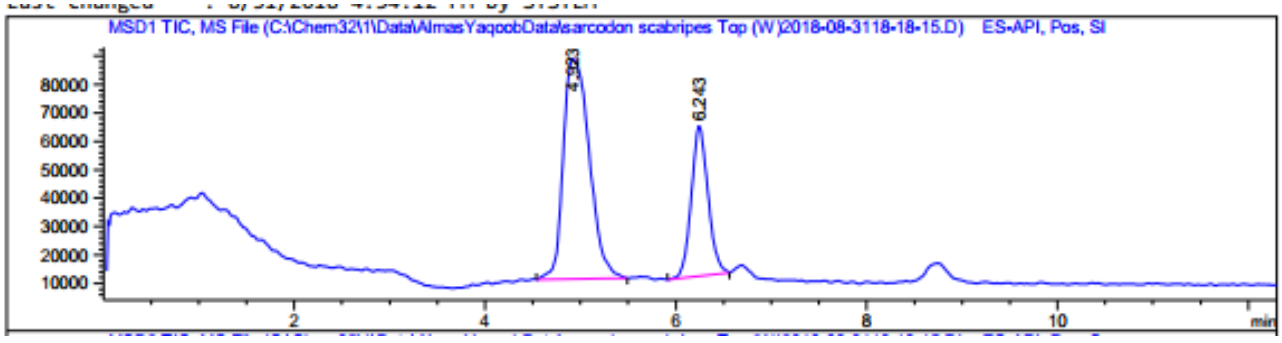

Figure 4. 33 MS SIM spectrum representing the relative abundance and retention time of the targeted masses, detected through ESI (Electrospray ionization) chamber. The type of column utilized was Phenomenex phenyl-hexyl column and sample was 1 µL of top water layer.

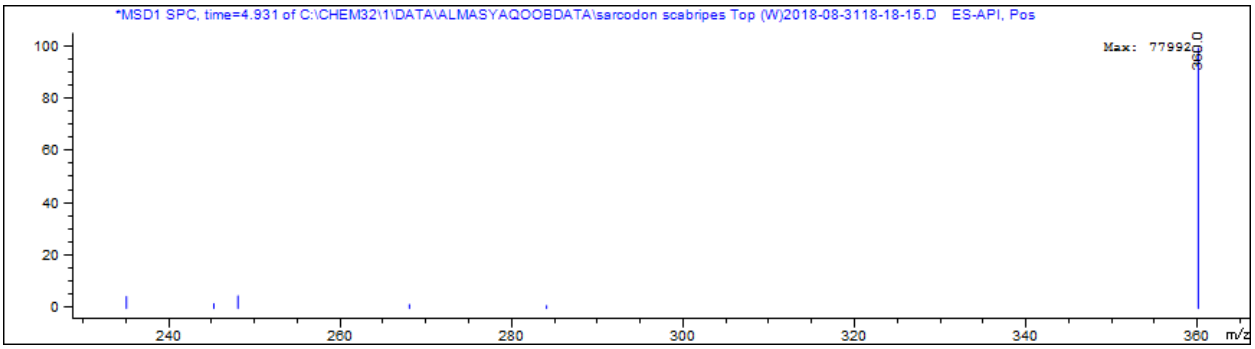

Figure 4. 34 Integration of MS SIM spectrum confirming the presence and abundance of compound with *m/z* 360.0 at 4.931 min.

4.2.7 Possibility of isolating novel compounds from *S. scabripes*

HPLC-MS analyses of the liquid-liquid extraction layers had provided an insight to the possibility of isolating novel compounds from *S. scabripes*. Tables 4.4 and 4.5 provide a summary of the identified compounds with different *m/z* present in the different liquid-liquid extraction layers. By comparing these *m/z* with known small molecules already identified from mushrooms of the same or different genus, it is possible to speculate which compounds could potentially be novel. An additional advantage is that *S. scabripes* has never been explored for its chemical constituents.

HPLC analysis revealed the compounds present in the bioactive Sephadex LH-20 fractions being smaller in size (Table 4.4 and 4.5). The molecular masses of the compounds present in *S. scabripes* (E1 extract) fell in the range of 360 to 526 *m/z*. The *m/z* $[M+H]^+$ of the most abundant compound present in chloroform layer was 484.0, which could be either methyl antcinate-B or a novel compound. Methyl antcinate-B is a cytotoxic compound purified from *Antrodia camphorata* (Yue et al., 2010). The *m/z* $[M+H]^+$ value of the compound present in water layer was 360.0, which could possibly be sarcodonin E (purified from *S. scabrosus*) (Dong et al., 2009) or it could also be a novel compound.

Table 4. 4 HPLC-UV data representing the peaks, their retention time and abundance in Sephadex fractions of chloroform layer.

Layer	HPLC column used	Retention time in UV signal (min)	Abundance based on UV signal	Molecular mass	Closest mass found in compounds isolated from other mushrooms	Reported Bioactivity of the compounds	Reference
Chloroform layer (exhibited cytotoxic activity on HeLa cells)	Zorbax C-18 analytical column	8.610	3.0807%	428	9,11-dehydroergosterol peroxide have molecular mass 426.63 found in *Sarcodon aspratus.*	Inhibitor of HL60 leukemia growth, apoptosis-inducer	Kobori *et al*., 2006.
		10.703	12.9368%	442	Scabronine H or Sarcodonin P both have molecular mass of 440.58 found in *S. scabrosus.*	Anti-bacterial and anti-fungal.	Ma *et al*., 2010.
		16.672	58.6614%	484	Methyl antcinate B have molecular mass 482.65 found in *Antrodia camphorata.*	Cytotoxic against several cancer cell lines.	Yue *et al*., 2012.
		27.921	6.4767%	526	Aurisin-K have molecular mass of 524.6 found in *Neonothopanus nambi*	Antimalarial activity (P. falciparum); antimycobacterial (M. tuberculosis)	Kanokmedhakul *et al* ., 2012.

Table 4. 5 HPLC-UV data representing the peaks, their retention time and abundances in top ethyl acetate and top water layer of the liquid-liquid extraction.

Layer	HPLC column used	Retention time in UV signal (min)	Percentage abundance based on UV signal	Molecular mass	Closest mass found in compounds isolated from other mushrooms	Reported Bioactivity of the compounds	Reference
Top layer ethyl acetate (did not show any activity on HeLa cells)	Phenyl-hexyl	4.963	48.3859%.	339	None	-	-
		6.464	8.2706 %.	444	Inonotsudiol A and inotodiol both have molecular mass of 442.72 found in *Inonotus obliquus.*	Cytotoxic against several cancer cell lines.	Handa *et al.,* 2010.
		7.738	34.8103%.	442 (also found in chloroform layer) Maybe It's a weak polar in nature	Scabronine H or sarcodonin P both have molecular mass of 440.58 found in *S. scabrosus*.	Anti-bacterial and anti-fungal.	Ma *et al*., 2010.
Top water layer (exhibited cytotoxic activity on HeLa cells)	Phenyl-Hexyl column	6.063	42.9028%	360	Sarcodonin E or 19-O-acetylsarcodonin G have molecular mass of 358.47 found in *S. scabrosus*.	-	Dong *et al*., 2009.

4.2.7 HPLC- semi-preparative (peaks collection)

The method developed and based on isocratic solvent system (water 43: acetonitrile 12: and methanol 45) using Agilent Zorbax C-18 semi-preparative column resulted in optimal separation of peaks (as shown in Figure 4.35). The abundance of peaks varied with different samples from different Sephadex fractions. Fraction collector was programmed to collect 10 fractions containing the different peaks. Once the compounds are purified in sufficient quantity, NMR analysis will be performed by other lab members to help elucidate the structure.

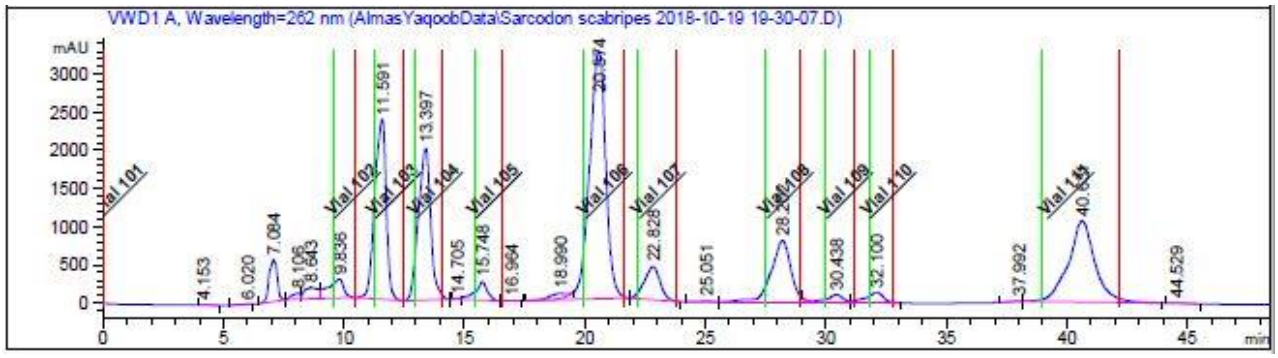

Figure 4. 35 UV spectrum representing the relative abundance and retention time of peaks at λ_{max} 262 nm (using semi-preparative column and Sephadex LH-20 fraction sample).

4.3 Discussion

This chapter describes the successful development of methods to purify growth-inhibitory compounds from *S. scabripes. Extracts* E1 (80% ethanol) and E2 (50% methanol) of *S. scabripes* exhibited potent growth-inhibitory activity. HeLa cell viability after treatment with both extracts (1 mg/mL) was less than 20%. For detailed study of chemical constituents, extract E1 was selected because of its potent growth-inhibitory activity. To obtain the bioactive compounds from E1 extracts, a series of purification steps were developed (Figure 4.36).

The E1 extract was first subjected to liquid-liquid extraction technique. This approach was based on two immiscible solvents (due to difference in polarity index). The first liquid-

liquid extraction was based on chloroform and water. The second sequential liquid-liquid extraction was based on same water layer with acetonitrile. Non-polar compounds were expected to move into the chloroform layer, while polar compounds were expected to solubilize and move into the water layer. Weakly polar molecules present in water layer were re-extracted with acetonitrile during the second step of liquid-liquid extraction.

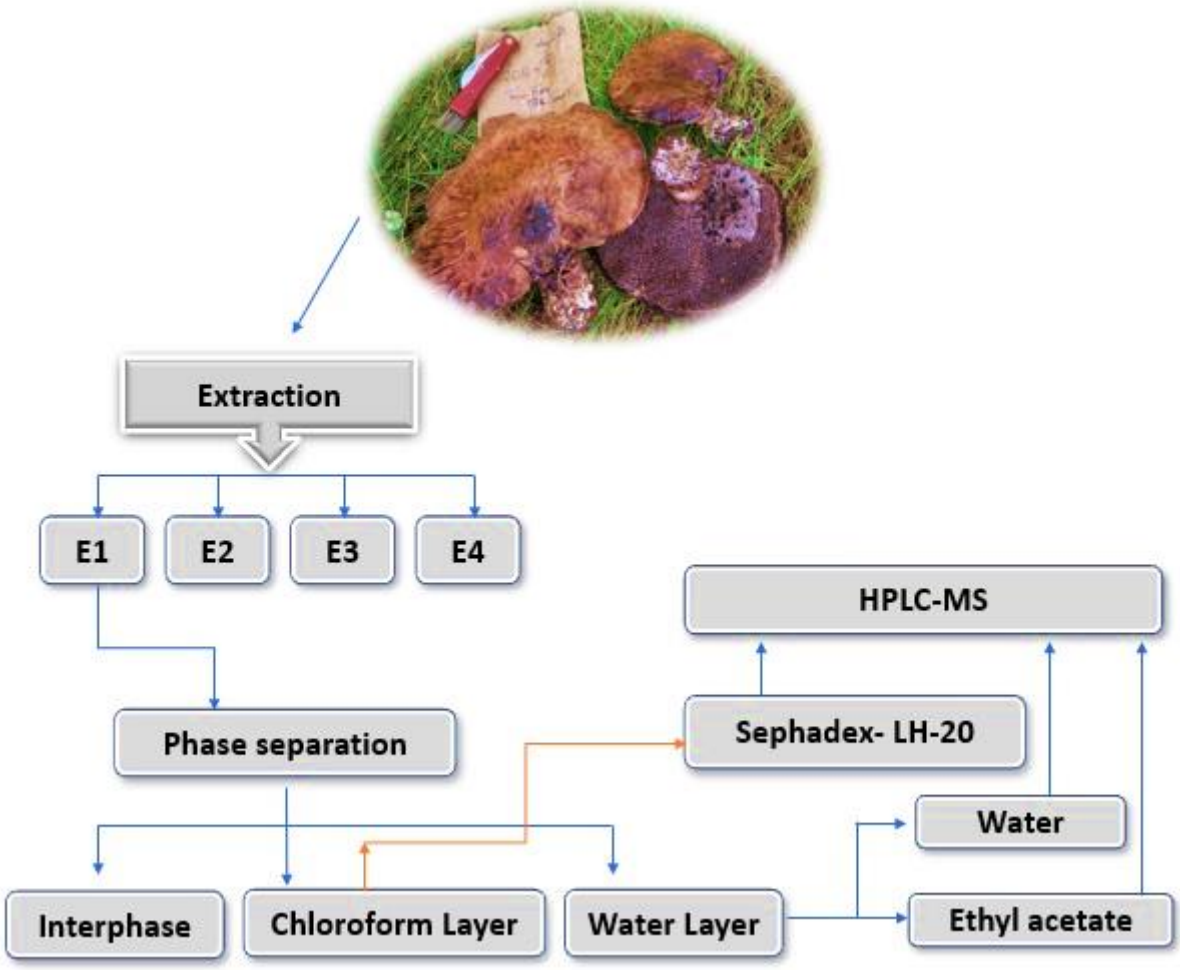

Figure 4. 36 Flow diagram representing the steps involved in the purification of compounds from *S. scabripes*.

Chloroform layer was then subjected to Sephadex LH-20 size exclusion chromatography. The volume of the fractions collected from Sephadex LH-20 columns were reduced by drying

($1/5^{th}$) and further assessed for growth-inhibitory potential. Even at 1 µL, the fractions were capable to reduce the cell viability down to 20% as compared to the negative control (Figure 4.5). A Nanodrop spectrophotometer was used to determine the λ_{max}=262nm of active Sephadex LH-20 fractions.

The post Sephadex LH-20 bioactive fractions were subjected to a second purification step using a high-resolution HPLC. Initially, a method was developed for optimal separation of compounds present in the bioactive post-Sephadex LH-20 fractions. The solvent system utilized for optimal separation of peaks was a gradient solvent system based on acetonitrile, methanol and water. The reverse phase (RP-HPLC) separation method was first developed using the non-polar analytical column (Zorbax eclipse, 5 µm C18, 150 x 4.6 mm) and a gradient solvent system (Figure 4.2). It was then scaled up to a semi-preparative column (Zorbax eclipse, 5 µm C18, 250 x 9.2 mm) using an isocratic solvent system (water 43: Acetonitrile 12: and methanol 45). The UV spectrum obtained using the semi-preparative column is shown in Figure 4.35. Peaks at ten different points of the UV spectrum were targeted for further collection, purification and mass determination of the compounds present in active Sephadex LH-20 fractions of chloroform layer (CL). The *m/z* $[M+H]^+$ of the compounds present in chloroform layer were 428.0, 442.0, 484.0 and 526.0.

No size-based separation using Sephadex LH-20 was performed on the water layer (TW) and top ethyl acetate layer (TEA). The HPLC method developed using analytical Phenyl-Hexyl column and isocratic solvent system (water 50%, acetonitrile 40% and methanol 10%) revealed the presence of three compounds present in the top ethyl acetate layer (TEA). The peaks obtained in the UV spectrum (Figure 4.29) of TW layer had different retention times than the peaks of TW in the MS Scan (Figure 4.30) and SIM spectrum (Figure 4.33).

4.4 Future directions

The E1 (80% ethanol) extract of *S. scabripes* could be a source to discover novel anti-cancer compounds. The purification of compounds present in the chloroform layer based on a semi-preparative HPLC method is still in progress. Purification of compounds in larger quantity is required for structural elucidation and biochemical characterization studies. Therefore, it is the priority of this study.

Chapter 5: General Discussion & Future Directions

5.1 General Discussion

5.1.1 Screening BC wild mushrooms for immuno-modulatory and growth-inhibitory activities

Wild mushrooms in North America have largely been unexplored for their medicinal properties. Recent studies by the research team at UNBC on wild mushrooms native to northern British Columbia showed that many species have never been reported for their growth-inhibitory, immuno-stimulatory or anti-inflammatory activities (Deo et al., in review; Smith et al., 2017). One of the major aims of this MSc thesis was to screen some of the wild mushrooms collected across Canadian forests for their immuno-modulatory and growth-inhibitory potential. To determine the growth-inhibitory and immuno-modulatory potential, HeLa human cervical cancer cells and Raw 264.7 mouse macrophage cells were used respectively. After successful screening of the growth-inhibitory and immuno-modulatory potential of extracts, I decided to focus on E1 extract (80% ethanol) of *A. flettii* because there has been no report of growth-inhibitory and anti-inflammatory activities of extract from this species. In addition, the E1 extract of *S. scabripes* was also explored for the same reason.

One of the objectives of this thesis was to reveal the immuno-modulatory potential of six genetically identified wild mushrooms collected from the forests in Canada: *F. officinalis, T. vaccinum, T. versicolor, A. flettii, S. scabripes* and *C. unicolor.* All twenty-four mushroom extracts were first screened for immuno-stimulatory activity. Eighteen extracts that showed weak or no immuno-stimulatory activity were further screened for anti-inflammatory activity.

Results from the screening of 24 crude mushroom extracts revealed that Canadian wild mushrooms have great potential for the discovery of novel immuno-modulatory and growth-inhibitory compounds. Out of the twenty-four extracts tested, five showed at least moderate (≥

40% stimulation) immuno-stimulatory activity. Among these, two extracts, E3 from *C. unicolor* and *T. versicolor* exhibited very strong (≥ 90%) immuno-stimulatory activity.

Out of 18 crude extracts tested, fifteen extracts showed at least moderate (≥ 40% inhibition) anti-inflammatory activity. Among these, twelve extracts from five species, *A. flettii* (E2, E3 and E4 only because E1 was cytotoxic), *F. officinalis* (E1 and E2), *S. scabripes* (E1, E2, E3 and E4), *T. vaccinum* (E1 and E2), and *T. versicolor* (E1), demonstrated very strong (≥ 90%) anti-inflammatory activity. The fact that there were more extracts with anti-inflammatory rather than with immuno-stimulatory activity is consistent with the earlier findings (Deo et al., in review; Smith et al., 2017). This suggests that in general, mushrooms have good anti-inflammatory activity.

In the case of growth-inhibitory activity screening, dose-dependent MTT assay was first performed on all twenty-four extracts. The extracts with potent growth-inhibitory activity (E1 and E2) from *F. officinalis*, *A. flettii* and *S. scabripes* were further studied for time-dependent MTT assay. Out of twenty-four extracts tested for dose-dependent MTT assay, twelve extracts demonstrated at least moderate (≥ 40% inhibition) growth-inhibitory activity. Among these, six extracts from three different mushrooms, *A. flettii* (E1 and E2), *F. officinalis* (E1 and E2), *S. scabripes* (E1 and E2), demonstrated very strong (≥ 90%) growth-inhibitory activity. These 6 extracts also showed potent growth-inhibitory activity in the time-dependent MTT assay. This study has further added to the list of wild mushrooms (Deo et al., in review; Smith et al., 2017) that should be explored for potential novel anti-cancer compounds. Taken together, it can be concluded that Canadian wild mushrooms are indeed good sources for the discovery of potential novel immuno-modulatory and growth-inhibitory compounds.

5.1.2 Purification, identification and characterization of growth-inhibitory compounds from *Albatrellus flettii*

This is the first study from Dr. Lee's lab describing purification, identification and characterization of small molecules from natural products, which in this case are mushrooms. I have carefully developed a purification strategy to isolate three growth-inhibitory compounds (grifolin, neogrifolin and confluentin) from *A. flettii* that can be generally adopted for the isolation of small molecules from any mushrooms (Figure 3.57). The first purification step involved liquid-liquid extraction that will provide clues as to the nature of the bioactive compounds. Presence of growth-inhibitory compounds (grifolin, neogrifolin and confluentin) in the chloroform layer suggested that they are more hydrophobic. Further purification based on Sephadex LH-20 size exclusion chromatography provided general information about the size of the bioactive molecules; smaller molecules will elute at later fractions. The last purification step using HPLC revealed the presence of three major growth-inhibitory small molecules present in bioactive fractions from Sephadex LH-20. Collection of the three bioactive small molecules from HPLC followed by 1-D and 2-D NMR analyses confirmed their identity as grifolin, neogrifolin and confluentin. The final yield of grifolin, neogrifolin and confluentin was 0.26, 0.16 and 0.025% respectively. These compounds possessing antibacterial property against *Bacillus cereus* and *Enterococcus faecalis* had been previously identified from *A. flettii* collected from California, USA, in January 2007 (Liu et al., 2010).

Grifolin and neogrifolin, both the synthetic form and naturally isolated from other *Albatrellus* species, had been extensively studied for their anti-cancer properties and most of the underlying mechanisms (as discussed in headings 3.1.3.1 and 3.1.3.2).

The underlying mechanisms of grifolin for the apoptosis induction in nasopharyngeal carcinoma cell CNE1 was found to be based on upregulation of DAPK1 via the p53–DAPK1

pathway (Luo et al., 2011) as well as by involvement of Bcl-2 family members and cytochrome c (Ye et al., 2005). Another mechanism involved in apoptosis induction in osteosarcoma cells was found out to be based on down-regulating the expression of the IAP (inhibitor of apoptosis protein) and induction of caspases (Jin et al., 2007). The autophagic cell death in human melanoma cells after treatment with grifolin was found mainly due to inhibition of Akt/mTOR/S6K pathway (Zhao et al., 2016). Grifolin resulted in reduced proliferation of osteosarcoma cells by reducing phosphorylation of Akt, FOXO transcription factor and GSK3 (Jin et al., 2007). The ability of grifolin to arrest tumor cells at G1 phase, was found mainly due to the inhibition of cyclin D, cyclin E and CDK 4 of the ERK1/2 or the ERK5 pathway (Ye et al., 2007).

Like grifolin, neogrifolin also has the ability to affect the AKT signaling pathway through the same mechanisms. Neogrifolin-treated osteosarcoma cells resulted in downregulation of phosphorylated AKT level, FOXO transcription factor, and glycogen synthase kinase 3 (GSK3) and IAP (inhibitor of apoptosis protein), while caspases were found upregulated (Chen et al., 2015).

Confluentin is a relatively new compound and it has not been explored for any of the anti-cancer properties nor underlying mechanisms (Hellwig et al., 2003).

In this study, grifolin, neogrifolin and confluentin purified from *A. flettii* were found to possess novel biochemical activity as described below.

5.1.2.1 Disrupting IMP1-KRas RNA interaction *in vitro* and inhibition of KRas expression in human colon cancer cells

In this study, grifolin, neogrifolin and confluentin isolated from *A. flettii* were assessed for their ability to disrupt IMP-1-KRas RNA interaction using an established fluorescent

polarization method. Both grifolin and neogrifolin dose-dependently inhibited the interaction between full-length IMP1 and KRas RNA but not the interaction between KH34 IMP1 and KRas RNA. This suggested that the compounds may bind to sites other than the KH34 di-domains of IMP1 (Barnes et al., 2015). At the time of writing this thesis, confluentin has not been tested on the fluorescent polarization assay.

Based on the results from the fluorescent polarization experiments, I hypothesized that the compounds could disrupt IMP1-KRas mRNA interaction in colon cancer cells leading to decrease in KRas expression (Mongroo et al., 2011). To test this hypothesis, the compounds were added to SW480 and HT-29 human colon cancer cells and KRas expression monitored using Western blot analysis. Interestingly, all three compounds were found to suppress KRas expression in both SW480 and HT-29 cells. To my knowledge, this is the first demonstration of the ability of grifolin, neogrifolin and confluentin in inhibiting KRas expression in cancer cells. Such inhibition on KRas expression could represent a mechanism whereby these compounds exert their growth-inhibitory effects on cells (Pagliuca et al., 2013).

The least abundant bio-active compounds present in *A. flettii*, confluentin, was investigated for its ability to induce apoptosis and cell cycle analysis in SW480 cells. This study shows for the first time that confluentin is a potent inducer of apoptosis in SW480 colon adenocarcinoma cells as well causing cell cycle arrest at G_2/M phase.

5.1.3 Purification and identification of growth-inhibitory compounds from *Sarcodon scabripes*

The techniques used in the purification of growth-inhibitory compounds from *S. scabripes* was based on the method developed earlier for *A. flettii*. However, the liquid-liquid extraction was done twice based on water/chloroform and water/ethyl acetate solvent system to

get a clearer separation of compounds based on polarity. Three layers were named as top ethyl acetate layer (TEA), top water layer (TW) and chloroform layer (CL). CL and TW were found to contain growth-inhibitory compounds. MTT assay results using Sephadex LH-20 fractions (of chloroform layer) suggested that the compounds were small in size (bioactive compounds present in later eluting fractions). Further analyses using HPLC confirmed that the compounds present in the bioactive Sephadex LH-20 fractions were small molecules (Table 4.4 and 4.5). The molecular masses of the compounds present in *S. scabripes* fell in the range of 360 to 526 *m/z*. The *m/z* of the most abundant compound present in chloroform layer was 484.0, which could be methyl antcinate-B or a novel compound. The molecular mass of methyl antcinate-B is 482.65 g/mole, a cytotoxic compound purified from *Antrodia camphorata* (Yue et al., 2010). The compounds with *m/z* 442.0 could be either Scabronine H or Sarcodonin P (anti-bacterial) which was isolated from *S. scabrosus* (Ma et al., 2010). TEA layer based HPLC-MS results revealed the presence of an abundant compound with 442.0 *m/z* ratio. Scabronine H or sarcodonin P both purified *S. scabrosus* have molecular mass of 440.58 (Ma et al., 2010). So, it could be either of these two or it could be a novel compound.

The *m/z* value of the compound present in water layer was 360.0, which could possibly be Sarcodonin E (purified from *S. scabrosus*) (Dong et al., 2009) or it could also be a novel compound. It is important to point out that Sarcodonin E has not been studied for any biological activity. Taken together, it is reasonable to speculate that for the possibility of finding novel growth-inhibitory compounds from *S. scabripes* is high because this mushroom has not been previously explored for its chemical constituents nor bioactivity.

The HPLC based purification technique was further scaled-up to a semi-preparative column in an effort to obtain sufficient quantity for further chemical analyses and compound identification purposes.

5.1.4 Conclusions

At the outset of this research, it was hypothesized that wild Canadian mushrooms contain potent small bioactive compounds. The results from this study showed that indeed northern BC is home to a large variety of mushrooms containing potent growth-inhibitory small molecules. Overall, the results generated from this study have provided an important platform for future investigations into discovering potential novel bioactive small molecules from Canadian wild mushrooms. For example, the crude extracts from *S. scabripes* and *T. vaccinum* may serve as potential sources for future discovery of novel growth-inhibitory or immuno-modulatory compounds. With the successful purification of three growth-inhibitory compounds (grifolin, neogrifolin and confluentin) from *A. flettii*, future studies could focus on understanding their mechanism of action in inhibiting KRas expression, a cellular effect that has not been previously described nor studied for these compounds.

There is a high possibility of isolating novel growth-inhibitory compounds from *S. scabripes.* This is based on the HPLC-MS analyses of the growth-inhibitory Sephadex LH-20 fractions from the chloroform layer sample. Further scaling-up the HPLC technique using a semi-preparative column will make the process of collection faster, hopefully leading to identification and characterization of the compounds.

References

Ahn, W. S., Kim, D. J., Chae, G. T., Lee, J. M., Bae, S. M., Sin, J. I., ... & Lee, I. P. (2004). Natural killer cell activity and quality of life were improved by consumption of a mushroom extract, *Agaricus blazei* Murill Kyowa in gynecological cancer patients undergoing chemotherapy. *International Journal of Gynecological Cancer*, *14*(4), 589-594.

Alves, M. J., Ferreira, I. C., Dias, J., Teixeira, V., Martins, A., & Pintado, M. (2012). A review on antimicrobial activity of mushroom (Basidiomycetes) extracts and isolated compounds. *Planta Medica*, *78*(16), 1707-1718.

Arora, D. (1986). Mushrooms demystified. A comprehensive guide to the fleshy fungi. Berkeley, California: Ten Speed Press.

Barros, L., Cruz, T., Baptista, P., Estevinho, L. M., & Ferreira, I. C. (2008). Wild and commercial mushrooms as source of nutrients and nutraceuticals. *Food and Chemical Toxicology*, *46*(8), 2742-2747.

Binder, M., & Hibbett, D. S. (2002). Higher-level phylogenetic relationships of homobasidiomycetes (mushroom-forming fungi) inferred from four rDNA regions. *Molecular Phylogenetics and Evolution*, *22*(1), 76-90.

Blanchette, R. A., Compton, B. D., Turner, N. J., & Gilbertson, R. L. (1992). Nineteenth century shaman grave guardians are carved *Fomitopsis officinalis* sporophores. *Mycologia*, *84*(1), 119-124

Bruggisser, R., von Daeniken, K., Jundt, G., Schaffner, W., & Tullberg-Reinert, H. (2002). Interference of plant extracts, phytoestrogens and antioxidants with the MTT tetrazolium assay. *Planta medica*, *68*(05), 445-448.

Burk, W. R. (1983). Puffball usages among North American Indians. *J. Ethnobiol*, *3*, 55-62.

Chakrabarti, M., Jang, H., & Nussinov, R. (2016). Comparison of the conformations of KRAS isoforms, K-Ras4A and K-Ras4B, points to similarities and significant differences. *The Journal of Physical Chemistry B*, *120*(4), 667-679.

Chang ST, Miles PG. (1992) Mushrooms biology—a new discipline. Mycologist. 6:64–5.

Che, X., Yan, H., Sun, H., Dongol, S., Wang, Y., Lv, Q., & Jiang, J. (2016). Grifolin induces autophagic cell death by inhibiting the Akt/mTOR/S6K pathway in human ovarian cancer cells. Oncology reports, 36(2), 1041-1047.

Chen, Y., Peng, G. F., Han, X. Z., Wang, W., Zhang, G. Q., & Li, X. (2015). Apoptosis prediction via inhibition of AKT signaling pathway by neogrifolin. *International journal of clinical and experimental pathology*, *8*(2), 1154.

Cheng, J. J., Huang, N. K., Chang, T. T., Wang, D. L., & Lu, M. K. (2005). Study for anti-angiogenic activities of polysaccharides isolated from *Antrodia cinnamomea* in endothelial cells. *Life sciences*, *76*(26), 3029-3042.

Chi, M., Jia, L., & Bao, H. (2014). Isolation, identification and cancer cell anti-proliferative activity of *Fomitopsis officinalis* fruit body constituents. *Acta Edulis Fungi*, *2*, 015, 284-285.

Daniel Silva, M. Sedlak, V. Slivova, T. Valachovicova, F. Llyod, N.W.Y. Ho. (2003) Biological activity of spores and dried powder from *Ganoderma lucidum* for inhibition of highly invasive human breast and prostate cancer cells. *The Journal of Alternative and Complementary Medicine* 9, 4, 2003, pp. 491-497.

Das, S. K., Mandal, A., Datta, A. K., Gupta, S., Paul, R., Saha, A., ... & Dubey, P. K. (2013). Nucleotide sequencing and identification of some wild mushrooms. *The Scientific World Journal*, *13*(1), 49-54.

De Monte, C., Carradori, S., Granese, A., Di Pierro, G. B., Leonardo, C., & De Nunzio, C. (2014). Modern extraction techniques and their impact on the pharmacological profile of *Serenoa repens* extracts for the treatment of lower urinary tract symptoms. *BMC urology*, *14*(1), 63.

Dembitsky, V. M., & Kilimnik, A. (2016). Anti-melanoma agents derived from fungal species. *MJ Pharma*, *1*(1), 002.

Dias, E. S., Abe, C., & Schwan, R. F. (2004). Truths and myths about the mushroom *Agaricus blazei*. *Scientia Agricola*, *61*(5), 545-549.

Dong, M., Chen, S. P., Kita, K., Ichimura, Y., Guo, W. Z., Lu, S., ... & Kashima, A. (2009). Anti-proliferative and apoptosis-inducible activity of Sarcodonin G from *Sarcodon scabrosus* in HeLa cells. *International journal of oncology*, *34*(1), 201-207.

Elsayed, E. A., El Enshasy, H., Wadaan, M. A., & Aziz, R. (2014). Mushrooms: a potential natural source of anti-inflammatory compounds for medical applications. *Mediators of inflammation*, *2014*, 805841.

Ferreira, I., A Vaz, J., Vasconcelos, M. H., & Martins, A. (2010). Compounds from wild mushrooms with antitumor potential. *Anti-Cancer Agents in Medicinal Chemistry (Formerly Current Medicinal Chemistry-Anti-Cancer Agents)*, *10*(5), 424-436.

Finimundy, T. C., Gambato, G., Fontana, R., Camassola, M., Salvador, M., Moura, S., ... & Roesch-Ely, M. (2013). Aqueous extracts of *Lentinula edodes* and *Pleurotus sajor-caju* exhibit high antioxidant capability and promising in vitro antitumor activity. Nutrition Research, 33(1), 76-84.

Fisher, M., & Yang, L. X. (2002). Anticancer effects and mechanisms of polysaccharide-K (PSK): implications of cancer immunotherapy. *Anticancer research*, *22*(3), 1737-1754.

Friedman, M. (2016). Mushroom Polysaccharides: Chemistry and Antiobesity, Antidiabetes, Anticancer, and Antibiotic Properties in Cells, Rodents, and Humans. *Foods*, *5*(4), 80.

Gibson, I., Gibson, E., & Kendrick, B. (2010). MatchMaker: mushrooms of the Pacific Northwest.

Ginns, J. (2017). Polypores of British Columbia. (Report No. 104), Province of British Columbia, Victoria, Canada.

Golovchenko, V. V., Khramova, D. S., Shinen, N., Jamsranjav, G., Chizhov, A. O., & Shashkov, A. S. (2018). Structure characterization of the mannofucogalactan isolated from fruit bodies of Quinine conk *Fomitopsis officinalis*. *Carbohydrate polymers*, *199*, 161-169.

Guillamón, E., García-Lafuente, A., Lozano, M., Rostagno, M. A., Villares, A., & Martínez, J. A. (2010). Edible mushrooms: role in the prevention of cardiovascular diseases. *Fitoterapia*, *81*(7), 715-723.

Han, J., Li, L., Zhong, J., Tohtaton, Z., Ren, Q., Han, L., ... & Yuan, T. (2016). Officimalonic acids A− H, lanostane triterpenes from the fruiting bodies of *Fomes officinalis.* Phytochemistry, 130, 193-200.

Handa, N., Yamada, T., & Tanaka, R. (2010). An unusual lanostane-type triterpenoid, spiroinonotsuoxodiol, and other triterpenoids from *Inonotus obliquus*. *Phytochemistry*, *71*(14-15), 1774-1779.

Hatvani N. (2001) Antibacterial effect of the culture fluid of *Lentinus edodes* mycelium grown in submerged liquid culture. Int J Antimicrob Agents; 17: 71–74.

Hawksworth, D. L. (2012). Global species numbers of fungi: are tropical studies and molecular approaches contributing to a more robust estimate? *Biodiversity and Conservation*, *21*(9), 2425-2433.

Hellwig, V., Nopper, R., Mauler, F., Freitag, J., Ji-Kai, L., Zhi-Hui, D., & Stadler, M. (2003). Activities of prenylphenol derivatives from fruitbodies of Albatrellus spp. on the human and rat vanilloid receptor 1 (VR1) and characterization of the novel natural product, confluentin. *Archiv der Pharmazie: An International Journal Pharmaceutical and Medicinal Chemistry*, *336*(2), 119-126.

Hu, M., Zhang, H., Feng, B., Liu, K., & Guo, S. (2013). Extraction of polysaccharides from Fomes officinalis Ames and their antitumor activity. *Experimental and therapeutic medicine*, *6*(2), 451-454.

Huang, W. H., Liao, W. R., & Sun, R. X. (2016). *Astragalus* polysaccharide induces the apoptosis of human hepatocellular carcinoma cells by decreasing the expression of Notch1. *International journal of molecular medicine*, *38*(2), 551-557.

Hur, J. M., Yang, C. H., Han, S. H., Lee, S. H., You, Y. O., Park, J. C., & Kim, K. J. (2004). Antibacterial effect of *Phellinus linteus* against methicillin-resistant Staphylococcus aureus. *Fitoterapia*, *75*(6), 603-605.

Ishii, N., Takahashi, A., Kusano, G., & Nozoe, S. (1988). Studies on the constituents of *Polyporus dispansus* and *P. confluens*. *Chemical and pharmaceutical bulletin*, *36*(8), 2918-2924.

Iwata, N., Wang, N., Yao, X., & Kitanaka, S. (2004). Structures and histamine release inhibitory effects of prenylated orcinol derivatives from *Rhododendron dauricum*. *Journal of Natural Products*, *67*(7), 1106-1109.

Javed, S. (2017). *In search of novel immuno-modulatory compounds from British Columbia wild mushrooms and their effectiveness in inflammatory micro-circulation of mice* (masters dissertation university of northern British Columbia).

Jaszek, M., Osińska-Jaroszuk, M., Janusz, G., Matuszewska, A., Stefaniuk, D., Sulej, J., ... & Jarosz-Wilkołazka, A. (2013). New bioactive fungal molecules with high antioxidant and antimicrobial capacity isolated from *Cerrena unicolor* idiophasic cultures. *BioMed research international*, *2013*. 497492.

Jin, S., Pang, R. P., Shen, J. N., Huang, G., Wang, J., & Zhou, J. G. (2007). Grifolin induces apoptosis via inhibition of PI3K/AKT signaling pathway in human osteosarcoma cells. Apoptosis, 12(7), 1317-1326.

Jing, S., Ying, P., Hu, X., Yu, Z., Sun, J., Ding, Y., ... & Song, S. (2017). Protective effect of grifolin against brain injury in an acute cerebral ischemia rat model. *Tropical Journal of Pharmaceutical Research*, *16*(6), 1299-1305.

Kang, J. H., Jang, J. E., Mishra, S. K., Lee, H. J., Nho, C. W., Shin, D., ... & Oh, S. H. (2015). Ergosterol peroxide from Chaga mushroom (*Inonotus obliquus*) exhibits anti-cancer activity by down-regulation of the β-catenin pathway in colorectal cancer. *Journal of ethnopharmacology*, *173*, 303-312.

Kidd, P. M. (2000). The use of mushroom glucans and proteoglycans in cancer treatment. *Alternative Medicine Review*, *5*(1), 4-27.

Kim, G. Y., Kim, S. H., Hwang, S. Y., Kim, H. Y., Park, Y. M., Park, S. K., ... & Lee, J. D. (2003). Oral administration of proteoglycan isolated from *Phellinus linteus* in the prevention and treatment of collagen-induced arthritis in mice. *Biological and Pharmaceutical Bulletin*, *26*(6), 823-831.

Kim, Y. S., Cho, N. S., Eom, T. J., & Shin, W. S. (2002). Purification and characterization of a laccase from *Cerrena unicolor* and its reactivity in lignin degradation. *Bulletin of the Korean Chemical Society*, *23*(7), 985-989.

Kim, J. H., Lee, Y., Sung, G. H., Kim, H. G., Jeong, D., Park, J. G., ... & Lee, S. Y. (2015). Antiproliferative and Apoptosis-Inducing Activities of 4-Isopropyl-2, 6-bis (1-phenylethyl) phenol Isolated from Butanol Fraction of *Cordyceps bassiana*. *Evidence-based complementary and alternative medicine: eCAM*, *2015*, 739874-739874.

Kim, K. C., Kim, J. S., Son, J. K., & Kim, I. G. (2007). Enhanced induction of mitochondrial damage and apoptosis in human leukemia HL-60 cells by the *Ganoderma lucidum* and *Duchesnea chrysantha* extracts. *Cancer letters*, *246*(1-2), 210-217.

Klein, E., Smith, D.L., Laxminarayan, R. (2007). Hospitalizations and deaths caused by methicillin-resistant *Staphylococcus aureus*, United States, 1999–2005. Emerging Infectious Diseases 13, 1840–1846.

Kobayashi, H., Matsunaga, K., & Oguchi, Y. (1995). Antimetastatic effects of PSK (Krestin), a protein-bound polysaccharide obtained from basidiomycetes: an overview. *Cancer Epidemiology and Prevention Biomarkers*, *4*(3), 275-281.

Kobori, M., Yoshida, M., Ohnishi-Kameyama, M., Takei, T., & Shinmoto, H. (2006). 5α, 8α-Epidioxy-22E-ergosta-6, 9 (11), 22-trien-3β-ol from an edible mushroom suppresses growth of HL60 leukemia and HT29 colon adenocarcinoma cells. *Biological and Pharmaceutical Bulletin*, *29*(4), 755-759.

Koch, B., & Steglich, W. (2007). Meroterpenoid pigments from *Albatrellus flettii* (Basidiomycetes). *European journal of organic chemistry*, *2007*(10), 1631-1635.

Kanokmedhakul, S., Lekphrom, R., Kanokmedhakul, K., Hahnvajanawong, C., Bua-Art, S., Saksirirat, W., ... & Kongsaeree, P. (2012). Cytotoxic sesquiterpenes from luminescent mushroom *Neonothopanus nambi*. *Tetrahedron, 68(39), 8261-8266.*

Kowalczyk, M., Sekuła, A., Mleczko, P., Olszowy, Z., Kujawa, A., Zubek, S., & Kupiec, T. (2015). Practical aspects of genetic identification of hallucinogenic and other poisonous mushrooms for clinical and forensic purposes. *Croatian Medical Journal*, *56*(1), 32-40.

Kozarski, M., Klaus, A., Nikšić, M., Vrvić, M. M., Todorović, N., Jakovljević, D., & Van Griensven, L. J. (2012). Antioxidative activities and chemical characterization of polysaccharide extracts from the widely used mushrooms *Ganoderma applanatum*, *Ganoderma lucidum, Lentinus edodes* and *Trametes versicolor*. *Journal of food composition and analysis*, *26*(1), 144-153.

Kozarski, M., Klaus, A., Jakovljevic, D., Todorovic, N., Vunduk, J., Petrović, P., ... & Van Griensven, L. (2015). Antioxidants of edible mushrooms. *Molecules*, *20*(10), 19489-19525.

Kucharzyk, K. H., Janusz, G., Karczmarczyk, I., & Rogalski, J. (2012). Chemical modifications of laccase from white-rot basidiomycete *Cerrena unicolor*. *Applied biochemistry and biotechnology*, *168*(7), 1989-2003.

Kuo, M. C., Weng, C. Y., Ha, C. L., & Wu, M. J. (2006). *Ganoderma lucidum* mycelia enhance innate immunity by activating NF-κB. *Journal of ethnopharmacology*, *103*(2), 217-222.

Kuriyama, I., Nakajima, Y., Nishida, H., Konishi, T., Takeuchi, T., Sugawara, F., ... & Mizushina, Y. (2013). Inhibitory effects of low molecular weight polyphenolics from Inonotus obliquus on human DNA topoisomerase activity and cancer cell proliferation. *Molecular medicine reports*, *8*(2), 535-542.

Lee, Y. S., Kim, Y. H., Shin, E. K., Kim, D. H., Lim, S. S., Lee, J. Y., & Kim, J. K. (2010). Anti-angiogenic activity of methanol extract of *Phellinus linteus* and its fractions. *Journal of ethnopharmacology*, *131*(1), 56-62.

Lin, Z. B. (2005). Cellular and molecular mechanisms of immuno-modulation by *Ganoderma lucidum*. *Journal of pharmacological sciences*, *99*(2), 144-153.

Lindequist, U., Niedermeyer, T. H., & Jülich, W. D. (2005). The pharmacological potential of mushrooms. *Evidence-Based Complementary and Alternative Medicine*, *2*(3), 285-299.

Liu, F. Y., Luo, K. W., Yu, Z. M., Co, N. N., Wu, S. H., Wu, P., ... & Kwok, T. T. (2009). Suillin from the mushroom *Suillus placidus* as potent apoptosis inducer in human hepatoma HepG2 cells. *Chemico-biological interactions*, *181*(2), 168-17.

Liu, K., & Woggon, W. D. (2010). Enantioselective synthesis of daurichromenic acid and confluentin. *European journal of organic chemistry*, *2010* (6), 1033-1036.

Liu, X. T., Winkler, A. L., Schwan, W. R., Volk, T. J., Rott, M. A., & Monte, A. (2010). Antibacterial compounds from mushrooms I: a lanostane-type triterpene and prenylphenol derivatives from *Jahnoporus hirtus* and *Albatrellus flettii* and their activities against Bacillus cereus and Enterococcus faecalis. *Planta medica*, *76*(02), 182-185.

Liu, Y., Guo, X., Duan, W., Wang, X., & Du, J. (2010). Accelerated solvent extraction of monacolin K from red yeast rice and purification by high-speed counter-current chromatography. *Journal of Chromatography B*, *878*(28), 2881-2885.

Luo, X., Yang, L., Xiao, L., Xia, X., Dong, X., Zhong, J., ... & Li, W. (2015). Grifolin directly targets ERK1/2 to epigenetically suppress cancer cell metastasis. *Oncotarget*, 6(40), 42704.

Luo, X., Namei Li, J. Z., Tan, Z., Liu, Y., Dong, X., Cheng, C., ... & Weng, X. (2016). Grifolin inhibits tumor cells adhesion and migration via suppressing interplay between PGC1α and Fra-1/LSF-MMP2/CD44 axes. *Oncotarget,* 7(42), 68708.

Luo, X. J., Li, L. L., Deng, Q. P., Yu, X. F., Yang, L. F., Luo, F. J., ... & Cao, Y. (2011). Grifolin, a potent antitumour natural product upregulates death-associated protein kinase 1 DAPK1 via p53 in nasopharyngeal carcinoma cells. European Journal of Cancer, 47(2), 316-325.

Ma, B. J., Wu, T. T., Ruan, Y., Shen, J. W., Zhou, H., Yu, H. Y., & Zhao, X. (2010). Antibacterial and antifungal activity of Scabronine G and H in vitro. *Mycology*, *1*(3), 200-203.

Matsuda, H., Akaki, J., Nakamura, S., Okazaki, Y., Kojima, H., Tamesada, M., & Yoshikawa, M. (2009). Apoptosis-inducing effects of sterols from the dried powder of cultured mycelium of *Cordyceps sinensis*. *Chemical and Pharmaceutical Bulletin*, *57*(4), 411-414.

Martin, K. J., & Rygiewicz, P. T. (2005). Fungal-specific PCR primers developed for analysis of the ITS region of environmental DNA extracts. *BMC microbiology*, *5*(1), 28.

Martin, K. R., & Brophy, S. (2009). Dietary mushrooms reduce mitogenesis and induce apoptosis and cytotoxicity in MCF-7 human breast cancer cells. *The FASEB Journal*, *23* (1 Supplement), 353-1.

Michniewicz, A., Ullrich, R., Ledakowicz, S., & Hofrichter, M. (2006). The white-rot fungus *Cerrena unicolor* strain 137 produces two laccase isoforms with different physico-chemical and catalytic properties. *Applied Microbiology and Biotechnology*, *69*(6), 682-688.

Mizerska-Dudka, M., Jaszek, M., Błachowicz, A., Rejczak, T. P., Matuszewska, A., Osińska-Jaroszuk, M., ... & Kandefer-Szerszeń, M. (2015). Fungus *Cerrena unicolor* as an effective source of new antiviral, immunomodulatory, and anticancer compounds. *International journal of biological macromolecules*, *79*, 459-468.

Mizutani, S., Kawai, T., Enoki, T., Sagawa, H., Shimanaka, K., Sakai, T., & Kato, I. (2006). Tumor-growth inhibitory activity of the terpene compound isolated from Buna-shimeji [*Hypsizigus marmoreus*] mushroom. *Journal of the Japanese Society for Food Science and Technology (Japan)*.36-36.

Morse, E. E. (1941). A new polypore in Washington. *Mycologia*, *33*(5), 506-509.

Naranmandakh, S., Murata, T., Odonbayar, B., Suganuma, K., Batkhuu, J., & Sasaki, K. (2018). Lanostane triterpenoids from *Fomitopsis officinalis* and their trypanocidal activity. *Journal of natural medicines*, *72*(2), 523-529.

Pagliuca, A., Valvo, C., Fabrizi, E. D., Di Martino, S., Biffoni, M., Runci, D., ... & Ricci-Vitiani, L. (2013). Analysis of the combined action of miR-143 and miR-145 on oncogenic pathways in colorectal cancer cells reveals a coordinate program of gene repression. *Oncogene*, *32*(40), 4806.

Park, Y. M., Won, J. H., Kim, Y. H., Choi, J. W., Park, H. J., & Lee, K. T. (2005). In vivo and in vitro anti-inflammatory and anti-nociceptive effects of the methanol extract of *Inonotus obliquus*. *Journal of Ethnopharmacology*, *101*(1), 120-128.

Park, B. T., Na, K. H., Jung, E. C., Park, J. W., & Kim, H. H. (2009). Antifungal and anticancer activities of a protein from the mushroom *Cordyceps militaris*. *The Korean Journal of Physiology & Pharmacology*, *13*(1), 49-54.

Patel, S., & Goyal, A. (2012). Recent developments in mushrooms as anti-cancer therapeutics: a review. *Biotech*, *2*(1), 1-15.

Pegler, D. (2002). Useful Fungi of the World: The Ling-zhi - The mushroom of immortality. *Mycologist, 16(3), 100-101*. doi:10.1017/S0269915X0200304

Perry, S. W., Norman, J. P., Barbieri, J., Brown, E. B., & Harris, A. (2011). Mitochondrial membrane potential probes and the proton gradient: a practical usage guide. *Biotechniques,* 50(2), 98–115.

Pouzar, Z. (1972). Contribution to the knowledge of the genus *Albatrellus* (Polyporaceae). I. A conspectus of species of the North Temperate Zone. *Ceska mykologie*. http://agris.fao.org/agris-search/search.do?recordID=US201301239473

Riss, T. L., Moravec, R. A., Niles, A. L., Duellman, S., Benink, H. A., Worzella, T. J., & Minor, L. (2016). Cell viability assays https://www.ncbi.nlm.nih.gov/pubmed/23805433.

Ren, G., Zhao, Y. P., Yang, L., & Fu, C. X. (2008). Anti-proliferative effect of clitocine from the mushroom *Leucopaxillus giganteus* on human cervical cancer HeLa cells by inducing apoptosis. *Cancer Letters*, *262*(2), 190-200.

Signoretto, C., Burlacchini, G., Marchi, A., Grillenzoni, M., Cavalleri, G., Ciric, L., ... & Pratten, J. (2011). Testing a low molecular mass fraction of a mushroom (*Lentinus edodes*) extract formulated as an oral rinse in a cohort of volunteers. *Journal of biomedicine & biotechnology*, *2011*, 857987-857987.

Schoch, C. L.; Seifert, K. A.; Huhndorf, S.; Robert, V.; Spouge, J. L.; Levesque, C. A.; Chen, W. (2012) Fungal Barcoding Consortium; Nuclear ribosomal internal transcribed spacer (ITS) region as a universal DNA barcode marker for Fungi. *Proc. Natl. Acad. Sci. U. S. A., 109*, 6241-6246.

Shieh, Y. H., Liu, C. F., Huang, Y. K., Yang, J. Y., Wu, I. L., Lin, C. H., & Lin, S. C. (2001). Evaluation of the hepatic and renal-protective effects of *Ganoderma lucidum* in mice. *The American journal of Chinese medicine*, *29*(03n04), 501-507.

Soares, R., Meireles, M., Rocha, A., Pirraco, A., Obiol, D., Alonso, E., ... & Balogh, G. (2011). Maitake (D fraction) mushroom extract induces apoptosis in breast cancer cells by BAK-1 gene activation. *Journal of medicinal food*, *14*(6), 563-572.

Stamets, P., & Zwickey, H. (2014). Medicinal Mushrooms: Ancient Remedies Meet Modern Science. *Integrative medicine (Encinitas, Calif.)*, *13*(1), 46-47.

Standish, L. J., Wenner, C. A., Sweet, E. S., Bridge, C., Nelson, A., Martzen, M., ... & Torkelson, C. (2008). *Trametes versicolor* mushroom immune therapy in breast cancer. *Journal of the Society for Integrative Oncology*, *6*(3), 122.

Statkiewicz, M., Matuszewska, A., Jaszek, M., Janusz, G., Osinska, M., Sulej, J., ... & Ostrowski, J. (2017). Antimelanomic Effects of High-and Low-Molecular Weight Bioactive Subfractions Isolated from the Mossy Maze Mushroom, *Cerrena unicolor* (Agaricomycetes). *International journal of medicinal mushrooms*, *19*(7). 619-628.

Stockert, J. C., Blázquez-Castro, A., Cañete, M., Horobin, R. W., & Villanueva, Á. (2012). MTT assay for cell viability: Intracellular localization of the formazan product is in lipid droplets. *Acta histochemica*, *114*(8), 785-796.

Sun, J., Zhao, Y., Chai, H., Wang, H., & Ng, T. B. (2011). A novel alkaline protease with antiproliferative activity from fresh fruiting bodies of the toxic wild mushroom *Amanita farinosa*. *Acta Biochim Pol*, *58*(4), 567-72.

Valverde, M. E., Hernández-Pérez, T., & Paredes-López, O. (2015). Edible mushrooms: improving human health and promoting quality life. *International journal of microbiology*, *2015*, 376387-376387.

van Meerloo, J., Kaspers, G. J., & Cloos, J. (2011). Cell sensitivity assays: the MTT assay. *Cancer cell culture: methods and protocols*, 237-245.

Wang, P., Henning, S. M., & Heber, D. (2010). Limitations of MTT and MTS-based assays for measurement of antiproliferative activity of green tea polyphenols. *PloS one*, *5*(4), e10202-e10202.

Wang, C. L., Meng, M., Liu, S. B., Wang, L. R., Hou, L. H., & Cao, X. H. (2013). A chemically sulfated polysaccharide from *Grifola frondosa* induces HepG2 cell apoptosis by notch1–NF-κB pathway. *Carbohydrate polymers*, *95*(1), 282-287.

Wu, Z., & Li, Y. (2017). Grifolin exhibits anti-cancer activity by inhibiting the development and invasion of gastric tumor cells. *Oncotarget*, *8* (13), 21454.

Wuliya, P., & Li, B. A. I. (2003). The immune-potentiating effect of *Fomes officinalis* polysaccharides [J]. *Journal of Xinjiang Medical University*, *6*, 022.

Yang, S., Wang, X., & Zhong, G. (2016). Grifolin, a potent anti-tumor natural product inhibits the growth and invasion of gastric cancer cells in vitro. *Int J Clin Exp Med,* 9(7), 12659-12668.

Ye, M., Liu, J. K., Lu, Z. X., Zhao, Y., Liu, S. F., Li, L. L., ... & Cao, Y. (2005). Grifolin, a potential antitumor natural product from the mushroom *Albatrellus confluens*, inhibits tumor cell growth by inducing apoptosis in vitro. FEBS letters, 579(16), 3437-3443.

Ye, M., Luo, X., Li, L., Shi, Y., Tan, M., Weng, X., ... & Cao, Y. (2007). Grifolin, a potential antitumor natural product from the mushroom *Albatrellus confluens*, induces cell-cycle arrest in G1 phase via the ERK1/2 pathway. Cancer letters, 258(2), 199-207.

Yue, P. Y. K., Wong, Y. Y., Chan, T. Y. K., Law, C. K. M., Tsoi, Y. K., & Leung, K. S. Y. (2012). Review of biological and pharmacological activities of the endemic Taiwanese bitter medicinal mushroom, *Antrodia camphorata* (M. Zang et CH Su) Sh. H. Wu et al.(higher Basidiomycetes). *International journal of medicinal mushrooms*, *14*(3).

Zhao, J., Wang, H., and Ng, T. (2009) Purification and characterization of a novel lectin from the toxic wild mushroom *Inocybe umbrinella*. Toxicon 53, 360-366.

Zhao, F., Wang, Y. F., Song, L., Jin, J. X., Zhang, Y. Q., Gan, H. Y., & Yang, K. H. (2017). Synergistic apoptotic effect of D-fraction from *Grifola frondosa* and vitamin C on hepatocellular carcinoma SMMC-7721 cells. *Integrative cancer therapies*, *16*(2), 205-214.

Zhao, G., Han, X., Zheng, S., Li, Z., Sha, Y., Ni, J., ... & Song, Z. (2016). Curcumin induces autophagy, inhibits proliferation and invasion by downregulating AKT/mTOR signaling pathway in human melanoma cells. Oncology reports, 35(2), 1065-1074.

Appendix

(i) ***Fomitopsis officinalis*** **(115)**

NLB4

NNNNNNNNNNGNNTCGTGCAGNNANGGTCCNGCGCGGANGCACTTCTCCAGACTAC
AACTCGGACGGCCAGAGACCGCCAGATTTTAAATTTGAGCTCTTCCCGCTTCACTCG
CAGTTACTAGGGGAATCCTTGTTAGTTTCTTTTCCTCCGCTTATTGATATGCTTAAGT
TCAGCGGGTAATCCTACCTGATTTGAGGTCAGAGGTCAAAAAAACAATTGTCCGAA
AGGACGATTGGAAGCCCAAACCCTCACAAAGTGTAAACCCTCCGGCGTAGACAAAA
CTATCACACCGGATTGAGCAAGATACACAGAGGTCCAAGCTAATGCATTCAAGAGG
AGCCGAACGTTTGACCGTCCGGCAGAAAACCTCCAAATCCAACCCCCCCCCNNACCA
ACAAAGGNNNGGGGGGTGAAAANTTCCTNGNCNNTCAACCAGGCTNGTTCCTCGAA
ATACCAAGGACCNAAGGGGGCGTTCAAAANTCCAATAATTCCNNAANTTNTGCATT
NNNTTNACTTATNGNTTTNNNTNCNNTNNNANCCNNNNANNNNNNNN

(ii) ***Sarcodon scabripes*** **(124)**

ITS3

NNNNNNNNNNATNATNNNTGCAGATTCANTGAATCATCGAATCTTTGAACGCACCT
TGCGCTCCTTGGTATTCCGAGGAGCATGCCTGTTTGAGTGTCATGAAATTCTCAACT
GCTTCAGCTTTGTTGAAGTGAAGTTGGACTTGGAGGATCTTTGCTGGCGTAAGTGTA
CACAATGTTGTAACATTTGCTTGTTGGCTCCTCTTAAAGATATGAAGCTTTTCTAGTA
GATCTTTGGCAGAAAAGTACCATTGATGTGATAATTATCTGCATCATTGAGAAAGCC
ATAGAGCAGAGTCCTACTTTATAAGGGCTCCTACAGAAAATGTTTATGATGTTCATT
GCCTTTCAACAATGATCACAATTGACCAAATTTGACCTCAAATCAGGTAGGACTACC
CGCTGAACTTAAGCATATCAATAAGCGGAGGAAAAGAAACTAACAAGGATTCCCCT
AGTAACTGCGAGTGAAGCGGGAAAAGCTCAAATTTAAAATCTGGCGTGCCTTTGGC
CGTCCGAGTTGTAGTCTGGAGAAGTGTTTTCTGTGCTGGACCGTGTACAAGTCCCTT
GGAACAGGGCGTCATAGAGGGTGAGAATNNNN

NLB4

NNNNNNNNNNNNCNNNNNGNTCCNCTCNCATGATGCNCTTCTCCAGACTACAACTC
GGACGGCCAAAGGCACGCCAGATTTTAAATTTGAGCTTTTCCCGCTTCACTCGCAGT
TACTAGGGGAATCCTTGTTAGTTTCTTTTCCTCCGCTTATTGATATGCTTAAGTTCAG
CGGGTAGTCCTACCTGATTTGAGGTCAAATTTGGTCAATTGTGATCATTGTTGAAAG
GCAATGAACATCATAAACATTTTCTGTAGGAGCCCTTATAAAGTAGGACTCTGCTCT
ATGGCTTTCTCAATGATGCAGATAATTATCACATCAATGGTACTTTTCTGCCAAAGA
TCTACTAGAAAAGCTTCATATCTTTAAGAGGAGCCAACAAGCAAATGTTACAACATT
GTGTACACTTACGCCAGCAAAGATCCTCCAAGTCCAACTTCACTTCAACAAAGCTGA
AGCAGTTGAGAATTTCATGACACTCAAACAGGCATGCTCCTCGGAATACCAAGGAG
CGCAAGGTGCGTTCAAAGATTCGATGATTCACTGAATTCTGCAATTCACATTACTTA
TCGCATTTCGCTGCGTTCTTCNATCGATGCAN

(iii) ***Tricholoma vaccinum*** **(125)**

ITS3

GNNNNNNNNANNNGNNNNANNNNNNGAANNNNNTGAATNATTCCGAATTCCTTNT
GAACGCACCTTGCGCTTCCCTTGGTATTTCCGAAGGAGCATGCCTGTTTGAGTGTCA
TGAAATTCTCAACCATTTCAGCTTTTTCTAGTTGATTTAGGCTTGGATGTGGGAGTTT
GCGGGCTTCTCTGAAGTCGGCTCTCCTTAAATATATTAGTAGGGACCTCTGTTGCCTC
AGCTCTTGGTGTGATAGTTATCTACGCCATTCTGCGAAGCAGCTTTAAAATGGGGTT
ACTGCTTTCTAACCGTCTCTACCGAGACAGCTTCTGACAATTTGACCTCAAATCAGG
TAGGACTACCCGCTGAACTTAAGCATATCAATAAGCGGAGGAAAAGAAACTAACAA
GGATTCCCCTAGTAACTGCGAGTGAAGCGGGAAAAGCTCAAATTTAAAATCTGAGG
GTCCTTGCGGCCTTCCGAGTTGTAATCTAGAGAAGTGCTATCCCCGCTGAACACCGA
GAACGCTCCGGGCACNCTGAGACTCAAAGAGTGACAGNNCACNTGCATCCATGAAC
AAAT

NLB4

NNNNNNNNNGNNNNNCGNTNCNCTCGCGGANGGNACTCTCTCTAGATTAANGCTCG
GAAGGCCGCAAGGACCCTCAGATTTTAAATTTGAGCTTTTCCCGCTTCACTCGCAGT
TACTAGGGGAATCCTTGTTAGTTTCTTTTCCTCCGCTTATTGATATGCTTAAGTTCAG
CGGGTAGTCCTACCTGATTTGAGGTCAAATTGTCAGAAGCTGTCTCGGTAGAGACGG
TTAGAAAGCAGTAACCCCATTTTAAAGCTGCTTCGCAGAATGGCGTAGATAACTATC
ACACCAAGAGCTGAGGCAACAGAGGTCCCTACTAATATATTTAAGGAGAGCCGACT
TCAGAGAAGCCCGCAAACTCCCACATCCAAGCCTAAATCAACTAGAAAAAGCTGAA
ATGGTTGAGAATTTCATGACACTCAAACAGGCATGCTCCTCGGAATACCAAGGAGC
GCAAGGTGCGTTCAAAGATTCGATGATTCACTGAATTCTGCAATTCACATTACTTAT
CGCATTTCNCTGCATTCTTGATCAATGCANCNTGNANGGNGANAANACAAAGGAGN

(iv) ***Cerrena unicolor*** **(127)**

ITS3

NNNNNNNNNNANNGANNNNTTGCAGAATTCNGTGAATCATCGAATCTTTGAACAGC
ACCTTGCGCCCCTTGGTATTCCGAGGGGCATGCCTGTTTGAGTGTCATGGTATTCTCA
ATACCCTAAATCTTTGCGGATGAGGGTGTATTGGATTTGGAGGTTTTTGCAGGCAAT
ATTCATTGTCAGCTCCTCTTAAATACATTAGCAGAGATATTACTGCTACTCTCCAGTG
TGATAATTGTCTACACTGTTAGTAGTGCGGTATAATCAAAGTCTTTGCTTCTAATCGT
CTTCGGACAATTCTTTGACATCTGACCTCAAATCAGGTAGGACTACCCGCTGAACTT
AAGCATATCAATAAGCGGAGGAAAAGAAACTAACAAGGATTCCCCTAGTAACTGCG
AGTGAAGCGGGAAAAGCTCAAATTTAAAATCTGGCAGCCTTCGGTTGTCCGAGTTGT
AGTCTGGANAAGCGTTTTCCGCGCTGGACCGTGTATAACTCCCTTGGANNAGGGGTG
TCCCAAAATGNTAAGAATCCAAAANTGCTGCAAAGCACAACCCCTATAGAANTCCC
GTGAATTCCAGGCCAAAAAGAAGANNTNANCCCCAAATN

NLB4

CNNNNNNNGGNNGNNNNNNNNNCCNCGNGGAAGCGCNCTNCNNGANNNNNNGNC
GGACAACCGAAGGCTGCCAGATTTTAAATTTGAGCTTTTCCCGCTTCACTCGCAGTT
ACTAGGGGAATCCTTCGTTAGTTTCTTTTCCTCCGCTTATTGATATGCTTAAGTTCAG
CGGGTAGTCCTACCTGATTTGAGGTCAGATGTCAAAGAATTGTCCGAAGACGATTAG
AAGCAAAGACTTTGATTATACCGCACTACTAACAGTGTAGACAATTATCACACTGGA
GAGTAGCAGTAATATCTCTGCTAATGTATTTAAGAGGAGCTGACAATGAATATTGCC
TGCAAAAACCTCCAAATCCAATACACCCTCATCCGCAAAGATTTAGGGTATTGAGAA
TACCATGACACTCAAACAGGCATGCCCCTCGGAATACCAAGGGGCGCAAGGTGCGT
TCAAAGATTCGATGATTCACTGAATTCTGCAATTCACATTACTTATCGCATTTCGCTG
CGTTCTTCATCGATGCNNGTTGGATTCTGCCCCTCNATGATGTGTTCTTCTTCNAAGC
ACCNNTTCTTTNAAAGAGGGGAGCTCCTATGGTCCACA

(v) ***Albatrellus flettii*** **(128)**

ITS3

NNNNNNNNNNGNNGNNNNNNNAANNNGTGAATATCGAATCTCGAACGCACCNNGC
GCCNNNNGGTATTCCGAGGGGCACACCNGTTTGAGTANCGTGAAATCATCAACCCA
GAACCCTTNTTTGTNGGGGGGTTCGAGGGCTTGGACTTGGAGGTCGTTGCCGGGTCC
CCCCCTTACGTGGGGGGGGAATCCGCTCCTCTTGAATGGATTAATGGGAACCCTCTC
TCCCCCTGCTCTCTTTGCCTCTCGGCGTGATAATTCCTCTGCGCCGACGTTGTGAGAA
AAGGGGGGAAAAGGAAACCGCTTCCAACCGTCTCTCGTCTGAAACAATTTTATGAA
CCCTTCCATCTCAAATCAGGGGGGACTACCCGCTGAACTTAAGCATATCAATAAACG
GAAGAAAAAAAACTAACAAGGATTCCCCTAATAACTGCCAGTGAAGCGGGAAAAG
CTCAAATTTGAAATCTGGCGGTCTTTGGCCGTCCGAATTGTAATCTGGAAAANCGCT
TTCCNCGCCNGAACATGTACAANTCCTCTGGAACGGGGCGTCATAAAAGGTGAAAA
TCCAANNTN

NLB4

GCNNNNNNNNNNGNNNNNNNCCGGNNGCTGGAAAGCGCTTTNTCCAGAACNACA
ACTCCGGACGGNNAAAGACCGCCAGATTNCNAATTCCGAGCTCCNTCCCGCTCTCA
CTCGCAGTTACTAGGGGAATCCNNGNTAGTTTCTTTTCCTCCGCTTATNGATATGCTT
AAGTTCAGCGGGTAGTCCCACCTGATTTGAGATCGAAGGGTTCATAAAATTGTCTCA
GACGAGAGACGGTTCGAAGCGGTCTCCTTTTCCCCCCTTTTCTCACAACGTCGGCGC
AGATGAATTATCACGCCGAGAGGCAAAGAGAGCAGGGTGAGAGAGGGCTCCCACT
AATGCATTCAAGAGGAGCCGATTCCCCCCCCCCCTAAGGGGGGGAACCGGGAACCA
CCTCCCAGTCCCAACCCTCCAACCCCCCAACAAAAAGGGTTCTGGGTTGAAGAATTC
CCNAAACTCCAACCGGGGTGCCCCTCCGAATACCCANAAGCCCNAGGGGGGTTCCA
ANAATCCATGAATCCCTGAATTCNGCNATTTNNNTTANTTATCNCATTTCCCTGCCTT
CTTNNNCCATGCAANGGAATCGGNANCCCCAGGGGGGNTTTTTAAAANTTNNANNN
NNCNCCCCCCNNNNCNCCGANNTNTTNNNNCN

(vi) ***Trametes versicolor (143)***

ITS3

NNNNNNNNNNNNNNNNNNNNAATTNNNTGATCATNNGAATNCTNTGAACGCACC
TTGCGCTCCTTGGTATTCCGAGGAGCATGCCTGTTTGAGTGTCATGGAATTCTCAACT
TATAAATCCTTGTGATCTATAAGCTNGGACTTGGAGGCTTGCTGGCCCTTGCTGGCC
GCTTCCCCTTGATGGCTTTACTTCATTCCCTAACGGTCCGCTCCTCATGGGGATATTT
GCCACCCCTGGGCCCGGGAATGGTTTTGCCAACTTTCTACCCTCCCATTAGACCAAT
TTTTTACNTTCGAACTTCAATCCAGGAAGAANTACCCCTTNACTTTAACCTAATCATT
AACCGAAGAAAAAAAACTAANNANGANTTCCCCTANAANNTGNAANGNANNCGGA
AAAACTCCAATTTTAAATCCGGNCGNCCTTTGNCCNNCCAATTTGNATCCGGAAAAA
CCTCCTTCNNCTTTGAACCTGGACCAATCNCCTTGAACCAAACCNCCTNNNAGGGGA
AAAATCCAA

NLB4

NNNCNNNNNNNNGNNNNNNNCANGCGGAGACGCTTCTCCAGACTACAACTCGGA
CGGCCAAAGACCGCCAGATTTTAAATTTGAGCTTTTCCCGCTTCACTCGCAGTTACT
AGGGGAATCCTTGTTAGTTTCTTTTCCTCCGCTTATTGATATGCTTAAGTTCAGCGGG
TAGTCCTACCTGATTTGAGGTCAGATGTTAAAAATTTGTCCTAATGGACGGTTAGAA
GCTCGCCAAAACACTTCACGGTCACAGCGTAGACAATTATCACACTGAGAGCCGAT
CCGTACGGAATCGAGCTAATGCATTCAAGAGGAGCCGACCGCCAGGGGCCAGCAGG
CCCCCAGTCCCAANCTAATAAATCACAGGGATTTAAGGTTGAAAAATTCCTGGACCT
TCAAACGGGCTGGCCCCTCGAAAAACCAGGGAGCGCAGGGGGCGTTCAAAAATCCA
AGAATTCNNGGATTTCGGCATTTCNATTTANTTACCGAATTTCNTGGCNTTCTCCATC
AAGNNN

(vii) ***Albatrellus flettii*** **(151)**

ITS3

NNNNNNANNTNGTGATNGNAGANTANNTGATCATCGAATCCTTTGAACGCACCTTG
CGCCTCTTGGTATTCCGAGGGGCACACCTGTTTGAGTATCGTGAAATCATCAACCCA
GAACCCTTTTTGTTGGGGGGTTCGAGGGCTTGGACTTGGAGGTCGTTGCCGGGTCCC
CCCCTTACGTGGGGGGGGAAACCGCTCCCCCTGGATGGCTTAATGGGAACCCTCCCC
CCCCCTGGTCTCCTTGGCTCCCGGCGTGGTAATTCCTCCGGCCCCAACTTGTGGAAA
AAGGGGGGAAAAGGGAAACCCTTCCAACCGTCTCTCCTCTGAAAAAATTTTATGAA
CCCTTCCATCCCCAATCCAGGGGGAATACCCGCTGAACTTAANCCTATCCATAAACG
GAAGAAAAAAAACTAACAANGGTTCCCCTAATAACTGGNAATGGAACGGGAAAAG
CTCCAATTTGAAATCTGGGGGTCTTTGGNCGTCCCAATTGNANTCTGGAAAAACCCT
TTCCNCGCCCGAACCTGGANNANNNCTCTGGAACGGGGCGTCNTTANNGGGGAAAA
TCCAA

NLB4

NNNNNNNNNNNNANTGGTCCGGCGCGGAAGCGCTTCTCCAGACTACAACTCGGACG
GCCAAAGACCGCCAGATTTCAAATTTGAGCTTTTCCCGCTTCACTCGCAGTTACTAG
GGGAATCCTTGTTAGTTTCTTTTCCTCCGCTTATTGATATGCTTAAGTTCAGCGGGTA
GTCCCACCTGATTTGAGATCGAAGGGTTCATAAAATTGTCTCAGACGAGAGACGGTT
CGAAGCGGTCTCCTTTTCCCCCCTTTTCTCACAACGTCGGCGCAGATGAATTATCAC
GCCGAGAGGCAAAGAGAGCAGGGTGAGAGAGGGCTCCCACTAATGCATTCAAGAG
GAGCCGATTCCCCCCCCCCCCGAAGGGGGGGGAACCCGGCACCAACTCCCAGTCCCAA
CCCCCCAACCCCCCCCACAAAAAGGGGTCCGGGGTGAAGAATTCCNNAAACTCCAAC
CGGGGGGGCCCCCCCGAAAAACCANAAGGGCCAGGGGGGGTCCAAAAATCCAAGAA
TCCNTGGATTTCGGCATTTCNNTTANTTANCCCATTTCCCTGGCNTCTNNNNCCNAN
GCAN